cAMP Signalling and Phosphodiesterase Activity in Cystogenesis of Autosomal Dominant Polycystic Kidney Disease

Thesis Submitted in Hilary Term, 2024

Ester Paolocci

Wolfson College

Department of Physiology, Anatomy, and Genetics

University of Oxford

Supervisors:

Manuela Zaccolo

David JP Henderson (Mironid)

Abstract

ADPKD affects 12 million people worldwide.(Igarashi and Somlo 2002) Characterised by the formation of fluid-filled kidney cysts, it is the fourth most common cause of end-stage renal disease. Yet, there is currently no cure for this disease. Tolvaptan, a V2R antagonist which blocks GPCR signalling, proved robust in clinical trials, but was also associated with numerous adverse side effects such as polyuria, nocturia, polydipsia, thirst, as well as hepatotoxicity.(Blair 2019) These collateral symptoms beg for the development of a better therapy for ADPKD. Enhanced cAMP signalling in the primary cilium of ADPKD cells drives cystogenesis, but thanks to the strict compartmentalisation of this second messenger, there is evidence to suggest the same cyclic nucleotide mitigates cyst formation when signalling from a domain in the cell body.(Hansen, Kaiser, Leyendecker, Stüven, Krause, Derakhshandeh, Irfan, Sroka, Preval, and Desai 2022) Thus, identifying these distinguished pools of cyst-protective cAMP would lead towards better treatment for ADPKD. Here, we set out to discover these domains of cAMP which reduce cystogenesis in vitro, and to identify the enzymes which regulate this second messenger at these locales. We provide evidence that in vitro inhibition of Phosphodiesterase 3 (PDE3), an enzyme which breaks down cAMP at the plasma membrane, ER, and Outer Mitochondrial Membrane, leads to mitigated cyst formation in vitro. PDE3 inhibition also decreased ER-mitochondrial contact sites in a renal cell line. The findings are consistent with a model where PDE3 alters organelle interaction and subsequent cystogenesis through a direct interaction with Polycystin 2 (PC2), one of the proteins mutated in 15% of ADPKD cases. Targeting PDE3, thus manipulating a cyst-protective nanodomain of second messenger, could be a selective therapeutic strategy for alleviating renal cystogenesis with minimal side effects.

Declaration of Work

The work presented in this thesis was primarily undertaken at the Department of Physiology, Anatomy, and Genetics, University of Oxford, in the laboratory of Manuela Zaccolo. Data was also obtained during my industrial placement at Mironid, in Glasgow, where I was supervised by David JP Henderson. All work presented is my own unless otherwise stated. This work has not been submitted for any other degree at University of Oxford or any other institution.

Ester Paolocci, April 2024

Thesis word count: ~45,000 words

Acknowledgements

There are many people I would like to thank for the last five years of work, culminating in this thesis. Firstly, I would like to acknowledge my supervisor, Manuela, who took a chance on me, because she saw potential at a time when I wasn't so sure of it myself. Secondly, I would like to thank all the post docs that helped guide me, Andreas, Inky, Guna, Stefania, Jianshu, and Jakub. Andreas, though your days experimenting in Oxford have reluctantly ended, you leave behind a legacy of DPhil students (including me) whom you have trained to excellent standards. I also will not forget the help you gave me during the pandemic, a time of great uncertainty. Inky, you are a great scientist, teacher, and friend, and your work ethic and passion for your research have inspired me throughout my own scientific endeavours. Guna, your cheery attitude was always welcome, particularly when I texted you at 6am for help, while I attempted new experiments alone in lab. Stefania, though no longer an official member of our group, knowing a helpful friend sat across the hall, was a great comfort. Down the science ladder, I also want to acknowledge all my DPhil peers, Anna, Milda, Emily, and Alex. In particular Milda and Anna have been by my side through all the ups and downs of this adventure. Without the pair of you, I would have never tried new things, like pitching a company or writing for OxSci. I owe it to you both, that I unexpectedly discovered these new passions, and more. I also want to thank Edoardo who contributed so much to last minute analyses in times of stress. I also feel privileged to have gotten to cox my Wolfson crew- the only thing better than your rowing were the unexpected swims and all the laughs we had on and off the boat. You guys truly made the Oxford experience special. Outside of Oxford, and in Glasgow, I want to mention my second "lab family" at Mironid. Dave, Maria, Susan, Jane, Faisa, Tom, Jazz, Martin, Catilin and Gemma, you all were great fun and so helpful throughout my internship. Particularly Faisa, you treated me more than a colleague, like a sister.

Finally, I would have never grown into the hardworking, international, curious scientist I am today, without the unwavering support, love, and sacrifices of my parents. Last but definitely not least, I thank Calum, who quite frankly deserves his own doctorate on the topic of how to love, support, and above all, tolerate a stressed out and sleep-deprived ambitious partner. To all the people mentioned, and many more, thank you, and lots of love!

N.B In practical terms I would like to acknowledge Mironid for providing me with the resources and materials for all cyst assay and qPCR experiments. I would also like to acknowledge that they provided the cell line I worked on throughout this thesis, IMCD3. Regarding execution of experimental protocols, all data was obtained by me, with some help from several undergraduate students and collaborators which will be specified. Jessica Zhang, an undergraduate student I supervised, set up, treated, fixed, and stained IMCD3 with Bay60. She imaged the resulting slides and analysed all the samples regarding ciliary length of Bay60 treated cells. Aparna Sridar, a second undergraduate I supervised, imaged a substantial number of slides for the cilia length chapter of this thesis. She also carried out FRET with the cGMP sensor cGi500. A third undergraduate student under my supervision, Wesley Donaldson, carried out a portion of FRET experiments in IMCD3 with FRET sensors OMM-EPAC, ER-cyto-H90, and AKAP79. He also analysed these experiments. Additionally, Wesley did a significant amount of the ER-mitochondria contact split-GFP imaging and some of the analysis. Edoardo Valli, a visiting undergraduate helped with the analysis of ciliary length. Finally, Faisa Omar and Caitlin Moore each did one round of the PDE assay to aid my effort in finishing three replicates before my stay in Glasgow ended. Faisa Omar also helped with some RNA extraction for qPCR.

Acronyms and Abbreviations

AC	Adenylyl Cyclase
ADPKD	Autosomal Dominant Polycystic Kidney Disease
AMPK	AMP-activated Protein Kinase
AKAP	A-Kinase Anchoring Protein
AKT	Protein Kinase B
ANOVA	Analysis of Variance
AQP2	Aquaporin 2
ATP	Adenosine Triphosphate
bPACs	photo-activatable Adenylyl Cyclases
cAMP	cyclic Adenosine Monophosphate
CEP290	Centrosomal Protein 290
CFP	Cyan Fluorescent Protein
CFTR	Cystic Fibrosis Transmembrane Conductance Regulator
CKD	Chronic Kidney Disease
CREB	cAMP response element binding protein
DMEM	Dulbecco's Modified Eagles Medium
DMSO	Dimethyl Sulfoxide
EDTA	Ethylene-diamine-tetra-acetic acid
EPAC	Exchange protein directly activated by cAMP
ER	Endoplasmic Reticulum
ERK	Extracellular signal-Regulated Kinases
FAO	Fatty Acid Oxidation
FEMP	FRET-based indicator of ER-Mitochondria Proximity
FRET	Fluorescence Resonance Energy Transfer
FSK	Forskolin
G-protein	Guanosine-binding protein
GAPDH	Glyceraldehyde 3-Phosphate Dehydrogenase
GFP	Green Fluorescent Protein
GPCR	G-protein Coupled Receptor
GSK	Glycogen Synthase Kinase
HEK	Human Embryonic Kidney cell line
IBMX	3-Isobutyl-1-Methylxanthine
IMCD3	Inner Medullary Collecting Duct cell line

IP	Immunoprecipitation
IP3	Inositol Triphosphate
KO	Knock Out
KD	Knock Down
KDa	KiloDaltons
LKB1	Liver Kinase B1
MAM	Mitochondria-Associated Membrane
MAPK	Mitogen Activated Protein Kinase
MDCK	Madine Darby Canine cells
MEF	Mouse Embryonic Fibroblasts
mTOR	mammalian Target Of Rapamycin
MW	Molecular Weight
OMM	Outer Mitochondrial Membrane
OXPHOS	Oxidative Phosphorylation
PBS	Phosphate Buffered Saline
PC	Polycystin
PCM1	Pericentriolar Material Protein 1
PDE	Phosphodiesterase
PKC	Protein Kinase C
PKD	Polycystic Kidney Disease
PGE2	Prostaglandin E2
PKA	Protein Kinase A
POPDC	Popeye-domain Containing
qPCR	real-time Polymerase Chain Reaction
RFP	Red Fluorescent Protein
RT	Room Temperature
RyR	Ryanodine Receptor
SD	Standard Deviation
SERCA	Sarcoplasmic Reticulum Ca^{2+}-ATPase
SHh	Sonic Hedgehog Signalling
$SPLIC_s$	Split-GFP-based contact site sensor
TSC	Tuberous Sclerosis Complex

UCR	Upstream Conserved Region
UPS	Ubiquitin Proteosome System
V2R	Vasopressin 2 Receptor
WCL	Whole Cell Lysate
WT	Wild Type
YFP	Yellow Fluorescent Protein

Table of Contents

Chapter 1: Introduction

What is Autosomal Dominant Polycystic Kidney Disease?

ADPKD is characterised by the formation of fluid-filled kidney cysts but also manifests with a variety of extra-renal symptoms, including arterial hypertension, hepatobiliary changes, and intracranial arterial aneurysms (**Schematic 1**).(Gattone et al. 2008; Bergmann 2015) It is estimated 1 in 500-1000 people suffer from this disease, with 12 million cases of ADPKD worldwide.(Igarashi and Somlo 2002) Of ADPKD patients, about 70% progress to renal failure and dialysis, making ADPKD the fourth most common cause of end-stage-renal disease globally.(Helal 2013; Chebib and Torres 2016) Currently, there is no cure for this disease.

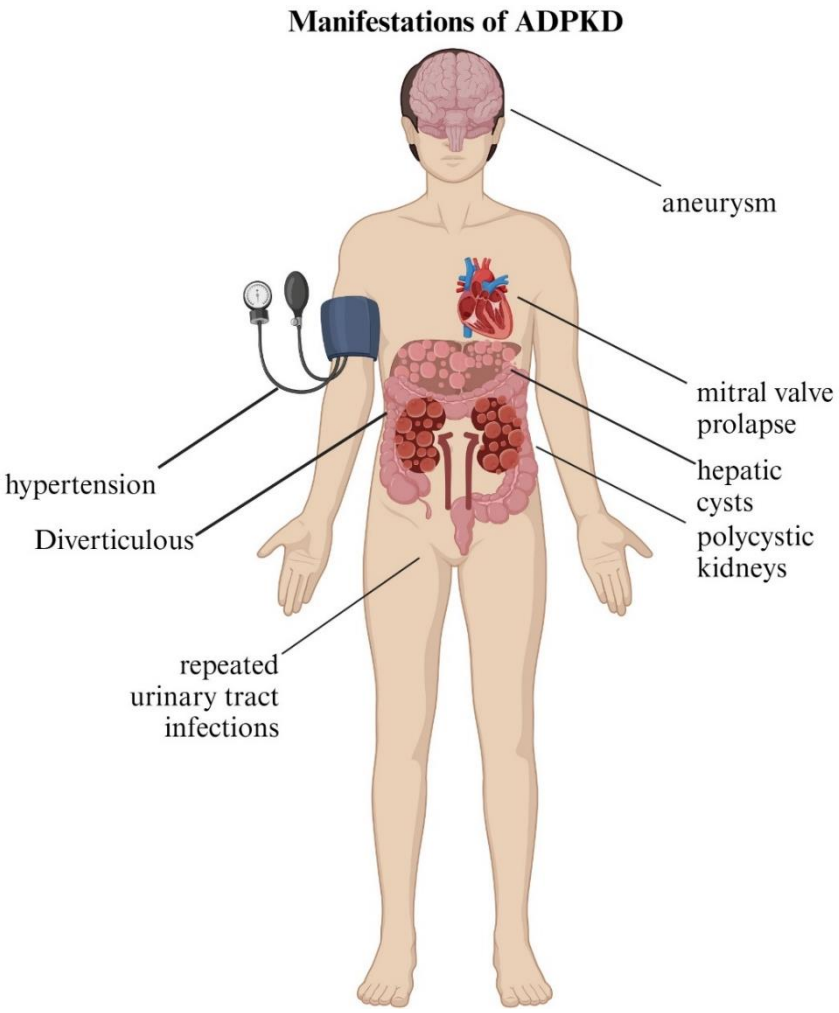

Schematic 1: ADPKD is characterised by fluid-filled kidney cysts but also manifests with extra-renal abnormalities and symptoms.

ADPKD, a ciliopathy

ADPKD was the first discovered ciliopathy, a class of diseases which develop when proteins of the primary cilium are mutated. The primary cilium is an organelle which was long ignored since it was first observed in 1898.(Zimmermann 1898) Thought to be a vestigial appendage, it has recently garnered increasing attention as a hub of intracellular signalling, hosting pathways primarily vital for embryonic development and tissue maintenance. The most prominent pathways include Sonic Hedgehog, Wnt, Notch, Hippo, PDGFP, TGF-beta, mTOR, Ca^{2+}, and cAMP signalling.(Wheway, Nazlamova, and Hancock 2018) The latter two pathways are particularly relevant to this thesis. This hair-like organelle projects from the surface of most mammalian cells, consisting of a microtubule-based axoneme and surrounding membrane. The cilium grows from the basal body, a derivative of the centrosome, in non-dividing cells.(Ishikawa and Marshall 2011) Its transition zone (TZ) gates entry of proteins from the cytosol into the cilium, with many mutations of TZ proteins leading to ciliopathies.(Reiter, Blacque, and Leroux 2012) Aside from its role in signalling, the cilium is also important for mechanosensory functions such as fluid-flow sensing, photoreception, and olfaction.(Kiesel et al. 2020; Bujakowska, Liu, and Pierce 2017; Doroquez et al. 2014)

ADPKD arises when proteins Polycystin 1 (PC1) or Polycystin 2 (PC2) are mutated (in 85% and 15% of cases respectively).(Porath et al. 2016) The polycystins function at the ER, plasma membrane, and eminently, at the primary cilium. PC1 is encode by the PKD1 gene, which sits on chromosome 16p13.3, while PC2 is transcribed from PKD2, a gene located on chromosome 4q22. ADPKD can also stem from other rare mutations, such as GANAB which encodes the glucosidase IIα subunit which, when altered, causes a mild cystic phenotype that does not lead to renal failure.(Porath et al. 2016) Another missense mutation in NAJB11 was also associated to polycystic kidneys in two relatives. NAJB11, is a cofactor of binding-immunoglobulin protein (BiP), a key chaperone in endoplasmic reticulum (ER) control of

folding, trafficking, and degradation of secreted and membrane proteins.(Cornec-Le Gall et al. 2018)

PC1 is a large 4,303 amino acid protein with 11 transmembrane domains and a prominent extracellular portion. Its partner, PC2, is a transient receptor potential (TRP) channel made up of 968 amino acids. This nonselective, cation-permeant, calcium-sensitive channel is expressed in all tissue types and can localise to the ER, primary cilium, and plasma membrane, where it also modulates the activity of other Ca^{2+} channels.(Brill and Ehrlich 2020) PC2 can conduct Ca^{2+} stores from the ER into the cytosol and mitochondria, but Ca^{2+} can also regulate PC2 activity. Lower levels of Ca^{2+} (<1μM) increase the channel's opening interval, while Ca^{2+} concentrations above 1μM have an inhibitory effect.(Cai et al. 2004) Cryo-electron microscopy studies showed PC2 forms a homotetrameric complex to conduct ions. However, it is possible that PC2 may heteromultimerize with other TRP channels as well as PC1.(Grieben et al. 2017) PC1 and PC2, the comprehensive functions of which are still to be elucidated, interact through their cytoplasmic carboxy termini.(Qian et al. 1997) It is believed PC1 is a strict regulator of PC2, thus why mutations in either polycystin lead to comparable extrarenal and cystic phenotypes. A more detailed structure, and some functions, of the polycystins can be seen in **Schematic 2**.

Though phenotype is comparable, patients with PKD1 mutations have more severe ADPKD, as opposed to their PKD2 counterparts, as the latter manifest with delayed onset of kidney cysts, hypertension, and renal failure. ADPKD cysts may form in any tubular segment of the kidney, sprouting from the nephron and spreading, thus impairing kidney function. Of note, while ADPKD is an autosomal dominant inherited disease, it is thought to occur through a two-hit model approach, whereby both copies of polycystins in germline and somatic mutations are required for considerable cystogenesis to develop later in life.(Pei 2001; Reeders 1992) Indeed, studies carried out in renal epithelial cells of nine ADPKD patients demonstrate somatic mutations in PKD1 or PKD2 in all participants, and in 90% of all

analysed cysts. Of these variants, 90% are truncating, splice site, or in frame predicted pathogenic mutations.(Tan et al. 2018)

The primary cilium converts fluid shear stress into intracellular Ca^{2+} signalling. In ADPKD, this ability of the cilium to translate extracellular mechanical stimuli into an intracellular response is compromised with mutations in the polycystins. (Kathem, Mohieldin, and Nauli 2014) Hence, Ca^{2+} concentrations are decreased in cilia of ADPKD cells, which lead to subsequent effects on intracellular signalling. Of importance, Adenylyl cyclase (AC) 5 and 6 localise to the cilium, and are Ca^{2+} inhibited. As ACs are responsible for the synthesis of cAMP, a downregulation of Ca^{2+} upon polycystin dysfunction, leads to excess AC activity and subsequently enhances cAMP signalling. This upregulation in second messenger has downstream effects which propagate the two main mechanisms driving cystogenesis- excessive cell proliferation and fluid secretion. The latter part of this introduction will go into detail, of how cAMP achieves such feats.

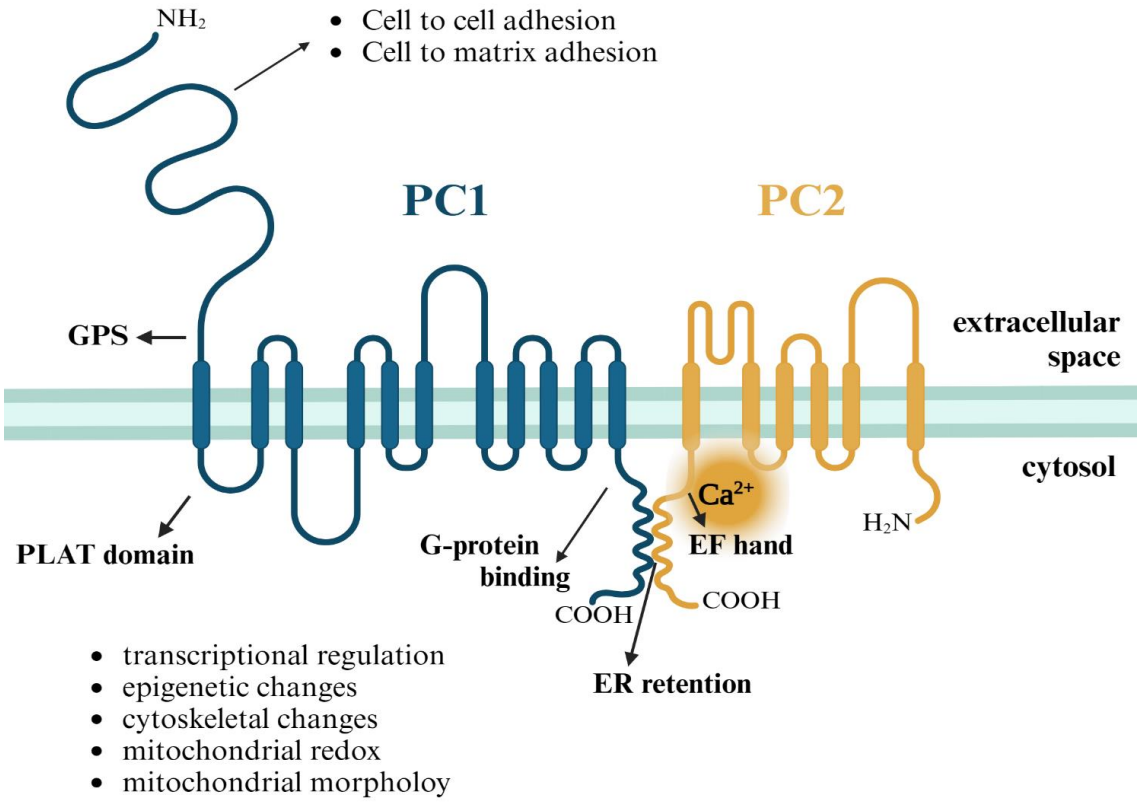

Schematic 2: Structure of Polycystins. PC1 is made up of 11 transmembrane domains with a prominent extracellular portion, containing a C-type lectin domain, leucine enriched repeats, immunoglobin-like repeats, as well as type III fibronectin domains. Together, the presence of these motifs on PC1, suggest this protein may mediate cell to cell or cell to matrix interactions.(Harris 1999; Koptides and Deltas 2000) Intracellularly, PC1 also has a polycystin-1 lipoxygenase and α-toxin (PLAT) domain. PKA phosphorylation of the PLAT domain anchors PC1 to the plasma membrane.(Xu et al. 2016) Additionally, PC1 also has a G-protein coupled receptor proteolytic site (GPS), which when cleaved, produces a large amino-terminal fragment which remains non-covalently anchored to the carboxy terminal fragment at the plasma membrane.(Qian et al. 2002) It is hypothesized, this cleaved product regulates PC1 biogenesis and trafficking.(Low et al. 2006) In addition, severance of the intracellular c-terminal tail releases PC1 fragments into the cytoplasm, which travel to the nucleus and interact with transcription factor modulators, ultimately regulating several signalling pathways.(Low et al. 2006; Bergmann et al. 2018) PC2 interacts with PC1 at their carboxy termini. The former is made up of 6 transmembrane domains. The EF hand of PC2, located on the cytosolic c-terminal tail, senses Ca^{2+} levels, and Ca^{2+} binding of this domain is required for opening of full-length PC2.(Kuo et al. 2014)

Molecular pathways propagating cyst formation in ADPKD

Several prominent pathways demonstrate altered signalling in ADPKD, downstream of Ca^{2+} and cAMP, to orchestrate transcriptional and metabolic changes regulating cell cycle, energy metabolism, cell proliferation, and fluid secretion. For example, the cAMP effector, protein kinase A (PKA) phosphorylates glycogen synthase 3β (GSK3β), which stabilizes β-catenin,

and thus enhances Wnt/ β-catenin transcriptional activity and cellular proliferation (Taurin et al. 2006).(Li et al. 2000) Also downstream of PKA, enhanced extracellular signal regulated kinase (ERK), and the protein kinase B (Akt) pathway activate mammalian target of rapamycin (mTOR).(Rowe, Chiaravalli, Mannella, Ulisse, Quilici, Pema, Song, Xu, Mari, and Qian 2013)

mTOR signalling orchestrates growth and metabolism,(Albert and Hall 2015) and is particularly prominent in renal biology.(Fantus et al. 2016) Tuberous sclerosis complex proteins TSC1 and TSC2 are notable inhibitors of mTOR complex 1 (mTORC1), and loss-of-function mutations in either protein can manifest with renal cystogenesis.(Henske et al. 2016) In fact, PKD1 and TSC2 have contiguous loci, with patients harbouring both mutations developing severe infantile ADPKD.(Brook-Carter et al. 1994) Increased mTOR signalling has been reported in several ADPKD models, with Rapamycin, an mTOR inhibitor, ameliorating cystogenesis in conditionally-induced PKD1-deletion mice.(Shillingford et al. 2006; Shillingford et al. 2010) It is believed PC1 and mTOR may function through a feedback mechanism in ADPKD.(Pema et al. 2016)

Downstream, mTORC1 stimulation promotes phosphorylation of eukaryotic translation initiation factor 4E-binding protein (4E-BP), propagating genetic translation relevant to proliferation, protein synthesis, metabolism, mitochondrial biogenesis, and mitochondrial functions linked to enhanced TCA cycle intermediates and ATP synthesis.(Hsieh et al. 2012; Morita et al. 2013) Another pathway, the S6 kinase (S6K)-dependent pathway also associates mTORC1 signalling to lipid synthesis and increased glycolysis through transcriptional control of hypoxia-inducible factor (Hif1α) and sterol regulator element-binding protein (SREBP1).(Düvel et al. 2010) In the alternative mTOR branch, mTORC2 is also a pivotal player in growth and nutrient signalling. It is speculated that mTORC2 promotes assembly of the IP3R/GRP75/VDAC1 complex(Betz et al. 2013), a linker of ER-mitochondrial contacts.(Li et al. 2022; Bartok et al. 2019) ER-mitochondria contact sites have recently been

reported to be altered in PKD2 KO cells, contributing to disease progression through regulation of mitochondrial structure and function.(Kuo et al. 2019) **Schematic 3** summarises some of the downstream effects of mTOR signalling in ADPKD.

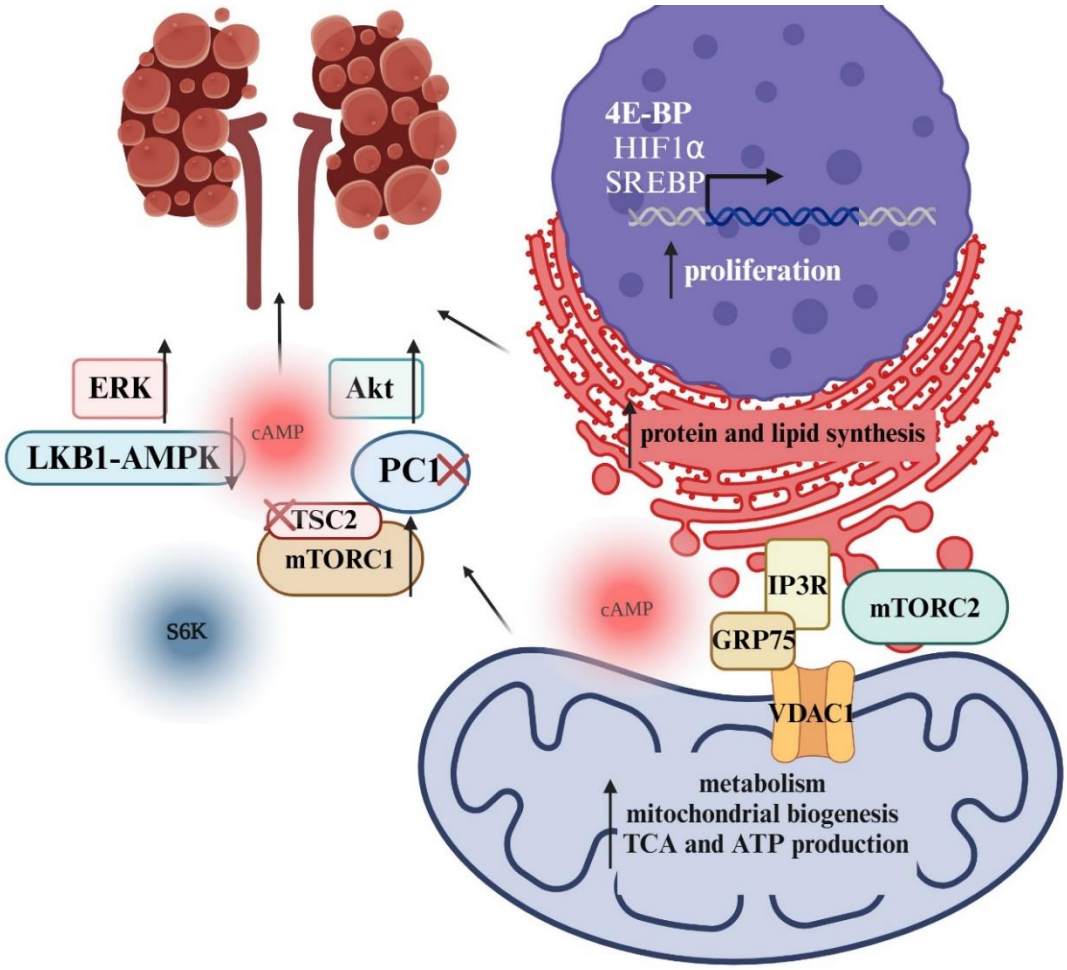

Schematic 3: mTOR signalling in ADPKD leads to upregulation of transcriptional regulators, 4E-BP, HIF1α, SREBP1, and SREPB2. Increased transcription is relevant to genes which propagate excess cell proliferation. Processes that contribute to proliferation are enhanced at the ER, such as protein and lipid synthesis, as well as at the mitochondria, including increase in TCA cycle intermediates and ATP production, as well as organelle biogenesis. TSC2 and PC1 as well as LKB1-AMPK can supress mTORC signalling. Downregulation of LKB1-AMPK by ERK signalling leads to upregulated mTORC signalling in ADPKD. KO of PC1 or TSC2 also leads to renal cystogenesis. mTORC2 has been associated to regulate ER-mitochondrial contact via the IP3R/GPR175/VDAC1 complex.

In ADPKD, Wnt/ β-catenin and mTOR are just some illustrations of how PKA, and thus cAMP, function to elicit secondary alterations in intracellular pathways driving renal cystogenesis. Yet, the list of intracellular responses, due to enhanced cAMP signalling, in this ciliopathy, are numerous and often paradoxical. cAMP achieves such varied and disparate outcomes through tight spatial and temporal control of its downstream signal, and ADPKD is a great example of this compartmentalization. Enhanced cAMP signalling in the primary cilium of kidney cells promotes excessive cell proliferation and fluid secretion, driving the formation of renal cysts which characterize ADPKD. Yet, emerging evidence suggests cAMP in the cell body, perhaps localized to specific and yet unidentified cAMP nanodomains, may actually play a mitigating role in cyst progression.(Hansen, Kaiser, Leyendecker, Stüven, Krause, Derakhshandeh, Irfan, Sroka, Preval, and Desai 2022) Therefore, targeting these unidentified domains of cAMP may be a selective therapeutic strategy for this ciliopathy. Indeed while this thesis begins in the cilium, it ends at the ER and mitochondrial contact sites. ADPKD, though a famous ciliopathy, also has a prominent metabolic component.

Extraciliary dysfunction in ADPKD

While ADPKD is a known ciliopathy, and many of the GPCRs which will be described below are thought to function at the cilium or plasma membrane to enhance cAMP, polycystins can also localise to intracellular domains, such as the ER and mitochondria, to alter metabolism in this disease.

Mitochondria are important in ADPKD, as numerous differences in gene expression in diseased and WT kidneys are in genes implicated in metabolism,(Podrini et al. 2018). Indeed, many of these genes are controlled by Hepatocyte nuclear factor 4α (HNF4α), (Menezes et al. 2012; Menezes and Germino 2019) a nuclear hormone receptor which binds linoleic acid to regulate Fatty Acid Oxidation (FAO). (Louet et al. 2002) PKD1-mutant mice with inactive HNF4α suffer from more severe renal cystogenesis.(Menezes et al. 2012) Yet, HNF4α is not the only factor contributing to altered FAO in ADPKD. MicroRNA cluster miR-17~92, is a

known oncogenic driver of metabolic reprogramming and regulates mTORC1 signalling.(Izreig et al. 2016) miR-17~92 is overexpressed in renal cystic samples of both mouse models and human patients of ADPKD. (Hajarnis et al. 2017) Anti- miR-17~92 treatment or KO mitigates cystogenesis in both PKD1 and PKD2 murine models. It is hypothesized miR-17~92 inhibits Peroxisome proliferator-activated receptor α (PPARα), a transcription factor, prominent for the regulation of glucose and lipid metabolism. (Hajarnis et al. 2017) Indeed, 30% of $Pkd1^{RC/RC}$ mice, a model of slow ADPKD progression, show downregulated PPARα and FAO. Fenofibrate, a PPARα agonist, increases PPARα expression and FAO in these mice, while reducing cyst volume by 60%.(Lakhia et al. 2018) In some studies, improving FAO shows promising effects on acute as well as chronic (CKD) kidney disease.(Kang et al. 2015) Of note, FAO is not the only metabolic process altered in ADPKD. Increased utilisation of glutamine is also observed in $PKD1^{-/-}$ Mouse Embryonic Fibroblasts (MEFs), as well as in PKD1-mutant embryonic cells.(Flowers et al. 2018)

It is hypothesized that PC1 receives signals (potentially at the cilium, which stimulate the release of the PC1 CTT fragment (PC1 C-Terminal tail)). Subsequently, these signals precisely adjust mitochondrial function, redox states, as well as acetyl-CoA levels, ultimately regulating epigenetic and cytoskeletal changes of the cell.(Xu et al. 2017; Wellen et al. 2009; Lee et al. 2014) As a consequence, cellular metabolism can respond to transcriptional regulation and thus change developmental processes.(Wong et al. 2017; Ghesquière et al. 2014). Indeed, subcellular localisation of both full-length PC1 as well as its PC1-C-terminal domain alone demonstrate colocalization of PC1 with mitochondrial markers.(Lin et al. 2018) In transgenic MEFs expressing full-length PC1, immunoblot staining highlighted a short PPC1-CTT fragment enriched in organelle fractions, suggesting PC1 is cleaved to release a CTT which is transported to the mitochondria.(Lin et al. 2018) In transgenic drosophila with the same overexpression of PC1, CTT trafficking to mitochondria results in obvious phenotypic changes including mitochondrial dysfunction, culminating in early embryonic lethality.(Lin et al. 2018) $PKD1^{-/-}$ cells also exhibit abnormal mitochondrial morphology and

altered mitochondrial membrane potential.(Lin et al. 2018) ADPKD rodent models, Ksp-Cre $PKD1^{flox/flox}$ mice and Hans:SPRD Cy/+ rats (a model of ADPKD which arises from a mutation in the Anks6 gene, coding for Samcystin, a protein relevant for cystogenesis) show mitochondrial anomalies in tubular cell morphology, particularly in cells of the cyst lining. In parallel, Human ADPKD cells, both with homozygous or heterozygous PKD1 mutations, also demonstrate mitochondrial structural abnormalities, alongside upregulation of mitochondrial superoxides.(Ishimoto et al. 2017)

Recently, it has been shown that, like cancer, ADPKD cells undergo the Warburg effect, or aerobic glycolysis. In culture, mouse embryonic fibroblasts (MEFs) from $PKD1^{-/-}$ embryos acidify their medium faster than their WT counterparts. This result is also observed in growth-arrested (100% density) $PKD1^{-/-}$ cells, implying metabolic changes are cell cycle independent.(Rowe, Chiaravalli, Mannella, Ulisse, Quilici, Pema, Song, Xu, Mari, Qian, et al. 2013) The KO cells have higher ATP levels, and NMR spectroscopy revealed the most pronounced differences in the diseased cells are reduced glucose and increased lactate concentrations. This data demonstrates a shift towards aerobic glycolysis in $PKD1^{-/-}$ cells. Phenotypically, glucose starvation decreases cell proliferation and increases apoptosis in the same cells. Further, both polycystins in LLC-PK1, or porcine renal epithelial cells, increased hydroxylation of PC1 by proline hydroxylase, Egl nine homologue 3 (EGLN3), an O_2 sensor. Inhibition of EGLN3 via dimethyloxaloylglycine (DMOG) decreases OXPHOS, corroborating PC1's role in mitochondrial metabolism. The authors of this study surmise that during hypoxia, PC1 relocates from the ER to the plasma membrane, possibly decreasing expression and function of the PC1/PC2 complex at the organelle, thus reducing PC2 channel activity. Cells without PC1 expression use less O_2 and demonstrate less mitochondrial Ca^{2+} uptake as a result of bradykinin (an inflammatory promoter)-induced ER Ca^{2+} release.(Padovano et al. 2017) Treatment of ADPKD mouse models with 2-deoxyglucose (2DG), an analogue of glucose which cannot be metabolised, reduce renal volume, cystic index, as well as cellular proliferation rate. The study also linked the metabolic alterations to

ERK signalling inhibiting the tumour suppressing LKB1-AMPK axis while also activating the mammalian target of rapamycin complex 1 (mTORC1)-glycolytic pathway.(Rowe, Chiaravalli, Mannella, Ulisse, Quilici, Pema, Song, Xu, Mari, Qian, et al. 2013) **Schematic 4** summarizes some of the downstream metabolic effects of mutated polycystin signalling at the ER and mitochondrial contact sites. The full scope of altered organelle signalling in ADPKD is yet still a mystery.(Menezes and Germino 2019)

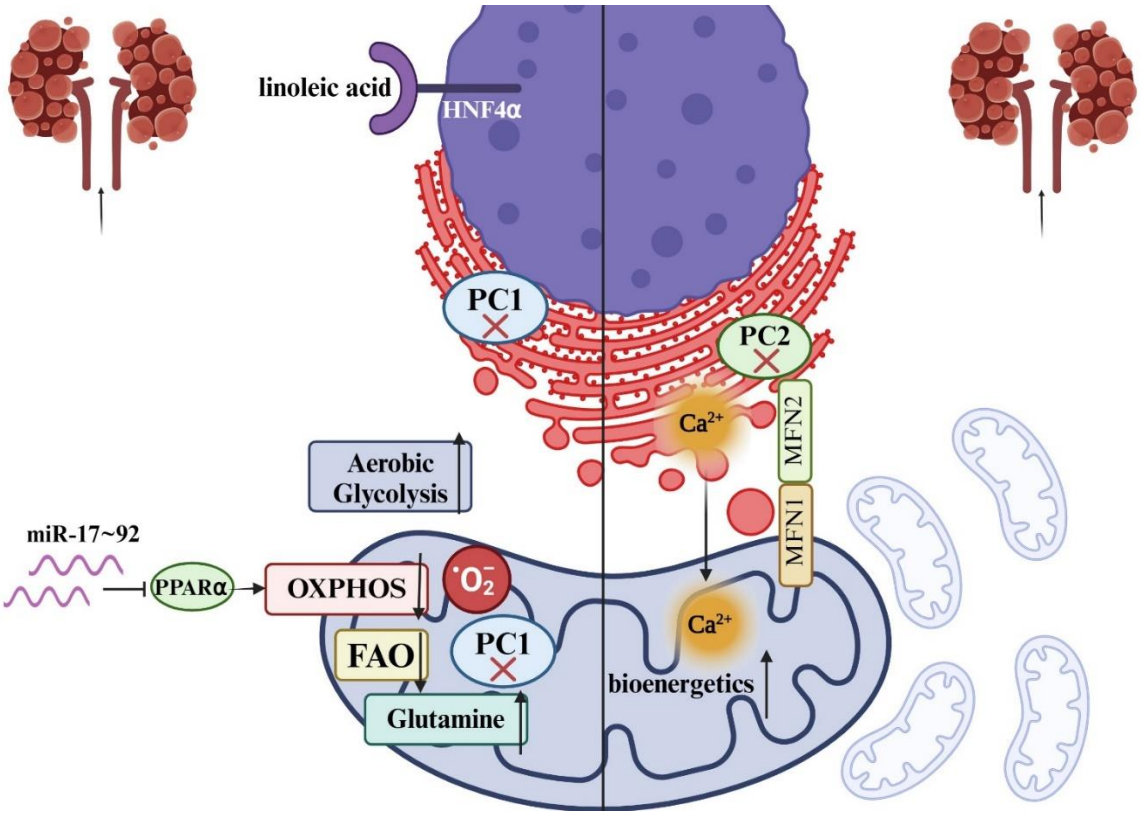

Schematic 4: Metabolic and bioenergetic downstream effects of either PC1 (left) deletion or PC2 (right) deletion.

Overall, based on this evidence and more, ADPKD is a complex disease. In this ciliopathy, aberrant signalling stems from the cilium, but goes on to have downstream effects in a variety of intracellular domains, eliciting changes such as altered organelle crosstalk, metabolic reprogramming, and transcriptional regulation. As aforementioned, one of the most fundamental drivers of renal cystogenesis is upregulation of cAMP signalling. Like the polycystins, cAMP regulates a variety of intracellular functions, but often achieves opposing

downstream outcomes. For example, in ADPKD, enhanced ciliary cAMP provokes cystogenesis, but there is evidence that cytosolic cAMP may mitigate cyst formation.(Hansen, Kaiser, Leyendecker, Stüven, Krause, Derakhshandeh, Irfan, Sroka, Preval, and Desai 2022) How this second messenger can achieve such disparate results in renal cyst growth is the broad aim of this thesis. However, before we can begin to dissect this aim, we must first understand how this cyclic nucleotide achieves compartmentalisation, and how this is relevant to ADPKD progression.

Compartmentalisation of the cAMP signal, and its involvement in ADPKD

cAMP was discovered more than 60 years ago by Earl Sutherland, when he demonstrated that this cyclic nucleotide bridged extracellular hormonal signals to the breakdown of glycogen in the liver(Beavo, Hardman, and Sutherland 1971). Since then, cAMP gave way to the fundamental idea of a "second messenger". This small molecule is capable of translating signals from hormones, neurotransmitters, and other extracellular stimuli into a variety of intracellular responses, ranging from cell proliferation to apoptosis, from cell differentiation to regulation of metabolic functions(Stork and Schmitt 2002; Weissinger et al. 1997) Such opposing outcomes are achieved through cAMP-dependent modulation of selected effectors that, in turn, can impact a plethora of different targets, such as receptors, channels, transporters and pumps, as well as, the cytoskeleton, transcriptional machinery, and metabolic enzymes, just to name a few. Accuracy of signal transduction from a particular extracellular stimulus to the appropriate cell function is achieved through tight spatio-temporal control of the cAMP signal.

G-Protein Coupled Receptors

cAMP signalling generally begins upon activation of a G-protein coupled receptor (GPCR) by a broad range of extracellular signals, (Levitzki 1988; Mons et al. 1998; Selbie and Hill 1998) including odours, hormones, and neurotransmitters.(Yang et al. 2021; Pal, Melcher, and Xu

2012; Billesbølle et al. 2023; Lovinger et al. 2022) Though most GPCRs are found at the cell surface, they can also function in intracellular compartments such as endosomes, endoplasmic reticulum (ER), mitochondria, and the nucleus, adding an extra degree of compartmentalization to the cAMP signal.(Irannejad et al. 2013; Köchl et al. 2002; Wang et al. 2016; Suofu et al. 2017; Buu, Hui, and Falardeau 1993)

GPCR activation leads to its association with a G protein, a trimeric αβγ complex, where the α subunit can either trigger ($G_{\alpha s}$) or supress ($G_{\alpha i}$) adenylyl cyclase(AC) activity, resulting in increased or reduced cAMP synthesis, respectively.(Rodbell et al. 1971) Multiple variants of heterotrimeric proteins also exist. $G\alpha_{olf}$ activates ACs in the olfactory neuron epithelium. G_{t1} and G_{t2}, transducins, stimulated by light-activated rhodopsins, increase cGMP-specific phosphodiesterase activity in retinal rods and cones respectively. Finally, a third example of heterotrimeric proteins, the G_q family, activate Phospholipase C-β (PLC) and downstream inositol 1,4,5-triphosphate [Ins(1,4,5)P3] (IP3) and diacylglycerol (DAG).(Hepler and Gilman 1992; Ross and Wilkie 2000; Wettschureck and Offermanns 2005)

The broad functions of GPCRs makes these receptors particularly interesting for drug discovery research. The encompassing GPCR families are labelled “class A” rhodopsins, “class B” secretins and adhesions, “class C” glutamates, and “class F” frizzled. Their classification dependent on their amino acid sequences. Of these, approximately 350 are non-olfactory receptors considered as potential drug targets, with 165 already valid for a range of therapeutics relevant to the nervous, cardiovascular, respiratory, and gastrointestinal systems.(Hauser et al. 2017; Shimada et al. 2019)

GPCRs themselves are made up of an extracellular amino-terminal domain, seven transmembrane spanning α-helices, which are connected by three intracellular and three extracellular loop regions, and an intracellular carboxyl tail.(Katritch, Cherezov, and Stevens 2013; Zhang, Zhao, and Wu 2015) (Weis and Kobilka 2018b). The amino terminus, along with the extracellular loops of GPCRs control ligand access, while the α-helices can display

different tilts and rotations, depending on the GPCRs. These helices form binding pockets for various ligands. When the ligand binds, the transmembrane helices are rearranged, resulting in the opening of the helical bundle into the cytosolic side of the membrane, where it allows for G-protein coupling and subsequent activation. To regulate its activity, the C-terminus of the GPCR usually has serine or threonine residues that can be phosphorylated to increase affinity of β-arrestin binding, which, in a canonical pathway, quenches receptor signal by blocking G protein interaction, acts as a scaffold for Phosphodiesterases (PDEs), and which also promotes receptor internalisation.(Weis and Kobilka 2018a; Peterson and Luttrell 2017) Internalised receptors in stable complex with β-arrestin, however, can also still signal from endosomes. For example, β-arrestin can activate mitogen-activated protein kinases (MAPK), which helps drive cellular proliferation in ADPKD.(Sussman et al. 2020) In addition to orthosteric ligands, GPCRs have allosteric binding sites for endogenous modulators to control their activity.(Hilger, Masureel, and Kobilka 2018) In the absence of a ligand, most GPCRs still display a level of basal signalling activity.(Weis and Kobilka 2018a) Of interest, the carboxy terminal tail of PC1 was shown to bind some Gα proteins in a Xenopus model. It is hypothesized PC1-bound Gα, sequesters free $G_{\beta\gamma}$, thus reducing the pool of $G_{\beta\gamma}$ available to interact with GPCR-bound G_{α}. Upregulation of $GPCR_{\alpha}$, due to loss of PC1, is thought to explain why PKD1 mutation leads to a more severe phenotype than PKD2-derived ADPKD. (Zhang, Tran, and Wessely 2018)

Due to their receptivity to a variety of endogenous ligands, it is no surprise GPCRs are implicated in an array of diseases from type 2 diabetes, obesity, depression, Alzheimer's, and cancer.(Sriram and Insel 2018) Of note, various GPCRs are suspected or known to drive cyst formation in Polycystic Kidney Disease (PKD).

For example, the first drug approved for the treatment of ADPKD, Tolvaptan, antagonizes one of these GPCRs, V2 receptor (V2R). In human ADPKD cells, stimulation of vasopressin receptors using arginine vasopressin (AVP) increases intracellular cAMP, ERK kinase activity,

cell proliferation, and Cl^- secretion.(Reif et al. 2011) Vasopressin acts on V2, a $G_{\alpha s}$-coupled GPCR which works via Adenylyl Cyclase 6 (AC) to synthesizes cAMP. In healthy kidneys the main function of V2R is the transfer of water, salt, and urea, through modification of the aquaporin 2 (AQP2) and epithelial Na^+ channels, the urea transports, and through regulation of vasodilation and stimulation of coagulation factors.(Juul et al. 2014; Yasuda and Jeffries 1998) In disease context, however, levels of circulating vasopressin are higher, triggering an increase in cAMP signalling (Zittema et al. 2012). It is hypothesized that the cAMP effector protein, protein kinase A (PKA), phosphorylates the Aquaporin 2 channel (AQP2), translocating it to the cell membrane where it plays a role in fluid secretion into the lumen of renal cysts.(Katsura et al. 1997) In ADPKD cells, Tolvaptan inhibits AVP-stimulated cAMP production in a concentration-dependent manner, mitigating ERK signalling and reducing cell proliferation and also Cl^- secretion. (Reif et al. 2011)

Other $G_{\alpha s}$-coupled GPCR which play prominent roles in renal cystogenesis are the EP2 and EP4 receptors which bind Prostaglandin (PGE). Microsomal PGE synthase 1 (mPGES-1), the enzyme which synthesizes PGE2, is highly expressed in renal collecting ducts, with heightened expression of mPGES1 observed in polycystic kidneys. Consequently, PGE2 is measured to greater concentrations in renal cyst fluid.(Sankaran et al. 2007; Yamaguchi et al. 2014) In vitro, PGE2 can drive cystogenesis of PKD and inner medullary collecting duct (IMCD3) cells in a 3D matrigel/collagen mix by orchestrating excessive cell proliferation and fluid secretion.(Belibi et al. 2004; Elberg et al. 2007; Liu et al. 2012)

Alternatively, the Calcium sensing receptor (CaSR) is $G_{\alpha q/11}$ and $G_{\alpha i/o}$ coupled.(Nagano 2006; Brown 2007) Divalent cations such as Ca^{2+} bind the extracellular domain of this GPCR in kidneys to elicit phosphate reabsorption in the proximal tubule and to decrease sodium chloride and calcium reabsorption in the thick ascending limb of Henle. Activation of CaSR, in healthy renal cells, also leads to the release of renin in the macula densa as well as enhanced AQP2 degradation in the inner medullary collecting duct.(Riccardi et al. 1998) In

ADPKD, disrupted calcium signalling leads to increased AC activity and subsequent upregulation of cAMP signalling.(Calvet 2015) Thus, stimulation of CaSR could relieve PKD by decreasing cAMP levels. Indeed, the calcimimetic R568 ameliorated early stage, but not late stage, PKD in Han:SPRD cy/+ rats, a preclinical model of PKD arising from a mutation in Samcystin, a protein seemingly implicated in cystogenesis.(Nagao et al. 2010)

V2R, EP2 and EP4, and CaSR are just four examples of GPCRs implicated in ADPKD. Yet, other GPCRs such as secretin, somatostatin, TGR5, adenosine, purinergic, dopaminergic, adrenergic, and endothelin receptors have all been entertained in the regulation of ADPKD, due to their association with G-proteins which either propel or attenuate the synthesis of cAMP.(Sussman et al. 2020)

Adenylyl Cyclases

Downstream of GPCR activation, cAMP is synthesized from ATP by adenylyl cyclases (ACs). Mammalian cells express nine different membrane-integral AC isoforms (AC1-9) and one soluble isoform, AC10, that is not activated by $G_{\alpha s}$ but by bicarbonate.(Dessauer et al. 2017; Wiggins et al. 2018) ACs can be inhibited or activated by messengers. For example, Calcium/calmodulin stimulate AC1 and AC8 while Ca^{2+} inhibits AC5 and AC6. AC6 is repressed by PKC and AC3 by CaMKII.(Bassler, Schultz, and Lupas 2018; Dessauer et al. 2017) Membrane-bound ACs have an intracellular N-terminus and two transmembrane domains bridged by the intracellu(Rees et al. 2014)lar C1a and C1b regions and the C2a and C2b regions of the C-terminus. When C1a and C2a associate, they form the catalytic domain.(Halls and Cooper 2017) This interface has two ligand-binding sites- the catalytic and a diterpene site. Forskolin is a diterpene which broadly activates membrane-ACs and is often used in cAMP studies as a non-selective AC activator.(Agarwal and Parks 1983) To generate cAMP, AC's create a cyclic phosphodiester bond at the α-phosphate group of ATP, with pyrophosphate as a byproduct. Byproduct release is the energy-producing and rate limiting step in this reaction.(Halls and Cooper 2017)

All nine membrane-ACs are expressed in ADPKD cells, with AC1,3, AC5, and AC6 localising to the collecting ducts and other kidney tubules. (Pinto et al. 2012) Of note, AC5/6 mRNA is increased in cyst tissue, while AC1,3, and 8 are decreased. AC5/6 protein expression mirrors this upregulation, with AC3 protein decreased in ADPKD.(Pinto et al. 2012) Since AC's synthesize cAMP, it is likely ACs also play a role in ADPKD cyst growth. Indeed, PKD cyst fluid contains an endogenous Forskolin-like molecule which may propagate cystogenesis.(Putnam et al. 2007) Additionally, AC3,5, and 6 produce cAMP in response to Vasopressin.(Strait et al. 2010) and collecting duct-specific KO of AC6 in mice leads to urine concentration defects.(Roos et al. 2012) In contrast, one study shows blunted cAMP upsurge in ADPKD, compared to non-disease cells, upon vasopressin stimulation, with any response mediated by AC3.(Pinto et al. 2012) The authors of the latter study suggest this discrepancy could be due to decreased Ca^{2+}, a consequence of excess cAMP produced from V2R over-stimulation. Reduced Ca^{2+} in ADPKD cells may have switched V2R coupling from Ca^{2+} inhibited AC5/6 to Ca^{2+}/Calmodulin enhanced AC3.(Pinto et al. 2012)

Further, in vivo studies demonstrate the contribution of AC isoforms in ADPKD. KO of both PC1 and AC6 in collecting ducts of mice show significant reduction in kidney and cyst volume, ameliorate renal function, and decrease B-RAF/ERK/MEK signalling compared to PC1 KO alone.(Rees et al. 2014) A different study demonstrates knock down (KD) of AC5 and AC6 using siRNA stunts cAMP production in PC2-ablated renal epithelial cells of the collecting ducts. Further, these mice have enhanced cAMP and AC5 mRNA levels. (Wang et al. 2018a) The role of ACs in cyst progression is clear, and several types of inhibitors exist for ACs. However, due to the fact that both the catalytic and diterpene sites are highly conserved among ACs, creating isoform specific antagonists of ACs is challenging.(Dessauer et al. 2017; Halls and Cooper 2017; Zhang et al. 2018) The next section discusses how ACs are often associated to certain A-kinase Anchoring Proteins (AKAPs), and several of these AKAPs are thought to propagate ADPKD.

A-Kinase Anchoring Proteins

AKAPs are a class of proteins that contributes to compartmentalise the cAMP signal by docking PKA to specific cellular locations, alongside proteins that are phosphorylated by PKA. Thus, when the AKAP-tethered PKA is activated by cAMP, it readily phosphorylates the nearby target. AKAPs also bind other molecules, orchestrating signalling platforms (signalosomes) where cAMP messaging can be locally initiated (e.g. via AKAP association with GPCR or ACs), conveyed (via tethered PKA or EPAC) and controlled (through interactions of AKAPs with PDEs, PPs, or other kinases). (Colledge and Scott 1999; Wong and Scott 2004) Several AKAPs have been linked to ADPKD. AKAP150 (also known as AKAP79) has been shown to form a complex, in the primary cilium, with AC5/6 , PKA, as well as PDE4C and PC1/PC2. (Choi et al. 2011b) In ADPKD, a reduction in ciliary Ca^{2+}, due to loss of the Polycystins, triggers AC5/6, enhancing intracellular cAMP and promoting cystogenesis.(Rees et al. 2014; Spirli et al. 2017; Wang et al. 2018b) One hypothesis is V2R couples with the PDE4C/AKAP150/PKA signalosome and AC5/6, to generate a local cAMP pool functioning in a feedback loop with Polycystin-coordinated Ca^{2+} , with the cAMP, in turn controlled by PDE4C function (**Schematic 5).** Measuring cAMP at AKAP150 using Fluorescence resonance energy transfer (FRET) microscopy, could confirm this hypothesis.

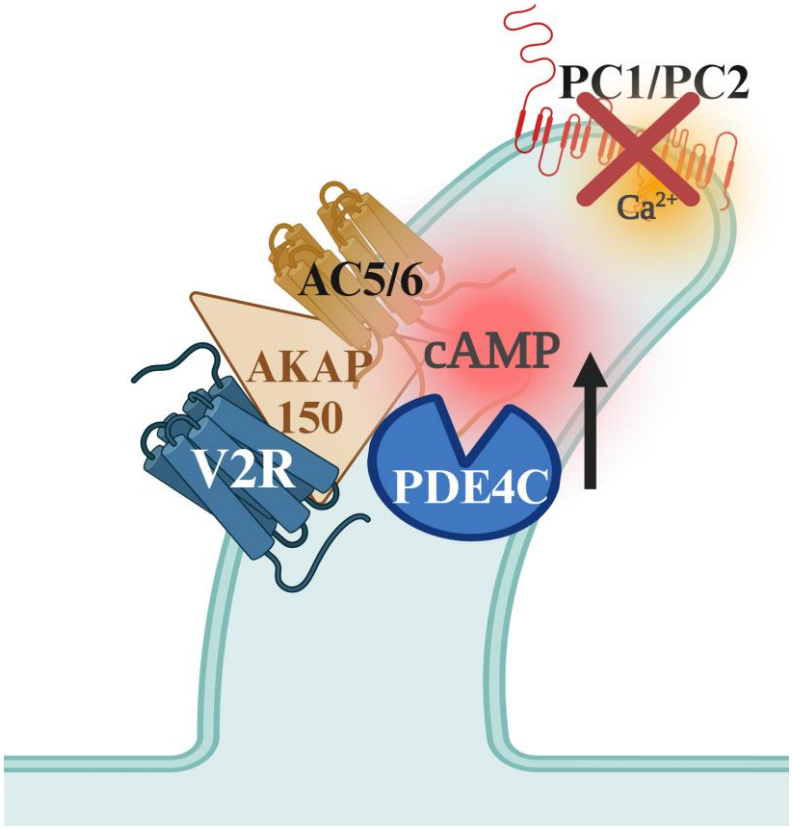

Schematic 5: Depiction of a possible cAMP signalosome at the primary cilium, anchored by AKAP150. With loss of Polycystin function in ADPKD, Ca^{2+} is decreased. AC5/6, which are normally inhibited by Ca^{2}, are now upregulated, and excess cAMP is subsequently synthesized. V2R signalling further enhances cAMP in the organelle, driving cystogenesis. PDE4C regulates this pool of cAMP, but in ADPKD, enzyme function may not be enough to control excess second messenger signalling.

Another AKAP that may function in ADPKD is thought to be the orphan receptor, Gpr161, which localises to the cilium.(Mukhopadhyay et al. 2013) Constitutive GPR161 activity enhances ciliary cAMP, altering Gli3 to its repressor state, resulting in suppressed Sonic Hedgehog signalling (SHh). Shh is a prominent, and best characterised, signalling pathway of the cilium. Gli transcription is altered through its phosphorylation by PKA, indeed suggesting, GPR161 regulation of Shh is cAMP-mediated. The reverse is also true, SHh activation results in GPR161 expulsion from the cilium, abolishing receptor signalling (**Schematic 6**).(Huangfu et al. 2003; Haycraft et al. 2005; Ho and Stearns 2021) Research in Zebrafish recently identified GPR161 as a high-affinity AKAP for the PKA regulatory subunit R1.(Bachmann et al. 2016) R1 binds the hydrophobic protein-protein interaction interface of the GPR161

cytoplasmic terminal tail. This complex localises in the plasma membrane, but upon overexpression is also found in the cilium. A L465 mutation in the receptor, which disrupts GPR161-PKA association leads to a significant decrease in ciliary R1α-GFP, hinting GPR161 indeed acts as an AKAP in the cilium. GPR161 has been found to interact with AC3 in primary hippocampal neurons, potentially constituting a cAMP signalosome.(Pal et al. 2016)

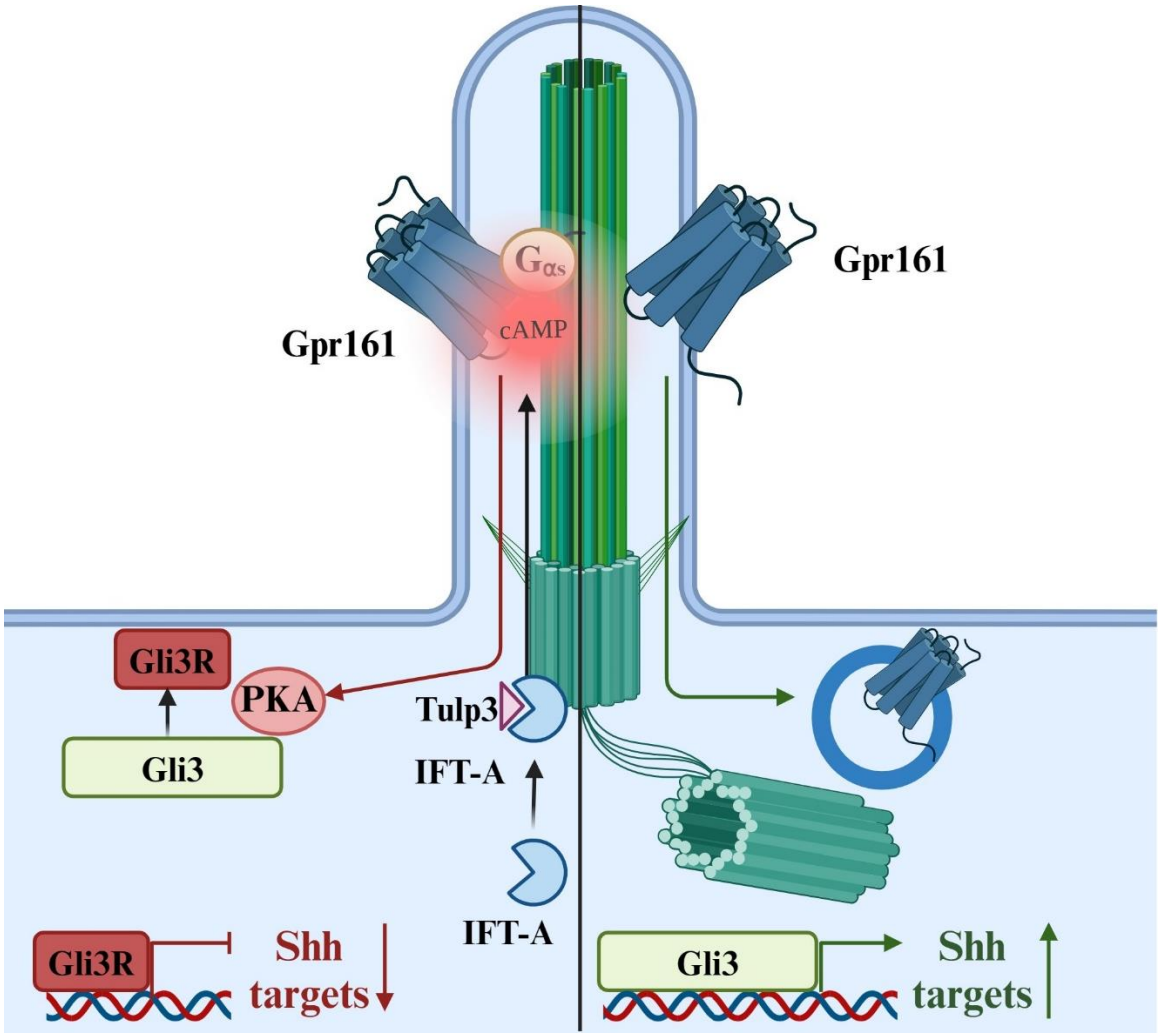

Schematic 6: GPR161 transport to the cilium is regulated by tubby family protein (Tulp3) and intraflagellar transport A (IFT-A). GPR161 signalling enhances ciliary cAMP, which activates PKA. PKA phosphorylation of Gli transforms the transcription factor into its repressor form, supressing Sonic hedgehog signalling (Shh). GPR161 removal from the cilium through endosomal internalisation leads to Shh transcription.

Though there is evidence for AKAP-bridged signalosomes in the cilium, less is known about cytosolic AKAPs that may play a role in ADPKD. While ciliary cAMP was shown to drive cystogenesis, evidence suggests cytosolic cAMP may help suppress cyst growth. (Hansen,

Kaiser, Leyendecker, Stüven, Krause, Derakhshandeh, Irfan, Sroka, Preval, and Desai 2022) Disruption of specific AKAPs within the cell could be a therapeutic strategy for PKD. For example, the AKAP, ezrin, is essential for PKA-mediated Cystic Fibrosis transmembrane receptor (CFTR) function.(Sun et al. 2000) Obstructing this interaction could stop Cl^- and subsequent fluid secretion into the cystic lumen. However, as AKAPs control effector localisation, tampering with this system could lead to PKA activity elsewhere in the cell, causing collateral responses.

Protein Kinase A and other cAMP Effectors

The main function of AKAPs is to harness the cAMP message to the right effector proteins. These proteins include: protein kinase A (PKA)(Walsh, Perkins, and Krebs 1968; Taylor et al. 2008) the exchange protein directly activated by cAMP (EPAC)(de Rooij et al. 1998), cyclic nucleotide-gated ion channels(Fesenko, Kolesnikov, and Lyubarsky 1985), and Popeye domain containing proteins (POPDC)(Brand 2005). PKA, the most thoroughly researched cAMP effector, is a heterotetramer in its inactive state, an association of a regulatory (R) dimer and two catalytic (C) subunits(Walsh, Perkins, and Krebs 1968; Corbin and Keely 1977; Taylor et al. 1993). Combinations of four R subunits (RIα, RIβ, RIIα, and RIIβ) and three C subunits (Cα, Cβ, and CϒΥ) can comprise the inactive PKA holoenzyme R2C2.(Diskar et al. 2010) cAMP binding to the R subunits, creates a conformational change, extricating the two c subunits from the inhibitory effect of R.(Kim et al. 2007; Taylor et al. 2013). Traditionally, it was thought cAMP binding to PKA led to dissociation of the C subunits to phosphorylate protein targets randomly in the cell. However, this would undermine strict compartmentalisation of the cAMP signal. The current model of PKA-dependent signalling suggests that binding of cAMP does not fully dissociate the C subunit from R, but instead triggers a conformational change, exposing a catalytic pocket in C which can then phosphorylate proteins in a 15-25nm radius.(Smith et al. 2017) Alternatively, excess of R subunits, not coupled to C subunits, may allow for the C subunit released on activation of

PKA to quickly bind a free R subunits nearby, thus resulting in C compartmentalisation.(Walker-Gray, Stengel, and Gold 2017)

PKA not only regulates CFTR function, but also works to control cilia length (Abdul-Majeed, Moloney, and Nauli 2012; Kim, Krishnaswami, and Gleeson 2008; Porpora et al. 2018), SHh transcription (Tuson, He, and Anderson 2011), and V2R-dependent Aquaporin 2 (AQP2) activity in regards to cystogenesis.(Raychowdhury et al. 2009) R1α is also specifically increased in mouse models of PKD. Indeed, PKA-1 downregulation in a kidney-specific dominant-negative R1αB allele in $PKD1^{RC/RC}$ mice, mIMCD3 3D cultures, or PKD1 mutant metanephric organ cultures, show PKA-1 inhibition abolished P-Ser133 cAMP Response Element Binding (CREB) expression and cystogenesis. PKA-1 activation achieves the opposite outcome. EPAC stimulation or PKA-II inhibition, in comparison, does not significantly affect cyst growth. (Wang et al. 2022; Ye et al. 2017) Another study showed PKA can also regulate cystogenesis through a different transcription factor, positive transcription factor b (P-TEFb) (Sun et al. 2019), suggesting PKA-1 is the central cAMP effector of cystogenesis.

Another effector of cAMP, EPAC, also functions in the kidneys. Expression of EPAC1 and EPAC2 is abundant in the renal epithelium, where it is believed the two effectors regulate water and electrolyte transport, specifically in the proximal tubule and collecting ducts. Mice lacking EPAC1 or EPAC2 show urinary concentration as well as Na^+ and urea excretion defects.(Tomilin and Pochynyuk 2019) In disease context, both PKA and EPAC have been implicated in hepatic cystogenesis in PCK rats, an animal model of Autosomal recessive polycystic kidney disease (ARPKD). cAMP also drives cystogenesis in the liver of these models, and second messenger inhibition supresses cyst growth. In the same study, healthy rat cholangiocytes express mRNA of EPAC1, EPAC2, and all PKA regulatory subunits, but in the diseased cell counterparts, both mRNA of EPAC isoforms and PKA- R1β are overexpressed. Activation of both effectors aggravate cystogenesis.(Banales et al. 2009) Despite regulating

hepatic cyst formation, little is known about EPAC involvement in renal cystogenesis. However, based on its expression in the kidneys, and its involvement in propagating the cAMP signal, it is highly possible this effector also contributes to cystogenesis in ADPKD.

Marking PKA, or other cAMP effectors, as a therapeutic treatment for ADPKD would no doubt cause collateral effects in cAMP signalosomes which do not contribute to cyst formation. However, elucidating phosphorylation targets of PKA which contribute to cystogenesis, would provide clues into the mechanisms of action in ADPKD. Therefore, while one would not target PKA directly, as a therapeutic strategy, one could control its phosphorylation activity through other compartmentalisation mechanisms that exist downstream of cAMP to combat this disease.

CREB and other transcription factors

Aside from immediate changes in cellular function upon cAMP upregulation, the second messenger can also have long-lasting affects via regulation of transcription. As mentioned above, two targets of PKA are P-TEFb and CREB transcription factors. In the context of ADPKD, cAMP also determines SHh transcription by regulating forms of Gli. SHh transcription is vital for ciliary function. In terms of cystogenesis, upon cAMP increase, P-TEFb, along with CREB-regulated transcription coactivator 2 (CRTC2) can translocate to the nucleus where it forms phase-separated condensates to disrupt the inhibitory 7SK snRNP complex. This upregulation of P-TEFb transcription due to elevated cAMP promotes cystogenesis in cystic epithelial cells of both mouse and human kidneys.(Mi et al. 2022)

In developing kidneys, CREB transcription shapes the ascending limb of Henle and the collecting ducts by marking nephron progenitor (NP) cells, later disappearing in differentiated and mature NP-derived proximal tubules. With upregulation of cAMP, using 8-Br-cAMP

analog, in a murine model of renal cystogenesis, ectopic p-CREB staining is observed in cystic segments of the proximal tubule which also stain positive for undifferentiated cells marker, lotus tratragonolobus lectin. Together, these findings suggest CREB transcription in mature kidneys reverts cells to an undifferentiated state which promotes cystogenesis.(Puri et al. 2018) Further studies have also implicated CREB transcription in PKD, demonstrating a positive feedback loop propagated via the serine/threonine kinase, Glycogen synthase kinase 3β (GSK3β). Vasopressin stimulation elevates cAMP, and thus the cAMP-responsive gene GSK3β. In turn, GSK3β promoter can bind CREB to propel its transcription. This feedback loop correlates with progression of cystogenesis in PKD mouse models.(Kakade et al. 2016b)

Phosphatases

Circling back to protein function, phosphatases undo PKA phosphorylation of target proteins, quenching a cAMP signal. Only recently have phosphatases been shown to contribute to cAMP signalling compartmentalisation. (Burdyga et al. 2018; Haj Slimane et al. 2014) In one study, PKA phosphorylation of PC2 at Ser829 localises PC2 to the ER. PC1 binding of PC2 greatly reduces PKA-mediated phosphorylation of Ser839 by recruiting protein phosphatase 1α to the polycystin complex.(Watnick and Germino 2013) While research on phosphatase involvement in ADPKD is still limited, identifying AKAPs and cAMP effectors contributing to cystogenesis may also reveal the phosphatases that regulate relevant messenger signals. Though phosphatases help control the impact of PKA phosphorylation on downstream targets, it is arguable that prevention of PKA phosphorylation of specific proteins would be even more effective than undoing an already-initiated signal. Thus, phosphodiesterases may prove the most effective therapeutic targets to battle excessive and compartmentalised cAMP driving ADPKD.

Phosphodiesterases (PDEs) and their role in normal and diseased renal function

Thus far, the components, which contribute to compartmentalise the cAMP signal, from GPCRs to phosphatases have also demonstrated roles in ADPKD disease progression. However, it was concluded aiming therapies at these specific levels of the cAMP cascade would ultimately cause collateral symptoms, as the higher up in the pyramid one targets, the greater the umbrella effect. However, in the last step of second messenger compartmentalisation- the cAMP signal is finally terminated at subcellular locations by Phosphodiesterases (PDEs).

cAMP is hydrolysed by PDEs, a super-family of enzymes encompassing 11 families (PDE1-11). Among these, PDE4, PDE7, and PDE8 specifically hydrolyse cAMP, while PDE1, PDE2, PDE3, PDE10 and PDE11 hydrolyse both cAMP and cGMP, and PDE5, PDE6 and PDE9 are cGMP specific. Some families of PDEs comprise several genes, with each gene expressing different proteins through alternative spicing, giving way to numerous PDE isoforms. These isoforms demonstrate varying affinities for cAMP and enzyme kinetics and their activity is controlled by diverse mechanisms (e.g. cGMP binding, phosphorylation, or Ca^{2+}-calmodulin binding). Individual isoforms function in specific subcellular sites, generating cAMP gradients, or confining cAMP pools through hydrolysis of the second messenger at different locations.(Jurevicius and Fischmeister 1996; Di Benedetto et al. 2008; Mongillo et al. 2004) Thus, since ADKPD is a disease driven by excess ciliary cAMP signalling, and PDEs function in very precise locations and mechanisms to regulate this second messenger, targeting isoforms of PDEs, which break down distinct pools of cAMP, could prove the most selective therapeutic approach for this ciliopathy. Several PDE isoforms have already been linked to ADPKD, including PDE4, PDE1, and PDE3.

PDE4

Indeed, novel PDE4 activators have been developed which inhibit cyst formation both in animal and human cell models of ADPKD. PDE4 is the largest family of PDEs, constituted by 4 genes (PDE4A, PDE4B, PDE4C, and PDE4D). These four genes are further spliced into alternative mRNA variants which encode long and short isozymes of PDE3 as well as 35 different PDE4 proteins.(Lugnier 2006a) This family of enzymes exclusively hydrolyse cAMP, and are characterised by unique regions of amino acid sequences called upstream conserved region 1 and 2 (UCR1 and UCR2).(Bolger et al. 1993) Long PDE4 forms contain both UCR regions, while short PDE4 isoforms only contain UCR2. Dead-short forms of the enzyme also exist which lack both UCR domains and have a truncated catalytic site, rendering them inactive.(Houslay, Sullivan, and Bolger 1998) The UCR domains are located between the amino terminus and the catalytic region of the enzymes. Linker, LR1, connects UCR1 to UCR2, while LR2 bridges UCR2 to the catalytic domain. UCR1's association with UCR2 regulates phosphorylation of PDE4 by several kinases. Indeed, PKA mediated phosphorylation of UCR1 upregulates PDE4 long-form cAMP-hydrolysing activity, providing a feedback loop for second messenger signalling.(Oki et al. 2000) Novel allosteric activators of PD4 exploit this feedback mechanism in an effort to combat ADPKD. The catalytic site of PDE4 isoforms (excluding PDE4A) is inhibited though phosphorylation by ERK. ERK signalling is upregulated in ADPKD, and thus it is believed enhanced cAMP levels in ADPKD are further aggravated by downregulated PDE4 function.(Omar et al. 2019; Bolger et al. 1993)

PDE4 inhibition with Rolipram has been shown to lead to the greatest intracellular increase in cAMP in ADPKD cells, suggesting it is the main PDE regulating ciliary cAMP and subsequent kidney cystogenesis (Omar et al. 2019) PDE4 also localises at the AKAP150 complex in the cilium (Choi et al. 2011b) and is likely responsible for Cl^- secretion in renal epithelial cells, leading to fluid build-up in cysts.(Pinto et al. 2016) However, PDE4 is not the

only cAMP-hydrolysing PDE functioning in the kidneys and, while the PDE4 activators hold promise in treating PKD, combination therapy which includes multiple PDE isoform targets could prove even more effective. In fact, a recent study has demonstrated that while ciliary cAMP drives cystogenesis, an increase in cytosolic cAMP followed by inhibition of PDEs via IBMX (but not Rolipram) protects from cyst development.(Hansen, Kaiser, Leyendecker, Stüven, Krause, Derakhshandeh, Irfan, Sroka, Preval, and Desai 2022) This finding suggests inhibition of PDE isoforms, other than PDE4, that may be responsible for the regulation of cytosolic pools of cAMP, may increase second messenger signalling in cytosolic nanodomains which help mitigate cystogenesis.

PDE1

Amongst the cAMP-hydrolysing PDEs which could help mitigate renal cystogenesis is PDE1A. Three genes with multiple splice variants per gene make up the PDE1 family. PDE1 isoforms are soluble enzymes which form homodimers. This family of enzymes is Ca^{2+} and calmodulin regulated, with sensitivity to Ca^{2+} and calmodulin dependent on individual isoforms.(Sonnenburg et al. 1995; Hashimoto, Sharma, and Soderling 1989) Additionally, phosphorylation of PDE1A1 and PDE1A2 by PKA, and of PDE1B1 by CaM Kinase II reduce sensitivity to calmodulin. PDE1 is a dual-hydrolyser of both cAMP and cGMP, but markedly prefers the latter as a substate.(Sonnenburg et al. 1995)

Mutations in PDE1A lead to renal cystogenesis in zebrafish (Matousovic et al. 1997b) and it is also hypothesized that loss of Ca^{2+} signalling due to changes in polycystin function leads to a lower degree of PDE1A activity, since this enzyme is positively regulated by Ca^{2+}-calmodulin. Like PDE4, PDE1 has been shown to bind AKAP150 in the cilium along with B-RAF, an upstream component of the B-RAF/MEK/ERK signalling pathway. Additionally, PDE1 and PDE4 are the main enzyme families expressed in collecting ducts.(Wallace 2011) PDE1 is up-regulated via vasopressin-induction, and possibly contributes to excessive cell proliferation seen in ADPKD.(Matousovic et al. 1997b) Unfortunately, at the time of this

project, selective PDE1 inhibitors were not commercially available, and thus the role of this dual-hydrolyser of cyclic nucleotides was not explored in this thesis.

PDE3

PDE3 expression levels are also downregulated in cystic kidneys. PDE3 targets to the endoplasmic reticulum (ER) and is inhibited by cGMP (which is also degraded by PDE1).(Shakur et al. 2000) PDE3 enzymes are transcribed from two genes, PDE3A and PDE3B.(Meacci et al. 1992; Miki et al. 1996) The PDE3A subfamily is further divided into three variants which arise from alternative transcription start sequences in the same gene as well as distinct starting sites in mRNA. The resulting amino acid sequences only differ in respect to the length of their N-termini. Thus, PDE3A1 is 996 amino acids long (MW 109,980) and is characterised by an N-terminus which can be phosphorylated by several kinases to modulate protein-protein interaction, including PKA at Ser302(Han et al. 2006; Pozuelo Rubio et al. 2005; Hunter, MacKintosh, and Hers 2009; Rahn et al. 1996). The PDE3A1 N-terminus also contains four hydrophobic loops which localise the enzyme to intracellular domains.(Shakur et al. 2000; Han et al. 2006) In contrast, PDE3A2 is 842 amino acids (MW 93,600) as it lacks the majority of the N-terminus phosphorylation sites and the transmembrane loops.(Hambleton et al. 2005) The shortest isoform, PDE3A3 is made up of 659 amino acids (MW 73,720) and has no hydrophobic loops and is also lacking upstream phosphorylation sites. Apart from the distinct N-termini, the three PDE3A enzymes share an identical basal catalytic activity, with indistinguishable sensitivity to catalytic site inhibitors.(Hambleton et al. 2005) Alternatively, the only known PDE3B isoform is 1112 amino acids long (MW 124,333) made up of an N-terminus encompassing six hydrophobic loops, phosphorylation sites, and a C-terminus containing the catalytic domain.(Leroy et al. 1996; Taira et al. 1993) The PDE3B sequence for the catalytic regions is 80% identical to that of PDE3A, with similar sensitivity as PDE3A, to catalytic site inhibitors.(Miki et al. 1996)

PDE3 had been linked to Cl^- secretion in shark rectal glands,(De Jonge, Tilly, Hogema, Pfau, Kelley, Kelley, Melita, Morris, Viola, and Forrest Jr 2014) and pig trachea submucosal glands.(Penmatsa et al. 2010) In ADPKD models, Pkd2($^{-/WS25}$) mice with PDE3A KO exhibit aggravated ADPKD and lead to an increase in CREB phosphorylation by PKA, though only a small percentage of cAMP is reported to be hydrolysed by PDE3 in the kidneys.(Ye et al. 2016) In another study PDE4 and PDE3 were shown to hydrolyse bulk cAMP in MDCK cells (85% and 15% respectively), but only PDE3 inhibition stimulates mitogenesis through BRAF activation, increasing ERK signalling and cyclin D and E_1 function.(Cheng et al. 2006) In yet a further investigation carried out in principle-collecting duct cells, mpkCCD_{c14}, PDE3, like PDE4, inhibition, increases NAPDH oxidase 4 (NOX4). NOX4 is thought to contribute to V2R-cAMP-PKA signalling, with enhanced activity of the oxidase resulting in greater expression of AQP2.(Feraille et al. 2014) To contrast, cells of renal cortical tubules, stimulated with Folic Acid, to induce proliferation, and treated with PDE3 inhibitor, demonstrate reduced cell growth, measured via decreased expression of proliferating cell nuclear antigen (PCNA).(Matousovic et al. 1997a) This latter study implies PDE3 pharmacological inhibition should aggravate cystogenesis. Yet, in cells isolated from human APDKD tissue, a further study found PDE3 inhibition induces ADPKD cell proliferation, but noticeably decreases proliferation of cells derived from healthy human tissue,(Pinto et al. 2016) Taken together, it is unclear whether PDE3 would ameliorate or aggravate cyst formation in vivo, and thus we sought to test PDE3 inhibition on in vitro assays of cystogenesis.

PDE2

A single gene encodes for three PDE2A family members of similar size (~106KDa), which localise to different subcellular domains. PDE2A1 degrades cAMP at the cytoplasm, PDE2A2 at the mitochondria and PDE2A3 at the plasmalemma.(Lobo et al. 2020a) All three variants of PDE2 share the same c-terminal sequence but have distinct N-termini which dictate enzyme

location to the respective subcellular domains. PDE2A preferentially hydrolyses cGMP, but can also hydrolyse cAMP.(Erneux et al. 1981) In fact, allosteric binding of cGMP to PDE2, increases enzyme hydrolysis of cAMP six-fold.(Martins, Mumby, and Beavo 1982; Wu et al. 2004) To achieve PDE2 activation, cGMP stoichiometrically binds one of two N-terminus domains, GAF-B. GAF-A is the other domain localising at the N-terminus, and is important for dimerization of PDE2. PDE2 can also be phosphorylated by PKC for post-translation upregulation, but can additionally be regulated at transcriptional level during pathophysiological changes. (Lugnier 2006b)

PDE2A expression has been observed in cilia of olfactory neurons, and is believed to work through cGMP signalling in this model, although localization to the primary cilium has not been reported otherwise (Juilfs et al. 1997). Apart from its localisation in olfactory cilia, PDE2A's role in renal cystogenesis is worth exploring for several reasons. Firstly, PDE2A has been linked to heterotaxy and Congenital Heart Disease (CHD), along with several ciliopathy proteins including PKD1 and CEP290.(Assenza et al. 2018; Li et al. 2015; Chaudhry and Henderson 2019; Burkhalter et al. 2019) Secondly, studies from our laboratory show PDE2A interacts with several ciliary proteins including Polycystin 2, which is mutated in ADPKD, and KIF13b, a kinesin motor protein known to affect ciliary signalling.(Schou et al. 2017a; Lobo et al. 2020b) It is possible that PDE2 may affect renal cyst growth through a process which directly alters ciliary phenotype, independently to modulation of bulk cAMP hydrolysis. It is also possible PDE2 may function to hydrolyse cAMP, and thus its inhibition would lead to increased cystogenesis.

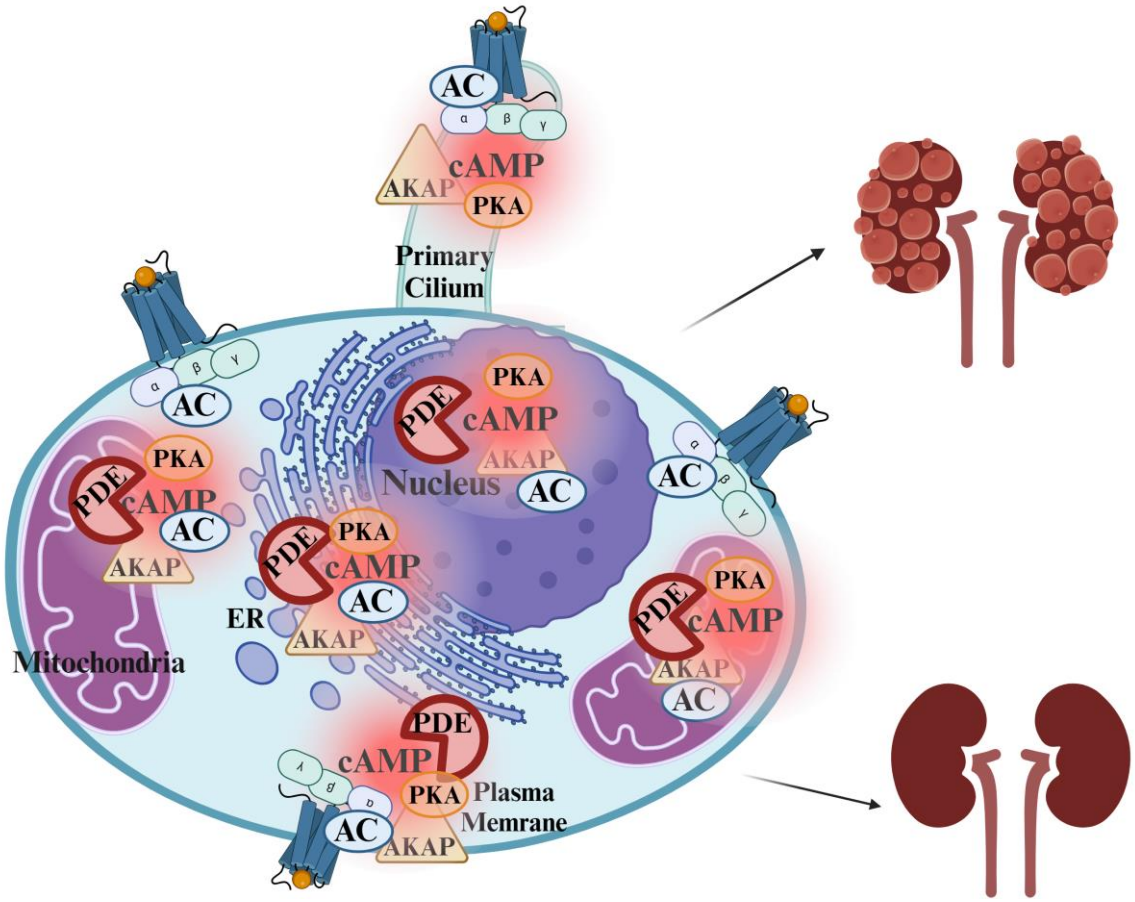

Schematic 7: Model of cAMP compartmentalisation depicting different pools of second messenger in distinct intracellular domains. Within each domain, are depicted some of the components which help compartmentalise the cAMP signal. It is believed that different pools of cAMP, located at specific subcellular domains either aggravate or mitigate cystogenesis in ADPKD.

It is known that both PDE1 and PDE4 are present at the cilium and contribute to excessive cell proliferation and fluid secretion observed in ADPKD. However, crosstalk of PDEs and the relationship between ciliary PDEs and PDEs at other subcellular domains (e.g PDE3 at the ER or PDE2A at the mitochondria) and its impact on cell proliferation or fluid secretion, has not been explored. This thesis endeavours to characterise the role of these enzyme isoforms, in both their effect on ciliary, as well as cytosolic second messenger signalling, and how this translates to altered renal cystogenesis in vitro.

Chapter 2: Rationale and aims of the project

In chapter 1, we have described in detail, how GPCR and cAMP signalling intercalates with other ciliary and intracellular pathways to bring about renal cystogenesis in ADPKD. Evidence suggests that a specific pool of cAMP at the cilium induces cystogenesis, but cytosolic cAMP subdomains may contribute to or mitigate cyst growth.(Hansen, Kaiser, Leyendecker, Stüven, Krause, Derakhshandeh, Irfan, Sroka, Preval, and Desai 2022) Identifying and characterising cAMP nanodomains involved in cyst formation would help pinpoint which pools of cAMP could be targeted as selective therapeutic approaches for ADPKD. One of the most effective ways cAMP is regulated is through its breakdown by PDEs. PDEs exist in a variety of isoforms with distinct affinities for cAMP hydrolysis, and which localise to highly specific cAMP nanodomains within the cell. Revealing which PDEs work to regulate specific pools of cAMP responsible for cystogenesis could be an effective, and free of side-effect, treatment of ADPKD, as the multitude of PDE isoforms available and the varied subcellular localisations they inhabit, would allow for highly selective manipulation of their function. Thus, characterising the role of lesser explored PDEs, which may contribute to renal cystogenesis, is the broad scope of this research project. To achieve this aim, several objectives are in place:

1. Engineer a FRET-reporter localising to the cilium, which can measure cAMP changes in the organelle, to assess the effects of selective PDE inhibition. Use this FRET reporter to identify which PDE isoforms regulate ciliary cAMP, the main pool of cAMP thought to drive renal cyst growth.
2. Set up cyst assays using Inner Medullary Collecting Duct ((IMCD3) cells, which model renal cystogenesis in vitro. Use these assays to test whether isoform-specific inhibition of PDEs alters cyst growth.

3. If a PDE isoform, upon inhibition, alters cyst growth, or more importantly, mitigates in vitro cystogenesis, explore where this PDE may function in the cell to decrease cyst formation, using localised FRET reporters for cAMP.
4. Define the effects of PDE inhibition on cell function.
5. Demonstrate how altered cAMP signalling and PDE activity, at this domain, could be relevant to renal cyst formation.

Chapter 3: Materials and Methods

Cell Culture

Inner medullary Collecting Duct cells (IMCD3 cells) were grown in 50% F12 and 50% DMEM medium, with 10% FBS, 1% pen-strep and 1% L-glutamine (**Table 1**). Cells were washed 4 times with PBS, trypsinised, and centrifuged to remove excess trypsin. Centrifuges settings for live cells was 1000rpm/4minutes/RT. The pellet was resuspended in 12ml of medium.

In preparation for FRET microscopy using the cilia reporter, Arl13b-H187, cells were starved (0.1% FBS and no added L-glutamine) to induce ciliogenesis for 48 hours before imaging. For experiments using the control H187 sensor and other non-ciliary sensors, cells were not starved, and FRET imagining was carried out 24hrs after cells were plated, unless stated otherwise.

Materials	**Source**
DMEM	*Gibco*
F12 nutrient mixture	*Gibco*
Foetal Bovine Serum	*Gibco*
Pen-strep	*Sigma*
L-glutamine	*Gibco*
PBS (1X)	*Gibco*
Trypsin 0.05%	*Gibco*
Table 1: Materials for cell culture of IMCD3 cells.	

Chemical Compounds

Compound	Source	Concentration
Bay60	*Cayman Chemical Company*	1nM, 3nM,10nM, 30nM, 100nM,300nM,1µM
Cilostamide	*Cayman Chemical Company*	1µM , 3µM, 10µM, 30µM
Rolipram	*Cayman Chemical Company*	1µM , 3µM, 10µM, 30µM
Forskolin	*Cayman Chemical Company*	25µM or (1µM as initial stimulus)
IBMX	*Sigma*	100µM
Prostaglandin 2 (PGE2)	*Sigma*	100nM
Bay41	*Cayman Chemical Company*	1mM, 5mM
Tunicamycin	*Sigma*	0.5µg/ml (0.6nM)
Rapamycin	*Sigma*	100nM
Rapalog	*Takara*	0.5µM
DMSO	Sigma 472301-1L	0.1%

Table 2: Concentrations of drugs and reagents used for experiments. Highlighted concentrations are the concentrations used for all FRET experiments and for ER-mitochondrial contact experiments.

Plasmids and Virus

Transfection of plasmids was carried out using *Polyplus jetPRIME* reagents and protocol. A list of all FRET sensors (**Table 3**), plasmids (**Table 3**), and viruses (**Table 4**) used are below.

Construct	Amount	Source
H187	0.5µg per six well	gift from Jaleenk lab
Arl13B-H187	0.5µg per six well	cloned
OMM-EPAC	0.5µg per six well	available in lab
ER-Cyto-H90	0.5µg per six well	available in lab
AKAP79	0.5µg per six well	available in lab
FEMP	0.5µg per six well	*Addgene*
OMM_{1-10} (SPLICS)	0.25µg per 24 well	*Addgene*
ER_s (SPLICS)	0.25µg per 24 well	*Addgene*
mcherry (plasmid)	5 µg per 100mm plate	available in lab
PDE2A1-RFP (plasmid)	2.5µg per 100mm plate	available in lab
PDE2A2-RFP (plasmid)	2.5µg per 100mm plate	available in lab
PDE2A3-RFP (plasmid)	2.5µg per 100mm plate	available in lab
PDE2A1-Flag (plasmid)	2.5µg per 100mm plate	available in lab
PDE2A2-Flag (plasmid)	2.5µg per 100mm plate	available in lab
PDE2A3-Flag (plasmid)	2.5µg per 100mm plate	available in lab
GFP (plasmid)	7.5 µg per 100mm plate	available in lab
PDE2A1-GFP (plsmid)	2.5µg per 100mm plate	available in lab
PDE2A2-GFP (plasmid)	2.5µg per 100mm plate	available in lab
PDE2A3-GFP (plasmid)	2.5µg per 100mm plate	available in lab
PC2-GFP (plasmid)	5 µg or 7.5µg per 100mm plate	*Addgene*
Kif13B-GFP (plasmid)	5µg per 100mm plate	*Addgene*
Kif1B-GFP (plasmid)	2.5µg per 100mm plate	cloned
Cav-1-RFP (plasmid)	5µg per 100mm plate	available in lab

Table 3: List of plasmids used in this thesis, with concentration and source.

Virus	Amount	Source
mcherry (virus)	5µl	*Vector Biolab*
PDE2A1-RFP (virus)	3µl	*Vector Biolab*
PDE2A2-RFP (virus)	3µl	*Vector Biolab*
PDE2A3-RFP (virus)	3µl	*Vector Biolab*
PDE3A1-RFP (virus)	15µl	*Vector Biolab*
PDE3A2-RFP (virus)	15µl	*Vector Biolab*

Table 4: List of viruses used in this thesis.

Generation of FRET-Reporters

A FRET reporter to measure changes in cAMP activity at the primary cilium was generated. The exclusive ciliary protein, Arl13b, was cloned into the N-terminus of the CUTie sensor CMM INF2, cutting at NHE1 sites, using forward and reverse primers found in **Table 5** below. For cloning of Arl13b into the EPAC-H187 sensor, HINDIII restriction enzyme sites were used, mirroring the method described in Jiang et.al.(Jiang et al. 2019) Forward and reverse primers for Arl13b-H187 are also found in **Table 5** below.

Primer Name	Primer Sequence
Forward primer **Arl13b-CUTie** (NHE1)	5' CTA GCTAGC ATG TTCAGTCTGATGGCC 3' 27bp, 52% GC
Reverse primer **Arl13b-CUTie** (NHE1)	5' CTA CGATCG TGA GAT CGT GTC CTG AGC 3' 27bp, 56% GC
Forward primer **Arl13b-H187** (HINDIII)	5' CCC AAGCTT ATG TTCAGTCTGATGGCC 3' 27bp, 52% GC
Reverse primer **Arl13b-H187** (HINDIII)	5' CCC TTCGAA TGA GAT CGT GTC CTG AGC 3' 27bp, 56% GC

Table 5: Engineered primers for construction of Arl13B-CUTie and Arl13b-H187.

FRET Microscopy

Coverslip was mounted into an imaging chamber kept at room temperature (RT) with 1ml E1 buffer (**Table 6**). Images were obtained by an OLYMPUS IX71 inverted microscope (**Table 7**). PDE inhibition was followed by saturation, achieved using 25µM of the AC activator, Forskolin, and 100µM of 3-isobutyl-1-methylxanthine (IBMX) (**Table 2**). For experiments

with Prostaglandin 2 (PGE2) or 1µM FSK, the cAMP-raising agent was applied before PDE inhibition and saturation.

FRET images were processed by MetaFluor molecular devices (*version 7.6.3.0*) and analyzed using excel and Prism software. Ratio was calculated for gain-of-FRET sensors by dividing YFP/CFP. For loss of FRET sensors Ratio was inverted to CFP/YFP, as a positive increase in trace reflected an increase in cAMP more appropriately. FRET change was calculated by dividing Ratio by average baseline ratio. To compare measurements from different sensors, FRET values were normalized to maximum FRET change, which was achieved via 25µM FSK and 100µM IBMX.

E1 buffer	(mM)
NaCl *(Sigma-Aldrich)*	140
KCL *(Sigma-Aldrich)*	3
$MgCl_2$ (x6H_2O) *(Sigma-Aldrich)*	2
$CaCl_2$ (x2H_2O) *(Sigma-Aldrich)*	2
Glucose *(Sigma-Aldrich)*	15
Hepes (pH=7.2) *(Sigma-Aldrich)*	10
Table 6: Composition of E1 buffer. Final pH is 7.4.	

oil immersion objective	PlanApoN , 60X or 100X, NA 1.42
FRET filters (*Chroma Technology*)	YFP excitation filter 535/30 m and CFP emission filter 480/30 m
beam splitter	simultaneous fluorescence emission measurements at 480 nm (CFP)/ 535 nm (YFP)
Excitation of cells	435nm
Table 7: Components of OLYMPUS IX71 inverted microscope set up.	

Immunostaining and Confocal Imaging

Cells were fixed with 4% Paraformaldehyde (PFA) at RT 72hrs after plating, washed in PBS, and permeabilized using 0.1% Triton X-100. Non-specific binding was blocked by Bovine Serum Albumin (BSA). Cells were incubated in primary antibodies (**Table 9**) overnight at 4◦C. After washing with Tween-20, cells were incubated in secondary antibodies (**Table 9**) for

1hr at RT. Coverslips were mounted with *Ibidi* mounting media and sealed. Z-stack images were obtained with a fixed distance of 0.5µm between slices (**Table 10**).

Reagents Immunostaining	**Source**	**Dilution**
Paraformaldehyde (PFA)	*Alfa-Aesar*	4%
Bovine Serum Albumin (BSA)	*VWR Chemicals*	1% diluted in 0.1% Triton X-100
Tween-20	*Sigma-Aldrich*	0.02%, diluted in PBS
Triton X-100	Promega	0.1%
Table 8: Reagents used for immunocytochemistry.		

Antibody	**Source**	**Dilution**
TUBA1A ace-40Lys Mouse McAb	*Proteintech*	1:200
ARL13B rabbit PolyAb	*Proteintech*	1:200
Anti-GFP rabbit monoclonal	*Abcam*	1:200
Alexa Fluor 488 goat anti-mouse IgG	*Invitrogen*	1:300
Alexa Fluor 568 goat anti-rabbit IgG	*Invitrogen*	1:300
Hoescht	*Invitrogen*	1:1000
Table 9: Antibodies and dyes used for immunocytochemistry.		

Nikon eclipse Ti confocal microscope	water immersion objective (40x or x60)
NIS elements Nikon confocal A1	version 4.13
ImageJ	version 1.53a
Table 10: Microscope and **s**oftware used for confocal image analysis.	

Cilia Measurements

Images of ciliated cells were analyzed using ImageJ and NIS elements software (**Table 10**). Pythagoras' Theorem was used to measure cilia length as shown in **Schematic 8**.

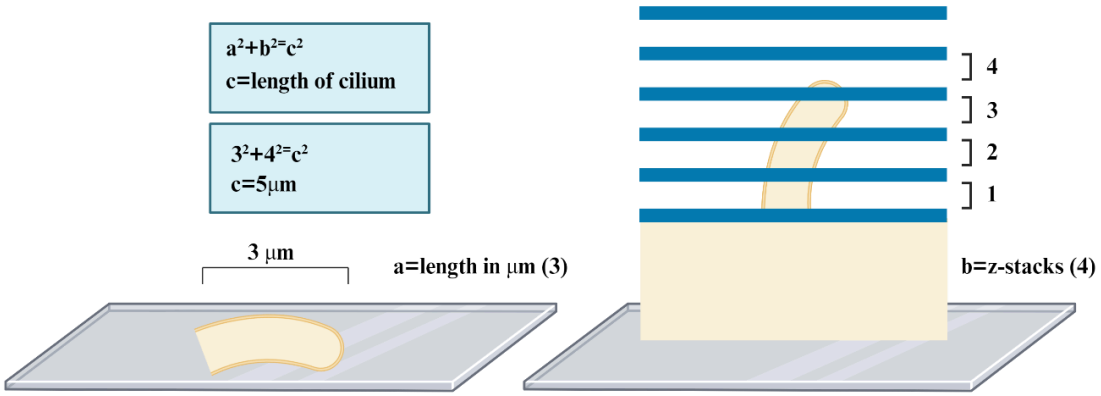

Schematic 8: a is calculated by measuring the length of the visible cilium in the composite image. b is calculated by counting the number of z-stacks in which any part of the cilium is observed times 0.5μM, the distance between z-stacks. The true length of the cilium is obtained by calculating c using Pythagoras' Theorem.

Co-Immunoprecipitation (Co-IP) and Western Blotting

Human Embryonic Kidney (HEK) cells were co-transfected with a GFP-plasmid and either an RFP or flag-plasmid (**Table 3**). Cells were harvested and lysed (**Table 11**). A sample of supernatant was collected for whole cell lysate (WCL) and Bradford concentration assay (*Thermo-Scientific*). Remaining lysate was blocked for 1hr at 4°C with protein-g beads. After blocking, lysate was incubated overnight at 4°C in either flag, GFP, or RFP beads (**Table 12**). The next day, beads were washed and boiled to release proteins.

WCL and Co-IP samples were loaded onto an SDS Mes *NuPage* Running gel then transferred onto a Transfer *NuPage* membrane. Membranes were blocked in 5% skim milk for 1hr, then incubated in primary antibody (**Table 12**) targeting GFP, GAPDH, and either flag or RFP overnight at 4°C. Next, membranes were washed, and secondary antibody was added for 1hr at RT (**Table 12**). Images were developed using an ECL machine (*BioRad*) and visualized using ImageLab software.

For Co-IP, probing for endogenous protein of interest, IMCD3 cells were infected with PDE isoforms tagged with mCherry (**Table 4**). Pull done was carried out with TRAP-RFP beads.

The protocol was identical to the aforementioned Co-IP method, but did not require blocking with protein-g.

For IPs carried out on fractionated samples the Qiagen Qproteome Mitochondria Isolation kit was used according to manufacturer's protocol.

Tris HCL (ice cold) (*Sigma-Aldrich)*	50mM
NaCl (ice cold) (*Sigma-Aldrich)*	150mM
EDTA (ice cold) (*CALBIOCHEM)*	1mM
Triton 100x (*Promega)*	0.5%
PBS (ice cold) (*GIBCO)*	1X
Protease inhibitor (*Roche)*	1 tablet per 10ml
Phosphatase Inhibitor (*Roche)*	1 tablet per 10ml
Table 11: Composition of Lyses Buffer.	

Flag-beads	Cell Signalling Technologies	20µl per sample
RFP-beads	Chromotek	20µl per sample
GFP-beads	Chromotek	20µl per sample
Protein-G Agarose Beads	Cell Signalling Technologies	20µl per sample
Anti-Flag antibody	Cell Signalling Technologies	1:1000 dilution
Anti-RFP antibody	Abcam	1:1000 dilution
Anti-GFP antibody	Abcam	1:1000 dilution
Anti-GAPDH mouse McAb	Proteintech	1:2,000 dilution
Anti-Polycystin-2	Proteintech	1:8000 dilution
Ponceau red	Thermoscientific	3ml
Anti-mouse IgG HRP-linked antibody	Promega	1:2000 dilution
Anti-rabbit IgG HRP-linked antibody	Cell Signalling Technologies	1:2000 dilution
Table 12: Reagents and Beads used for Co-IP		

Cyst Assays

To generate in vitro 3D cysts, IMCD3 cells were plated in a 96-well culture dish in a collagen/Matrigel mix. Matrigel and collagen, plates, and all supplies used were kept on ice/cold. 30µl of collagen/Matrigel/media (**Table 13**) was added to the bottom of the wells and allowed to set for 15 minutes at 37ºC. Afterwards a second layer of 100µl mix with $2.75x10^6$ cells was added to each well and left overnight at 37ºC. The subsequent day, the medium was replaced with medium containing a final concentration of either 100nM PGE2 or 1µM FSK (to stimulate cyst formation) and increasing concentrations of test compounds

(**Table 15**) with a final DMSO vehicle concentration of 0.1% (control). The treatments were reenforced two days after.

Material	**Source**
Rat Collagen 1	*Fisher Scientific 11519816*
Matrigel	*Corning 356235*
Bio-Rad counting slides	*Bio-Rad 1450011*
Trypan blue	*Sigma T8154*
Deep well plates	*Starlab*
Table 13: Materials for cyst assay	

Material	**Amount**
Collagen	1.2ml
1M NaOH	90µl
DMEM F12	2.4ml
Matrigel	4ml
Table 14: Composition of Matrigel/collagen mix	

Compound	**Concentrations**
Bay60	1nM, 3nM,10nM
Cilostamide	3uM,10µM, 30µM
Rolipram	3uM,10µM, 30µM
FSK	10nM, 30nM, 100nM, 300nM, 1µM, 3µM, 10µM, 30µM
PGE2	1nM, 3nM,10nM, 30nM, 100nM, 300nM, 1µM, 3µM
Isoproterenol	0.3nM, 1nM, 3nM, 10nM, 30nM, 100nM, 300nM
A1 Purinergic	1nM, 3nM, 10nM, 30nM, 100nM, 500nM, 1 µM
Table 15: Drugs used for cyst assay treatments. Highlighted concentrations were used to induce cystogenesis for non-optimisation experiments.	

A Nikon Ti2E was used to obtain z stacks of in vitro cysts a week after plating. Plates were scanned via an automated platform and JOBS software. Minimum intensity projections were generated, and the z stack bright field images were collated into one image per well. The Nikon General Analysis software was then used to measure mean cyst area, number of cysts, and total cyst area per well. Most parameters were fixed- cyst size was set to 60.58µM and circularity to 0.2units. Threshold was the only parameter that could be altered between experiments, to accommodate for the exclusion of different background shadowing and artifacts such as bubbles. Data from the software was exported to excel.

PDE ratiometric assay

HEK293 cells are washed with PBS and KHEM, and then lysed using the dounce homogeniser. Lysate is centrifuged and separated from cell debris. The lysate is further ultra-centrifuged to remove lipid membrane components. Cytosolic fractions are then collected and protein concentration assessed using a Bradford assay. Final concentration of protein used for ratiometric assay is typically 20µg. This cell lysate reflects the physiological confirmation of PDEs at the time of lysis. The lysate is incubated with PDE inhibitors prior to addition of reaction substrate, cAMP with a trace of ^{3}H-cAMP. With the addition of substrate, the reaction continues for 10 minutes at 30ºC before it is quenched via enzyme denaturation at 95ºC for 2 minutes. The solution is cooled on ice and subsequently incubated with snake venom for 15 minutes at 30ºC, to convert the product of the prior reaction, AMP, to adenosine. Dowex ion exchange resin is then added to filter out unreactive substrates, leaving behind adenosine and ^{3}H-adenosine in the solution. Proteins attached to the Dowex resin are removed via centrifugation, and thus the filtered ^{3}H-adenosine is quantified using scintillation. Controls include background activity of assay (heat-inactivated lysate), and lysate not treated with PDE inhibitor (total cAMP).

Role in reaction	**Name**	**Amount**	**Source**
washing buffer	Ice-cold PBS	1ml per smaple	*Sigma Aldrich*
washing buffer	KHEM buffer: (50 mM KCl, 10 mM EGTA, 50 mM HEPES (pH 7.2), 1.92 mM MgCl2, pH 7.2 with KOH) contains protease inhibitors (leupeptin 10 mg/ml, PMSF 50 mg/ml, aprotinin 10 mg/ml and DTT 1M)	1ml per sample	
resin	Dowex in a 1:1:1 ratio with water and ethanol	400µl per sample	*Sigma Aldrich*
assay buffer	Tris buffer, pH 7.4, containing 10 mM $MgCl_2$ cAMP	20mM	*made in lab*
substrate	cAMP	1µM	*Sigma Aldrich*
substrate	^{3}H-cAMP	111 KBq/mL (3 uCi/mL)	*Perkin Elmer*
5'nucleotidase	snake venom	1mg/ml	*Sigma Aldrich*

Table 16: Reagents for PDE ratiometric assay.

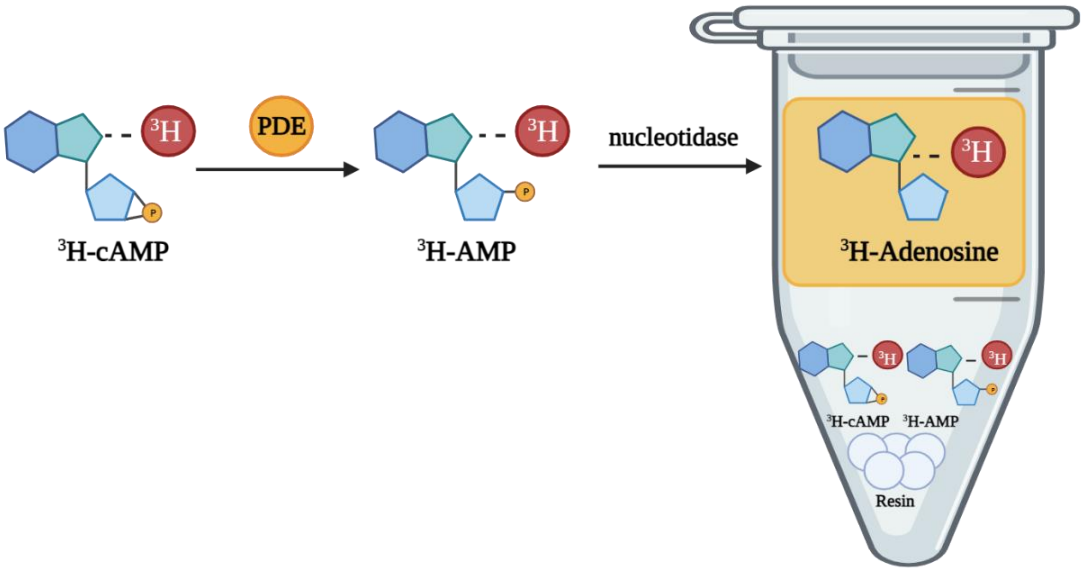

Schematic 9: The PDE ratiometric assay measures ^{3}H-adenosine as the product of the two-step reaction. ^{3}H-cAMP is hydrolysed to ^{3}H-AMP by PDEs. In the second step ^{3}H-AMP gets converted to ^{3}Hadenosine by the 5'nucleotidase found in snake venom. Since the first reaction is terminated while still in its linear phase, and the second reaction goes to completion, the end-product, ^{3}H-adenosine is a direct indicator of the rate of PDE catalysis.

Flow Cytometry

Flow cytometry was carried out on IMCD3 cells starved, or treated with FSK, PDE inhibitors, or DMSO control. Cells were trypsinised, centrifuged, and washed in PBS. After washing, cells were resuspended in 500µl of PBS. Cells were gently vortexed and fixed in 1.5ml ice cold ethanol and kept up to two weeks at 4ºC before measurements. On the day of FACs analysis cells were pelleted to remove ethanol and resuspended in 2ml PBS (or a volume allowing for a final concentration of ~1x10^{6}cells/400µl). 50µl RNAse A was added to the cells at RT for two hours before measuring. Propidium Iodide (PI) was added to each sample (except PI- control) immediately before running experiments on the BD Fortessa X20 with laser 561nm wavelength.

Material	Working Concentration	Source
RNase A	1mg/ml	Sigma
Propidium Iodide	1mg/ml	Sigma

Table 17: Reagents used for floc cytometry experiments, with concentrations per sample.

SPLICS

75,600 IMCD3 cells were plated on 12-well plates with glass coverslips. 24 hours after plating, cells were pre-treated with different PDE inhibitors. With introduction of PDE inhibitors, cells were also fed starvation media (or normal media for control wells). Tunicamycin, Rapamycin, or DMSO treatment was initiated 4 hours before SPLICs transfection (replacement media for this timepoint also contained fresh doses of PDE inhibitors). SPLICs transfection (**Table 18**) occurred 52 hours after plating for all treatments. **Schematic 10** shows the sequence of preparation for these experiments.

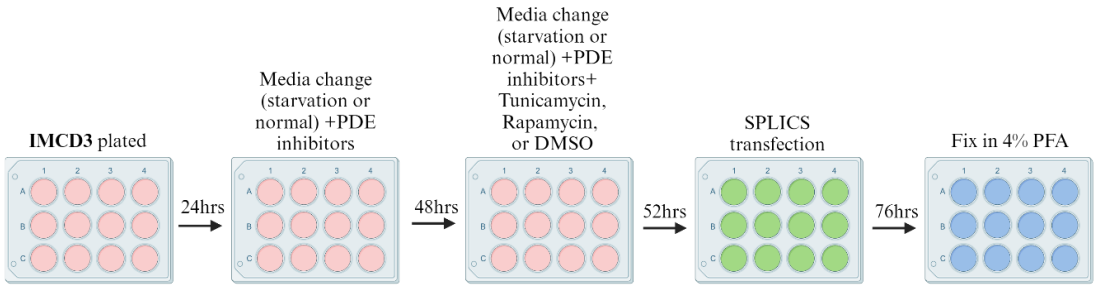

Schematic 10: Sequence of treatment for IMCD3 samples for SPLIC$_s$ experiments.

24 hours after transfection cells were washed in PBS and fixed in 4% PFA and stained for GFP primary and 568 goat anti-rabbit IgG secondary antibodies according to the immuno-staining protocol. GFP antibody recognised both the 11th strand and the 1-10 β-barrels of the GFP. Images were taken using the OLYMPUS IX71 inverted microscope (**Table 19**). Analysis of images was carried out using ImageJ software. GFP average fluorescent intensity was also normalized to GFP antibody staining average intensity (red) in order to correct for transfection efficiency. All IMCD3 samples were normalized to "Not Starved DMSO" control for PDE inhibitor and Tunicamycin/Rapamcyin/starvation treatments respectively.

Construct	**Amount**	**Source**
Sac1 ML GFP Strand 11 Short	0.5µg per six well	*Addgene*
Sac1 ML GFP Strand 11 Long	0.5µg per six well	*Addgene*
OMMGFP 1-10	0.5µg per six well	*Addgene*

Table 18: Constructs used for ER-mitochondrial quantification.

Filter	**Excitation Wavelength**	**Emission Wavelength**
GFP	470+/- 20nm	535+/- 25nm
Texas Red	560+/-20nm	630+/- 37.5nm
Table 19: Filters used for SPLICs experiments.		

Statistical Analysis

Prism software was used for analysis. Data was assessed for normal distribution using the Shapiro-Wilk test. Parametric t-test or the non-parametric Mann Whitney test were used when comparing two conditions for normally distributed or not normally distributed data respectively. For three or more conditions One-way ANOVA (parametric) or Kruskal-Wallis (nonparametric) were executed. Significance level for all tests was set at 95%. For all experiments with three or more conditions, I corrected with multiple comparisons tests specified in each figure legend.

PDE assay statistics

For PDE assay experiments the same amount of protein was loaded for each sample, as protein content had been previously measured using Bradford. Each n number represents an independent round of experiments, with each data point of each experiment, an average of triplicates. SD was calculated for each sample using the three data points, which were averaged to yield a mean. No statistical test was carried out as we were interested in the shape of the curve. The control was DMSO, which was not graphed as it had a 0% effect.

FRET statistics

Unless specified otherwise, for FRET experiments, each data point represents one coverslip. If multiple cells were imaged on one coverslip, the average of these cells was taken for a single data point. N is specified in figure legends, where n is one day of FRET

experimentation, with cells obtained from a single flask passage. The control treatment for FRET experiments was DMSO. Statistical analysis can be found in figure captions.

Cyst assay

Cyst assays were carried out with a fixed number of cells plated in each well. For every 96 well plate there were four repeats per condition and a DMSO only control. There was a stimulus (either PGE2 or FSK) only control for each plate. The DMSO control measurements were averaged, this average was subtracted from all drug treatment well measurements. Stimuli + PDE inhibitor measurements were normalised to stimuli-only measurements. Each well per condition represents one data point. Four data points were obtained for each independent round of experiments, for which there were four total rounds (N=4). An independent experiment consisted of cells obtained from different passages and plated on different days. Parameters analysed included total cystic area and cyst number. A third parameter, average cyst size, was calculated by dividing total cyst area by cyst number. SD was calculated from the 16 data points. Kruskal Wallis was used to test non-parametric data and ANOVA for parametric. Post hoc tests differed between experiments and are thus stated in figure legends.

Cilia length statistics

For cilia length experiments, the length of every cilium was measured in each coverslip. Data points represent the average cilia length per coverslip, from which SD was calculated. N is stated in figure legends, where n is one round of experiments (an independent flask passage). Datapoints obtained from each drug treatment were normalised to the DMSO control. Statistical analyses used nested t-test or nested ANOVA. Post hoc tests differed between experiments and are thus stated in figure captions.

Flow cytometry statistics

For flow cytometry experiments one n is equivalent to one batch of cells obtained from an independent flask passage. All conditions are normalised to a DMSO control sample. The Mann Whitney test was used to calculate statistical significance of non-parametric data. Statistical data is found in figure legends.

Co-IP

For Co-IP, each experiment was done three times, thus N=3. Gels were not clean enough to quantify, so data remains qualitative.

ER-mitochondrial contacts

Er-mitochondrial contacts were measured so that one data point represents the median of one coverslip. Data was normalised to DMSO control. N is stated in figure legends, where one n represents one round of experimentation from one independent flask passage. Each median was transformed to Log(Y) and analysed using nested t-test or nested ANOVA, depending on the number of conditions. Post hoc tests differed between experiments and are thus stated in figure legends.

Chapter 4- Detection of cAMP and Phosphodiesterase Activity in the Primary Cilium

Introduction

Since the discovery of the primary cilium as a central hub for intracellular signalling, there has been much debate over whether the organelle could foster an independent pool of cAMP from the cytosol. The structure of the cilium allows for a higher surface area to volume ratio, 13-fold greater than that of the cell body.(Arena and Hofer 2021) This increased surface area would benefit GPCR localisation to the organelle, which upon stimulus, could generate a highly concentrated pool of cAMP in a small compartment.(Bangs and Anderson 2017) Additionally, numerous studies indicate that stimulation of a receptor localising to the cilium has a distinct downstream effect to the activation of the same receptor localising to the cytosol (Masyuk et al. 2008; Loktev and Jackson 2013; Yao et al. 2016), supporting a model where the cilium operates through cAMP networks that are distinct from those that function in the cell body. Yet, the transition zone of the cilium was found to be Ca^{2+} and cAMP permeable (Jiang et al. 2019), suggesting that second messenger signalling in the organelle may not be compartmentalised.

Several studies report detection of cAMP signalling in the cilium, however the findings are inconsistent. Jiang et al generated ciliary FRET sensors, Arl1b-H187 and Arl13b-H188, based on loss-of-FRET reporters, EPAC-H187 and EPAC-H188 respectively. No difference was observed, using either Arl13b-H187 or Arl13b-H188, in ciliary versus cytosolic cAMP in IMCD3. When V2R was stimulated with Vasopressin, and cAMP levels were recorded with Arl13b-H187 in the cytosol and cilium of the same cell, a similar increase in cAMP was observed in the two compartments. As, V2R primarily localises to the plasma membrane, the finding was interpreted as diffusion through the ciliary transition zone of cAMP generated in the cytosol. This observation supported the hypothesis that the cilium is not an independent

cAMP signalling subdomain. The same group also generated a sensor targeted to the serotonin receptor, 5-hydroxytryptamine (5HT6). Stimulation of 5HT6-EpacH187, with Serotonin, equally raised ciliary and cytosolic cAMP in cells where the 5HT6 receptor localised to the main body plasma membrane, but did not increase cAMP at either subcompartment when the 5HT6 sensor was only localised in the cilium. These experiments hint that while bulk cAMP can diffuse freely between cilium and cytosol, ciliary versus cytosolic localisation of GPCRs can alter their downstream cAMP response.(Jiang et al. 2019) Therefore the cilium may still provide a degree of cAMP compartmentalisation despite its lack of a selective border with the cytosol.

Using a different approach to Jiang et al., Moore et al. sought out to measure cAMP levels in the cilium and the cytosol by generating a PKA activity sensor targeted to the cilium by fusing 5HT6 to AKAR4, a FRET-based sensor that measure PKA-dependent phosphorylation.(Depry and Zhang 2011) 5HT6-AKAR4 expressed in Mouse Embryonic Fibroblasts (MEFs) demonstrated markedly higher PKA activity in the cilium than the cytosol. Increased PKA activity in the cilium is not necessarily due to increased levels of cAMP at the organelle. Enhanced PKA activation could be due to more PKA, better anchoring of PKA in vicinity to cAMP, different buffering of cAMP at the cilium versus the cytosol, or decreased phosphatase activity, and thus Moore's findings do not necessarily contradict Jiang's observations. However, Moore et al also measured basal cAMP levels using the cAMP Difference Detector in situ (cADDis) reporters, which works on the principle that cADDis fluorescence decreases as more cAMP binds.(Tewson et al. 2016) Moore et al then cleverly fused the cADDis to mcherry, which does not change in fluorescence upon cAMP increase, thus providing a value for transfection efficiency which cADDis fluorescence can be normalised to. The mcherry/cADDis ratio gives absolute cAMP basal levels. mcherry-cADD in the cell body measured a basal concentration of 800nM cAMP, while 5-HT6-mcherry -cADDis in the cilium reported 4μM basal cAMP in MEFs, a five-fold difference between compartments.(Moore et al. 2016) A higher cAMP concentrations in the cilium than in the

cytosol cannot be explained by diffusion of cAMP from the main cell body to the cilium, as Jiang et al. reported.

With these examples of cAMP imaging in the cilium, it is clear that detecting second messenger signalling in the organelle remains elusive and controversial. Additionally, FRET sensors have been shown to report artificial levels in cAMP changes when fused to targeted proteins, as this insertion could alter sensor conformation or affinity to cAMP. Thus, I sought to generate my own reporter, localising to the cilium, with the same backbone, CUTie, as other reporters, localising to alternative subcellular domains, and readily available in the lab.(Surdo et al. 2017) The gain-of-FRET sensor was demonstrated to tolerate well fusion to a variety of targeting domains without impact of the FRET signal. This approach would make findings measured via a ciliary-CUTie sensor comparable to data obtained with CUTie sensors targeted to other intracellular pools of cAMP.

Results 1-Generating and Optimizing a Ciliary FRET Reporter

The initial FRET construct was created by fusing Arl13b, a protein with exclusive expression to the cilium (Duldulao, Lee, and Sun 2009), at the N-terminus of the cytosolic CUTie construct (**Figure1.a**). Sequencing confirmed Arl13b was inserted correctly. Additionally, Arl13b-CUTie ciliary localisation was demonstrated via immunostaining with anti-Arl13b (**Figure1.b**). Unfortunately, upon cAMP-raising stimuli, such as 1µM FSK, this reporter failed to show any FRET change (**Figure1.d**). Saturation with 25µM FSK and 100µM IBMX led to a small but detectable FRET change. (**Figure1.d**) However, a less than 10% increase in FRET and the fact that, while CFP fluorescence decreased, the YFP intensity also decreased, suggests only a small amount of energy transfer is afforded by the sensor, as functioning gain-of-FRET sensors should correlate a marked CFP decrease to a YFP increase upon cAMP binding.

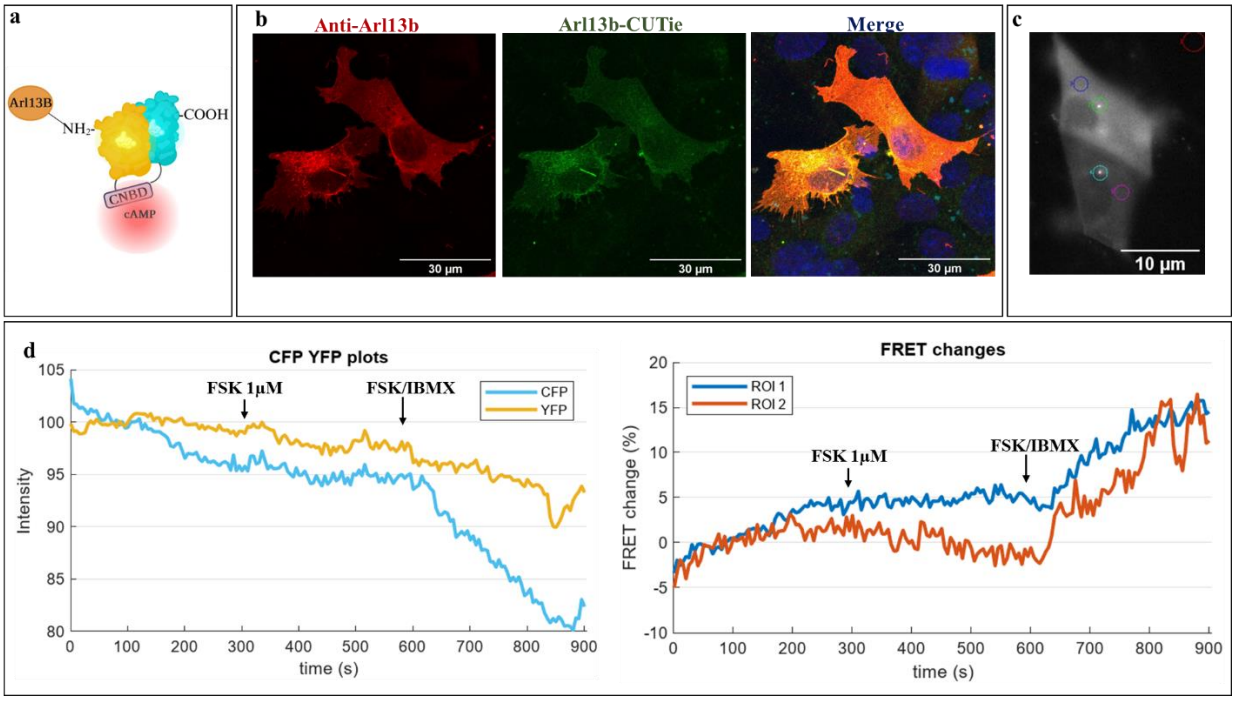

Figure 1: a Schematic of Arl13b-CUTie. **b** Overlap of Arl13B-CUTie to anti-Arl13b in fixed IMCD3 to confirm ciliary localisation of the FRET reporter. **c** Example of live IMCD3 imaging transfected with Arl13B-CUTie, with ciliary (green and cyan) as well as cytosolic (pink and dark blue) Regions of Interest (ROIs). **d** Traces for fluorophore intensities and FRET upon 1µM FSK and saturation with 25µM FSK and 100µM IBMX.

Given the poor performance of Arl13b-CUTie, I next decided to generate a ciliary FRET reporter that replicates a successful design previously published (Jiang et al. 2019) by fusing Arl13b to the CFP fluorophore of H187. As mentioned above, H187 is a loss-of-FRET sensor where the cAMP effector, EPAC, is sandwiched between YFP and CFP at the C-terminus and N-terminus, respectively (**Figure 2a**). Both Arl13b insert and H187 were readily available in the lab, and at the time Arl13b-H187 was not commercially available. Although the fusion of H187 to Arl3b may impact the maximal FRET change displayed by the sensor (Surdo et al. 2017) we reasoned that, given the large dynamic range of H187 (250% at saturation) the cilium-targeted version of H187 should still generate a clearly detectable signal. The expression of Arl13b-H187 into IMCD3 showed clear localisation to the cilium (**Figure 2b.c**), with some mistargeting of the sensor into the main body of the cell (**Figure 2b.c**). On application of FSK (1µM) an increase in CFP emission concomitant with a decrease in YFP emission was observed, resulting from the conformational change that occurs on cAMP

binding to the sensor, separating the two fluorophores, and decreasing the FRET signal. However, it should be noted, during analysis, fluorophore ratio was inverted to reflect an increase in FRET, upon an increase in cAMP, for all loss-of-FRET sensors (**Figure 2d**). A further change in fluorescence was observed upon maximum cAMP stimulation via FSK and IBMX (**Figure 2d**). The normalised ratio of fluorescence intensities yields a FRET trace (**Figure 2d**) thus providing a genuine measure of changes in cAMP. Therefore, Arl13b-H187 was demonstrated as a functional tool for measuring cAMP, in real-time, at the cilium. However, as H187 is an EPAC-based sensor, absolute cAMP responses measured with this reporter cannot be compared to absolute measurements of cAMP obtained using reporters with a CUTie backbone. To account for this, the FRET change detected upon drug treatments was expressed as a percent of maximal FRET change, achieved with FSK and IBMX. This normalisation method was also applied when comparing signals, measured with the same sensor, but in different compartments within the same cell (**Figure 2.c**).

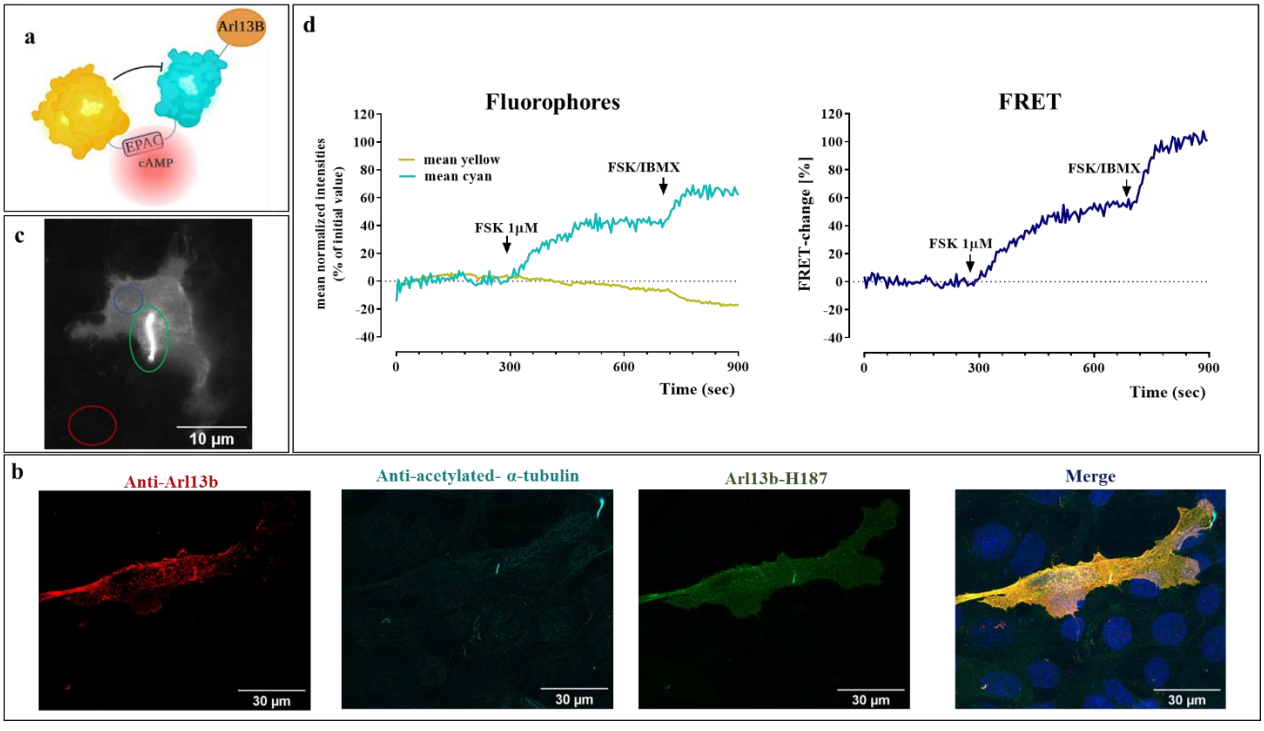

Figure 2: a Schematic of FRET-reporter, Arl13B-H187. **b** Overlap of Arl13B-H187 to anti-Arl13b and anti-acetylated α-tubulin in fixed IMCD3, confirming ciliary localisation of generated FRET reporter. **c** Example of live IMCD3 imaging transfected with Arl13B-H187, with ciliary (green) as well as cytosolic (blue) ROIs. **d** Traces for fluorophore intensities, and FRET upon 1µM FSK and saturation with 25 µM FSK and 100µM IBMX.

To establish whether fusion of Arl13B to H187 may have compromised dynamic range of the FRET change of the sensor, either via conformational modifications or altered localisation of Arl13b-H187 into the small ciliary compartment, the maximum FRET change at saturating cAMP concentration detected using Arl13b-H187 was compared to that measured using the untargeted cytosolic H187 (**Figure 3.a.b**). As expected, the analysis did show a significant decrease in maximum cAMP detected by Arl13b-H187 in the cell and cytosol of IMCD3 compared to H187 (**Figure 3.b**). However, the mistargeting of Arl13b-H187 to the cytosol of the cell created an opportunity to measure cAMP in the cilium and the cell body of the same cell using the same sensor, ultimately rendering H187 redundant, and allowing for a more direct comparison of cAMP levels between two subdomains.

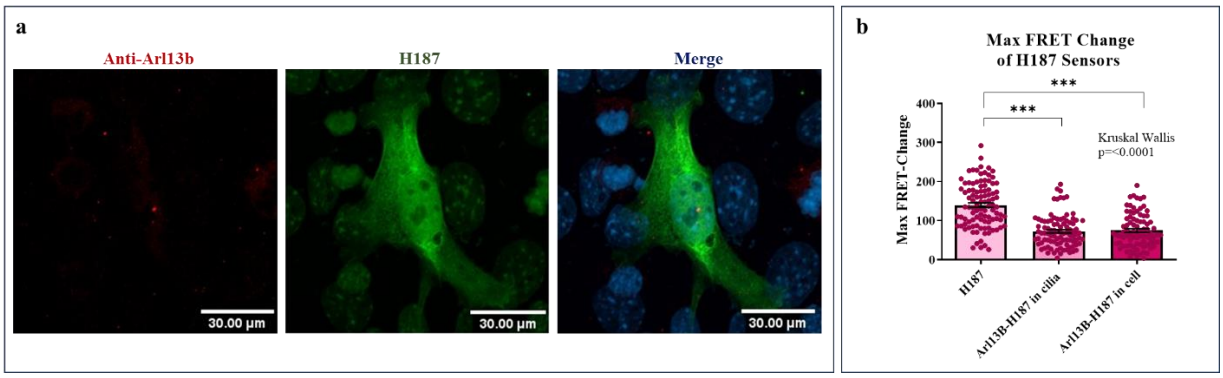

Figure 3: a Overlap of H187 sensor with ciliary antibody marker anti-Arl13b. **b** Comparison of max FRET change, induced via 25µM FSK and 100µM IBMX, measured by H187, Arl13b-H187 targeted to the cilium, or Arl13b-H187 mistargeted to the cytosol of IMCD3. Each data point is a single cell. N=3 where each n is a round of experimentation on an independent flask passage. Kruskal Wallis was used to compare non-parametric data. Mutliple comparison was carried out using Dunn's post hoc test.

Results 2-Measuring cAMP-hydrolysing activity of PDEs in cilium and cytosol of IMCD3

Though Jiang et al. found no difference in ciliary versus cytosolic cAMP using Arl13b-H187, their experiments focused on quantifying cAMP changes upon activation of GPCRs and did not explore cAMP response to PDE inhibition. Thus, it was still possible that Arl13b-H187 could help identify which PDEs hydrolyse localised pools of cAMP in the cilium. Indeed, with the help of Mironid collaborators, Faisa Omar and Caitlin Moore, using a PDE

ratiometric assay, carried out in IMCD3 cells treated with one of three respective PDE inhibitors, we demonstrated that there is cAMP hydrolysing activity from all three PDEs (though it appears there is no PDE2 hydrolysis in the average of three separate assay rounds, some n numbers did show PDE2 cAMP hydrolysing activity) (**Figure 4**). However, as PDE hydrolysis in solution does not reflect activity of the same PDE in intracellular subdomains, I next sought to assess PDE contribution to hydrolysis of cAMP generated on inhibition of PDEs in the cilium and the cytosol of IMCD3 using Arl13b-H187 (**Figure 5 and 6**). After, baseline FRET was measured, one of three PDE inhibitors was added (Bay60 for PDE2, Cilostamide for PDE3, and Rolipram for PDE4). The response upon PDE inhibition was expressed as percent of maximal FRET change at saturation using FSK/IBMX (**Figure 6a**). Results showed no significant difference for any of the PDEs tested between Arl13b-H187 in the cilium versus Arl13b-H187 or H187 in the cytosol. The latter was tested as a control for mistargeted Arl13b-H187 in the cytosol (**Figure 6b**). Measurements obtained with H187 or with the mistargeted Arl13b-H187 in the cytosol showed no difference in PDE activity reported with either sensor, demonstrating Arl13B-H187 can be used to faithfully report cytosolic cAMP changes.

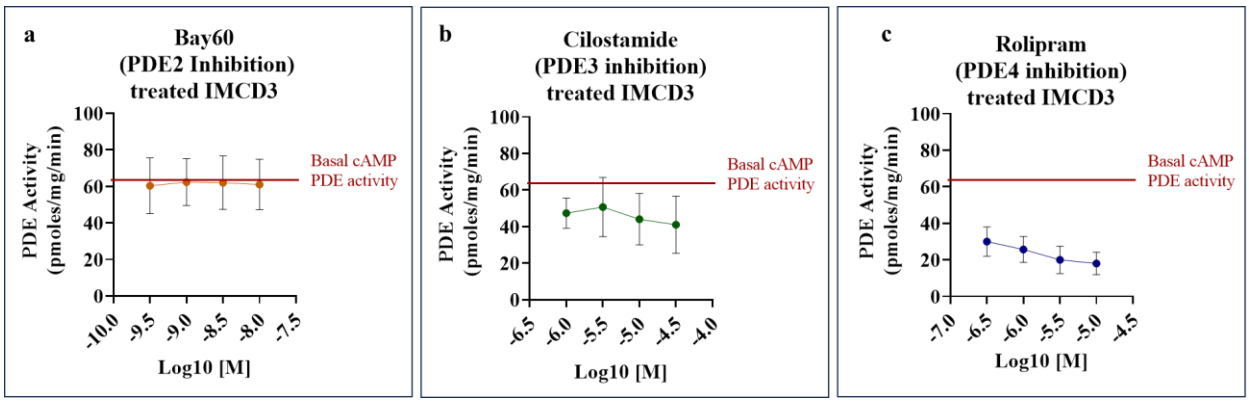

Figure 4: Results of PDE ratiometric assay carried out on IMCD3 cells pre-treated with either **a** Bay60 (PDE2 inhibitor), **b** Cilostamide (PDE3 inhibitor), or **c** Rolipram (PDE4 inhibitor). Concentrations of PDE inhibitors are in Log10 scale. N=3, where n is 3 independent rounds of experimentation. Data shows mean of n=3 with SD. No statistical test was carried out for this analysis.

PDE4 inhibition led to the greatest increase in ciliary and cytosolic cAMP in IMCD3 cells, with comparable activity in the two sub compartments (**Figure 6**). While there is no evidence

that PDE2 or PDE3 localise to the cilium of renal cells, Arl13b-H187 also reported similar cAMP hydrolysis activity for PDE2 or PDE3 in the cytosol and cilium of IMCD3 (**Figure 6**). Overall, these findings align with results from Jiang et. Al, supporting the conclusion that there is no difference in cAMP signalling or PDE activity in the cilium and the cytosol of the same cell. However, Arl13b-H187 did confirm all three PDE families function at basal cAMP levels in IMCD3, supporting the rationale that these enzymes may play a role in regulating cystogenesis of ADPKD. Indeed, when expression levels of PDEs in IMCD3 were profiled using qPCR **(Figure 7),** in IMCD3 grown in 3D culture, expression of all three isoforms was detected, with the highest levels observed for PDE4 long-form isoforms and some detectable expression of PDE2A and PDE3A (**Figure 7**).

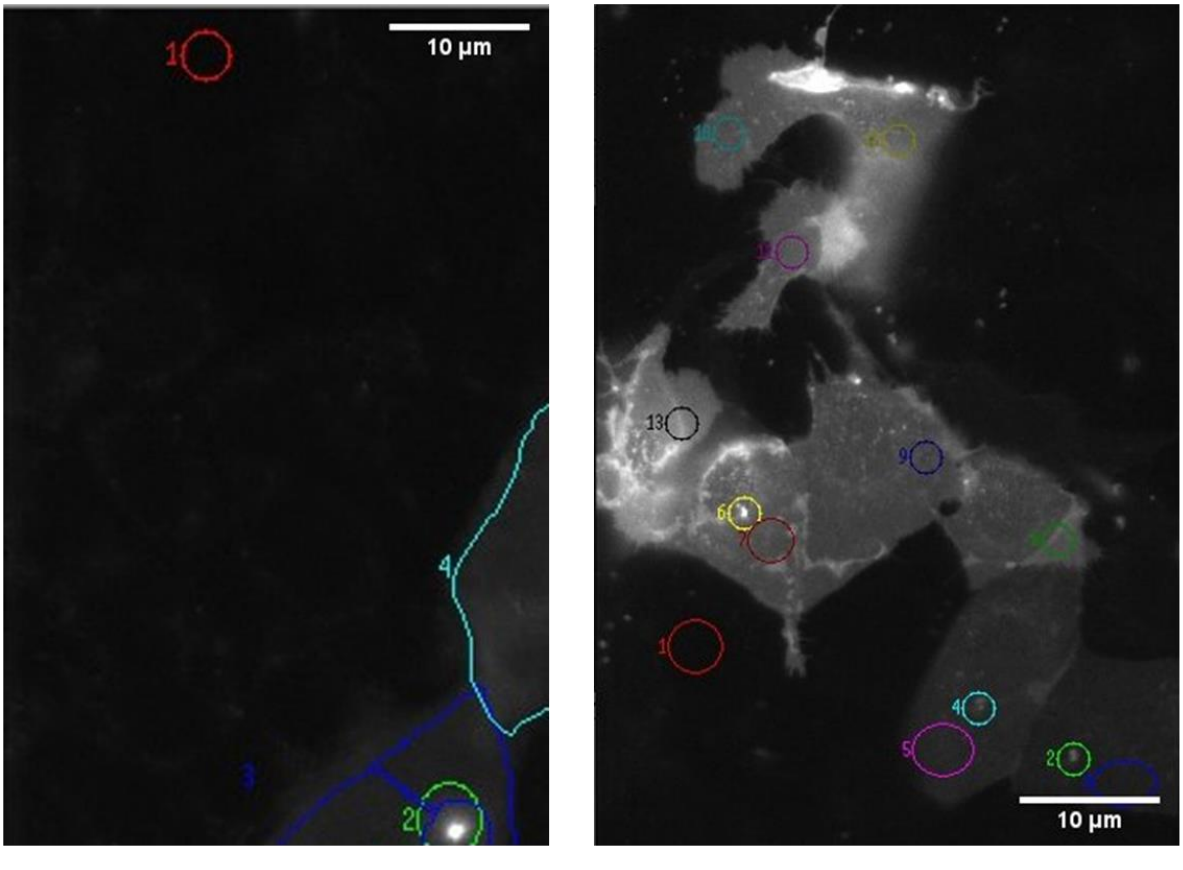

Figure 5: Examples of FRET sensor Arl13b-H187 in ciliated versus non-ciliated cells within the same coverslip. ROIs were drawn around cilium and in the cytosol of ciliated IMCD3. ROIs were only drawn in the cytosol of non-ciliated IMCD3.

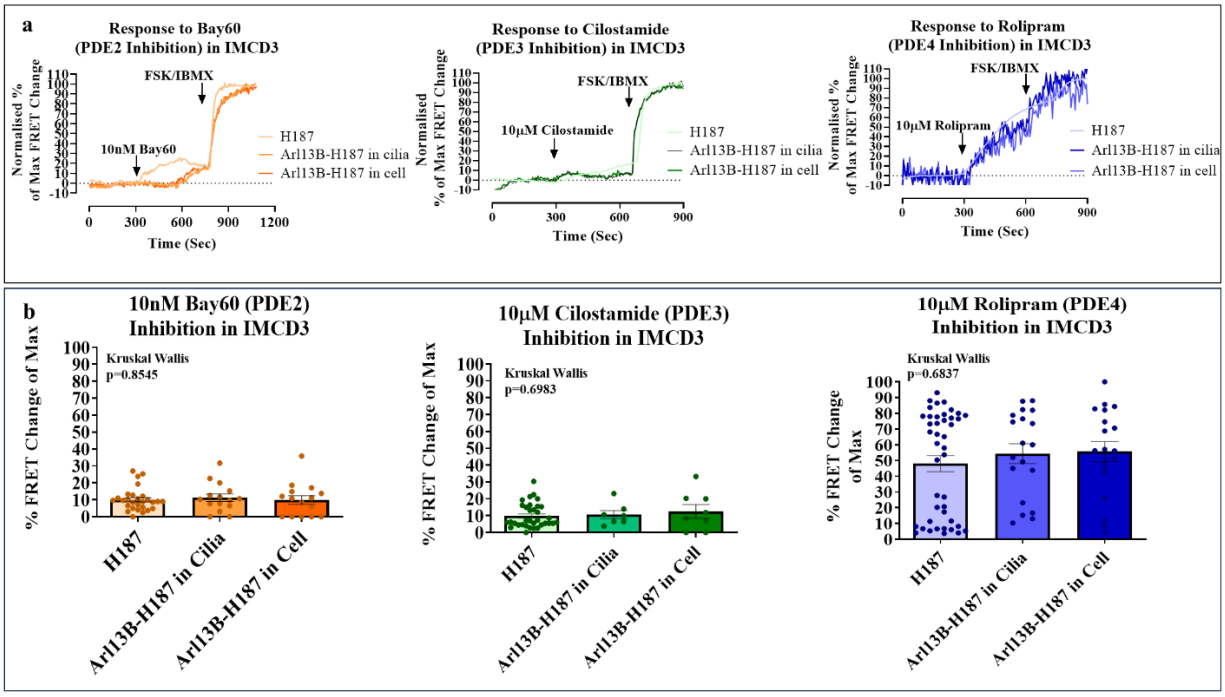

Figure 6: a shows example FRET traces for IMCD3 cells treated with either 10nM Bay60 (PDE2 inhibitor), 10µM Cilostamide (PDE3 Inhibitor), or 10µM Rolipram (PDE4 inhibitor), followed by maximum stimulation of cAMP via FSK/IBMX. FRET was either measured in the cytosol with H187, or in the cytosol with Arl13B-H187, or in the cilium with Arl13B-H187. **b** shows the quantified data from **a** normalised to maximal FRET change on stimulation with FSK/IBMX. Each data point represents cell measurements obtained from one coverslip. N=3, where n is one day of imaging (cells from different flask passages). Kruskal-Wallis was used to test for non-parametric significance, data show mean with SD. Mutliple comparison was carried out using Dunn's non-parametric post hoc test.

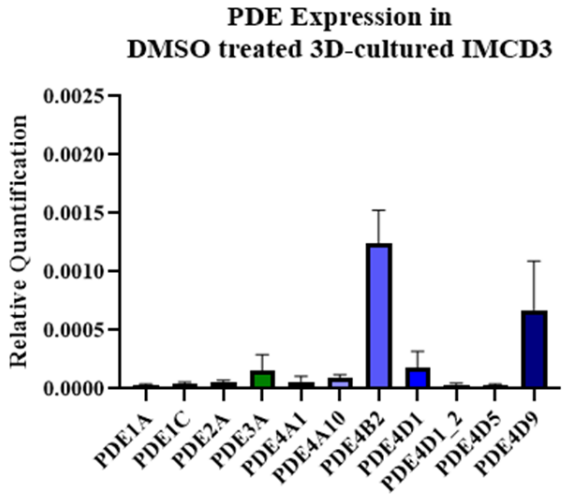

Fig. 7: Relative expression of PDEs, measured via qPCR, in IMCD3 cells treated with DMSO and grown in a 3D-matrigel collagen mix. N=2, so no statistical analysis was carried out. SD from two data points is shown.

Though Arl13b-H187 failed to differentiate independent pools of cAMP in the cilium and the cytosol, the sensor could distinguish ciliated cells from non-ciliated cells, a novel pursuit. The primary cilium is only present in non-dividing cells, as the basal body, from which the organelle grows, stems from centrioles, vital regulators of the cell cycle.(Loukil, Tormanen, and Sütterlin 2017) Therefore, I asked whether ciliated cells, which are not undergoing mitosis, have different cAMP signalling profiles compared to cells without a cilium that are dividing. Additionally, several GPCRs have been shown to communicate distinct downstream signals based on their localisation to the cilium or the plasma membrane.(Paolocci and Zaccolo 2023) Thus, GPCR signalling in ciliated cells may also differ to cells where GPCR signalling is restricted to the plasma membrane in the main cell body, altering downstream cAMP compartmentalisation as a consequence. Ciliary and mistargeted cytosolic localisation of Arl13b-H187 provided the opportunity to explore whether this was indeed the case, and the sensor was used to assess any difference in cAMP and PDE activity in the cytosol and cilia of ciliated versus non-ciliated IMCD3. Since in vitro cyst assays are performed by treating the cells with cAMP-raising agents such as FSK or PGE2 to induce cystogenesis, cAMP-hydrolysing activity of PDEs was next measured after initial addition of cAMP stimuli- FSK or PGE2. **Figure 8** shows FRET traces recorded in IMCD3 cells where addition of 1μM FSK was followed by one of three selective PDE inhibitors. cAMP changes were measured using Arl13b-H187 in the cilium, or the cell body of ciliated and non-ciliated cells. Results show the majority of cAMP generated upon FSK stimulation is hydrolysed by PDE4 in ciliated and non-ciliated cells alike, with minimal contribution from PDE2. A drop in cAMP levels after FSK and PDE3 inhibition suggest minimal, if no detectable cAMP hydrolysis by PDE3, as a drop in cAMP is also observed with addition of DMSO, the control vehicle (**Figure 9**). Though minimal activity of PDE2, and no activity of PDE3 is observed in the cell body of IMCD3 after FSK stimulation, this does not rule out the possibility that these PDEs may function in highly selective cAMP nanodomains to potentially affect cystogenesis, as we previously observed PDE2 and PDE3 activity at baseline cAMP levels (**Figure 6b**).

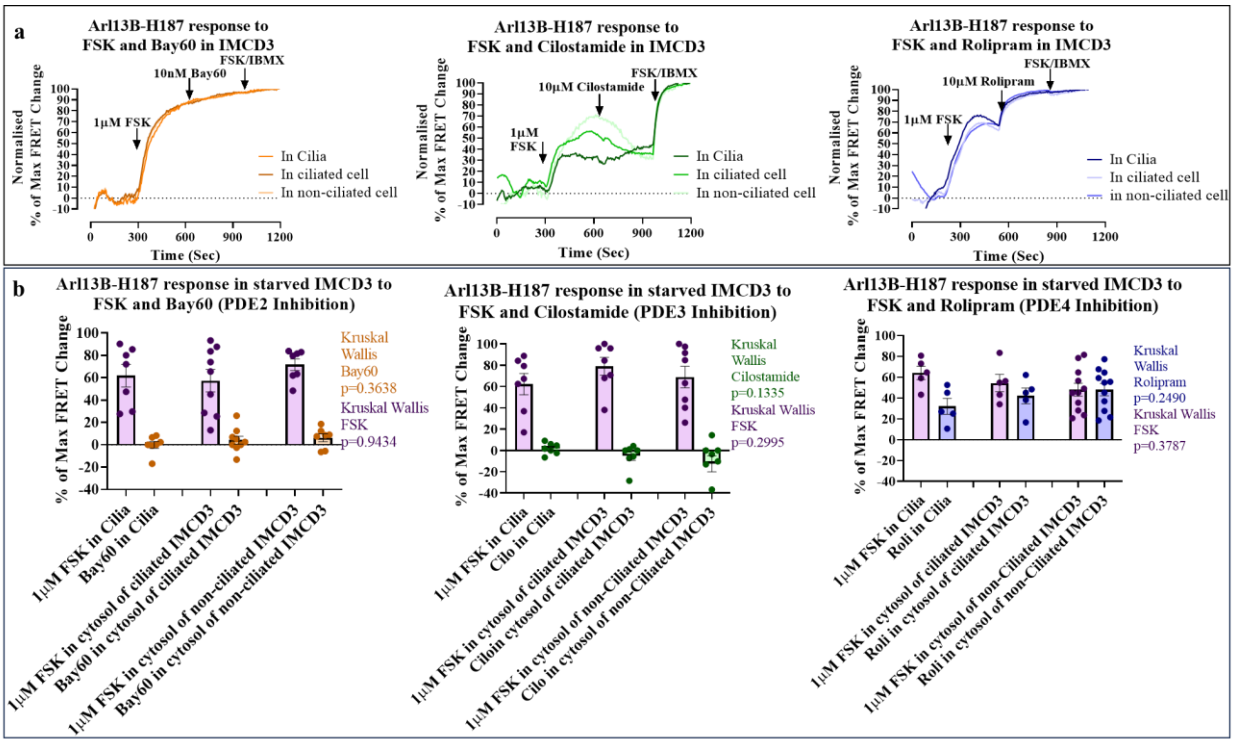

Figure 8: a shows example FRET traces for IMCD3 cells treated with 1μM FSK followed by either 10nM Bay60 (PDE2 inhibitor), 10 μM Cilostamide (PDE3 Inhibitor), or 10μM Rolipram (PDE4 inhibitor), and concluded with maximum stimulation of cAMP via FSK/IBMX. FRET was either measured in the cytosol of non-ciliated cells with Arl13B-H187, the cytosol of ciliated cells with Arl13B-H187, or in the cilium with Arl13B-H187. **b** shows the quantified data from **a,** normalised to maximum stimulation of FSK/IBMX. Each data point is one coverslip. N=3, where n is one day of imaging (cells from different flask passages). Kruskal-Wallis was used to test for non-parametric significance. Data show mean with SD. Mutliple comparison was carried out using Dunn's post hoc test.

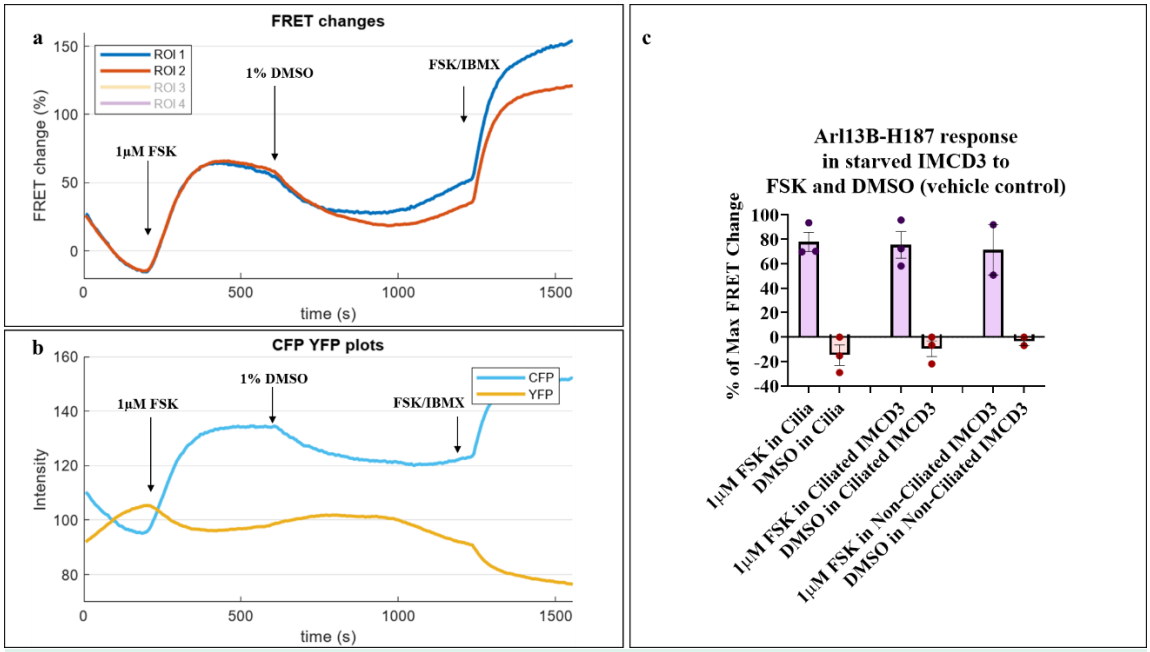

Figure 9: a shows example FRET traces for IMCD3 cells treated with 1µM FSK followed by DMSO (vehicle control) and concluded with maximum stimulation of cAMP via FSK/IBMX. FRET was either measured in the cytosol of non-ciliated cells with Arl13B-H187, the cytosol of ciliated cells with Arl13B-H187, or in the cilium with Arl13B-H187.**b** shows the change in fluorophore intensity upon drug addition. **c** shows the quantified data from **a,** normalised to maximum stimulation of FSK/IBMX. Bars show mean with SD. N=3 for experiments carried out in the cilia and cytosol of ciliated cells. N=2 for experiments in non-ciliated cells.

Next, cAMP-hydrolysing activity of PDEs was assessed in the presence of 100nM of PGE2 (**Figure 10**). cAMP-hydrolysing activity of PDE4 after PGE2 stimulation mirrored enzyme function after initial FSK addition. In contrast, PDE3 inhibition after PGE2 administration led to 20% increase in cAMP in cilia and in the cytosol of ciliated IMCD3, but did not result in any increase in cAMP levels in non-ciliated cells. The same observation was made for PDE2 inhibition as in the cilium and cell body of ciliated IMCD3 a ~16% increase in cAMP levels was detected, while minimal hydrolysing activity by PDE2 was measured in non-ciliated cells. These findings support the hypothesis that ciliated and non-ciliated IMCD3 may harbour different cAMP signalling profiles.

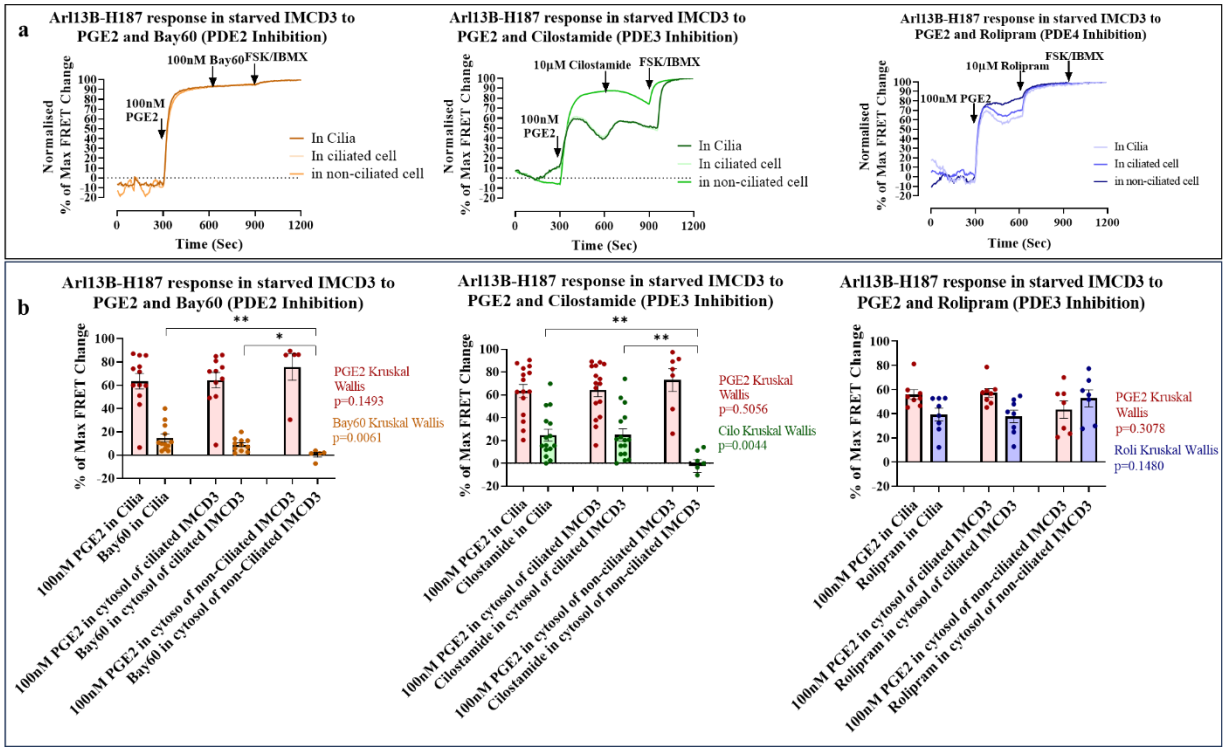

Figure 10: a shows example FRET traces for IMCD3 cells treated with 100nM PGE2 followed by either 10nM Bay60 (PDE2 inhibitor), 10 µM Cilostamide (PDE3 Inhibitor), or 10µM Rolipram (PDE4 inhibitor), and concluded with maximum stimulation of cAMP via FSK/IBMX. FRET was either measured in the cytosol of non-ciliated cells with Arl13B-H187, the cytosol of ciliated cells with Arl13B-H187, or in the cilium with Arl13B-H187. **b** shows the quantified data from **a,** normalised to maximum stimulation of FSK/IBMX. Each data point is one coverslip. N=3, where n is one day of imaging (cells from different flask passages). Kruskal-Wallis was used to test for non-parametric significance. Data shows mean with SD. Multiple comparison was carried out using Dunn's post hoc test.

While PDE4 was found to localise to the cilium at AKAP150(Choi et al. 2011a), and thus, equal hydrolysis of cAMP by PDE in the cilium and the cytosol of IMCD3 supports this finding, there is no evidence of PDE2 and PDE3 localising to the organelle. Yet FRET results using Arl13b-H187 reported no difference in cAMP increase upon PDE2 or PDE3 inhibition between the cytosol and the cilium of the cell, which could not be possible unless PDE2 or PDE3 localised to the organelle, or unless cAMP equilibrium between the cytosol and cilia is rapidly achieved. Regardless, these findings are in line with results reported by Jiang et. al, who also used Arl13b-H187 to measure cAMP in the cilium and concluded there was no difference between cAMP signalling between the cytosol and the cilium and suggest that the transition zone of the organelle is permeable to second messengers. However, FRET reporters are not the only optogenetic tools available to study cAMP signalling, and studies implicating

light-activated adenylyl cyclases (bPACs) localising to the cilium and the cytosol have indeed demonstrated differential cAMP activity between the two subcompartments.(Truong et al. 2021)

There are several explanations to why FRET reporters may not be sensitive enough to detect robust change in ciliary cAMP signalling compared to the cytosol. As aforementioned, the surface area to volume ratio of the cilium could allow for the generation of high concentrations of cAMP, and indeed Moore et al. demonstrated higher basal concentrations of cAMP at the cilium compared to the cytosol of MEFs.(Moore et al. 2016) Thus one hypothesis is that cAMP diffusion from the cilium into the cytosol, which usually occurs in the range of 10-780$\mu m^2/s$(Agarwal, Clancy, and Harvey 2016; Lohse et al. 2017), and could even be faster if cAMP is moving down its concentration gradient, is not detected by FRET microscopy. Cilium length is on average 3-8μm, thus even with the slowest cAMP diffusion rate, and the longest cilium, FRET measurements, which occurred every 5 seconds, could still miss cAMP movement out of the organelle. To test this hypothesis, FRET imaging with an acquisition interval of 333milliseconds was attempted in an effort to observe cAMP diffusion, but still no change was observed between ciliary and cytosolic cAMP signalling (**Figure 11**).

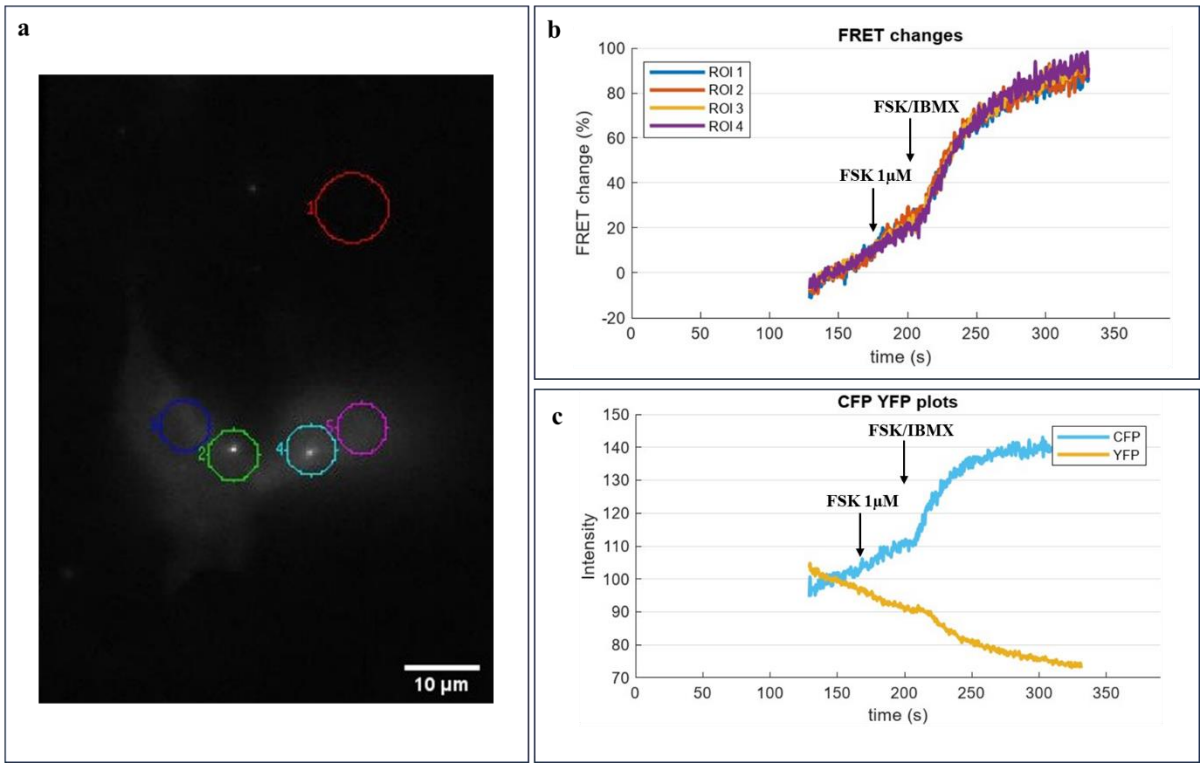

Figure 11: a image of IMCD3 expressing Ar13b-H187 in cilia (2 and 4 regions) and cytosol (3 and 5 regions). **b** example FRET traces from cilia (blue and yellow traces) and cytosol (red and purple) of an IMCD3 cell. **c** average fluorophore intensity trances for CFP and YFP. Experiments were carried out with fluorescent exposure every 333msec. Intracellular cAMP was stimulated with 1µM FSK and max saturation was achieved using FSK/IMBX. N=1 so no statistical analysis was carried out.

A second explanation is that Arl13b may direct the sensor to a ciliary domain that does not overlap with a ciliary cAMP nanodomain. However, in order to select an anchoring protein for a ciliary cAMP sensor able to detect very localised second messenger changes, one would need to know where in the cilium such cAMP nanodomains reside.

Discussion and Conclusion

Arl13B-H187 failed to detect a difference in ciliary versus cytosolic cAMP signalling. While this mirrored findings by Jiang et al (Jiang et al. 2019) it did not support results from Truong et al. demonstrating different cAMP levels between the two subcompartments using bPACs (Truong et al. 2021). However, the use of exogenous ACs to measure cAMP, may not truly reflect endogenous second messenger signalling. Overexpression of ACs might lead to mistargeting of these enzymes to domains they do not normally occupy, altering regulatory

mechanisms as a consequence and reporting non-physiological cAMP activity. Thus, we cannot exclude the possibility that, indeed, there is no difference between cAMP signalling in the cilium and the cytosol of the same cell.

Despite its shortcomings in confirming differences in cAMP signalling at the cilium and the cytosol, Arl13b-H187 proved useful in distinguishing ciliated from non-ciliated cells, and to test the hypothesis that the ciliary phenotype of a cell may have an impact on the cell's cAMP signalling activity. Indeed, after PGE2 stimulation, cAMP-hydrolysing activity was observed by all three PDEs in the cytosol and cilia of ciliated cells, but no increases in cAMP was observed upon PDE2 and PDE3 inhibition in non-ciliated cells. This discrepancy may hint at the possibility that cAMP and thus PDE hydrolysis of the second messenger may indeed be dependent on the ciliary phenotype, or position in the cell cycle, of individual cells. Additionally, these results may also suggest that a ciliary pool of PGE2-initiated cAMP is under the control of PDE3 and PDE2, supporting the hypothesis that perhaps cAMP signalling in the cilium and the cytosol do operate separately. Further, the fact that PDE2 and PDE3 do not hydrolyse cytosolic cAMP downstream of FSK, corroborates that their hydrolysing function is compartmentalised to a pool of cAMP downstream of PGE2. Indeed, using bPACs, Hansen et al have demonstrated that signalling downstream of ciliary cAMP has separate effects to cAMP signalling in the cytosol. As mentioned in the introduction, ADPKD is characterised by increased levels of cAMP, but little was previously known about which pool of the second messenger is responsible for renal cystogenesis. With the use of bPACs, Hansen et al proved, in vitro, that it is ciliary cAMP which drives cyst formation in this disease.(Hansen, Kaiser, Leyendecker, Stüven, Krause, Derakhshandeh, Irfan, Sroka, Preval, Desai, et al. 2022) If this is the case, then cysts generated by PGE2 stimulation in the cilium should be enhanced upon PDE3 or PDE2 inhibition. The following chapter focuses on the effects of enzyme inhibition on cyst formation, explored in a 3D in vitro model of cystogenesis.

Chapter 5: PDE pharmacological inhibition leads to altered cystic phenotype *In Vitro*

Introduction

An increase in cAMP drives cystogenesis in ADPKD and as thoroughly aforementioned, there is evidence implicating a variety of GPCRs to renal cyst formation. Excessive cell proliferation and fluid secretion into the cyst lumen propagate cyst growth, and cAMP plays a role in both these processes. In normal human kidney cells cAMP inhibits mitosis, but the reverse is true in disease, where cAMP stimulates PKD cells to grow.(Belibi et al. 2004) In the initial stages, cysts are isolated structures throughout renal tissue, but at end-stage ADPKD, the kidneys host very large and bloated fluid-filled cysts. Cysts can arise from all parts of the nephron, but dissection of ADPKD patient kidneys suggests the collecting ducts give rise to the most prominent renal cystogenesis, with individual cysts measuring 1mm or more in diameter.(Heggö 1966) cAMP propels abnormal renal cell proliferation via crosstalk with Ca^{2+}. In kidneys, AC5 and AC6 are the predominant synthesizers of cAMP and are enzymes normally inhibited by Ca^{2+}.(Shen et al. 1997) When mutations in the polycystins arise, ciliary and intracellular Ca^{2+} levels drop, stimulating AC activity. Thus, when intracellular Ca^{2+} is reduced, cAMP signalling is increased. In culture, epithelial cells from ADPKD patients have a basal $[Ca^{2+}]_i$ ~20nM lower than normal human kidney (NHK) cells. Decreased Ca^{2+} signalling enhances cell proliferation through a mechanism that has yet to be fully elucidated. One hypothesis is that a reduction of Ca^{2+} upregulates BRAF, which is normally repressed, and which triggers cAMP to activate MEK-ERK signalling.(Yamaguchi et al. 2004), Indeed, BRAF stimulation, specific to collecting ducts, was shown to induce cystogenesis in WT cells, and further aggravated cyst growth, inflammation, and fibrosis in slowly progressive PKD models.(Ramalingam et al. 2021) Treatment of healthy renal epithelial cells with Ca^{2+} channel blockers enhanced BRAF signalling and consequent cAMP and MEK/ERK activation. Furthermore, the MEK inhibitor, PD98059, effectively abolished

cell proliferation in response to cAMP agonists, a feat that was not observed upon receptor tyrosine kinase inhibitor, genistein.(Yamaguchi et al. 2000a) PKA inhibition via H89 also recapitulated these results.(Hanaoka and Guggino 2000) In a different study, human ADPKD cells treated with Ca^{2+} channel activator, Bay K8644, or the Ca^{2+} ionophore A23187, had increased intracellular Ca^{2+} and a restored anti-mitogenic response to cAMP.(Yamaguchi et al. 2006) In contrast, a study which used Bay 43-9006 to directly inhibit Raf and block cAMP upregulation in jck mice, a spontaneous model of recessive polycystic kidney disease brought about from a mutation in NEK8,(Menezes and Germino 2013) did not yield significant changes in disease development.(Yamaguchi et al. 2010) As Bay 43-9006 is a broad inhibitor of multiple kinases, it is conceivable that the lack of an effect on ADPKD progression may be due to its promiscuity. Additionally, B-RAF inhibition on ERK may be more complex than originally thought- as B-RAF and RAF-1 can heterodimerize, impacting the activity of both kinases.(Rushworth et al. 2006; Heidorn et al. 2010; Hatzivassiliou et al. 2010) Therefore, targeting B-RAF signalling may not be the best approach for tackling ADPKD. Strategies increasing intracellular Ca^{2+} are also being explored as possible treatment. Triptolide, a medicinal herb which is hypothesized to activate PC2 was shown to arrest the cell cycle in $PKD1^{-/-}$ cells and slow down cyst progression.(Leuenroth et al. 2008; Leuenroth et al. 2007) Finally, arresting the cell cycle indirectly through cyclin kinase inhibitors showed a promising decrease in cystogenesis, and improved renal function in jck mice.(Bukanov et al. 2006) These inhibitors had long-lasting effects, a useful characteristic for prolonged treatment.

Of importance, in healthy renal tissue, cAMP normally inhibits ERK and subsequent cell proliferation, and thus this mechanism is not the only process that must contribute to cystogenesis.(Hanaoka and Guggino 2000; Yamaguchi et al. 2000b) Another study implicated cAMP, and subsequent PKA phosphorylation, to upregulation of positive transcription elongation factor b (P-TEFb), an important regulator of transcription elongation. The P-TEFb/HEXIM1/7SK complex is normally inactive, but its phosphorylation by PKA was shown to stimulate this complex and increase cystogenesis in zebrafish models. In mice

models of ADPKD ($Pkd^{-/-}$), pharmacological inhibition of P-TEFb mitigates cystogenesis. Furthermore, P-TEFb is hyperactive in kidneys of ADPKD patients.(Sun et al. 2019) Thus cAMP may also play an independent role to Ca^{2+} or B-RAF to propagate cyst formation. In addition to P-TEFb, cAMP also activates cAMP response element-binding protein (CREB), a transcription factor that upregulates expression of ribosomal biogenesis and protein synthesis genes. Genetic and pharmacological inhibition of CREB showed delayed cystogenesis in ADPKD rodent models.(Liu et al. 2021) Upregulated CREB activity has also been linked to PC1 mutation and deletion.(Aguiari et al. 2012) Finally, the serine/threonine protein kinase Glycogen synthase kinase β positively regulates cAMP in response to Vasopressin signalling, in healthy renal murine cells.(Rao et al. 2010) Mice with collecting duct-specific KO of GSK3β show reduced AC activity, decreased cAMP, and defective urine concentration. GSK3β likely works in a positive-feedback loop with CREB and cAMP, whereby GSK3β stimulates cAMP activity and subsequent CREB transcription to express more GSK3β.(Kakade et al. 2016a) In ADPKD mice models, GSK3β renal expression progressively enhances with age, parallel to increased cAMP. KO of GSK3β in collecting ducts in cpk (mouse model with mutation in Cys1, the ortholog gene for Autosomal Recessive PKD) and kidney specific Pkd1 KO mice mitigated ADPKD. These results were recapitulated with pharmacological inhibition of GSK3β via 4-Benzyl-2-methyl-1,2,4-thiadiazolidine-3-5-dione (TDZD-8). GSK3β KO/inhibition resulted in a marked reduction in cyclin-D1 and c-Myc, suggesting the kinase works to propagate excess cell proliferation, contributing to cystogenesis.(Tao et al. 2015)

The second process driving cystogenesis, fluid secretion, works through Cl^- movement into the lumen of the cyst via Na-K-Cl contransporter (NKCC1) and the apical cystic fibrosis transmembrane conductance regulator (CFTR) chloride channel.(Sullivan, Wallace, and Grantham 1998; Grantham et al. 2006) cAMP functions in many secretory epithelia, including healthy collecting ducts and kidney tubules, to regulate Cl^- expulsion. Extracellular Cl^- enters the cell via basolateral NKCC1, raising the intracellular Cl^- concentration above the

electrochemical gradient which allows Cl^- efflux. When cAMP is present, CFTR channels are phosphorylated by PKA and activated, leading to NaCl flow into the cysts. Indeed, CFTR inhibitors administered to $PKD1^{-/-}$ mice renal organ cultures and to PKD $flox^{/1;KsP}$-Cre mice slowed cystogenesis.(Yang et al. 2008) Alternatively, Ouabain, an inhibitor of Na^+, K^+, -ATPase also stopped cAMP-dependent fluid secretion by cysts (Grantham et al. 1995), as well as anion expulsion by polarised ADPKD cell monolayers.(Mangoo-Karim et al. 1995) However, Ouabain would likely inhibit Na^+ absorption by kidneys, causing excess water loss. Additionally, ouabain was also shown to bind a specific site on the NA+, K+ ATPase, resulting in stimulation of the MEK/ERK pathway independently of cAMP or growth factors, suggesting ouabain as an ADPKD therapy may cause significant side effects.(Nguyen, Wallace, and Blanco 2007)

K^+ channels present in collecting ducts help regulate the chemical and electrochemical gradient used by active transports. ATP inhibits these channels while cAMP activates them. Cl^- drives osmotic movement of water into the cyst lumen via aquaporin channels. Aquaporin-2 (AP-2) localisation and subsequent activity is regulated by V2R signalling. As aforementioned, Arginine vasopressin (AVP) is a vital antidiuretic hormone that works through cAMP production, primarily in collecting ducts and the distal nephrons, the major sites of cystogenesis. AVP binds V2R receptors, increasing cAMP. Subsequent phosphorylation of AQP-2 by PKA leads to its insertion into the apical membrane, and channel upregulation. Renal cAMP levels are markedly higher in PKD animal models such as pcy mice, jck mice, PCK rats, and $PKD^{225/-}$ mice.(Torres et al. 2003; Smith et al. 2006; Torres et al. 2004; Yamaguchi et al. 1997) These elevated levels of the second messenger are thought to arise from overstimulation of the V2R receptor, which is also overexpressed in ADPKD models.(Torres et al. 2003; Torres et al. 2004; Nagao et al. 2006; Nagao et al. 2008) Several therapeutic strategies that are being considered for ADPKD target V2R. OPC-31260, a V2R antagonist, when given to ADPKD models such as $PKD2^{WS25/-}$ mice, PKC rats, and PCY mice decreased renal cAMP and reduced kidney volume, cyst area, blood urea nitrogen (BUN) as

well as number of mitotic and apoptotic cells, ultimately inhibiting disease progression. Additionally, OPC-31260 downregulated the B-RAF/MEK/ERK pathway.(Torres et al. 2003; Smith et al. 2006; Wang et al. 2005) Tolvaptan, a treatment in clinical trials for ADPKD, is a highly selective V2R antagonist, and showed similar affects to OPC-31260 when administered to animal models. (Wang et al. 2005) However, Tolvaptan clinical trials are showing significant side effects of this treatment, including thirst, polyuria, nycturia, polakisuria and polydipsia.(Torres et al. 2012; Torres et al. 2018)

Overall cAMP orchestrates multiple downstream functions to propagate renal cystogenesis in ADPKD. Various therapies targeting these subsequent effects of the second messenger are being explored as treatment. Many of these options, however, show negligible reduction in disease progression or come with significant side effects. Targeting just one branch downstream of second messenger signalling does not seem like a comprehensive strategy for developing a therapy for ADPKD. cAMP is a highly compartmentalised signalling pathway, regulated by several downstream players, such as PDEs, which breakdown the second messenger at specific subcellular domains. Thus, therapies aiming at localised pools of cAMP or specific PDE isoforms driving cyst formation could be more effective approaches for curing ADPKD. Indeed, long-form PDE4 activators show promise in reducing cystogenesis in vitro.(Omar et al. 2019) Yet, while we know that GPCR signalling propagates various cAMP signals throughout the cell, data still reports inconclusive results regarding exact mechanisms of how cAMP drives cyst growth, or which PDEs regulate these specific pools of second messenger. Thus, in this chapter, to understand cAMP compartmentalisation in ADPKD, cystogenesis was simulated in vitro, and the consequences of GPCR signalling as well as PDE inhibition were investigated in these preparations.

Protocols which mimic in vitro 3D cystogenesis have been established and are often implemented to study PKD. The principle of the assays is to grow renal cells such as IMCD3, in a 3D collagen/Matrigel mix and induce cyst growth through an increase in intracellular

second messenger. Several agents can be used to stimulate cAMP levels, FSK and PGE2 are both known inducers of in vitro cystogenesis. However, G_{α} -coupled GPCRs can also raise intracellular cAMP significantly, and may also propagate cyst growth in vitro.

For example, adenosine receptors bind extracellular adenosine. Two types of adenosine GPCRs, A2A and A2B, signal through $G_{\alpha s}$.(Jacobson et al. 2012) In certain stress conditions, such as hypoxia, or upon GPCR stimulation, ATP is converted to AMP by ectonucleoside triphosphate diphosphohydrolase (CD39) then into adenosine by ecto-5'-nucelotidases (CD73). Adenosine can also occur intracellularly under hypoxic conditions, travelling across the cell membrane via nucleoside transporters in order to bind signalling receptors.(Kishore, Robson, and Dwyer 2018) Additionally, it can be created through the extracellular cAMP adenosine pathway.(Jackson and Raghvendra 2004; Oyarzún et al. 2017; Kishore, Robson, and Dwyer 2018) In this third alternative, the activation of ACs by other (non-adenosine) $G_{\alpha s}$ -GPCRs increases intracellular cAMP which is converted into AMP by PDEs or exonucleases, then dephosphorylated by 5'nucleotidases. The resulting adenosine binds A2A and A2B receptors resulting in a positive feedback loop of cAMP signalling.(Jackson and Raghvendra 2004) Adenosine signalling is important for renal vasoconstriction and for regulating local renin production.(Oyarzún et al. 2017) Relevant to ADPKD, the adenosine pathway has been shown to promote cell proliferation in various tissues, including primary human and cultured rat collecting duct.(Jackson et al. 2003) (Jackson and Gillespie 2013) Despite various evidence suggesting adenosine receptors play a role in ADPKD progression, the P1 purinergic GPCRs have not garnered much attention compared to P2Y receptors in the context of ADPKD. However, it is possible, in vitro, stimulation of adenosine receptors could result in cystogenesis.

Other GPCRs which could stimulate in vitro cyst formation are adrenergic receptors. Both adrenaline and noradrenaline are released by sympathetic nerve fibres near proximal and distal tubules, loops of Henle, and collecting ducts. These hormones act on two adrenergic

receptors, α and β. β1 and β2 signal through $G_{\alpha s}$ while β3 can function via both $G_{\alpha s}$ and $G_{\alpha i}$. Epinephrine was shown to produce the greatest increase in receptor-mediated cAMP in human ADPKD as well as ARPKD cells, with this effect entirely muted when the same cells were treated with β-blockers. (Belibi et al. 2004) Denervation of the kidneys in Han:SPRD cy/+ rats diminished cyst size and volume density, as well as systolic blood pressure, overall improving organ function.(Gattone et al. 2008) Indeed, CKD patients have enhanced noradrenaline levels as well as sympathetic nerve activity. Yet, adrenergic signalling in renal cystogenesis has hardly been explored. In this chapter we test whether adrenergic or adenosine stimulation could propel in vitro cyst formation, in a further effort to characterise the contribution of cAMP compartmentalisation in renal cystogenesis.

Results 1-Establishing a cystogenesis model in vitro

Several agents can be used to stimulate cAMP levels, inducing in vitro cyst growth. As different GPCRs are linked to distinct cAMP pools, I sought to test a number of agonists which could potentially signal downstream pools of cAMP responsible for cystogenesis. Indeed, a few GPCRs linked to possible renal cyst formation, such as Purinergic receptors and β-adrenergic receptors, were tested to establish whether they would yield in vitro cysts (**Figure 12**). Unfortunately, purinergic signalling, upon treatment of IMCD3 with Adenosine 2A agonist, did not contribute to cyst formation in these assays (**Figure 12a, b**). However, β-adrenergic signalling via Isoproterenol did show a small concentration-dependent increase in cystogenesis (**Figure 12c, d**).

While the finding that Isoproterenol stimulated mild cystogenesis in a concentration-dependent fashion would have been interesting to pursue further, due to time constraints, in vitro cysts for consequent assays were induced via FSK or PGE2, the most common and successful cAMP-raising agents used to achieve the cystic phenotype.(Omar et al. 2019) In addition, in Chapter 4 we tested cAMP-hydrolyses, by PDEs, downstream of FSK and PGE2 signalling, and were therefore curious to see how this measured PDE activity translated to in

vitro cyst formation. Thus, **Figure 13** shows concentration dependent growth of cysts in the presence of FSK or PGE2. Patterns of cystogenesis differ slightly between PGE2 or FKS-stimulated cysts- with PGE2-derived growth manifesting in increased cystic area of smaller-diameter cysts (**Figure 13a**), while FSK-induced cystogenesis displays larger independent blebs (**Figure 13c**). Both FSK and PGE2-stimulated cysts were tested, alongside PDE inhibitors, to investigate which enzymes are responsible for the breakdown of cyst-generating pools of cAMP.

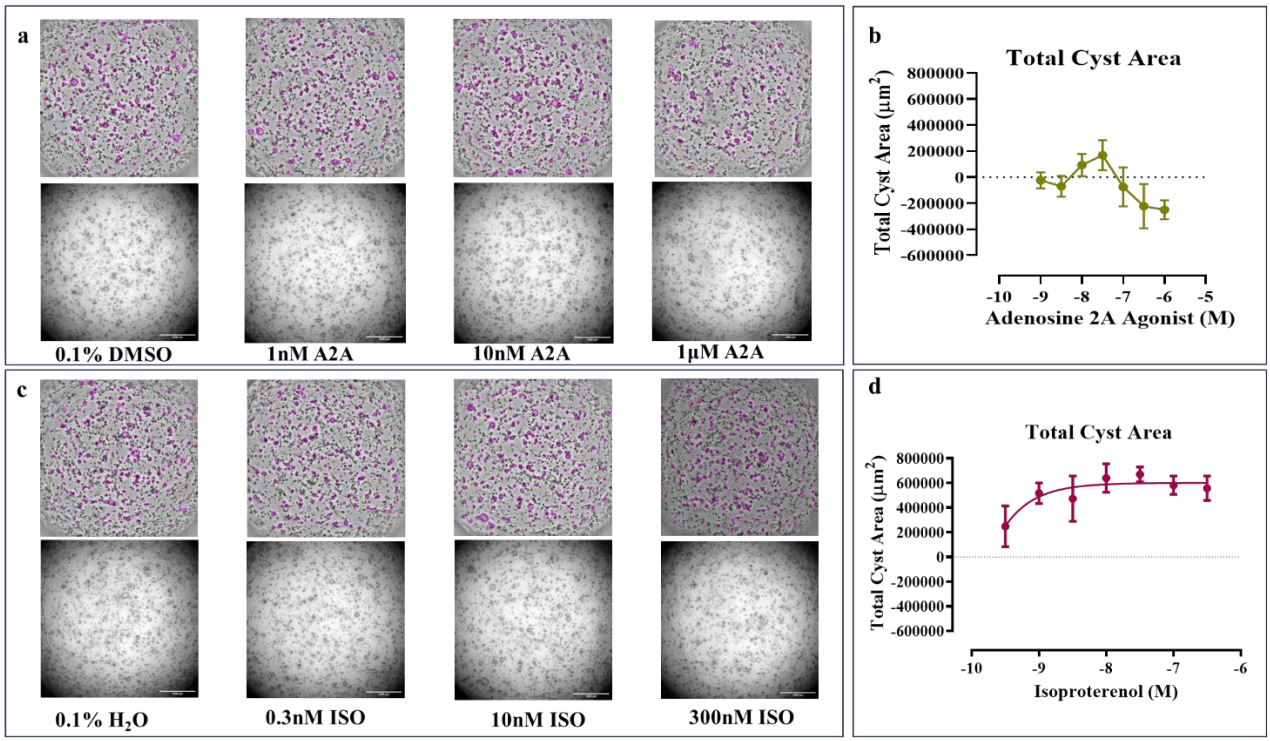

Figure 12: shows concentration dependent growth of cysts in the presences of Adenosine 2A Agonist with (above) and without (below) the mask threshold applied to produce a quantified analysis. **b** shows the quantified analysis for **a**. **c** shows concentration dependent growth of cysts in the presences of Isoproterenol with (above) and without (below) the mask threshold. **d** shows analysis of **c**. Each data point represents the mean of n with SD. N=2, where n is an independent 96 well plate with cells from different flask passages. Scalebar depicts 1000µm.

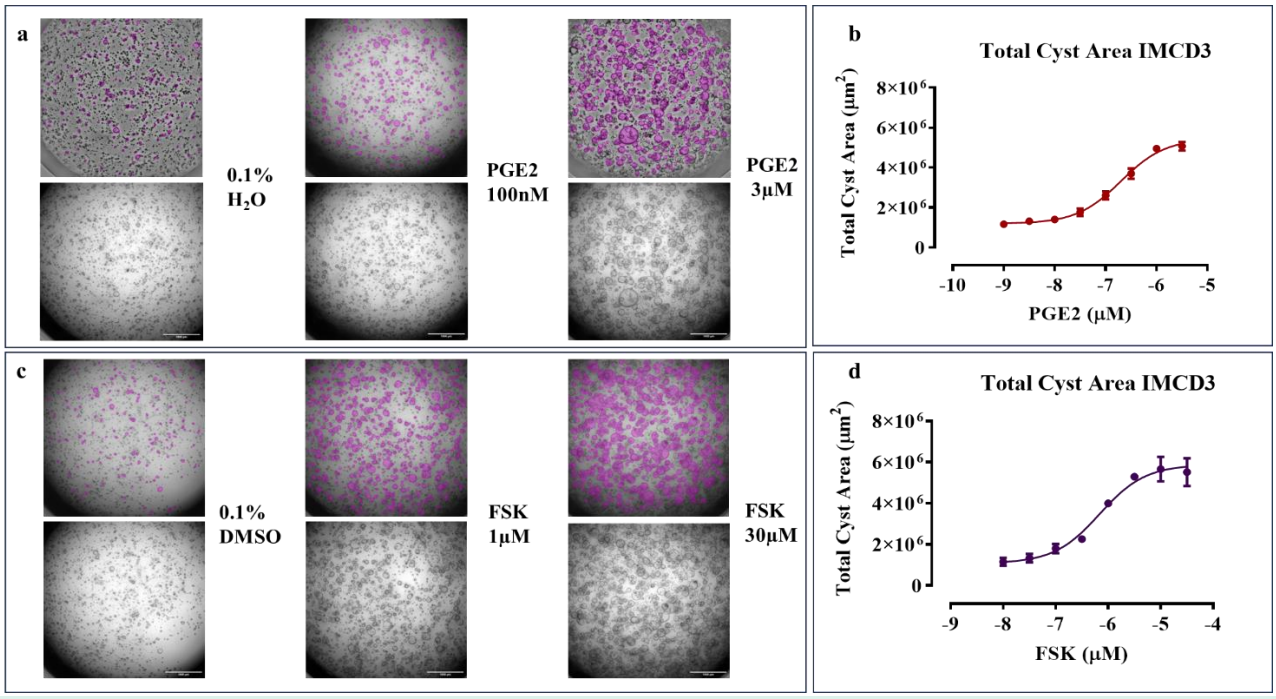

Figure 13: a shows concentration dependent growth of cysts in the presences of PGE2 with (above) and without (below) the mask threshold applied to produce a quantified analysis. **b** shows the quantified analysis for **a**. **c** shows concentration dependent growth of cysts in the presences of FSK with (above) and without (below) the mask threshold. **d** shows analysis of **c**. Each data point represents the mean of

n with SD. N=2, where n is an independent 96 well plate with cells from different flask passages. Scalebar depicts 1000µm.

Results 2-PDEs Regulate Cyst Growth

PDEs breakdown cAMP, and cAMP drives cystogenesis, thus it is expected that inhibition of the enzymes which eliminate cAMP should lead to aggravated cyst growth, while the activation of such enzymes would mitigate it. Indeed, novel activators of long-form PDE4 are being explored as potential therapeutic targets for PKD.(Omar et al. 2019) However, while it is known PDE4 hydrolyses a prominent pool of cAMP relevant to cystogenesis, other PDE isoforms and their role in cyst progression has not yet been fully characterised. Thus, an in vitro cyst assay was generated using PGE2 to stimulate cAMP in 3D-cultured IMCD3, and cells were subsequently treated with either PDE2 (Bay60), PDE3 (Cilostamide), or PDE4 (Rolipram) inhibitor, to study the effects of enzyme inhibition on cystogenesis (**Figure 14, 15,16**). Indeed, as expected, inhibition of PDE4, which is the main hydrolyser of cAMP in IMCD3, led to significantly exacerbated cyst growth (**Figure 14**). PDE2 inhibition via Bay60 also led to a slight enhancement in cystogenesis, and a significant increase in cyst number (**Figure 15**). Finally, no significant change in cystic growth was observed with Cilostamide treatment, the PDE3 inhibitor, regarding total cyst area, though a significant decrease in average cyst area was measured (**Figure 16**). This latter finding may be explained due to the non-significant but concentration-dependent increase in cyst number upon PDE3 inhibition (**Figure 16.d**), decreasing average cyst size despite total cyst area remaining constant.

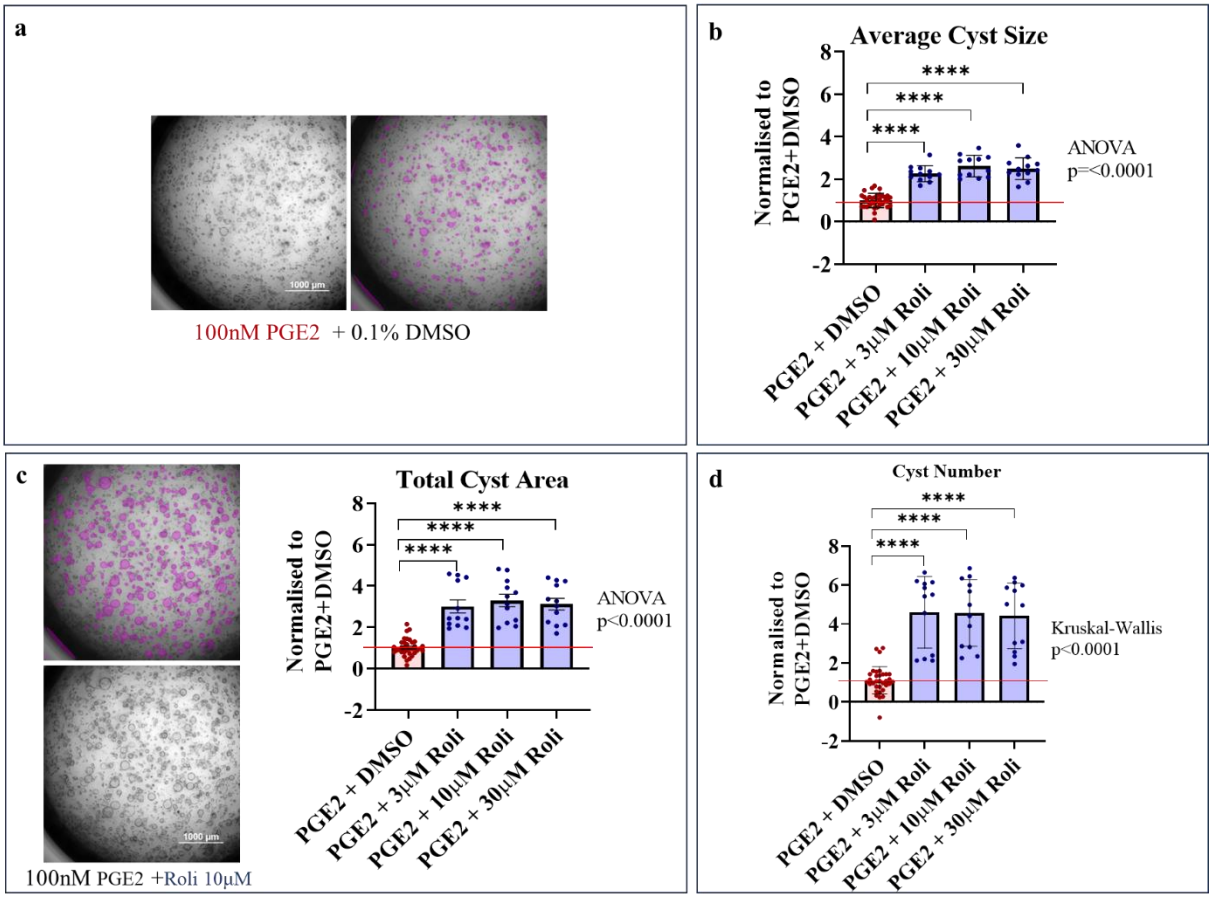

Figure 14: a shows unmasked (left) and masked (right) images of control wells treated with 100nM PGE2 and DMSO. b is average cyst size in wells treated with 100nM PGE2 and Rolipram concentrations (calculated by dividing total cyst area (c) by cyst number (d)). **c** is total cyst area in wells treated with 100nM PGE2 and Rolipram concentrations. **d** is total cyst number in wells treated with 100nM PGE2 and Rolipram concentrations. Each data point represents one well. N=3, where n is an independent flask passage. ANOVA was used for statistical analysis of normally distributed data. Kruskal-Wallis was used to test non-parametric data. Data shows mean with SD. Multiple comparisons were carried out with Tukey's multiple comparisons test for parametric data and Dunn's post hoc test for non-parametric data.

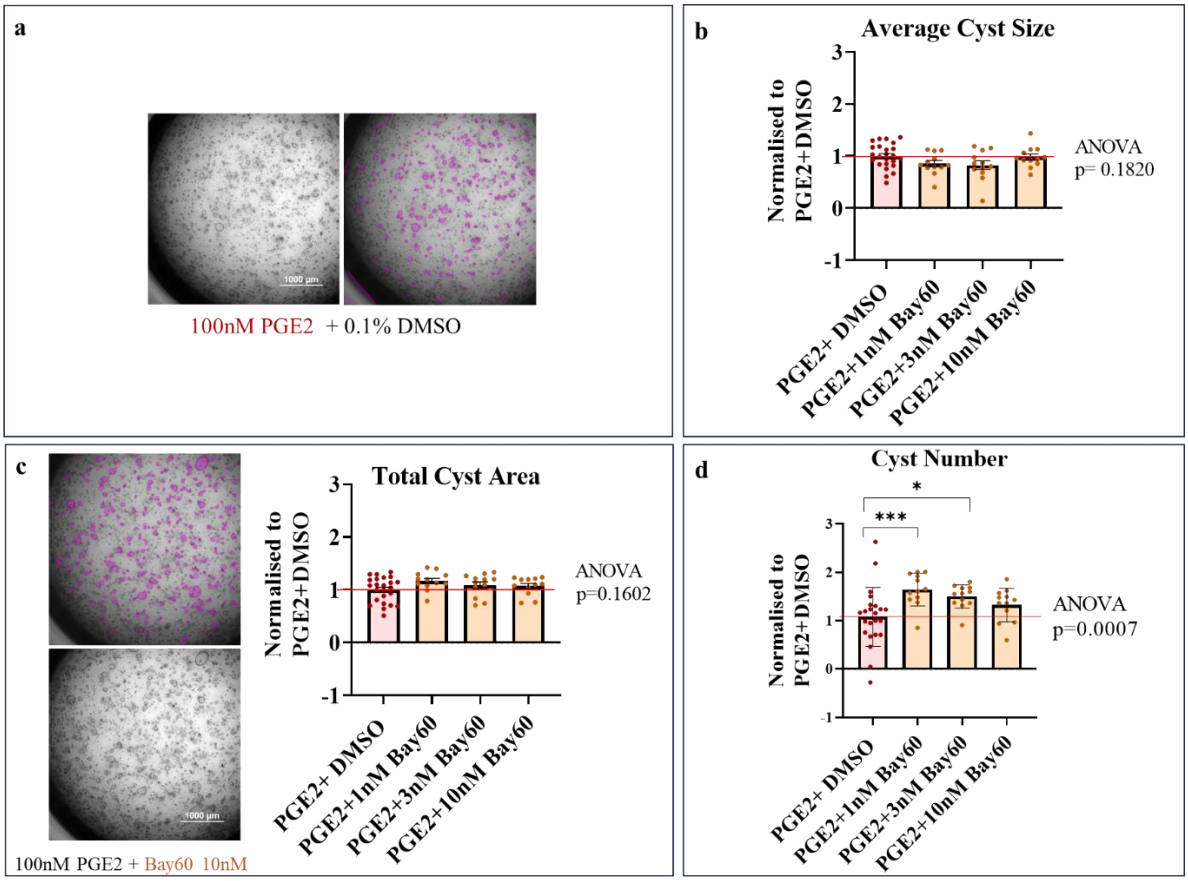

Figure 15: a shows unmasked (left) and masked (right) images of control wells treated with 100nM PGE2 and DMSO. **b** is average cyst size in wells treated with 100nM PGE2 and Bay60 concentrations (calculated by dividing total cyst area (c) by cyst number (d)). **c** is total cyst area in wells treated with 100nM PGE2 and Bay60 concentrations. **d** is total cyst number in wells treated with 100nM PGE2 and Bay60 concentrations. Each data point represents one well. N=3, where n is an independent flask passage. ANOVA was used for statistical analysis of normally distributed data. Data shows mean with SD. Multiple comparisons were carried out with Tukey's multiple comparisons test.

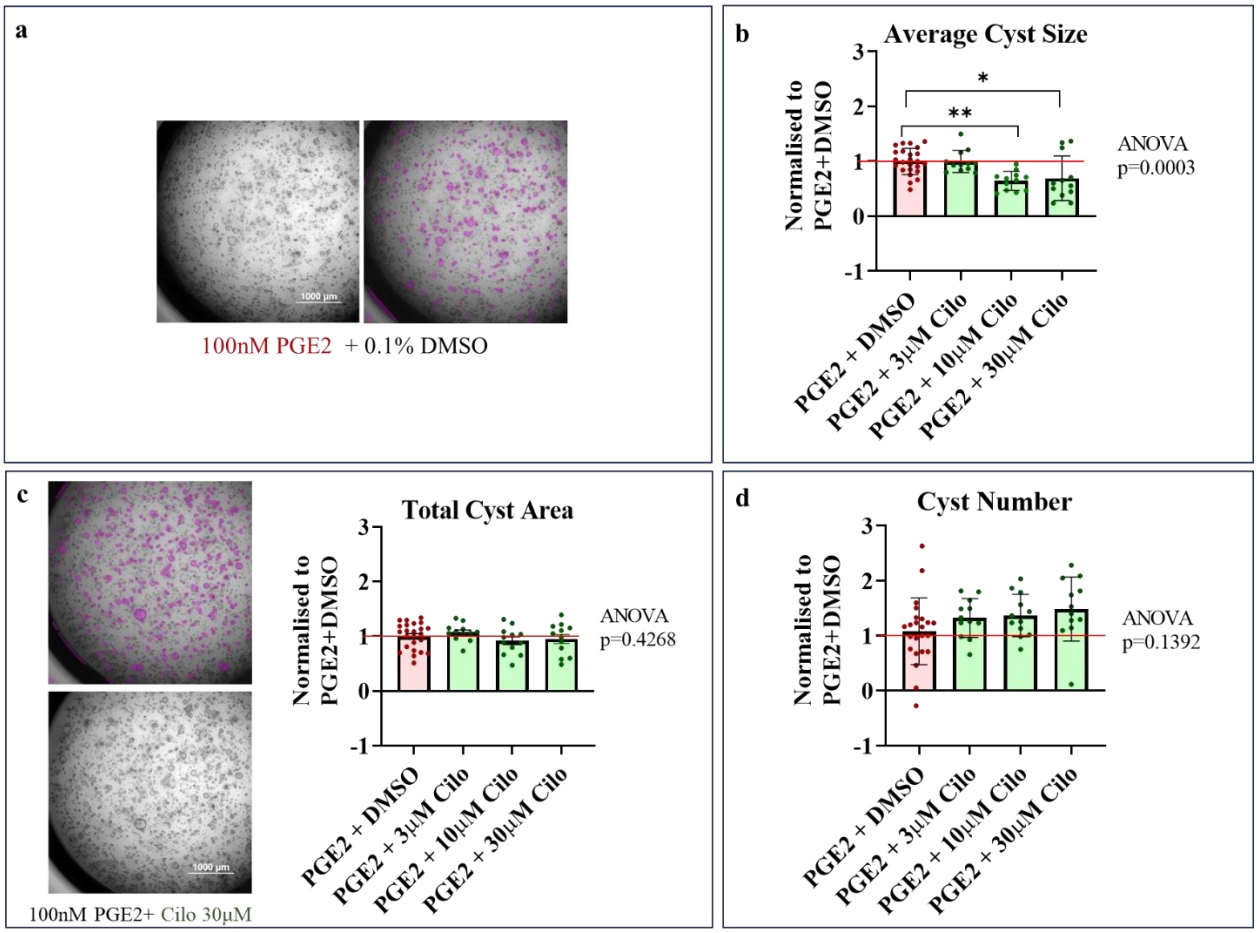

Figure 16: a shows unmasked (left) and masked (right) images of control wells treated with 100nM PGE2 and DMSO. **b** is average cyst size in wells treated with 100nM PGE2 and Cilostamide concentrations (calculated by dividing total cyst area (c) by cyst number (d)). **c** is total cyst area in wells treated with 100nM PGE2 and Cilostamide concentrations. **D** is total cyst number in wells treated with 100nM PGE2 and Cilostamide concentrations. Each data point represents one well. N=3, where n is an independent flask passage. ANOVA was used for statistical analysis of normally distributed data. Data shows mean with SD. Multiple comparisons were carried out with Tukey's multiple comparisons test.

We next tested PDE inhibition in FSK-stimulated cystogenesis (**Figure 17,21,22).** PDE4 inhibition once again aggravated cyst formation significantly (**Figure 17**) as expected, though not to the same magnitude as was observed with PGE2-driven cysts (**Figure 18)**. To show how PDE4 inhibition in in vitro cyst formation and PDE4 cAMP-hydrolysing activity correlated, a statistical comparison of cAMP generated upon PDE4 inhibition, downstream of 1μM FSK or 100nM PGE2, was made from previous FRET experiments (**Figure 19**). PDE4 inhibition downstream of 1μM FSK did generate significantly more cAMP in the cilium than downstream of 100nM PGE2. To confirm PDE4 activity downstream of PGE2 and FSK was stimuli-dependent, and not due to the combination of one stimuli and PDE4 inhibition

saturating the cell with cAMP, before the full effect of PDE4 inhibition could be measured, a statistical comparison of cAMP increase after 1µM FSK or 100nM PGE2 was also performed (**Figure 20a**). Though not significant, 100nM PGE2 enhances ciliary cAMP in the cilium to a greater extent than 1µM FSK, suggesting Rolipram only increases cAMP significantly in the cilium, downstream of 1µM FSK, simply because the range of cAMP change available is greater after 1µM FSK as compared to 100nM PGE2. The degree of cystogenesis between FSK or PGE2-derived cysts was also compared (**Figure 20b**) and showed that 100nM PGE2 stimulates markedly less total cyst formation compared to 1µM FSK. This suggests, once more, that PDE4 inhibition may aggravate PGE2-derived cysts to a greater extent, because the range of cyst growth available in PGE2-derived in vitro cystogenesis is greater than in 1µM FSK-derived cyst formation.

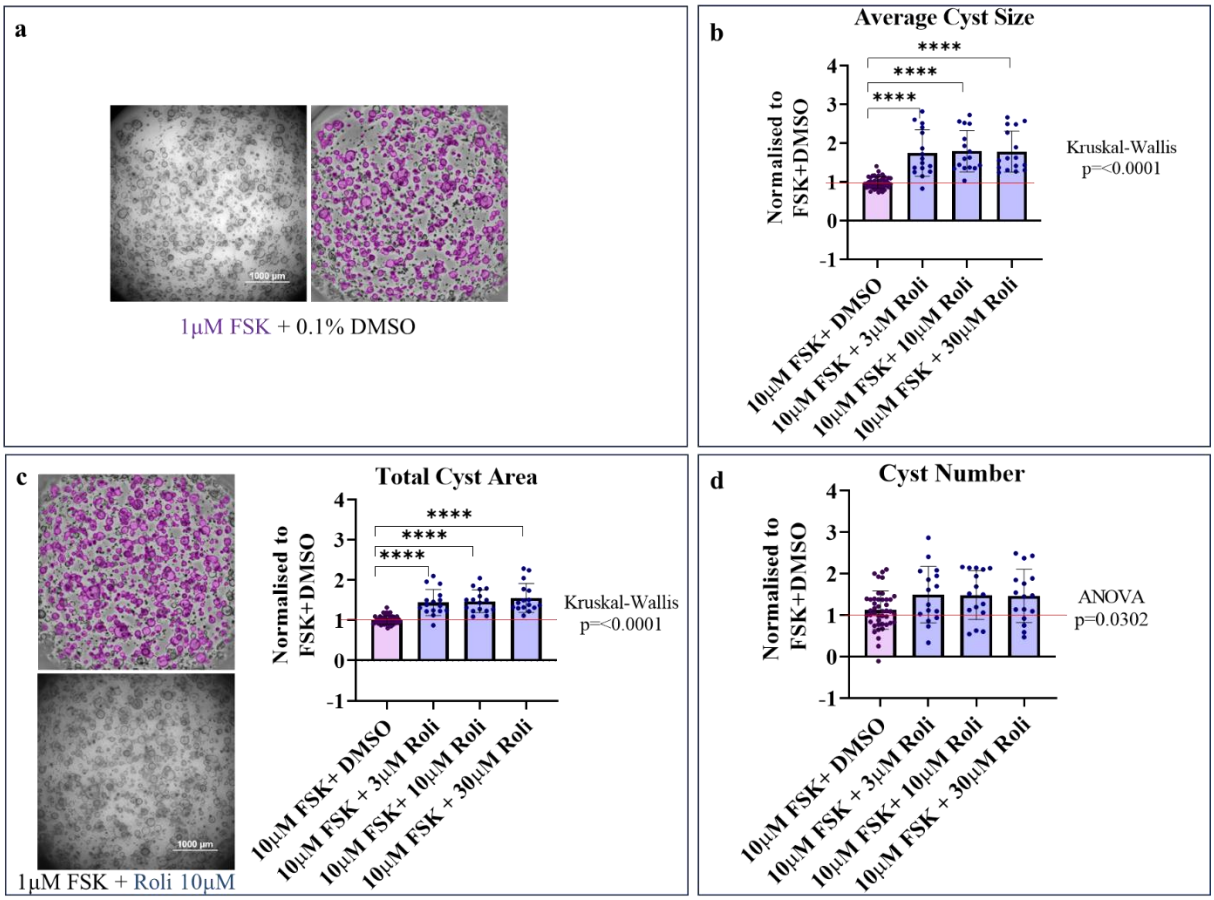

Figure 17: a shows unmasked (left) and masked (right) images of control wells treated with 1µM FSK and DMSO. **b** is average cyst size in wells treated with 1µM FSK and Rolipram concentrations (calculated by dividing total cyst area (c) by cyst number (d)). **c** is total cyst area in wells treated with 1µM FSK and Rolipram concentrations. **D** is total cyst number in wells treated with 1µM FSK and Rolipram concentrations. Each data point represents one well. N=4, where n is an independent flask passage. ANOVA was used for statistical analysis of normally distributed data, Kruskal-Wallis for non-

parametric data. Data shows mean with SD. Multiple comparisons were carried out with Tukey's multiple comparisons test for parametric data and Dunn's post hoc test for non-parametric data.

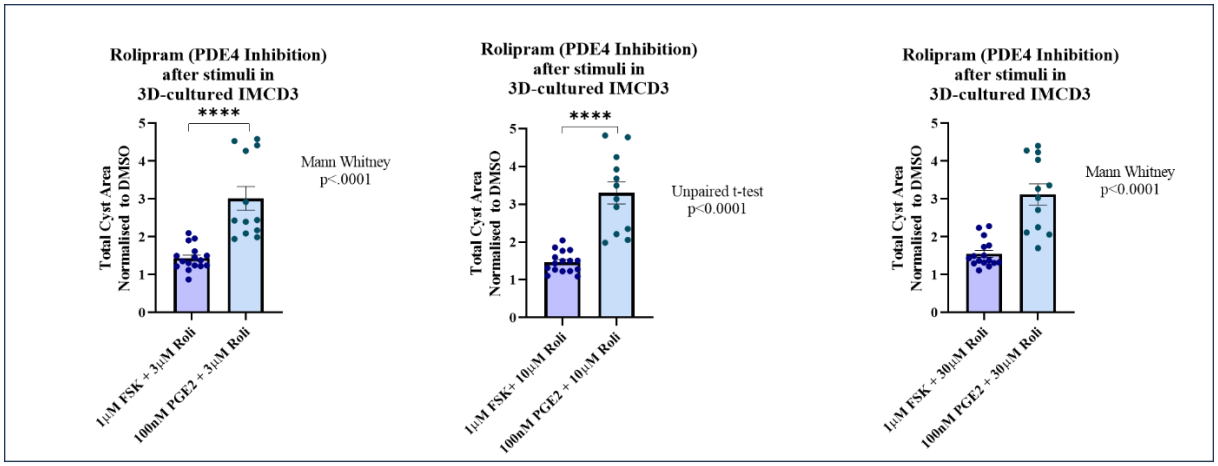

Figure 18: Comparison of cystogenesis induced upon PDE4 Inhibition (Rolipram) in FSK-derived versus PGE2-induced cyst assays, at increasing concentrations of Rolipram. Each data point represents one well. N=4 for FSK experiments. N=3 for PGE2 experiments. Parametric data was tested using unpaired t-test, while Mann Whitney test was applied to non-parametric data. Bars show mean with SD

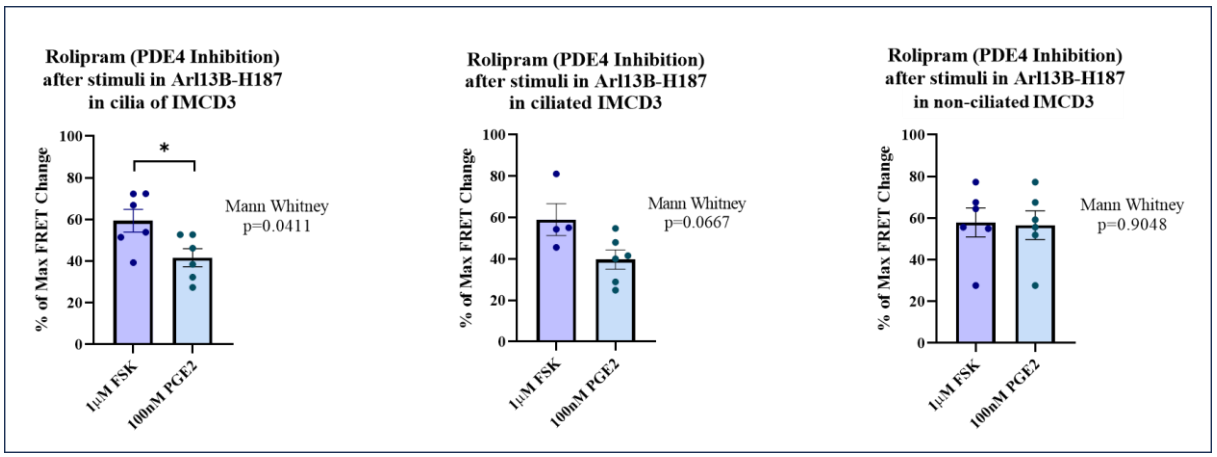

Figure 19: Comparison of PDE4 cAMP-hydrolysing activity measured via Arl13B-H187 in cilia of IMCD3, ciliated IMCD3, or non-ciliated IMCD3 that were first stimulated with either FSK or PGE2. Each datapoint represents a single coverslip. N=3, where n is one round of experimentation from an independent flask passage. Non-parametric data was analysed using Mann Whitney test. Bars show mean with SD.

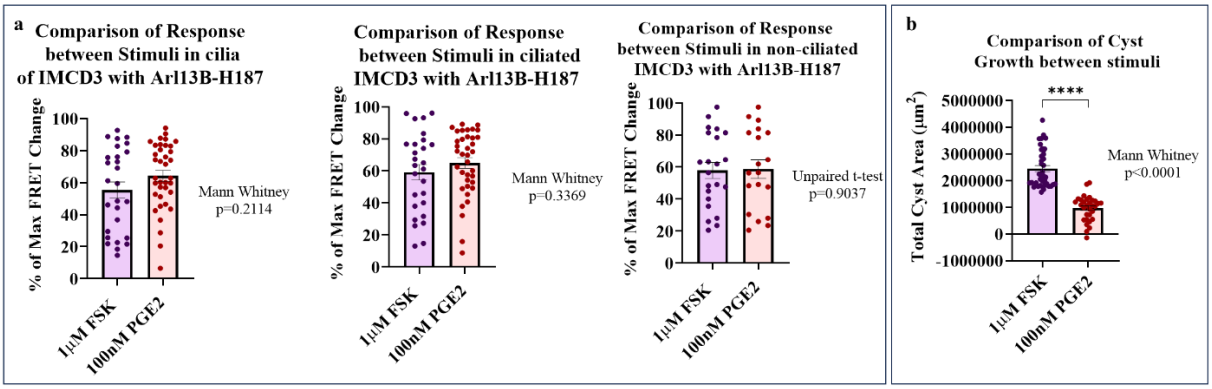

Figure 20: a comparison of cAMP increase, as measured via Arl13B-H187 in cilia of IMCD3, ciliated IMCD3, or non-ciliated IMCD3, in response to 1μM FSK or 100nM PGE2. **b** degree of cystogenesis compared for 1μM FSK versus 100nM PGE2 stimulation. Parametric data was tested using unpaired t-test. Non-parametric data was tested with Mann Whitney test. Bars show mean with SD. Datapoints are single coverslips. N=3, where n is one round of experimentation from an independent flask passage.

While PDE2 was shown to readily hydrolyse a small pool of cAMP downstream of PGE2 signalling (**Figure 10b**), minimal cAMP enhancement was observed in cilia of IMCD3, ciliated IMCD3, or non-ciliated IMCD3 when this enzyme was inhibited after initial stimulation with FSK in FRET experiments with Arl13b-H187, in chapter 4 (**Figure 8b**). Therefore, just as the 16% increase in cAMP after PGE2 stimulation and subsequent PDE2 inhibition led to a comparable increase in cystic wells subjected to the same treatment, FSK-induced cysts treated with PDE2 inhibitor (Bay60) led to no change in total cyst growth, reflecting the negligible change in intracellular cAMP (**Figure 21c**). However, PDE2 inhibition in FSK-derived cysts did significantly decrease average cyst size in a concentration dependent manner (**Figure 21b**). This observed effect is likely due to the fact that PDE2 inhibition also markedly multiplied cyst number in FSK-induced in vitro cystogenesis (**Figure 21d**), thus reducing cyst size while not affecting total cyst area.

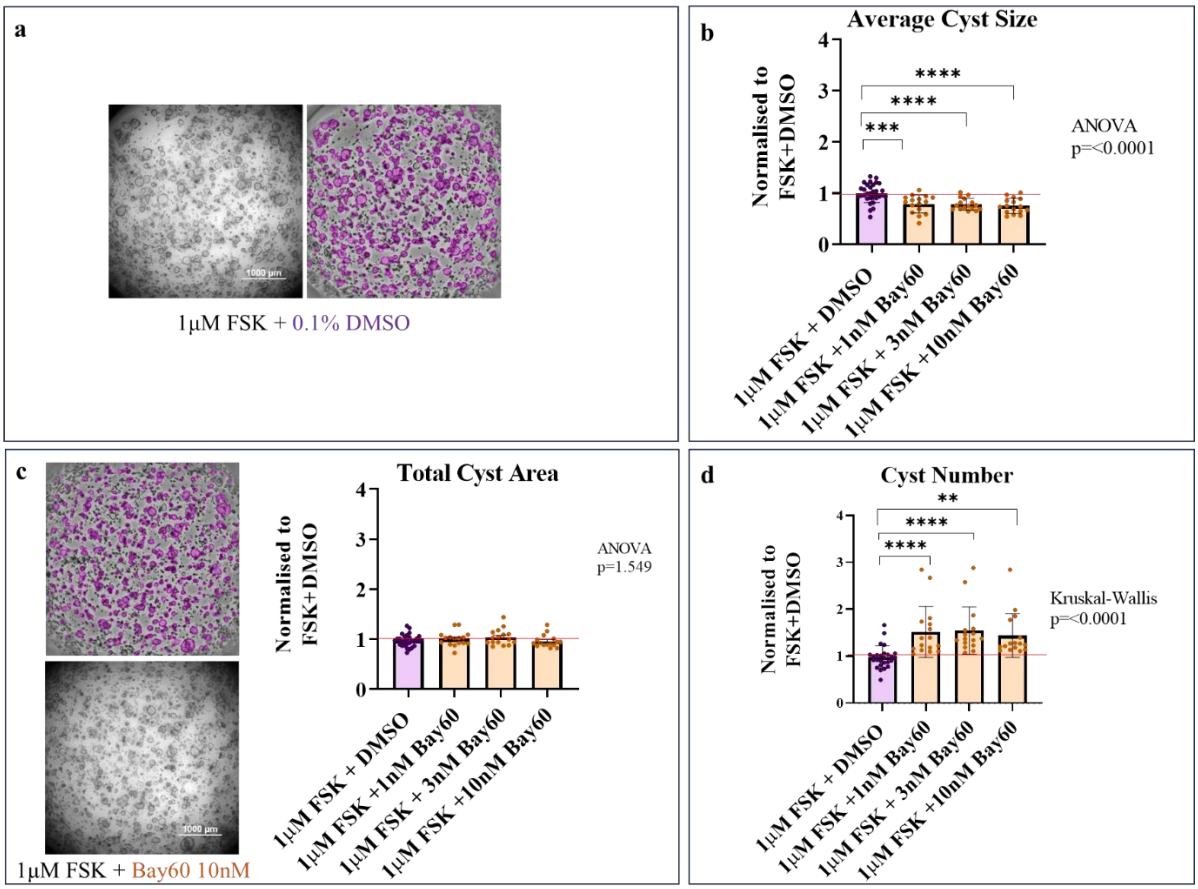

Figure 21: **a** shows unmasked (left) and masked (right) images of control wells treated with 1µM FSK and DMSO. **b** is average cyst size in wells treated with 1µM FSK and Bay60 concentrations (calculated by diving total cyst area (c) by cyst number (d)). **c** is total cyst area in wells treated with 1µM FSK and Bay60 concentrations. **D** is total cyst number in wells treated with 1µM FSK and Bay60 concentrations. Each data point represents one well. N=4, where n is an independent flask passage. ANOVA was used for statistical analysis of normally distributed data, Kruskal-Wallis for non-parametric data. Data shows mean with SD. Multiple comparisons were carried out with Tukey's multiple comparisons test for parametric data and Dunn's post hoc test for non-parametric data.

Unexpectedly, PDE3 inhibition via Cilostamide treatment led to a significant and concentration dependent decrease in total cyst area (**Figure 22c**). This finding is in contrast with the observation that PDE3 inhibition in IMCD3, was found to have no effect on bulk intracellular cAMP after FSK, as detected with Arl13b-H187, in chapter 4 (**Figure 8b**). PDE3 inhibition did not have a significant effect on cyst number (**Figure 22b**), but did markedly reduce average cyst size. Thus, PDE3 inhibition decreased both total and average cyst size in in vitro cysts generated via FSK stimulation.

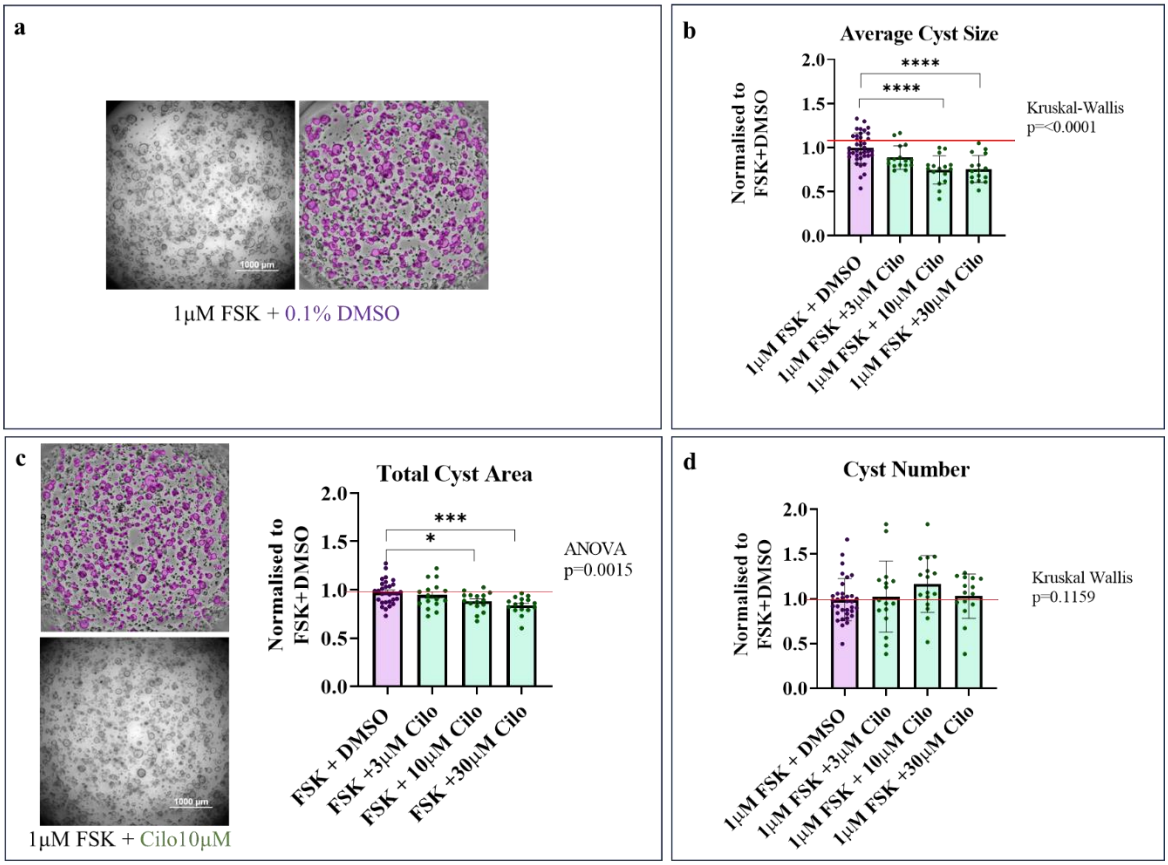

Figure 22: a shows unmasked (left) and masked (right) images of control wells treated with 1µM FSK and DMSO. **b** is average cyst size in wells treated with 1µM FSK and Cilostamide concentrations (calculated by diving total cyst area (c) by cyst number (d)). **c** is total cyst area in wells treated with 1µM FSK and Cilostamide concentrations. **D** is total cyst number in wells treated with 1µM FSK and Cilostamide concentrations. Each data point represents one well. N=4, where n is an independent flask passage. ANOVA was used for statistical analysis of normally distributed data, Kruskal-Wallis for non-parametric data. Data shows mean with SD. Multiple comparisons were carried out with Tukey's multiple comparisons test for parametric data and Dunn's post hoc test for non-parametric data.

Discussion and Conclusions

It is established knowledge that cAMP drives cyst formation in ADPKD, with recent studies suggesting it is a pool of ciliary cAMP which specifically propagates cystogenesis.(Hansen, Kaiser, Leyendecker, Stüven, Krause, Derakhshandeh, Irfan, Sroka, Preval, Desai, et al. 2022) PDEs hydrolyse cAMP and thus their inhibition should further increase intracellular second messenger, and should therefore also aggravate cyst formation. Indeed, PDE4 inhibition has previously been shown to exacerbate cystogenesis in vitro (Omar et al. 2019), but paradoxically, PDE inhibition via IBMX, in the same studies, has hinted to be cyst-protective.(Hansen, Kaiser, Leyendecker, Stüven, Krause, Derakhshandeh, Irfan, Sroka, Preval, Desai, et al. 2022) Since cAMP is a highly compartmentalised second messenger, it is

possible that its presence in one subcellular locale may lead to the opposite downstream effects of cyclic nucleotide signalling in a different subdomain. PDEs are part of a big family of enzymes, whereby individual isoforms differ in cAMP-hydrolysing activity as well as tissue expression and subcellular localisation.(Bender and Beavo 2006) Therefore, we sought to characterise PDE isoforms' role on cyst formation in in vitro cyst assays, to see how individual enzyme isoforms affected cyst growth.

PDE4 inhibition, as expected, led to increased cyst formation in both PGE2 (**Figure 14**) and FSK-derived cysts (**Figure 17**). However, Rolipram did aggravate cystogenesis more, in assays stimulated with PGE2 rather than FSK (**Figure 18)**, suggesting PDE4 may function downstream of PGE2 signalling to regulate cyst growth. However, upon closer analysis, when the response to Rolipram after PGE2 or FSK is compared from FRET experiments (**Figure 19**), there is greater cAMP hydrolysing activity from PDE4 after FSK stimulation rather than PGE2, in cilia and the cell body of ciliated cells, thus questioning this hypothesis. If we contrast FSK versus PGE2 stimulation of cysts, while the levels of intracellular cAMP they raise, measured with Arl13B-H187, in IMCD3, is comparable, the degree of cystogenesis induced by 1μM FSK is markedly higher than that generated by 100nM PGE2 (**Figure 20**). Though this data should be taken with cation, as analysis parameters for labelling objects as "cysts" differed between PGE2 and FSK experiments, as the two stimuli gave rise to slightly different cyst patterns. Overall, as PDE4 inhibition appears to saturate both cAMP and cystic growth after either agonist, it is likely Rolipram treatment may aggravate cyst formation to a higher degree in PGE2-induced cysts, simply because there is a greater opportunity for cyst growth with PDE4 inhibition, after treatment with PGE2 compared to FSK.

In the same assay, PDE2 inhibition also increased PGE2-derived cyst formation in proportion to the percent increase in cAMP observed upon PDE2 inhibition using FRET (~16%), though this trend is not significant (**Figure 15, 10b**). In FSK-derived cysts, no change to total cyst formation was observed upon PDE2 inhibition (**Figure 21c**), which aligns with the lack of

cAMP fluctuation measured, via FRET, upon FSK stimulation and subsequent Bay6o administration (**Figure 8b**) In line with the results observed upon PDE4 and PDE2 inhibition in the in vitro cyst assays, it was concluded that PDE inhibition increases intracellular cAMP and thus promotes cyst formation.

However, as aforementioned, data from chapter 4 suggested PDE3 also hydrolyses a specific pool of PGE2-generated cAMP in ciliated IMCD3 (**Figure 10b**) and since ciliary cAMP propagates cystogenesis, it was thus hypothesized that PGE2-stimulated in vitro cysts, treated with PDE3 inhibitor, Cilostamide, should also increase bulk cAMP and markedly aggravate cyst growth. Yet, surprisingly, we found no evident correlation between PDE3 inhibition and PGE2-induced total cyst formation (**Figure 15c**). From this observation it was hypothesized that a cAMP nanodomain, regulated by PDE3, must exist, to counteract the consequences of enhanced bulk second messenger signalling on in vitro cystogenesis. To test this theory, PDE3 inhibition was applied to FSK-stimulated cysts, with the rationale that PDE3 inhibition would not give rise to an increase in bulk cAMP, as PDE3 inhibition measured during FRET experiments where FSK was chased by Cilostamide, showed no changes in cytosolic cAMP (**Figure 8b**) in chapter 4. Thus, upon Cilostamide treatment, PDE3 inhibition of FSK-induced cysts should lead to a reduction in cystic growth. Indeed, results showed that PDE3 inhibition, in FSK-derived cysts, led to a significant and concentration dependent decrease in total cyst area (**Figure 22c**). This finding suggests that PDE3 may function in a specific cAMP nanodomain, somewhere in the cell, to regulate a pool of cAMP which counteracts cystogenesis (**Schematic 11**).

Of interest, both PDE2 and PDE3 inhibition reduced average cyst measurements in FSK-induced in vitro cystogenesis. PDE3 inhibition also markedly reduced average cyst size in PGE2-derived in vitro cysts. While it is clear PDE3 inhibition reduces cyst growth in general, it appears PDE2 inhibition limits the size of individual FSK-derived cysts but ultimately does not change total cyst formation. Whether this smaller cyst phenotype is relevant to

progression of ADPKD is unclear. One publication does suggest that the size of individual cysts matter for disease prognosis, with larger cysts indicating faster progression of ADPKD.(Prince, Weiss, and Blumenfeld 2023) Ultimately, however, PDE3 inhibition led to a more robust change in in vitro cystogenesis as compared to PDE2 inhibition, and was thus selected as the PDE of interest for consequent experiments.

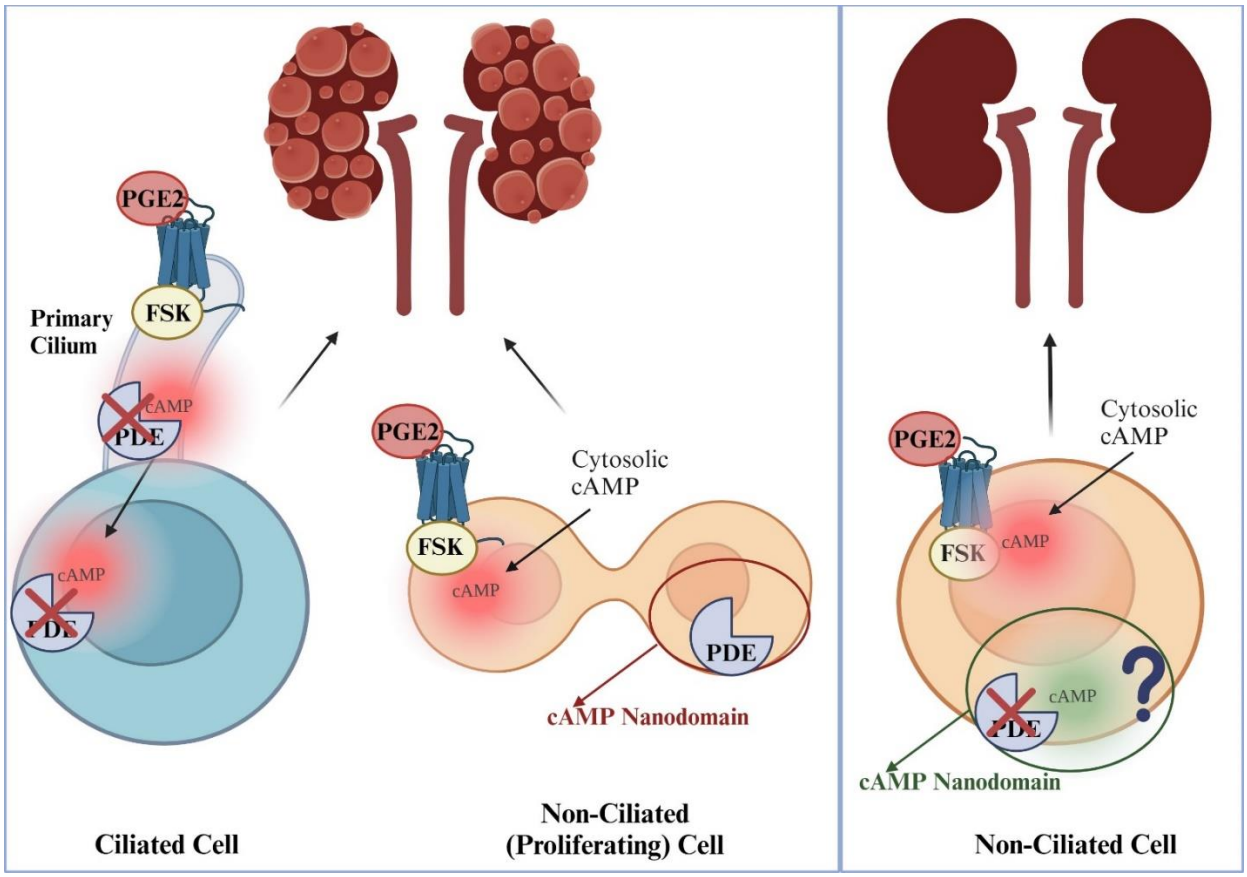

Schematic 11: Example diagram of working hypothesis for distinct cAMP signalling and PDE activity in ciliated versus non-ciliated IMCD3. Ciliary cAMP, from ciliated cells, induces downstream bulk effects to drive cystogenesis (left). Cytosolic bulk cAMP, in non-ciliated IMCD3, also contributes to cystogenesis, as non-ciliated IMCD3 are the dividing cells which excessively proliferate in ADPKD (middle). In the cytosol of non-ciliated cells, we have shown, using FRET, there is limited cAMP-hydrolysing activity by PDE2 and PDE3, but PDE3 inhibition in these cells still leads to decreased cystogenesis. Thus, it is hypothesized, PDE3 works to regulate a specific intracellular subdomain of cAMP, most likely in non-ciliated IMCD3, to regulate cyst formation. In this subdomain, when PDE3 is functioning, there is no cAMP signalling, and non-ciliated cells still divide, contributing to cyst formation (middle). However, in the same subdomain, if PDE3 is inhibited, there is a surge in localised cAMP signalling whose downstream effects culminate in mitigated cyst formation (right).

Previous literature holds cryptic clues as to which nanodomain PDE3 may be functioning to regulate cyst growth. In addition, former findings do not necessarily support our results. In one study, carried out in Pkd2($^{-/WS25}$) mice, PDE3A, but not PDE3b, KO aggravated ADPKD

and led to an increase in CREB phosphorylation by PKA, even though only a small subset of cAMP is reported to be hydrolysed by PDE3 in the kidneys.(Ye et al. 2016) Upon PDE3 KO this study saw an increase in cyst formation, while our data suggests decreased cystogenesis. It is important to note that our cysts were not generated via mutations in ADPKD proteins, but only simulated cystogenesis by direct cAMP upregulation. The contrasting study used Pkd2($^{-/WS25}$) mice to model ADPKD, and thus likely better reflects real disease conditions. Additionally, our study looked at PDE inhibition, whereas the Pkd2($^{-/WS25}$) mice genetically abolished the PDE3 gene. Pharmacological inhibition and complete deletion of a protein may not have the same consequence. It is also possible, that like cAMP, which mitigates cell proliferation in healthy kidneys, but accelerates cell division in ADPKD, through BRAF, PDE3 may also achieve opposing outcomes in homeostatic and disease conditions. Indeed, a separate study showed PDE4 and PDE3 hydrolyse bulk cAMP in MDCK cells (85% and 15% respectively). However, only PDE3, not PDE4, inhibition stimulated mitogenesis through activation of BRAF, subsequently increasing ERK signalling and cyclin D and E_1 function.(Cheng et al. 2006) However, in cells of renal cortical tubules, stimulated with Folic Acid to induce proliferation, a different group showed PDE3 inhibition led to reduced cell growth, measured via decreased expression of proliferating cell nuclear antigen (PCNA).(Matousovic et al. 1997a) Yet, in a further investigation carried out in principal-collecting duct cells, mpkCCD$_{c14}$, PDE3, like PDE4, inhibition, increased NAPDH oxidase 4 (NOX4). NOX4 is thought to contribute to V2R-cAMP-PKA signalling, with enhanced activity of the oxidase resulting in greater expression of AQP2.(Feraille et al. 2014) This alternate study implies PDE3 pharmacological inhibition should aggravate cystogenesis, and thus also contrasts our findings. Yet, in cells isolated from human APDKD tissue, a further study found PDE3 inhibition induced ADPKD cell proliferation, but noticeably decreased proliferation of cells derived from healthy human tissue,(Pinto et al. 2016) alluding to the possibility that PDE3 plays opposing roles in disease and healthy intracellular signalling. Of

note, in this study, PDE4 inhibition was found to have negligible effects on proliferation, shedding some doubt on the validity of these findings.

While in the aforementioned experiments, cell proliferation was the main parameter for cystogenesis, other research also explored PDE3's role in fluid secretion. One seminal study demonstrated PDE3 inhibition, including via Cilostamide, mimics C-type natriuretic peptide (CNP) fluid secretion in shark rectal glands. PDE3 was implicated in a complex with CNP/cGMP/cAMP/PKA to upregulate CFTR activity.(De Jonge, Tilly, Hogema, Pfau, Kelley, Kelley, Melita, Morris, Viola, and Forrest 2014) Similar results were found in cells from pig trachea submucosal glands. PDE3 was shown to interact with CFTR at the plasma membrane, and PDE3 inhibition augmented CFTR function.(Penmatsa et al. 2010) Contrary, Pinto et al found only a small increase in CFTR activity upon PDE3 inhibition. (Pinto et al. 2016) Taken together, data cannot conclude whether in vivo, PDE3 inhibition would ameliorate or aggravate cyst formation in ADPKD. Nevertheless, regardless of which direction PDE3 may function to affect cyst formation, our results indicate that this enzyme plays a role in regulating cystogenesis.

Another question raised by these studies is which isoform of the PDE3 family is responsible for cyst growth? PDE3A and PDE3B are the main subfamilies of PDE3. Research has shown decreased protein expression of PDE3B and PDE4A, but no change in PDE3A, in ADPKD patient tissue, implying PDE3B plays a role in ADPKD not PDE3A. (Pinto et al. 2016) Contrastingly, as aforementioned, Ye et. Al demonstrated PDE3A is more likely implicated in renal function and dysfunction, as PDE3A KO, not PDE3B KO aggravated cystogenesis in Pkd2($^{-/WS25}$) mice. Furthermore only PDE3A KO led to a significant decrease in PDE activity with 13.1% drop in total PDE activity and 64% drop in PDE3 activity in Pkd2($^{-/WS25}$) mice.(Ye et al. 2016) Additionally, Cilostamide, the PDE3 inhibitor, has greater affinity to PDE3A (IC_{50} 27nM) over PDE3b (IC_{50} 50nM), suggesting that PDE3A is more prominently inhibited in our assays which led to cyst reduction. Data from our laboratory, carried out in

cardiomyocytes, also shows PC2 is found in the interactome of PDE3A1. (Subramaniam et al. 2023) Together this evidence implicates PDE3A over PDE3B in renal cystogenesis.

The unexpected finding that PDE3 inhibition leads to an increase in intracellular cAMP but a decrease in cystogenesis in vitro, demonstrates the power of compartmentalised cAMP signalling and suggests that PDE3 may function in a specific cAMP nanodomain, somewhere in the cell, to regulate renal function. This pool of cAMP, controlled via PDE3, may be altered in ADPKD. The remainder of this thesis attempts to narrow down the possible locations where this cAMP nanodomain may exist, functioning, in particular with the PDE3A1 isoform.

Chapter 6: cAMP and PDEs may affect cystogenesis by altering primary cilium length and number

Introduction

In the previous chapter we demonstrated that PDE3 inhibition, which should raise cAMP levels in the cell, and thus increase cystogenesis in vitro, unexpectedly reduces cyst development. To explain this observation, we hypothesized that PDE3 functions in a specific subcellular domain somewhere in the cell, to counteract cystogenesis brought about via bulk cAMP signalling. Since PDE3 has not been shown to localise in the primary cilium, and since PDE3 hydrolysis of cAMP was observed downstream of PGE2 signalling in ciliated cells, but PDE3 inhibition did not exacerbate PGE2-induced cyst growth, it is unlikely, PDE functions inside the cilium to regulate cystogenesis. However, while it may not directly regulate ciliary cAMP signalling, PDE3 could still influence cystic formation by altering cilia length, thus also changing the organelle's downstream signalling. In a phosphoproteomics study previously carried out in the lab, PDE3A1 inhibition was shown to increase PKA phosphorylation of pericentriolar material 1 (PCM1), a protein vital for ciliary growth. (Subramaniam et al. 2023)

The primary cilium and the centrosome are interconnected and are both controlled by an intricate network of PKA phosphorylation targets. Ciliogenesis begins when cells exit the cell cycle and transition to G_0 phase.(Porpora et al. 2018) A ciliary vesicle docks at to the basal body of the centrioles, from which the nascent cilium will extend.(Sánchez and Dynlacht 2016) Axonemal microtubules orchestrate ciliogenesis, with the pericentriolar matrix functioning as a scaffold in this process. PCM1 is part of this pericentriolar complex, which is made up of multiple proteins. Thus PCM1 is essential for ciliogenesis, and its deletion leads to loss of primary cilia.(Kim, Krishnaswami, and Gleeson 2008) Of importance, PCM1 also operates as an AKAP for PKA at the centrosome. GPCR activation leads to downstream PKA phosphorylation of NIMA-related Kinase 10 (NEK10), a kinase which is also necessary for

ciliary biogenesis. PKA phosphorylation of NEK10 leads to the latter's ubiquitination and proteolysis by E3 ligase CHIP, thus abolishing ciliogenesis.(Porpora et al. 2018) In a separate complex, PKA also phosphorylates Orofacial Digital Type 1 (OFD1) at the centrosomes, to regulate cilia length. Phosphorylation of OFD1 coordinates its proteolysis through the E3 ubiquitin ligase praja2 and the ubiquitin-proteosome system (UPS). Non-phosphorylatable mutants of OFD1 in Medaka fish led to altered cilia morphology and dynamics, and subsequent developmental defects. Furthermore, OFD1 syndrome, an X-linked congenital ciliopathy, expresses with facial, oral cavity, and digital malformations, and in many cases PKD.(Senatore et al. 2021) Thus PKA phosphorylation, and therefore cAMP, regulates ciliogenesis and subsequent organelle length.

While the effects of global cAMP on ciliary phenotype are not fully understood, the consequences of primary cilium elongation in the context of cystogenesis also remain unclear. In ADPKD, mutations in polycystins lead to elongated cilia, and obvious cyst growth.(Shao et al. 2020) It is also now accepted that a specific pool of ciliary cAMP drives cystogenesis (Liu et al. 2018; Hansen, Kaiser, Leyendecker, Stüven, Krause, Derakhshandeh, Irfan, Sroka, Preval, and Desai 2022) Therefore, it seems that the greater the length of the cilium, the greater ciliary cAMP signalling and subsequent cyst growth. However, when cilia of WT mice were abolished through loss of Kif3α or Ift20, two proteins relevant to ciliogenesis, this also provoked renal cyst formation. Yet paradoxically, when Kif3α or Ift20 were knocked out, in addition to Pkd1 or Pkd2, cyst formation in these mice models was mitigated.(Ma et al. 2013) It thus appears that, in either direction, loss or elongation of cilium, alters cellular homeostasis and in some organ systems, leads to cystogenesis.

Both cAMP and the polycystins affect ciliogenesis as well as cystogenesis, and PDEs obviously function downstream of the second messenger to regulate its effects. Additionally, PDE2 and PDE3, from a proteomics study previously undertaken in our lab, could also interact with PC2,(Subramaniam et al. 2023) while an interaction between PDE4C and PC2

has already been observed at AKAP150. (Choi et al. 2011b) Thus, it is possible that PDEs function to alter ciliary structure. Of interest, PDE2A mutations were linked to congenital heart defects alongside mutations in many prominent ciliary proteins such as PC1 and CEP290.(Li et al. 2015) PDE2A KO in the interventricular septum of mice also slowed down cardiomyocyte proliferation,(Assenza et al. 2018) with universal PDE2A KO leading to embryonic lethality. The primary cilium hosts the hedgehog signalling pathway which plays a prominent role in foetal development; thus it is possible PDE2 mutations function through the cilium to achieve these congenital defects. However, PDE2 inhibition did not significantly reduce cystogenesis, instead, PDE3 inhibition decreased cyst formation in vitro. Aside from its potential regulatory role in the phosphorylation of PCM1, PDE3 mutations are also linked to a ciliopathy like phenotype. Members of a Turkish family with a PDE3A missense heterozygous mutation suffered from cardiac hypertension, but also manifested with brachydactyly, or shortened fingers. Brachydactyly is a common phenotype of ciliopathies.(Focșa, Budișteanu, and Bălgrădean 2021) Though not relevant to ciliogenesis, but of interest, in the same family, the PDE3A mutation was also shown to protect the kidneys from hypertension induced damage.(Sholokh et al. 2023) Therefore, altered PDE3 activity has been shown to improve renal health in more than one disease model. It is possible that PDE3 inhibition achieves cyst protective effects by altering ciliary length or number. In this chapter, with the assistance of three undergraduate students, Jessica Zhang, Aparna Sridar, and Edoardo Valli, we tested this hypothesis by measuring the length of cilia in IMCD3 treated with PDE inhibitors and cyclic nucleotide activators.

Results 1- PDEs affect ciliogenesis

To measure cilia length in response to PDE inhibition, we depleted IMCD3 cells of nutrients to induce ciliogenesis (50:50 DMEM:F12 with 0.1% FBS instead of 10%, with no added glutamine), while also treating the cells with one of three PDE inhibitors Bay60 (PDE2), Cilostamide (PDE3), or Rolipram (PDE4). After 48 hours of nutrient-depletion (starvation)

and treatment, IMCD3 were fixed and stained for ciliary markers acetylated α-tubulin (green) and Arl13b (red). Cilia length was obtained based on Pythagoras theorem, whereby "a" was the length of the cilia measured in the composite stack of the image, "b" was the number of z-stacks a single cilium occupied, multiplied by 0.5µm, the distance between stacks. To obtain c, the square root of $a^2 + b^2$ was calculated, yielding the true length of the organelle (**Schematic 7**). Results for Bay60 treated IMCD3 were calculated manually (**Figure 23**) by Jessica Zhang. The remaining cilia analysis was carried out by Edoardo Valli using the CiliaQ ImageJ plugin.(Hansen et al. 2021)

Figure 23 shows a concentration dependent decrease in cilia length upon PDE2 inhibition, with 100nM Bay60 markedly reducing organelle size.

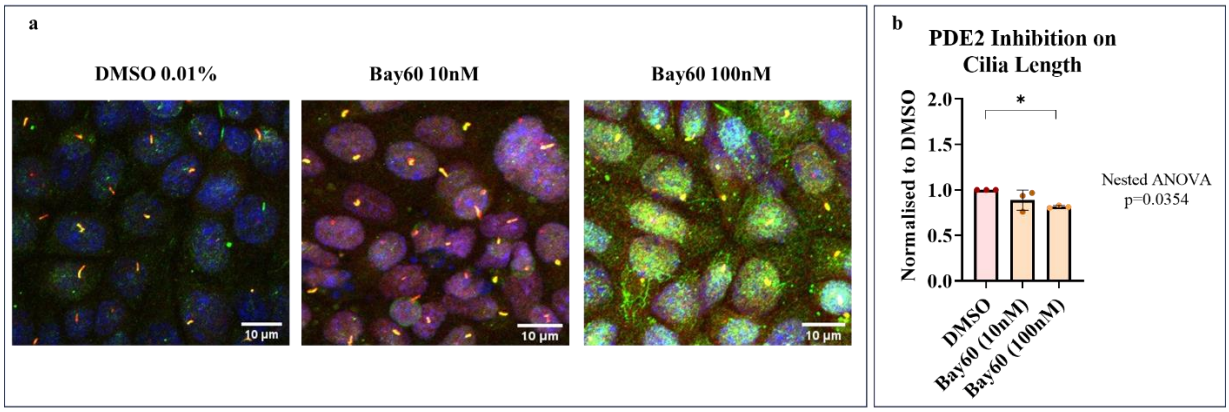

Figure 23: a shows IMCD3 cells starved and treated for 48 hours with either DMSO, 10nM Bay60, or 100nM Bay60. Cells were then fixed and stained for ciliary markers acetylated α-tubulin (green) and Arl13b (red). Hoechst dye identifies the nucleus. **b** length of cilium was measured from images in a, and nested ANOVA was used for statistical analysis. Tukey's multiple comparisons was used for post hoc testing. Each data point represents values from one coverslip (counted cilia per coverslip >50), normalised to the DMSO control. N=3 where each n is a separate round of experimentation with an independent flask passage. Bars represent mean with SD. Experiments, images and analysis were carried out by Jessica Zhang.

Since PDE2 has three splice variants, which are all inhibited by Bay60, I also wanted to test which PDE2A isoform was responsible for regulation of ciliogenesis. To test this, I transfected IMCD3 with either PDE2A1-DN-RFP, PDE2A2-DN-RFP, or PDE2A3-DN-RFP then fixed and stained for ciliary marker, acetylated alpha tubulin. PDE2A1 degrades cAMP at the cytoplasm, PDE2A2 at the mitochondria and PDE2A3 at the plasmalemma.(Lobo et al.

2020a) By transfecting the dominant negative (DN) versions of each PDE2A isoform, tagged with RFP, the endogenous enzyme would be displaced from its intracellular subcompartment, and one could assess how loss of PDE isoform localisation would affect ciliogenesis. For this experiment, the length of the cilia was measured and in addition, the percent of ciliated cells was also calculated. **Figure 24** shows the results. PDE2A2-DN-RFP markedly reduced cilia length, as well as the percent of ciliated cells in each coverslip.

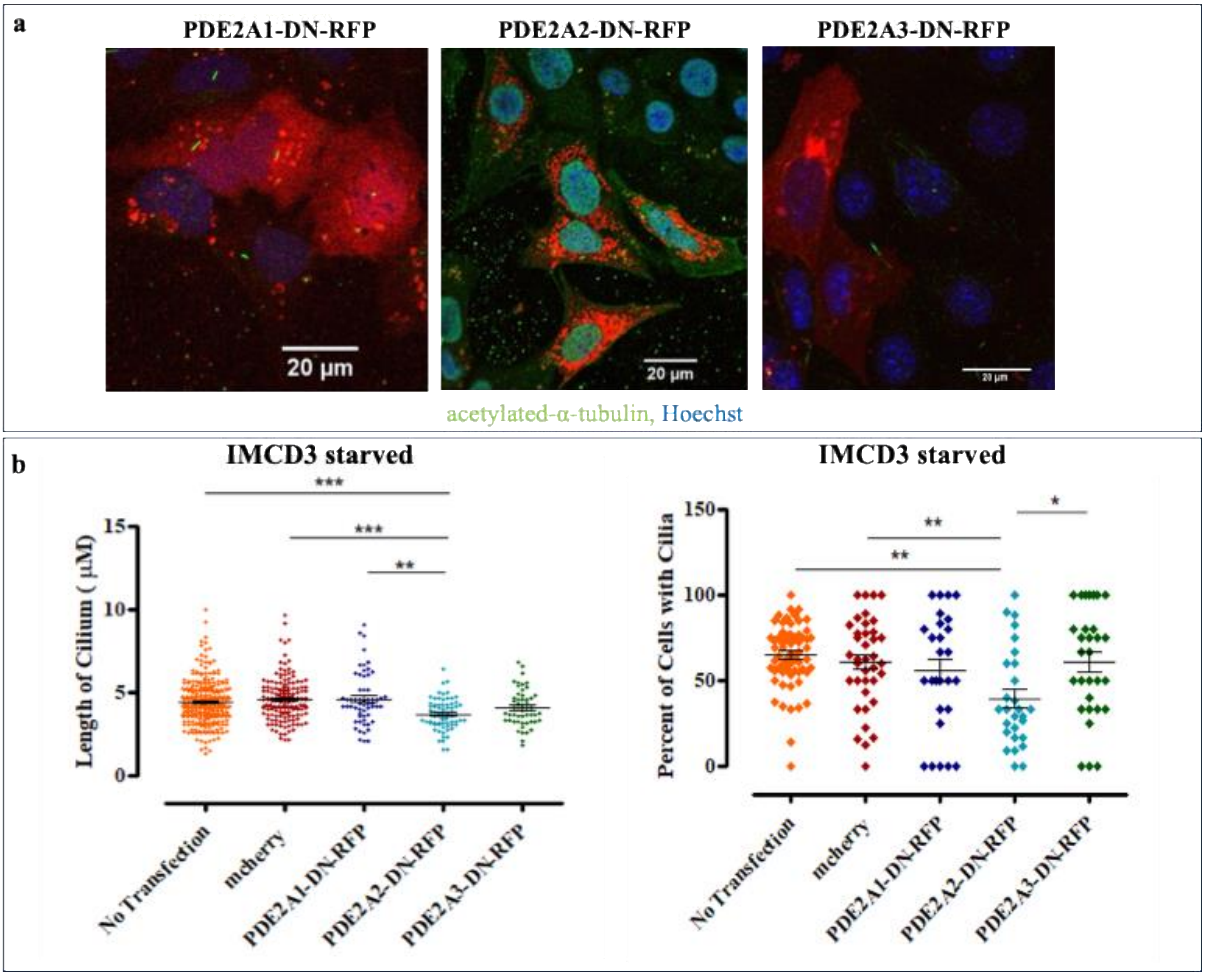

Figure 24: a IMCD3 were transfected with either PDE2A1-DN-RFP, PDE2A2-DN-RFP, or PDE2A3-DN-RFP then fixed and stained for ciliary marker acetylated alpha tubulin. **b** Cells with PDE2A-DN-RFP expression were analysed for presence of cilium and cilium length. ANOVA was used for statistical analysis. Tukey's multiple comparisons was also carried out. Each datapoint is a single cell. N=3, where n is one independent round of experiments from a single flask passage. Bars show mean with SD

Due to the surprising finding that PDE2 inhibition reduced cilia length, I briefly pursued an explanation for this result. Data from a mass spectrometry study carried out in a mouse neuroblastoma cell line, HT-4 showed that PDE2A2 likely interacted with Kif13B (Lobo et al.

2020b), a prominent kinesin involved in ciliogenesis, and in translocation of PC2 to the cilium.(Schou et al. 2015; Juhl et al. 2023a; Schou et al. 2017b; Rezi et al. 2024) To confirm this interaction, one of three PDE2A flag-tagged isoforms was co-transfected with Kif13B-GFP in HEK293. Upon pull down with GFP, all three PDE2A isoforms did interact with KIF13B-GFP (**Figure 25**).

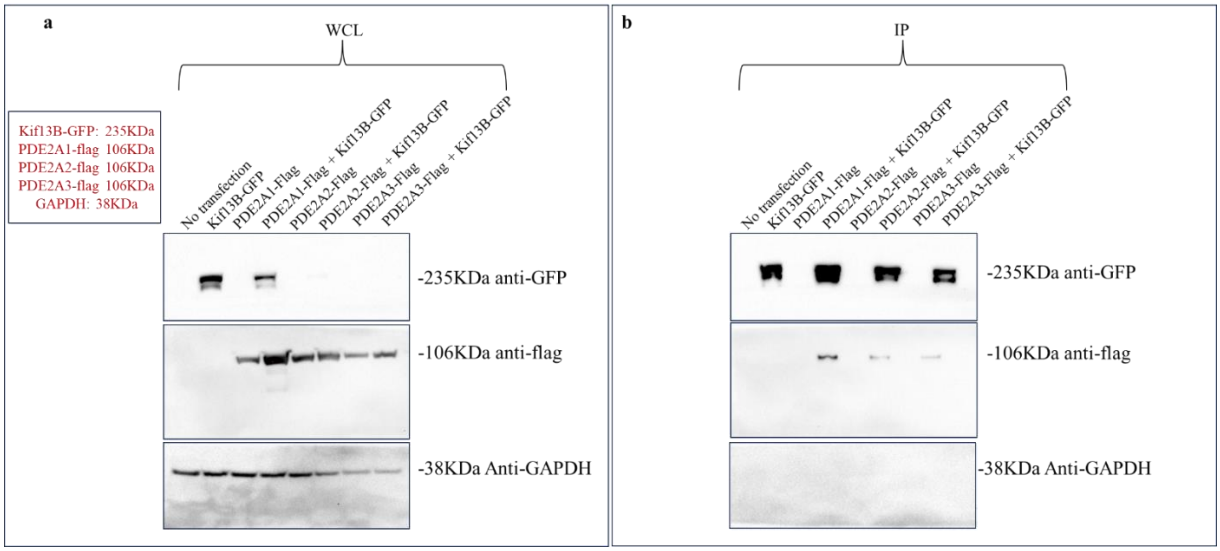

Figure 25: HEK293 cells transfected with either KIF13B-GFP or one of three PDE2A-flag-tagged isoforms, or co-transfected with KIF13B-GFP and a PDE2A-flag isoform. **a** shows whole cell lysate (WCL) stained for anti-GFP, anti-flag, or anti-GADPH. **b** shows co-immunoprecipitation (IP) samples, stained for anti-GFP, anti-flag, or anti-GADPH. Pull down was achieved with GFP. This experiment was repeated three times (N=3). No statistical analysis was performed.

Next, we measured cilia length in IMCD3 treated with increasing concentrations of Cilostamide, as PDE3 was our primary enzyme of interest (**Figure 26)**. However, no marked difference in cilia length was observed between Cilostamide treated cells and DMSO control.

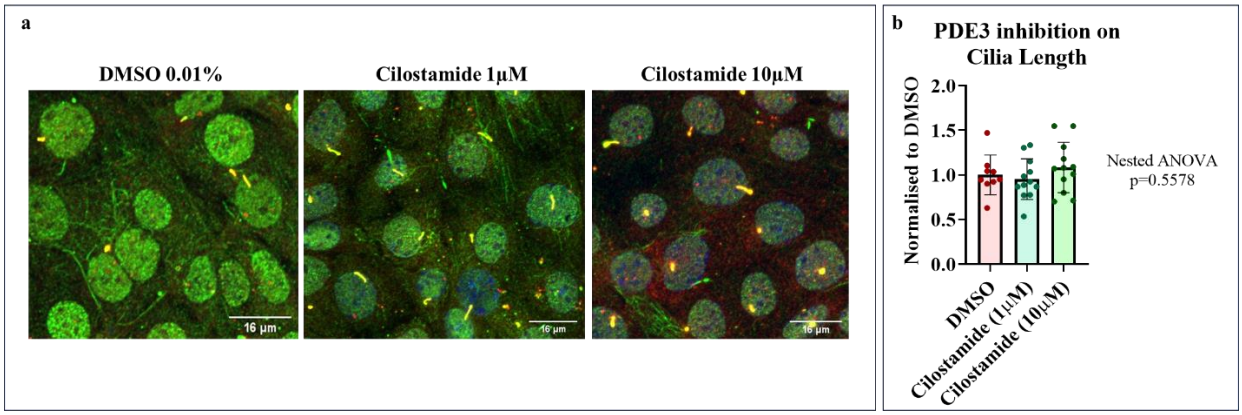

Figure 26: a shows IMCD3 cells starved and treated for 48 hours with either DMSO, 1µM Cilostamide, or 10µM Cilostamide. Cells were then fixed and stained for ciliary markers acetylated α-tubulin (green) and Arl13b (red). Hoechst dye identifies the nucleus. **b** length of cilium was measured from images in **a** with CiliaQ. Nested ANOVA was used for statistical analysis, no post hoc test was required. Each data point represents values from one coverslip (counted cilia per coverslip >100), normalised to the DMSO control. N=6 where n is one independent round of experimentation from an independent flask passage. Bars represent mean with SD. Analysis, in part, carried out by Edoardo Valli.

The third PDE inhibitor tested, Rolipram, led to a concentration dependent increase in cilia length of IMCD3, though this elongation upon PDE4 inhibition was not statistically significant (**Figure 27**).

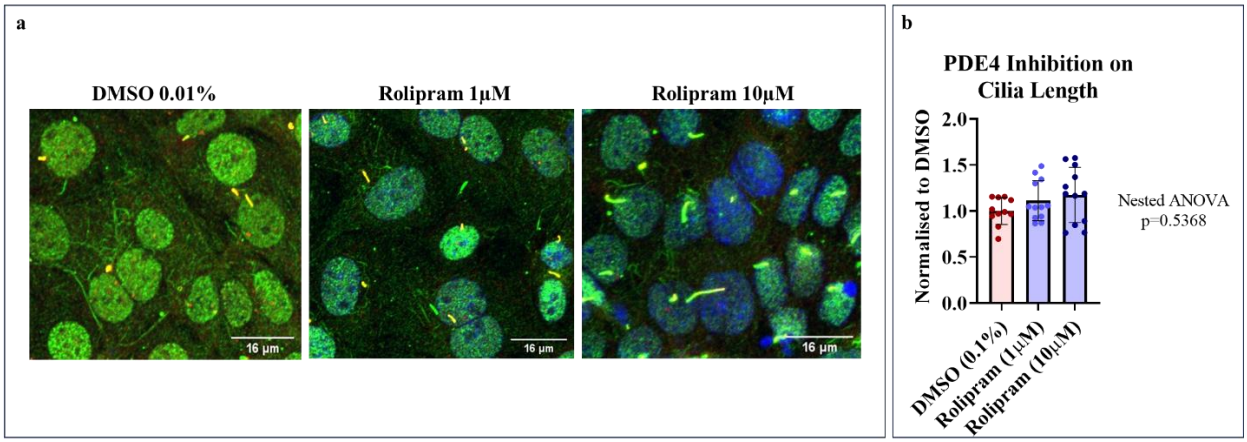

Figure 27: a shows IMCD3 cells starved and treated for 48 hours with either DMSO, 1μM Rolipram, or 10μM Rolipram. Cells were then fixed and stained for ciliary markers acetylated α-tubulin (green) and Arl13b (red). Hoechst dye identifies the nucleus. **b** length of cilium was measured from images in **a** with CiliaQ. Nested ANOVA was used for statistical analysis. Images were captured by Aparna Sridar. Data point represents values from one coverslip (counted cilia per coverslip >100), normalised to the DMSO control. N=6 where n is one independent round of experimentation from an independent flask passage. Bars represent mean with SD.

Results 2- PDEs may work through cyclic nucleotide signalling to affect ciliogenesis

As PDEs hydrolyse cAMP, and as it is uncertain whether enhanced levels of cAMP in ADPKD are a consequence or driver of elongated cilia, we next aimed to confirm whether increased second messenger promotes ciliogenesis. Starved IMCD3 cells treated with AC activator, FSK, indeed demonstrated a significant increase in organelle length (**Figure 28**). Of note, 25μM FSK experiments could not be compared to 1μM and 10μM experiments, as the former required a different control of 0.25% DMSO.

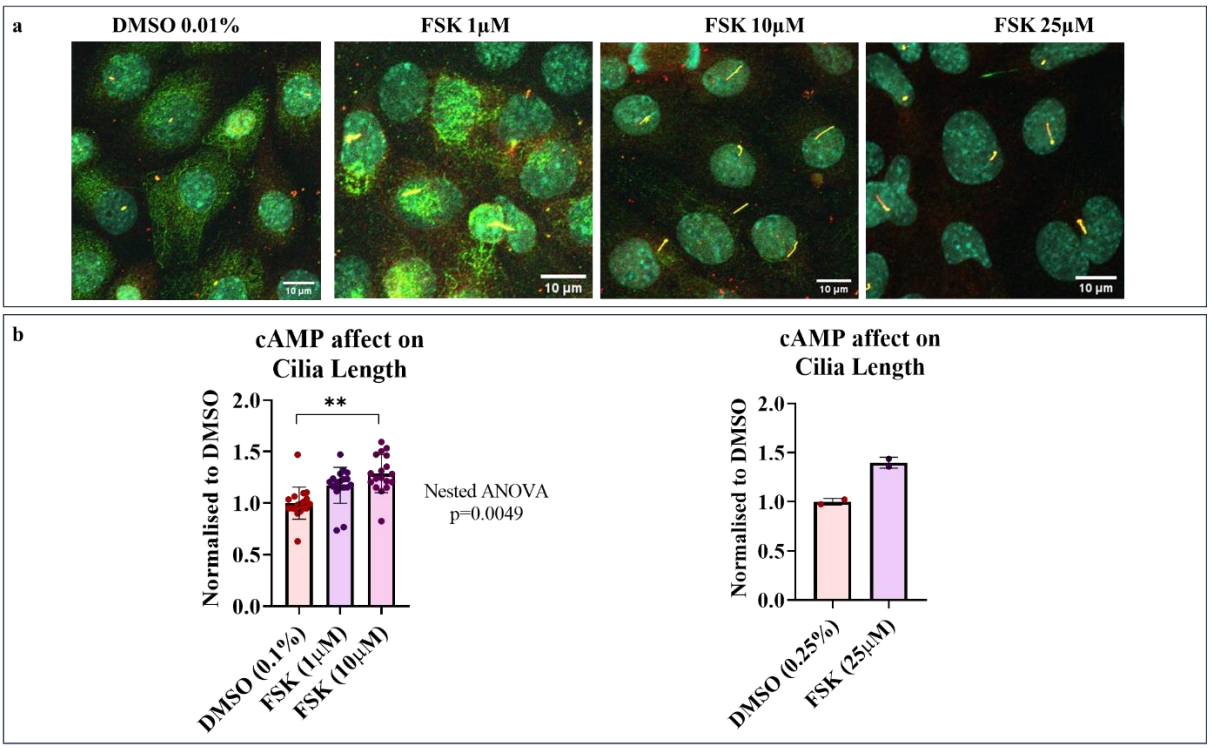

Figure 28: a shows IMCD3 cells starved and treated for 48 hours with either DMSO, 1µM FSK, 10µM FSK, or 25µM FSK. Cells were then fixed and stained for ciliary markers acetylated α-tubulin (green) and Arl13b (red). Hoechst dye identifies the nucleus. **b** length of cilium was measured from images in **a** with CiliaQ. Nested ANOVA was used for statistical analysis of graph to the left, post hoc analysis was achieved with Tukey's multiple comparisons test. For graph to the left n=4, where each n is one round of experiments from an independent flask passage. No statistical analysis was performed for graph to the right, as n=2. Each data point represents values from one coverslip (counted cilia per coverslip >100), normalised to 0.1% DMSO control for 1-10 µM FSK and 0.25% DMSO control for 25µM FSK. Bars represent mean with SD. Analysis was, in part, performed by Edoardo Valli.

Finally, since PDE2 inhibition led to a decrease in cilia length, but we have previously demonstrated cAMP elongates the cilium, we also wondered whether PDE2 inhibition functions through hydrolyses of cGMP to reduce ciliogenesis. Firstly, we confirmed whether PDE2A and PDE3 indeed hydrolysed cGMP, in IMCD3, as compared to cGMP-specific hydrolysing PDEs, PDE5 and PDE9. For this, we employed the cGMP cytosolic FRET sensor, cGi500. IMCD3 cells transfected with cGi500 were treated with one of four PDE inhibitors (Bay60, Cilostamide, Sidenafil, and PZ044613) followed by Bay41/IBMX to achieve cGMP saturation. All four PDEs were found to hydrolyse cGMP at comparable levels in IMCD3 (**Figure 29**).

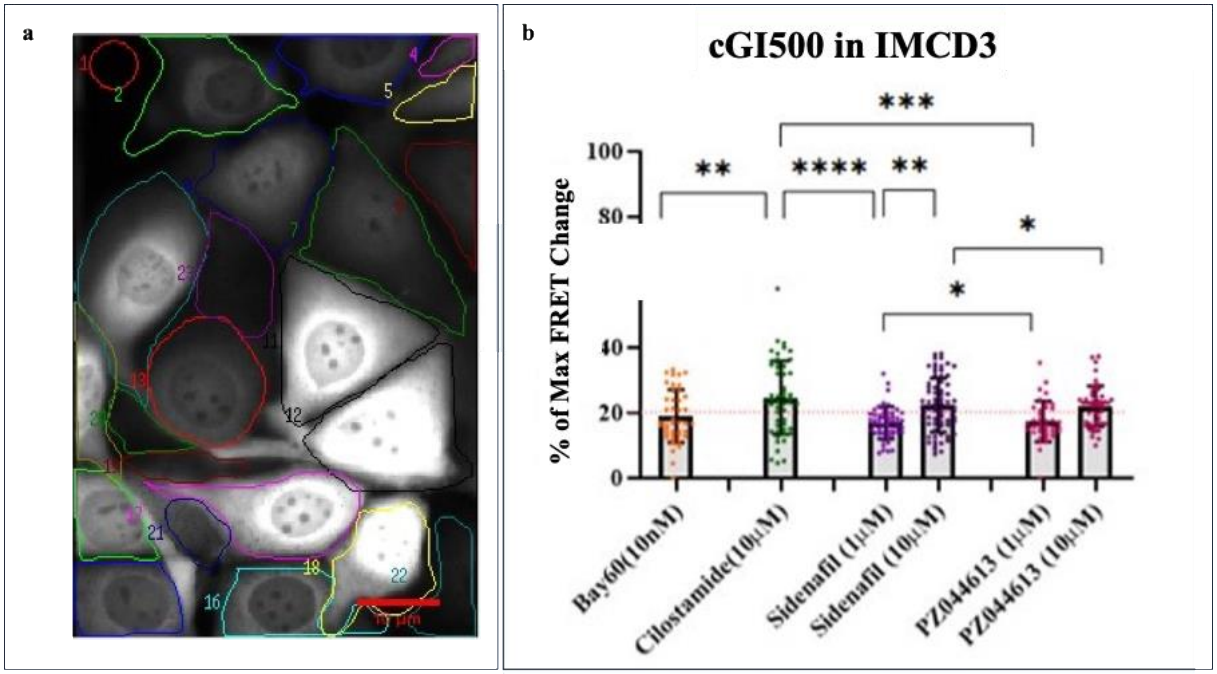

Figure 29: a shows localisation of cGi500 in IMCD3. **b** is the quantification of cGMP signalling in IMCD3 cells transfected with cGMP FRET reporter, cGI500, after administration with one of several inhibitors of PDEs known to hydrolyse cGMP, such as PDE2 (Bay60), PDE3 (Cilostamide), PDE5 (Sidenafil), or PDE9 (PZ044613). FRET activity upon PDE isoform inhibition was normalised to total intracellular cGMP levels, achieved by saturation via Bay41 and IBMX. One-way ANOVA was carried out on parametric data, with Bonferroni for multiple comparisons. Each data point in a single coverslip. N=3, where n is one round of experimentation from an independent flask passage. Bars represent mean with SD. Experiments and analysis were carried out by undergraduate student Aparna Sridhar.

Since both PDE2 and PDE3 were shown to hydrolyse cGMP, and since we previously demonstrated PDE2A2 inhibition alters ciliogenesis, we next wanted to see whether organelle length responded to an increase in cGMP. For this, we treated IMCD3 with Bay41, the guanylyl cyclase activator. Upon cGMP activation we did not observe significant alterations in cilium length (**Figure 30**).

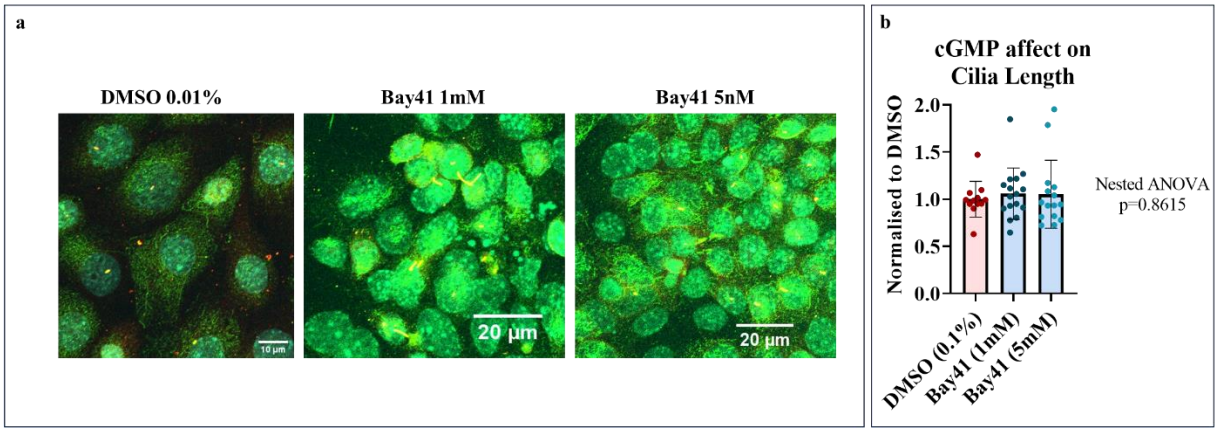

Figure 30: a shows IMCD3 cells starved and treated for 48 hours with either DMSO, 1mM Bay41, or 5mM Bay41. Cells were then fixed and stained for ciliary markers acetylated α-tubulin (green) and Arl13b (red). Hoechst dye identifies the nucleus. **b** length of cilium was measured from images in **a,** with CiliaQ. Nested ANOVA was used for statistical analysis. No post hoc test was required. Each data point represents values from one coverslip (counted cilia per coverslip >100), normalised to DMSO control. N=4 where each n is one round of experimentation from an independent flask passage. Bars represent mean with SD. Analysis was carried out, in part by Edoardo Valli.

Results 3- PDEs alter cell cycle

Since ciliogenesis begins in the G_0 phase of the cell cycle, changes in cell cycle could affect cilia length. As cells treated with PDE inhibitors may undergo altered cell cycles, we also wanted to test whether any effects on cilia length upon PDE inhibition could be secondary to changes in cell growth. Thus, IMCD3 were starved and treated with PDE inhibitors. Cells were collected and dyed with propidium iodide. Flow cytometry was used to measure the proportion of cells in G_0/G_1 and G_2 phase. **Figure 31** shows that upon PDE2 inhibition, a larger proportion of cells were in G_0/G_1 phase, with no difference in the proportion of cells in G2. PDE3 and PDE4 inhibition had the opposite effect, whereby a smaller proportion of cells treated with Cilostamide or Rolipram were in G_0/G_1 phase, with no changes in number of cells in G_2 interval. Of note, the difference in number of cells in G_0/G_1 phase was significant for Cilostamide treatment, but not Rolipram. Some of these results were also recapitulated in IMCD3 that were not starved but instead treated with FSK and PDE inhibitors (**Figure 32**). While in this case PDE2 inhibition led to no differences, PDE3 inhibition and PDE4 inhibition mirrored the results observed for G_0/G_1 with starvation. Meanwhile, upon FSK

treatment, Cilostamide and Rolipram treated cells were found in larger proportion to be in G2 phase, something not observed in starved cells.

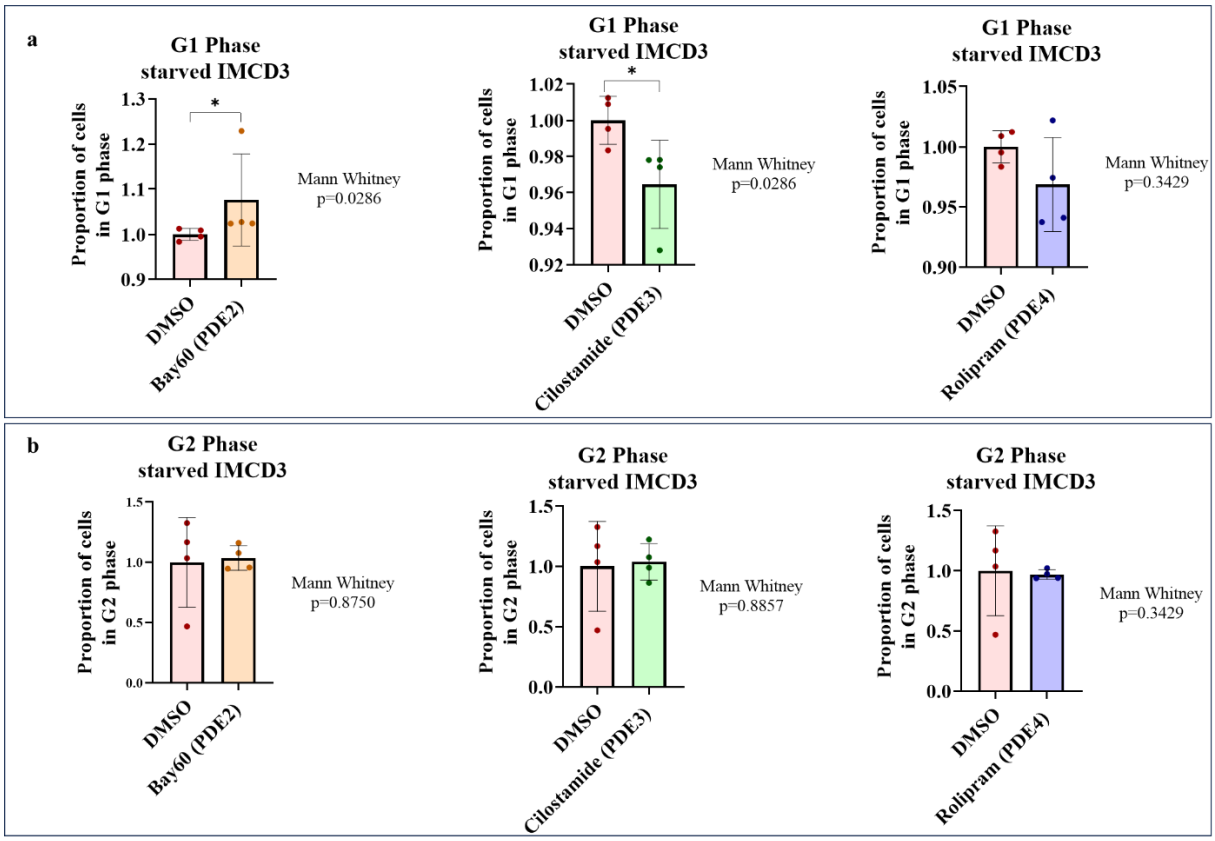

Figure 31: Flow cytometry analysis of IMCD3 treated with PDE inhibitors. **a** shows proportion of cells found in G_0/G_1 phase, normalised to DMSO treated control cells. **b** shows proportion of cells in G_2 phase, normalised to DMSO treated control cells. Mann Whitney test was carried out on non-parametric data. N=4, where each n is one round of experiments from an independent flask passage. Bars represent mean with SD.

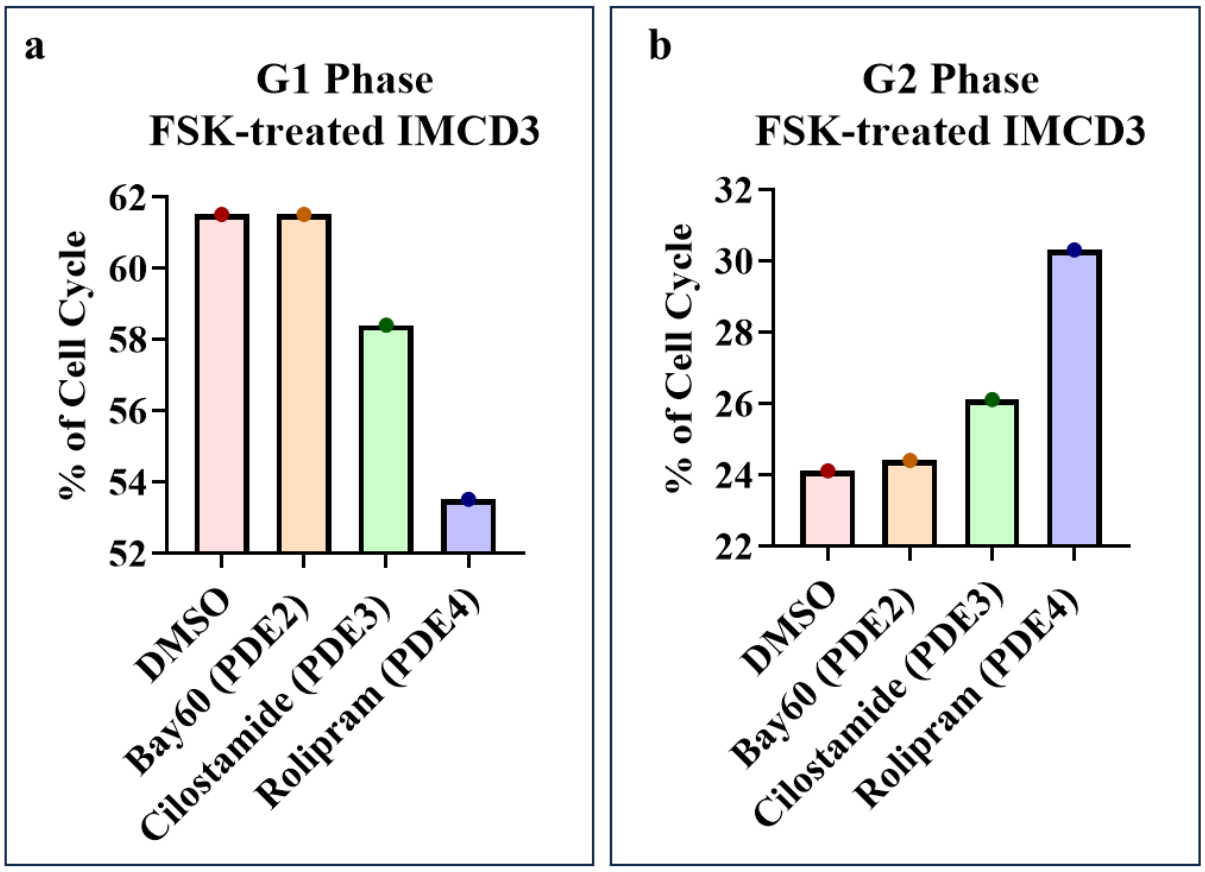

Figure 32: Flow cytometry analysis of IMCD3 cells treated with FSK and one of three PDE inhibitors. **a** shows percent of cell cycle spent in G_0/G_1 phase. **b** shows percent of cell cycle spent in G_2 phase. N=1, where n is one round of experimentation from an independent flask passage. No statistical analysis was carried out since N=1.

Discussion and Conclusions

In the previous chapter, we observed PDE3 inhibition leads to mitigated cystogenesis in vitro, but no cAMP hydrolysis was measured upon inhibition of PDE3 downstream of FSK stimulation. This counterintuitive finding led to the hypothesis that PDE3 functions in a nanodomain of cAMP to regulate cystogenesis in IMCD3. While PDE3 has not been shown to localise to the primary cilium, it was thought that perhaps PDE3 inhibition mitigates cyst growth by indirectly altering ciliary cAMP signalling through regulation of organelle length. To test this, we starved and treated IMCD3 cells with PDE inhibitors as well as cyclic nucleotide activators. Upon PDE3 inhibition, despite the enzyme's association with ciliary proteins such as PCM1 and PC2, we did not observe any marked changes in cilia length (**Figure 26**). It should be highlighted, that this study, due to time restraints, did not quantify

the percent of ciliated cells, a parameter that could have made PDE3's contribution to ciliogenesis more thorough. Nevertheless, 10μM Cilostamide treatment did elongate the organelle, even if this finding was not significant. Thus, PDE3 inhibition followed the same trend as PDE4 inhibition (**Figure 27**) and FSK treatment (**Figure 28**) - an increase in ciliogenesis. However, since FSK and PDE4 inhibition aggravate cystogenesis in vitro and elongate cilia, but PDE3 increases cilia length and reduces cyst growth, it was concluded PDE3 does not function through this mechanism to mitigate cystogenesis in vitro.

Of interest, PDE2 has been linked to congenital heart defects alongside known ciliary proteins such as PC1 and CEP290. Indeed, PDE2 inhibition led to a concentration dependent decrease in cilia length, which was significant at 100nM Bay60. Interestingly, we demonstrated that PDE2A isoforms, when overexpressed, interact with the kinesin-3 motor protein KIF13B (**Figure 25**). Kif13B has been shown to regulate both intraflagellular transport (IFT) within the cilium, as well as transition zone composition and recruitment of Sonic Hedgehog signalling intermediates.(Schou et al. 2017b; Juhl et al. 2023b) Therefore, PDE2 inhibition may work through this Kinesin to alter organelle length. However, it should be noted, 100nM Bay60 inhibits 100% of PDE2 but also blocks about 40% of PDE1 activity (Boess et al. 2004), therefore confounding clear association between PDE2 and ciliogenesis. Though not shown, in vitro, 100nM Bay60 treatment also exacerbated cystogenesis. Therefore, while it seems that agents which increase cilia length, such as FSK and Rolipram, also increase cyst formation, in this case, 100nM Bay60 contradicts this finding by decreasing cilia length while aggravating cystogenesis. This particular result, though not relevant to PDE3's role in ciliogenesis, upholds the idea that modified organelle length in either direction may contribute to cyst formation.

Finally, we also wanted to test PDEs contribution to regulation of cell cycle, as ciliogenesis is dependent on centrosome activity. G_0/G_1 is the phase in which the cilium is born and the organelle is resorbed directly preceding mitosis, in G2 phase.(Ishikawa and Marshall 2011)

Using FACs and propidium iodide, a fluorescent dye which can intercalate into DNA, we measured proportion of cells in G_0/G_1 or G_2 phase in IMCD3 cells treated with one of the three PDE inhibitors (**Figure 31**). Surprisingly, FACs analysis directly contradicted ciliary length findings, for all three PDE inhibitors. PDE2 inhibition led to decreased cilia length, but a significantly larger proportion of cells in G_0/G_1, the phase during which ciliogenesis occurs. The opposite was observed for PDE3 and PDE4 inhibition whereby IMCD3 treated with Cilostamide or Rolipram had longer cilia but fewer cells in G_0/G_1 phase (**Figure 31**). When cells were stimulated with FSK instead of starvation, PDE3 and PDE4 inhibition also led to more cells in G_2 phase (**Figure 32**), the part of the cell cycle where cilia should be resorbed. Together, this data suggests that the effect of PDE inhibition and FSK stimulation on cilia length is direct and not secondary to any changes, brought about by these treatments, on cell cycle.

While we discovered a potential role for PDE2 in ciliogenesis, and confirmed that bulk cAMP enhancement drives cilia elongation, we also concluded that PDE3 does not function by altering cilium length to mitigate cyst growth in vitro. With our null hypothesis confirmed, we set out in search of clues that may lead us towards the identification of the intracellular nanodomain where PDE3 functions to hydrolyse cAMP and reduce cyst formation. A hint was found in a proteomics study previously carried out in our lab, as PC2 appeared in the interactome of PDE3A1.(Subramaniam et al. 2023) Indeed, the next chapter explores this potential interaction between PDE3 and PC2, and where it might occur within renal cells.

Chapter 7: PDEs interact with PC2

Introduction

As described in chapter 5, PDE3 inhibition led to a cyst protective effect in an in vitro assay modelling ADPKD. Paradoxically, PDE3 inhibition after PGE2 stimulation or after FSK treatment increased or led to no change in cAMP respectively, in ciliated IMCD3. Since upregulation of cAMP signalling is thought to fuel cystogenesis, the fact that PDE3 inhibition does not increase cyst formation, but in the case of FSK-induced cysts, markedly decreases cyst area, suggests PDE3 must function to regulate a specific nanodomain of cAMP, somewhere in the cell, to alter cyst growth. Therefore, I sought to narrow in on where this intracellular nanodomain could be. To help with this investigation, the results of a PDE isoform integrated proteomics study, which had been previously carried out in the lab, was consulted. In this study, PDE2A2, PDE3A1, and PDE3A2 were tagged with mCherry fluorophore, and expressed in neonatal rat ventricular myocytes (NRVM).(Subramaniam et al. 2023) The cardiomyocytes were lysed and RFP-Trap beads used to pull down the PDEs and their associated proteins. Mass spectrometry identified candidate interactors for the three PDE isoforms. Subsequently, I searched these interactomes of PDE3A1 and PDE3A2 to see whether any proteins stood out which could begin to explain the cyst-protective effects of PDE3 inhibition. PC2 was found as a candidate interactor of PDE3A1, but not of PDE3A2. Of note, PDE2A2 did not appear to interact with PC2 in NRVM, but was found to associate with this protein in another interactome, carried out in a the neuroblastoma cell line, HT-4.(Lobo et al. 2020b) As aforementioned, PC2 is mutated in 15-20% of ADPKD cases,(Brill and Ehrlich 2020) therefore it was hypothesized that the effect on cyst size observed on PDE3 inhibition may involve a domain where PDE3, and possibly PDE2, interact with PC2.

As a first step to test this hypothesis, I sought to validate the interaction between PDE3A1 and PDE2A2 with PC2.

Results 1- Over-expressed PDE2A isoforms interact with overexpressed PC2

To validate the PDE2A:PC2 interaction, all isoforms of PDE2A, tagged with flag, were overexpressed alongside PC2-GFP in Human Embryonic Kidney (HEK) cells. HEKs were used, as co-transfection of two plasmids proved inefficient in IMCD3. Unfortunately, no expression of PDE3A1 was observed when the cells were transfected with a plasmid encoding for this protein. Infection of HEK cells with a virus encoding for PDE3A1 was also attempted alongside transfection of PC2-GFP, with no positive results. Co-transfection of PDE3A1 and PC2 constructs in other cell types including, IMCD3 and Chinese Hamester Ovarian (CHO), was also tested unsuccessfully. Therefore, only PDE2A, and not PDE3A1, isoform interaction with PC2 in HEKs, where both proteins were overexpressed, could be tested. Cells were lysed and pull down was achieved via GFP-beads (**Figure 33**). Membranes were stained with anti-GFP antibody. The expected molecular weight for PC2 is 109 kilodaltons (KDa). When tagged with GFP, which is ~30Kda, a band should appear at 139KDa. Indeed, **Figure 33b** shows clear co-immunoprecipitation of PC2 only in the samples obtained from lysate of cells, where PC2 was transfected. In the whole cell lysate of the same experiments (**Figure 33a**), expression of PC2-GFP in samples co-transfected with PDE2A2-flag and PDE2A3-flag is very faint, likely a consequence of reduced protein loading (as suggested by lower signal detected by anti-GAPDH for those samples). However, PC2-GFP expression in HEK was confirmed via fluorescence microscopy before lysis, for all PC2-GFP samples, thus the protein was present in the lysate. Of note, promiscuous anti-GFP antibody gave rise to non-specific bands above and below 139KDa. After confirming PC2-GFP expression and successful pull down, I probed for an interaction by staining the membrane with anti-flag antibody, as all PDE2A isoforms were flag-tagged. Indeed, all three PDE2A-tagged isoforms interacted with PC2-GFP, confirmed with a band at ~106KDa (**Figure 33b**). Of note, PDE2A2-flag and PDE2A3-flag showed a thicker band than PDE2A1-flag, despite similar expression levels of PDE observed in the WCL, as well as less PC2-GFP expression in the

PDE2A2-flag and PDE2A3-flag samples compared to PDE2A1 (**Figure 33a**), suggesting PDE2A2 and PDE2A3 may form a stronger interaction with PC2-GFP.

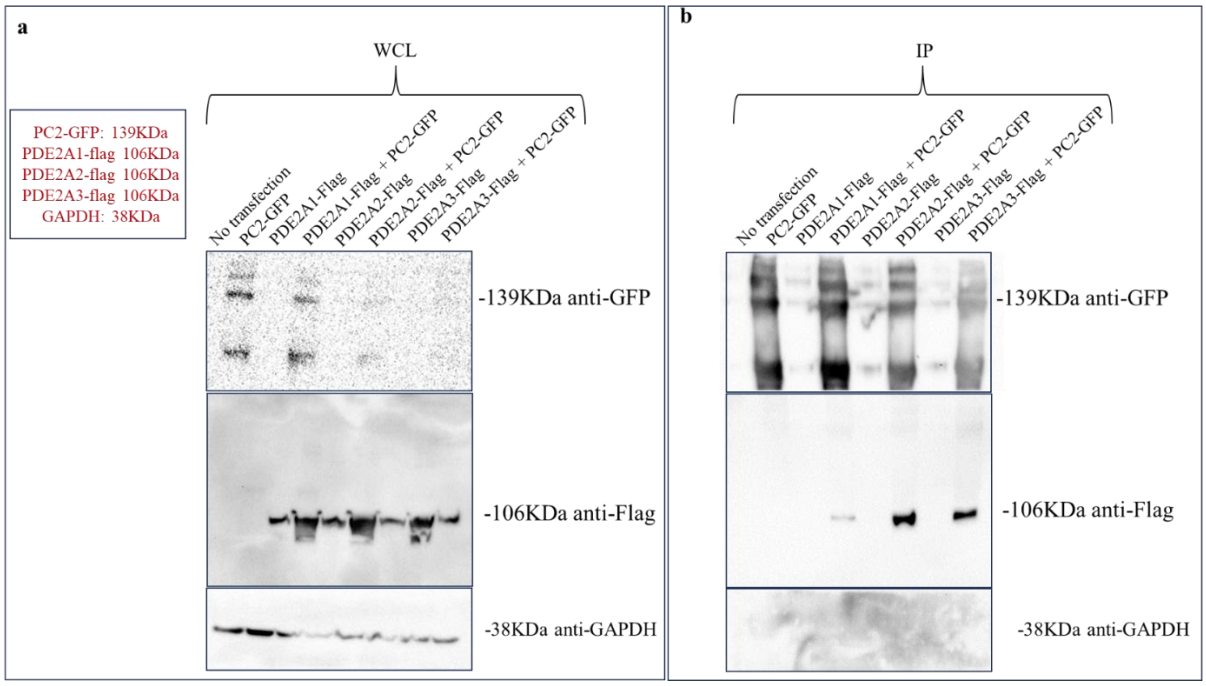

Figure 33: HEK cells were transfected with PC2-GFP or one of PDE2A-flag isoforms as controls. Co-transfection of PDE2A-flag isoforms with PC2-GFP was used to test the interaction between these proteins. **a** shows membrane with whole cell lysate (WCL) samples, and stained with anti-GFP, anti-flag, and anti-GAPDH. Pull down was achieved with GFP-Trap beads. **b** shows membrane with immunoprecipitation (IP) samples, again stained for anti-GFP, anti-flag and anti-GAPDH. The same interaction was tested three times for PDE2A2 (n=3), and once for PDE2A1 and PDE2A3 (n=1). No statistical analysis was performed.

Results 2-PDE3A1, but not PDE2A, interact with endogenous PC2

Co-transfection of PDE3A1 with PC2-GFP proved unsuccessful, therefore only PDE2A isoform interaction with PC2-GFP was confirmed. Thus, I next infected HEK cells with either mCherry (control), one of three PDE2A-RFP isoforms, or PDE3A1-RFP, and then probed the RFP-immunoprecipitate for endogenous PC2 (**Figure 34**). Upon staining with anti-PC2 antibody, similar, multiple bands, for PC2 detection in the WCL, were observed, as obtained previously in **Figure 33a**. However, the band of interest at 109KDa was also present (**Figure 34b**), confirming anti-PC2 antibody could be used to successfully probe for PC2. A very faint band was also present at 109KDa in the IP membrane (**Figure 34b**), for the PDE3A1-RFP sample lane, suggesting PDE3A1-RFP can interact with endogenous PC2. mCherry control or

any of the PDE2A-RFP samples did not show an interaction with endogenous PC2 in the same membrane (**Figure 34b**). To next confirm mCherry and PDE-RFP expression, the membrane was stained with RFP antibody. No RFP expression was observed for any sample in the WCL (**Figure 34a**), with RFP recognising mCherry, PDE2A1-RFP, PDE2A2-RFP, PDE2A3-RFP, but not PDE3A1-RFP in the IP membrane (**Figure 34a**). Residual bands in the WCL at the 38KDa marker are due to poor stripping of previous staining with anti-GAPDH antibody. This result suggests that expression of proteins from the plasmids was not sufficient to be detected, particularly in the WCL where the protein of interest is diluted more than in concentrated RFP-bead samples. However, before lysing cells, expression levels of all RFP-tagged proteins, including PDE3A1-RFP had been confirmed using fluorescence microscopy. PDE3A1-RFP expression in HEK was not as strong as PDE-RFP isoform infection but was clear.

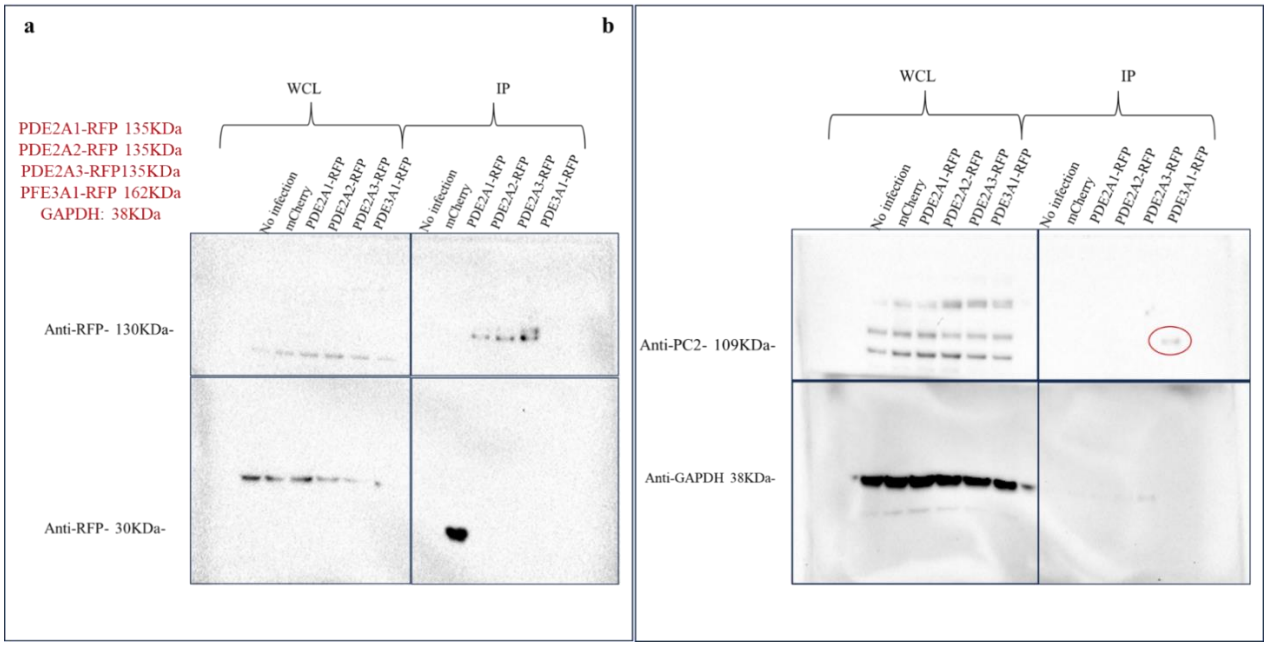

Figure 34: HEK cells were infected with mcherry, one of three PDE2A-RFP isoforms, or PDE3A1-RFP. Pull Down was achieved via RFP nanobeads. **a** shows membrane with WCL (left) or IP (right) samples and stained with anti-RFP **b** shows membrane with WCL (left) or IP (right) samples, stained for anti-PC2, or anti-GAPDH. Experiment was carried out three times (n=3) with PDE3A1 interaction with PC2 confirmed each time. Bands were not good enough to perform statistical analysis.

Results 3-PDE3A1 interacts with endogenous PC2 in the cytosol and ER

Having tested PDE interaction with endogenous PC2 and finding a band for PC2 interaction in the PDE3A1-RFP sample, but no band confirming PDE3A1-RFP expression in the fragment lysate, it was next decided to carry out the same IP on fractionated samples of IMCD3. This was done for several reasons. Firstly, switching to IMCD3 cells might yield stronger PDE3A1-RFP expression than in HEKs. Secondly, separating the cell lysate using the Qiagen fractionation kit could allow for the proteins of interests to be more prominently visible, as each protein would be more concentrated in the relevant fraction. This was not only important to potentially enhance PDE3A1-RFP detection, but also because it had not been possible to confirm the interaction between endogenous PC2 and PDE2A-flag isoforms. Focusing on specific cellular subdomains to probe for PDE2A:PC2 interaction, might increase the chance of detection. The third, and most important, reason for carrying out fractionation IP was to identify where in the cell, PDE3A1-RFP may be interacting with endogenous PC2.

IMCD3 cells were infected with mCherry, PDE2A2-RFP, or PDE3A1-RFP. As all three PDE2A isoforms were shown to interact with PC2-GFP, PDE2A2-RPF only was selected for further experiments, to reduce the number of samples handled simultaneously and because PC2 was originally found in an interactome for the PDE2A2 isoform specifically. Efficient infection of all viruses was confirmed using fluorescence microscopy before lysing the cells. **Figure 35a** shows the input (or whole fractions) for this experiment. Of note, anti-RFP staining demonstrated PDE2A2-RFP (~135KDa) primarily localises to the mitochondria, but also showed expression in the ER fraction as well as in the cytosol, confirming previous findings (Lobo et al 2020). PDE3A1-RFP expression, demarcated by a band at ~162KDa was observed primarily at the ER, with some expression also seen in the mitochondria (**Figure 35a**). Of note, the band representative of PDE3A1-RFP is the higher band, and not the immediately lower band, that appears in the ER sample. The identity of the latter band is unknown. In the IP samples (**Figure 35b**) PDE2A2-RFP primarily localised to the ER but also

showed some expression in cytosol and mitochondria. PDE3A1-RFP, primarily localised to the ER, but also showed some expression in the cytosol. A hint of PDE3A1-RFP in the mitochondrial fraction of the IP could also be noticed (**Figure 35b**). Surprisingly, mCherry expression was not detected using anti-RFP antibody in either the input or the IPs (**Figure 35b**), which is unexpected as mCherry expression was quite strong when assessed through fluorescence microscopy before lysis. Nevertheless, since PDE2A2-RFP did not interact with PC2 at any of the subcellular fractions, but PDE3A1-RFP did interact with PC2 in the cytosolic and ER fractions of IMCD3 (**Figure 35b**), it was assumed that PC2 interaction with PDE3A1-RFP was not occurring through random association with RFP, but through PDE3A1. Outside the interaction, in fraction samples PC2 can be seen to localise primarily to the ER, but also slightly to the mitochondria, with no obvious localisation to the cytosol (**Figure 35a**). Also from the input, GAPDH confirmed the cytosolic fraction, and no GAPDH staining in the ER and mitochondrial fraction suggests fractionation was clean. Equally, ponceau red stained a band at ~16 KDa in the mitochondrial fractions of the input only, which is believed to be TOM20. Unfortunately, this was the only way to visualise the mitochondrial marker, as the TOM20 antibody failed to stain. The same problem occurred with ER antibodies, so firm confirmation of the purity of the ER fraction was not achieved. However, based on PC2 and PDE3A1 expression in the ER sample, it is highly likely this fraction is indeed ER, as both those proteins are known to localise to the organelle. One final note, non-specific staining with RFP led to non-specific bands between 40-100KDa in the non-infected cytosolic and ER IP samples. Overall, this experiment strongly indicates an interaction between PDE3A1-RFP and endogenous PC2 at the cytosol and ER of IMCD3.

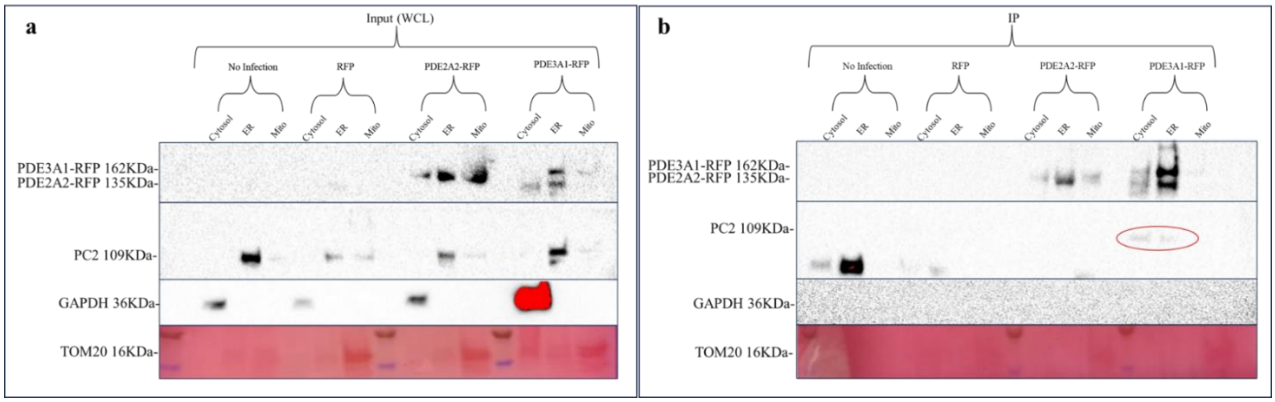

Figure 35: IMCD3 cells were infected with mCherry, PDE2A2-RFP, or PDE3A1-RFP viruses. Cells were then lysed according to the Qiagen fractionation kit protocol to obtain cytosolic, ER, and mitochondrial fractions for each sample. Pull down was achieved with RFP-Trap nanobeads and input (**a**) and IP membranes (**b**) were stained with ponceau red, anti-PC2, anti-RFP, and anti-GAPDH. Experiment was attempted five times with mixed success (n=5). No statistical analysis was performed.

Discussion and Conclusions

Proteomics studies carried out in NRVM and HT-4 indicated PDE3A1 and PDE2A2, respectively, may interact with PC2, which is mutated in 15-20% of ADPKD cases. Since PDE3 inhibition leads to decreased cystogenesis in vitro, and since PC2 mutations, or deletion, leads to cystogenesis in this disease, it was hypothesized that PDE3A1 inhibition mitigates cyst growth by regulating a pool of cAMP at a subcellular site where PC2 localises. Therefore, I sought to carry out co-immunoprecipitation experiments to validate these interactions. Despite some limitations in the biochemical analysis conducted, it can still be confidently concluded that PDE3A1 interacts with endogenous PC2, as demonstrated in both HEK and IMCD3 cell lines. The main issue with these experiments, however, was a failure of the anti-RFP antibody to detect PDE3A1-RFP, despite it being able to detect PDE2A-RFP isoforms. The same issue was sometimes also observed with anti-RFP staining of mCherry (**Figure 34**). Troubleshooting for this problem included ordering fresh RFP antibody and increasing mCherry and PDE3A1-RFP expression levels in IMCD3. However, the former gave inconsistent results, as sometimes the anti-RFP would stain mCherry and sometimes not, despite equal expression levels of mCherry being observed with fluorescence microscopy before lysis. A colleague carrying out similar experiments in Mouse embryonic fibroblasts (MEFs) and cardiomyocytes also encountered this problem. Although extensive optimisation

was carried out to try to resolve this issue, time limitations did not allow successful resolution. The anti-RPF antibody also stained non-specific bands in the IP from non-infected samples. Overall, it is likely the lack of PDE3A1-RFP detection in samples, confirmed to have been infected with the virus, was a mix of low expression levels paired to weak antibody performance. However, in the non-fractionated endogenous IP (**Figure 34**) a PC2 band was still observed at 109KDa, in the PDE3A1-RFP sample alone, and since pull down was achieved with RFP-trap beads, this hints that, though undetected, PDE3A1-RFP pulled down PC2. Furthermore, in the IP from subcellular fractions, PDE3A1 did successfully pull down PC2 in the cytosolic and ER fractions of IMCD3. The interaction was stronger at the cytosol than the ER, despite expression of individual PC2 and PDE3A1 showing more intense signal in the ER fraction. Although this finding may indicate that the interaction takes place in the cytosol of the cell, it should be considered that the lysis of the plasma membrane and intracellular membranes were achieved via different buffers and the interaction could have been affected more readily in the intracellular membrane samples than in the cytosolic ones.

Of note, while the main protein of interest was PDE3A1, PDE2A isoforms were also shown to interact with PC2-GFP, when both proteins were overexpressed (**Figure 34b**). Unfortunately, this interaction was not recapitulated in HEK or IMCD3 when only the PDE2A isoforms were overexpressed and endogenous PC2 was probed. In these latter cases, there is no doubt of either PDE2A or PC2 expression, but the interaction was still not observed. From this data, it is concluded that all three PDE2A isoforms can interact with PC2, but most likely do not do so at physiological expression levels of both proteins in IMCD3. It is important to remember that the initial interaction between PDE2A2 and PC2 was observed in a neuroblastoma cell line (Lobo et al. 2020b), so one hypothesis is that PC2 interaction with specific isoforms of PDEs is cell type dependent, as PDE2A is highly expressed in the brain, with less expression in kidneys (according to the human protein atlas). Another possibility is that PDE2A only interacts with PC2 in specific physiological conditions. In chapter 9 it is suggested that PDE3 and PDE2 function at ER-mitochondrial contact sites to regulate inter-organelle crosstalk.

PC2 is also present at these contact sites and functions to keep them apart (Kuo et al. 2019). One hypothesis is therefore that PDE2A2 localises to the outer mitochondrial membrane (OMM) and when mitochondria make contact with the ER, PC2 localising to the latter organelle can associate with PDE2. In contrast to PDE2, PDE3A1, which localises to the ER and is expressed at higher levels in IMCD3 (**Figure 7**), more consistently interacts with PC2. This interaction could potentially help mitigate cystogenesis in vitro, upon PDE3 inhibition.

For PDE3 to function through PC2 to mitigate cyst formation, it would likely have to control a pool of cAMP, whose upregulation would lead to phosphorylation of PC2 by one of the cAMP effector proteins. Indeed, PC2 can be phosphorylated by PKA to affect its localisation and function. One study reported findings which complement the in vitro phenomenon observed in the cyst assays described in chapter 5. Cantero et al linked PC2 channel activity to PKA phosphorylation in human term syncytiotrophoblasts (hST). Overexpression of the catalytic subunit of PKA increased spontaneous endogenous PC2 channel activity by 566%, with the cAMP analogue, 8-Br-cAMP, also increasing channel function. Addition of alkaline phosphatases attenuated both the PKA and the 8-Br-cAMP stimulated increase in PC2 channel activity. Vanadate, a phosphatase inhibitor reversed the latter finding. PKA and 8-Br-cAMP did not alter PC2 ion conductance but increased the average time the channel remained open. Finally, PKA phosphorylation did not have an effect on PC2 channels with a S829A mutation, suggesting altered conductance time was directly regulated through S829 phosphorylation.(Cantero Mdel et al. 2015) These findings align with the hypothesis that PDE3 inhibition leads to mitigated cystogenesis via interaction with and phosphorylation of PC2. In this model, PC2 mutations lead to loss of channel function at the ER, and subsequent ADPKD. PDE3A1 inhibition in in vitro cystogenesis, upregulates PKA phosphorylation of PC2, increasing channel function, resulting in reduced cyst formation (**schematic 12**). However, this is possibly an oversimplified explanation, as alternative literature demonstrates the mechanism by which the polycystins work together, and are orchestrated by cAMP and PDE activity, will likely be a complex one.

In a different study, authors demonstrated that Ser829 was phosphorylated by PKA when PC2 localises to the ER only. Phosphorylation of the same residue is regulated by Aurora Kinase A when the protein is located at the mitotic spindle poles.(Watnick and Germino 2013) The study proposed a checks and balances relationship between the polycystins, as PC1 binding to PC2 greatly reduced PKA-mediated phosphorylation of Ser839 by recruiting protein phosphatase 1α to the polycystin complex. Corroborating this finding, phosphorylation of PC2 Ser829 was enhanced in embryonic kidney cells of PKD1 mutant mice, as well as from renal tissue of ADPKD patients. This increased phosphorylation of Ser829 had subsequent effects. HEK cells expressing phosphomimic mutants of Ser829 had increased ATP-stimulated calcium currents compared to their WT PC2 counterparts. Furthermore, overexpression of WT PC2, but not the phosphomimic mutant, decreased cell proliferation in HEKs.(Watnick and Germino 2013) The authors posed a fundamental question of whether PC2 phosphorylation, and its regulation by PC1, is thus detrimental or beneficial to ADPKD progression. Based on the data, increased PKA phosphorylation of PC2 upon PC1 mutation/deletion would aggravate cyst formation, as likely occurs in PKD1-mutated patients and models. However, it is also known that knock out of PC2 would mean no Ser829 phosphorylation, and yet cystogenesis is still observed, hence contradicting the idea that upregulating PKA phosphorylation of PC2 is detrimental. In the context of our findings, it is proposed that PDE3 inhibition mitigates cystogenesis through a direct interaction with PC2. This would likely mean PDE3 inhibition leads to enhanced phosphorylation of PC2, possibly at Ser829, aggravating disease in this scenario. Yet, the opposite effect was observed in vitro, where PDE3 inhibition significantly mitigates cystogenesis. However, the experiments in this thesis were carried out in a model of ADPKD propagated by increasing promiscuous cAMP, and not in a model of ADPKD fuelled by mutations in the polycystins. Therefore, it is unpredictable whether PDE3 inhibition, in a more faithful replica of ADPKD, would still ameliorate or aggravate cyst formation without further experimentation.

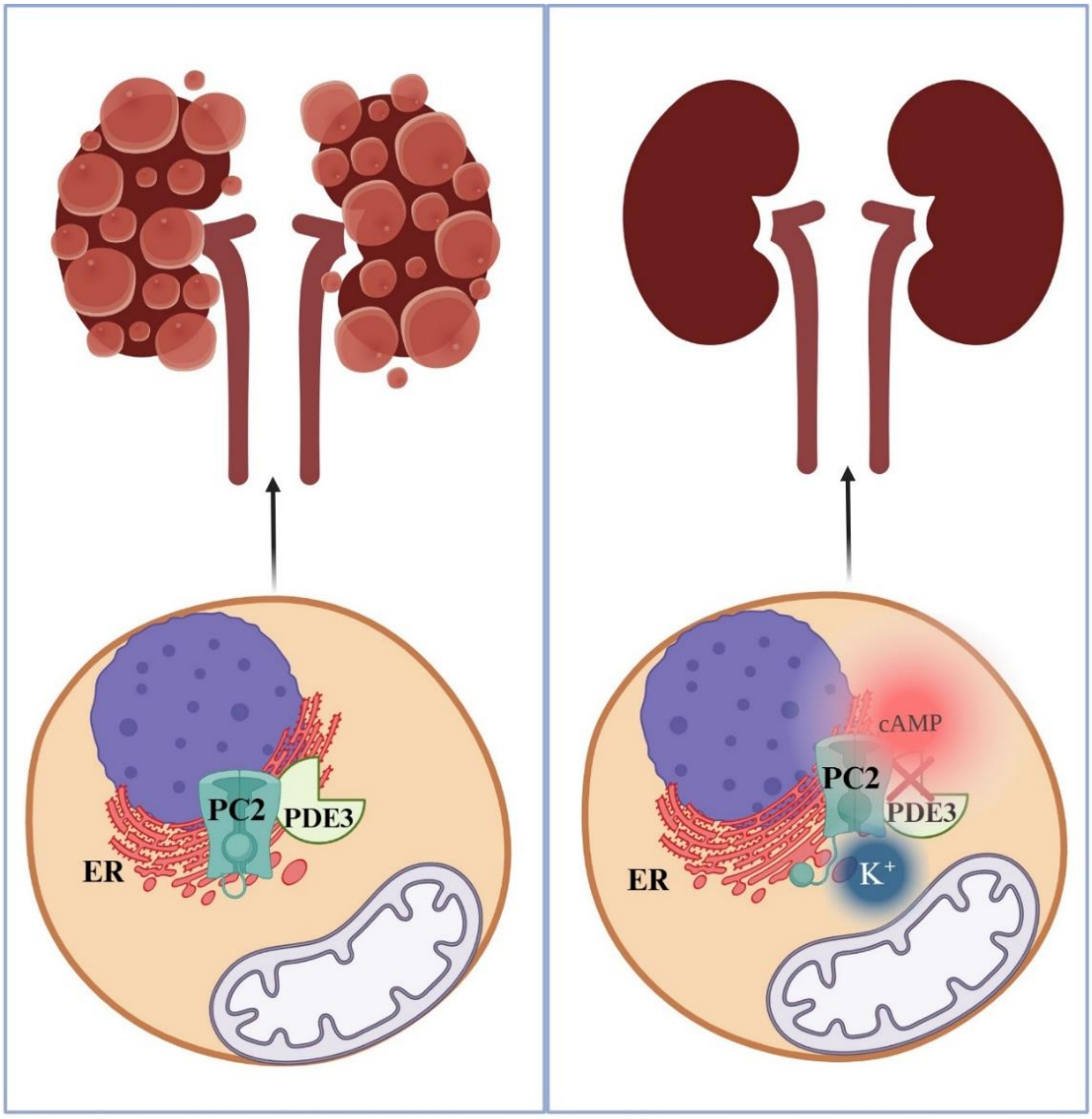

Schematic 12: The schematic illustrates a potential mechanism for how PDE3 inhibition leads to reduced cystogenesis in vitro. PDE3 functions to hydrolyse a pool of cAMP where the effector protein, PKA, phosphorylates PC2. With active PDE3, there is reduced cAMP and subsequent PKA phosphorylation of PC2 (left). This leads to lower PC2 channel conductance and cyst formation, in the presence of FSK. When PDE3 is inhibited (right), cAMP in this nanodomain is upregulated, thus PKA phosphorylation of PC2 is increased, and PC2 channel stays open longer, increasing K^+ conductance. Increased K^+ signalling in this domain mitigates cystogenesis through a mechanism that remains to be elucidated.

Had time allowed, western blots probing for phosphoserine in DMSO versus Cilostamide treated IMCD3, could have been performed to test whether PDE3 inhibition indeed leads to increased phosphorylation of PC2 by PKA. However, this thesis was particularly focused on locating the cAMP nanodomain believed to regulate renal cytogenesis, so these experiments were not prioritised. An aforementioned study demonstrated PKA phosphorylates PC2 at the

ER, and Aurora Kinase A phosphorylates PC2 at the mitotic spindles where the centrioles are located.(Watnick and Germino 2013) Therefore, it is hypothesized the cAMP nanodomain of interest may be proximal to the ER. The next chapter will use FRET reporters, to monitor cAMP responses at specific subcellular domains, including the ER, to measure cAMP changes upon PDE inhibition. Identifying subdomains with high levels of PDE3 cAMP hydrolysis will narrow in on where PDE3 may function to regulate cyst formation.

Chapter 8: PDEs hydrolyze cAMP at subcellular domains of IMCD3, and their activity is dependent on ciliary phenotype

Introduction

In chapter 5, PDE3 inhibition led to a decrease in cystogenesis in an in vitro model of ADPKD (**Figure 22**). Yet, FRET microscopy with ciliary and cytosolic reporter, Arl13B-H187, did not detect any changes in cAMP upon FSK administration and subsequent PDE3 inhibition (**Figure 8b**) in chapter 4. These observations suggest that PDE3 functions to regulate cystogenesis by modulating cAMP levels in a subcellular nanodomain, that escapes detection with Arl13b-H187.

Traditionally, cAMP signalling has been described as a linear cascade, whereby ligand binding to a GPCR initiates cAMP synthesis by ACs and activates PKA to phosphorylate target proteins. However, recently, this model was recognised as an inadequate explanation to how this second messenger can achieve different outcomes in distinct subcellular domains. A better model was developed, where G_{as} -coupled receptors generate isolated pools of cAMP which only stimulate specific PKA subsets, which are anchored in proximity to their phosphorylation target via AKAPs. These complexes, structured by AKAPs, also include phosphatases and PDE isoforms to quench the cAMP signal. With unique combinations of effector proteins, AKAPs, and enzymes, each nanodomain can achieve distinct cellular functions downstream of cAMP.(Lohse, Bock, and Zaccolo 2024)

Indeed, cAMP levels differ at subcellular sites, and are not uniform, as previously thought. Evidence for this model was primarily observed through β-AR signalling in cardiomyocytes, but was also demonstrated in other cell types.(Annamdevula et al. 2018; Agarwal et al. 2017; Monterisi et al. 2012; Hansen, Kaiser, Leyendecker, Stüven, Krause, Derakhshandeh, Irfan, Sroka, Preval, and Desai 2022) For example, the smallest cAMP nanodomains were observed in HEK293 cells, where spacers, incorporated in cAMP FRET sensors, measured a specific distance between a GPCR and the FRET reporter. A cAMP diameter of 60nms per domain was observed, using these spacers, after low agonist concentrations. Proximal nanodomains operated distinctly from one another and were isolated from cAMP signalling outside of the domain. These domains were called receptor-associated independent cyclic adenosine monophosphate nanodomains (RAINs).(Anton et al. 2022) Furthermore, similar spacers were used to separate cAMP sensors from PDEs. In HEKs, these constructs unveiled even smaller nanodomains with radii of less than 10nm.(Bock et al. 2020) Therefore, it is possible that PDE3 functions in a RAIN which is so small, it could not be detected with cytosolic expression of Arl13b-H187. Thus, I sought to measure PDE3 cAMP hydrolysis in more precise cAMP compartments, using localised FRET reporters, to narrow in on this potential domain.

Ciliary cAMP has been shown to drive cyst formation, (Hansen, Kaiser, Leyendecker, Stüven, Krause, Derakhshandeh, Irfan, Sroka, Preval, and Desai 2022) yet PDE3 inhibition, which should increase cAMP, led to decreased cyst growth. This knowledge, paired with the facts that PDE3 has not been shown to localise to primary cilia, and that, according to data from chapter 6, PDE3 inhibition does not alter ciliogenesis, indicates that the cAMP nanodomain by which PDE3 functions to control cyst formation is unlikely at the cilium. Therefore, to narrow in on where PDE3 does function within IMCD3 cells, FRET reporters, readily available in the lab, and localising to three subcellular domains were used to measure cAMP changes upon PDE inhibition. The three intracellular domains selected were the ER

(ER-cyto-H90), the Outer Mitochondrial Membrane, also known as OMM (OMM-EPAC), or the plasma membrane (AKAP79-CUTie).

The first domain of interest is the ER, as both PDE3A1 and PC2 have been shown to localise to this organelle.(Kuo et al. 2019; Shakur et al. 2000) I have also demonstrated ER localisation of PDE3 and PC2 in the previous chapter. Of note, PC2 has many phophorylation sites, for a variety of kinases, which alter the proteins localisation and function.(Cantero Mdel et al. 2015) Interestingly, while Aurora Kinase A phoshorylation of PC2 targets the polycystin to the mitotic spindles, PKA phosphorylation of PC2, instead, localises the protein to the ER,(Watnick and Germino 2013) hinting that the cAMP pathway is a regulator of PC2 at the latter organelle. Additionally, as Chapter 9 will later highlight, PC2 regulates crosstalk between the endoplasmic reticulum and the mitochondria.(Kuo et al. 2019) PDE3A1 has also been shown to localise to intracellular membranes, unlike its counterpart PDE3A2 which is mainly cytosolic.(Vandeput et al. 2013) Though PDE3A1 has been primarily linked to the regulation of the sarcoplasmic reticulum Ca^{2+} reuptake in cardiac contractility (Ahmad et al. 2015), a proteomics study carried out in our lab shows PDE3A1, but not PDE3A2, interacts with a variety of proteins which function at the ER. Some of these proteins, such as Calnexin, Fis1, and Cav1 are also implicated in ER-mitochondrial crosstalk. (Bravo-Sagua et al. 2019; Subramaniam et al. 2023) Therefore, the second nanodomain selected for further investigations was the outer mitochondrial membrane (OMM). Limited literature is available to indicate whether PDE3 functions at this domain. PDE3B localises to T-tubules and was reported to function in proximity of mitochondria to regulate their activity in cardiomyocytes, yet no evidence has linked PDE3A1 to this organelle thus far. (Movsesian, Ahmad, and Hirsch 2018) Our aim here was to measure cAMP hydrolysis by PDE3 in mitochondria of IMCD3 using targeted FRET sensor OMM-EPAC.

The final domain of interest is the plasma membrane, as PDE3 was reported to interact with CFTR at this site, where PDE3 inhibition augments CFTR function.(Penmatsa et al. 2010)

Though this finding would suggest that PDE3 inhibition aggravates cystogenesis, by increasing fluid secretion via CFTR Cl^- expulsion, the possibility that PDE3 functions at the membrane to mitigate cystogenesis, cannot be excluded, unless no PDE3 activity at this domain is observed. Furthermore, in Chapter 7, we demonstrated PDE3A1 interacts with PC2, a protein which can localise to the ER, the cilium, but also to the plasma membrane.(Hanaoka et al. 2000) In line with this, endogenous PC2 interacted more strongly with PDE3A1-RFP in the cytosolic fraction, rather than the ER, where both proteins were found at a higher concentration. This observation hints that PDE3A1 and PC2 could interact at the plasmalemma. Finally, AKAP79 (also known as AKAP150), the protein used here to anchor the FRET sensor to the plasma membrane, interacts with PC2, in a complex localising to the cilium, along with PDE4, PKA, and AC5/6. Disruption of this complex was implicated in renal cystogenesis. (Choi et al. 2011b) While it is unlikely PDE3 functions at the cilium, since AKAP79 also localises to the plasma membrane, PDE3 may regulate membrane AKAP79 cAMP signalling while PDE4 controls ciliary signalling of the same domain. Indeed, there are multiple examples where the same GPCR, signalling at the plasma or ciliary membrane, achieves disparate outcomes depending on its location.(Paolocci and Zaccolo 2023) It could be, alternate downstream signals are modulated by different PDEs.

Results 1- PDEs function to hydrolyse cAMP at the ER

To identify the subcellular domain controlled by PDE3 and responsible for reduced cyst growth, we first set out to measure PDE cAMP hydrolysing activity at the ER. IMCD3 cells were transfected with loss -of-FRET sensor, ER-cyto-H90, which measures cAMP changes at the cytosolic interface of the organelle, as it is anchored using the protein P450 2C1/2.(Lobo 2018) FRET was recorded in response to one of three PDE inhibitors. This response was normalised to sensor saturation, achieved through adenylyl cyclase activator, FSK, and the non-selective PDE inhibitor, IBMX. Of note, cells were discriminated based on the presence and absence of a cilium, as previous experiments with the FRET reporter, Ar1lb-H187,

demonstrated that the ciliary phenotype determined the PDE activity detected in the bulk cytosol. In these experiments, the primary cilium was identified via co-transfection of the sensor with SSTR3-RFP, a protein known to localise to the cilium.(Barbeito and Garcia-Gonzalo 2021) Upon PDE3 inhibition with Cilostamide, in non-ciliated IMCD3, we observed an increase in cAMP corresponding to ~15% maximal FRET change, and a ~10% increase in ciliated IMCD3 (**Figure 36**). PDE2 inhibition via Bay60 led to a 20% increase in FRET change at the ER of non-ciliated cells, and a 15% increase in ciliated IMCD3 (**Figure 36**). Rolipram, the PDE4 inhibitor, yielded a 40% increase in FRET change in non-ciliated IMCD3, and a 50% increase in ciliated cells. (**Figure 36**)

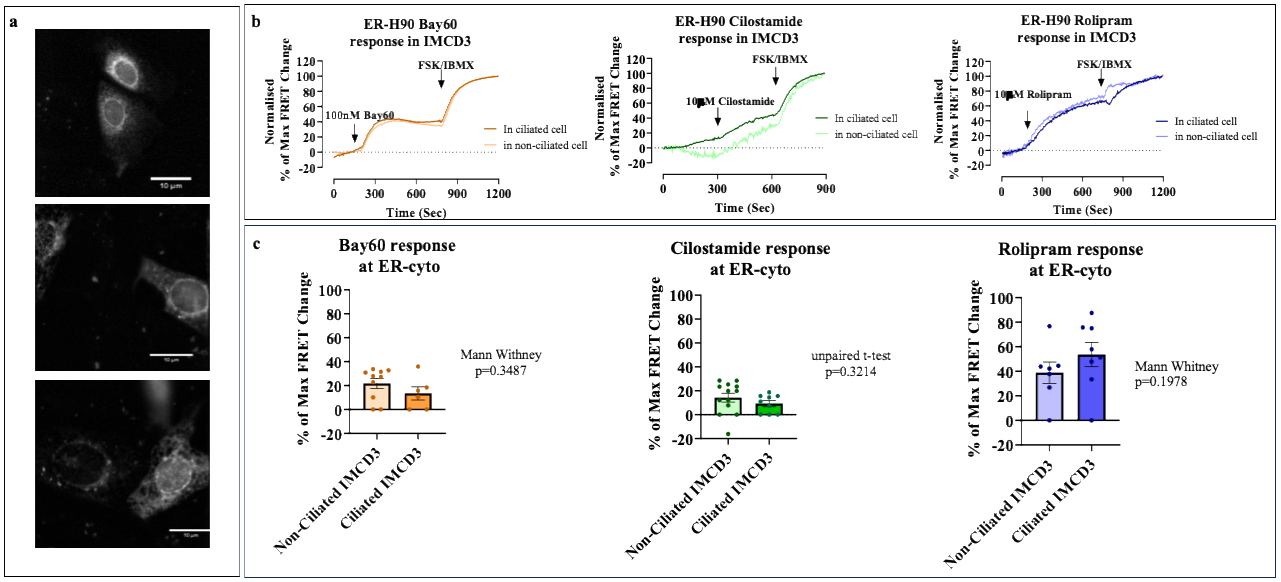

Figure 36: a shows examples of ER-Cyto-H90 localisation in IMCD3 **b** Example FRET curves for IMCD3 ciliated or non-ciliated, transfected with ER-H90 reporter and treated with either 100nM Bay60 and FSK/IBMX (left), 10μM Cilostamide and FSK/IBMX (middle), or 10μM Rolipram and FSK/IBMX (right). FRET curves are normalised to max FRET change (response to FSK/IBMX). **c** quantification of FRET curves **a.** Parametric data was analysed using unpaired t-test. Non-parametric data was analysed with Mann Whitney test. Each datapoint is a single coverslip. N=3, where n is one round of experimentation from one independent flask passage. Bars represent mean with SD.

Results 2- PDEs function to hydrolyse cAMP at the OMM of non-ciliated cells

We next wanted to measure PDE hydrolysis of cAMP at the OMM, as PDE3 activity at the mitochondria of renal cells had not been previously explored. OMM-EPAC, a loss-of-FRET reporter, was expressed into IMCD3, and a similar experimental protocol as used with ER-cyto-H90 was applied. After analysis, we observed a 16% increase in cAMP upon PDE3

inhibition in non-ciliated IMCD3, but no PDE3 cAMP-hydrolysing activity was observed at the OMM of ciliated renal cells (**Figure 37**). Similar findings were observed with PDE2 inhibition via Bay60, which reported a 12% increase in cAMP at the OMM of non-ciliated cells, with minimal cAMP hydrolysis in ciliated IMCD3 (**Figure 37**). The third inhibitor, Rolipram, showed an increase of 22% in non-ciliated IMCD3 and 27% in ciliated renal cells, upon PDE4 inhibition (**Figure 37**).

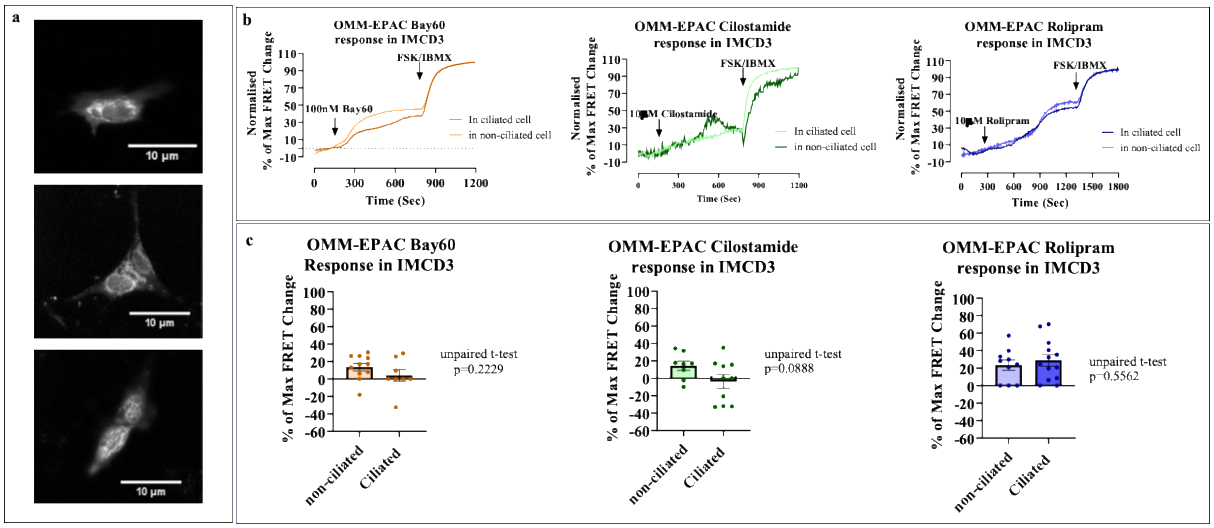

Figure 37: a shows examples of OMM-EPAC localisation in IMCD3 **b** Example FRET curves for IMCD3 ciliated or non-ciliated, transfected with OMM-EPAC reporter and treated with either 100nM Bay60 and FSK/IBMX (left), 10µM Cilostamide and FSK/IBMX (middle), or 10µM Rolipram and FSK/IBMX (right). FRET curves are normalised to max FRET change (response to FSK/IBMX). **c** quantification of FRET curves **d.** Parametric data was analysed using unpaired t-test. Each datapoint is a single coverslip. N=3, where n is one round of experimentation from one independent flask passage. Bars represent mean with SD.

Results 3- PDEs function to hydrolyse cAMP at the plasma membrane

The final cAMP domain of interest, the plasma membrane, was measured using AKAP79-cutie, a gain-of-FRET sensor. Of note, AKAP79 plasmid transfection proved difficult and inconsistent, and co-transfection of AKPA79-CUTie with SSTR3-RFP was entirely unsuccessful. Therefore, we infected AKAP79-CUTie with no SSTR3 and could thus not discriminate our analysis based on ciliary phenotype. Despite this, we found a comparable increase in cAMP upon PDE3 inhibition at this domain, as we did at the ER and OMM of non-ciliated IMCD3 (about 15%). **Figure 38** also shows minimal cAMP hydrolysis by PDE2

at this site, and reduced cAMP hydrolysis by PDE4 at the plasma membrane (22%) compared to PDE4 activity at other subcellular domains.

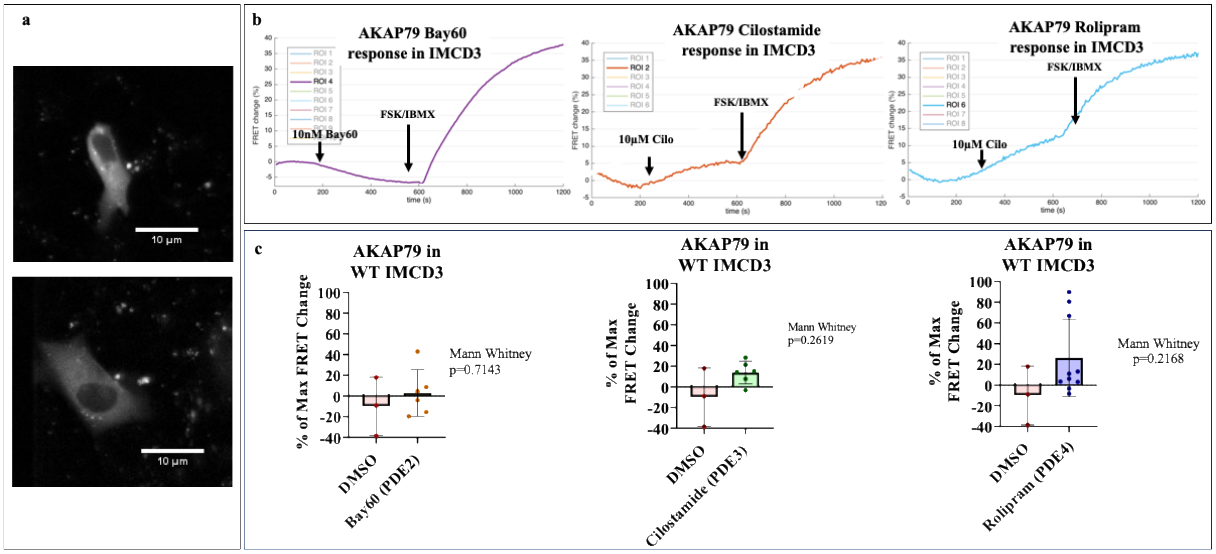

Figure 38: a shows examples of AKAP79 localisation in IMCD3 **b** Example FRET curves for IMCD3 transfected with AKAP79-CUTie reporter and treated with either 100nM Bay60 and FSK/IBMX (left), 10µM Cilostamide and FSK/IBMX (middle), or 10µM Rolipram and FSK/IBMX (right). FRET curves are normalised to max FRET change (response to FSK/IBMX). **c** quantification of FRET curves. Non-parametric data was analysed using unpaired Mann Whitney test. Each datapoint is a single coverslip. N=3, where n is one round of experimentation from one independent flask passage. Bars represent mean with SD.

Discussion and Conclusions

PDE3 inhibition reduced cyst formation in an in vitro assay of cystogenesis, but upon measurement of cAMP, using ciliary and cytosolic FRET reporter, Arl13B-H187, we found negligible activity of PDE3, downstream of AC activation with FSK (**Figure 8b**). Thus, we hypothesized, that while PDE3 does not function to hydrolyse cAMP at the bulk cytosol or cilium, it might do so in a compartmentalised intracellular domain of IMCD3. Identifying where PDE3 activity is upregulated, in comparison to other PDEs and other subcellular locations, could point to the mechanism by which PDE3 inhibition mitigates cyst growth. Thus, we measured cAMP hydrolysis of PDEs at the ER (ER-cyto-H90) (**Figure 36**), OMM (OMM-EPAC) (**Figure 37**), and the plasma membrane (AKAP79-CUTie) (**Figure 38**). We found that PDE3 hydrolyses cAMP to comparable degrees at all three subdomains, with slightly higher activity at the ER. Surprisingly, PDE3 breakdown of cAMP, particularly at the

OMM, was dictated by ciliary phenotype, as no PDE3 function was observed at the OMM of ciliated IMCD3 (**Figure 37**). A similar pattern was observed, where there was increased PDE2 activity at both the OMM and the ER of non-ciliated cells compared to their ciliated counterpart, again, particularly at the OMM. Of interest, PDE2 hydrolysis of cAMP was greater at the ER, despite its reported function at the OMM, suggesting a potential role for this enzyme at the former organelle(Monterisi et al. 2017) Also of note, PDE4 inhibition led to greater cAMP enhancement in ciliated cells, following the opposite pattern to PDE2 and PDE3. This finding aligns with studies which show PDE4 can localise to the cilium to breakdown cAMP, while PDE2 and PDE3 are not thought to function in this organelle.(Choi et al. 2011b; Omar et al. 2019)

Using AKAP79-CUTie we could not express SSTR3, so we were unable to differentiate between ciliated and non-ciliated cells. Nevertheless, we still saw an increase in cAMP upon PDE3 inhibition at this domain (**Figure 38**). As it was previously reported that PDE3 functions at the plasma membrane to control CFTR activity, (Penmatsa et al. 2010) we could not exclude the possibility that PDE3 inhibition works through CFTR at the plasmalemma, to control fluid secretion and mitigate cystogenesis. Indeed, this hypothesis thus still stands. We also surmised PDE3 could interact with PC2 at AKAP79, as PC2 was shown to form a complex with this AKAP, PKA, AC5/6 and PDE4C.(Choi et al. 2011b) It was hypothesized PDE3 may regulate this complex at the plasma membrane, while PDE4C would control a cAMP pool in the cilium. PDE4 is known to be highly expressed in IMCD3, thus its activity is relatively ubiquitous (**Figure 7**). Surprisingly, however, PDE4 inhibition at AKAP79 led to its smallest increase in cAMP (20%) of all domains investigated, supporting the hypothesis that AKAP79 cAMP signalling is regulated by PDE3 at the plasma membrane.

Overall, the three subcellular cAMP domains showed comparable levels of PDE3-driven cAMP hydrolysis. Thus, we could not select a clear domain likely responsible for the regulation of cystogenesis through this evidence alone. However, we observed PDE3

breakdown of cAMP at the OMM and comparable PDE2 hydrolyses of the second messenger at the ER of non-ciliated IMCD3. These two results had not previously been reported and shed light on a possible role for the two enzymes in their respective novel domains. Further experiments would need to be carried out to fully characterise the role of PDEs in these domains. Yet, recent advances have shown the ER and the mitochondria interact to achieve a multitude of downstream effects. Both PC2 and PKA were demonstrated to function at these organelle contact sites.(Kuo et al. 2019; Bravo-Sagua et al. 2019) We have validated that PDE3 and PDE2 interact with PC2, but in a proteome study carried out previously in the lab, these two enzymes are also involved with a plethora of proteins known to function at the mitochondria-associated-membranes (MAMs). Therefore, we hypothesize that PDE3 works at the MAMs, alongside PC2, to regulate cystogenesis. The following chapter explores the role of PDE inhibition on ER-mitochondrial contact sites.

Chapter 9: PDEs may interact with PC2 to regulate ER-mitochondrial crosstalk.

Introduction

PDE3 inhibition and the Endoplasmic Reticulum

PDE3 inhibition was shown to mitigate cystogenesis in vitro (Chapter 5), and in Chapter 7 it was demonstrated PDE3A1 interacts with PC2 at the plasma membrane and the Endoplasmic Reticulum (ER). Thus, it is hypothesized that PDE3 interacts with PC2, in a specific subcellular domain, to reduce cyst formation. In an attempt to identify this domain, PDE3 cAMP-hydrolysing activity was measured using FRET reporters targeted to specific subcellular locations (Chapter 8). PDE3 activity was observed at the ER and the plasma membrane, as well as at the outer mitochondrial membrane (OMM) of non-ciliated cells. Recently, PC2 has been shown to reduce ER-mitochondrial contacts. (Kuo et al. 2019) KO of PC2 in LLC-PK1, a porcine renal epithelial cell line, increased expression of Mitofusin 2 (MF2N), an outer mitochondrial membrane (OMM) protein which helps tether mitochondria to ER. Through increased organelle contacts, PC2 KO led to upregulated Ca^{2+} release from the ER into the mitochondria, resulting in bioenergetic activation, and increased overall mitochondria density. KO of MFN2 in PC2 KO LLC-PK1 restored defective mitochondrial Ca^{2+} transfer, and significantly reduced cell proliferation in in vitro-induced renal cysts. In the study, tissue derived from ADPKD patients showed a 2 fold increase in mitochondria as well as MFN2 expression.(Kuo et al. 2019) Together, this evidence suggests a primary role for PC2 in ER-mitochondrial dynamics, and by extension, genetic deletion of PC2 may drive cystogenesis by altering organelle contact and consequent oxidative metabolism and cellular proliferation in ADPKD. On these grounds, we hypothesized that PDE3 inhibition may also function at the ER-mitochondrial interface to reduce cyst formation. Indeed, many interactors of PDE3A1 regulate ER-mitochondrial contact sites.

PDEs interact with proteins of the MAMs

Intra-organelle crosstalk at the mitochondria-associated ER membranes (MAMs) orchestrates a variety of processes such as glucose metabolism,(Rieusset 2018) lipid synthesis, and mitochondrial bioenergetics, as well as apoptosis. Consequently, ER-mitochondrial collaboration is emerging as a prevalent driver in all sorts of diseases from cancer to neurodegeneration.(Tubbs and Rieusset 2017; Wilson and Metzakopian 2021; Csordás, Weaver, and Hajnóczky 2018; Bravo-Sagua et al. 2017; Cárdenas et al. 2010; Pennanen et al. 2014; Sutendra et al. 2011; Arruda et al. 2014) Emerging evidence suggests ADPKD could be one these diseases, where altered organelle crosstalk leads to changes in mitochondrial metabolism and bioenergetics.(Kuo et al. 2019)

Polycystins co-fraction with long chain fatty acid-CoA ligase 4 (FACL4), a mitochondria-associated-membranes (MAM) identifier (Padovano et al. 2017). Of note, our proteomics studies also link PDE3A1 and PDE2A2 to a multitude of proteins implicated in ER-mitochondrial crosstalk. For example, PDE2A2 was shown to hydrolyse a pool of cAMP where subsequent PKA phosphorylation of Dynamin-related protein 1 (DRP1) controlled apoptosis.(Monterisi et al. 2017) DRP1, but also Cav1, another interactor of both PDE3A1, PDE2A2 and PC2, were shown to function, alongside cAMP to regulate ER-mitochondrial contact. (Subramaniam et al. 2023; Bravo-Sagua et al. 2019)

During early ER-stress, crosstalk between the mitochondria and the ER increases, enhancing ATP production, but the mechanism by which this is achieved is still unknown (Bravo et al. 2011) Bravo-Sague et al. showed that Caveolin-1 (Cav1) localises to the MAMs of tumour cells, to impair organelle contact and subsequently quench Ca^{2+} transfer into the organelle, making mitochondria unresponsive to ER stress.(Bravo-Sagua et al. 2019) Interestingly, both ER stress and mTOR inhibition can lead to PKA upregulation at this site, where evidence suggests Cav1 may function as a PKA scaffold.(Cohen et al. 2004) At the MAMs, PKA phosphorylates DRP1 on Ser637, to inhibiting the GTPase and elongate mitochondria. In

addition, PKA phosphorylation of DRP1 relocates the GTPase to the ER, working in concert with various ER-associated proteins to expand the organelle.(Friedman et al. 2011; Ortiz-Sandoval et al. 2014) (Wikstrom et al. 2013) This process, is believed to be, in part, a protective mechanism to combat ER stress, triggered by protein misfolding.(Arasaki et al. 2015) Therefore, PKA contributes to both ER expansion and mitochondrial elongation, allowing for increased contact between the organelles. Bravo-Sagua also demonstrated Cav1 expression reduced PKA signalling, impairing DRP1 phosphorylation by the kinase, ultimately leading to enhanced cell death as a consequence of ER stress.

Calnexin is a chaperone at the ER, which controls Ca^{2+}-associated machinery at the MAMs. During ER stress, Calnexin moves from the MAMs to the ER to reinforce protein folding as well as to enhance ER-mitochondria Ca^{2+} transfer. Interactions with Cav1 and Calnexin suggest PDEs may play a prominent role in ER-stress related pathways. Indeed, one experiment described in this chapter will test PDE's role in ER-mitochondrial contact alongside Tunicamycin-induced ER stress.

The interaction of MAM associated proteins with PDE2A2/PDE3A1 goes even further, as various proteins implicated in ER-mitochondrial contacts appear in the PDEs' interactomes. For example, PDE2A2 controls PKA-mediated phosphorylation of MIC60, a component of the mitochondrial contact site and organizing system (MICOS) complex. PKA phosphorylation of MICOS modulates Parkin recruitment to the mitochondria and mitophagy.(Lobo et al. 2020a) Of interest, Parkin has also been shown to regulate ER-mitochondrial contacts via MFN2 in human cells as well as in a Drosophila models of Parkinson's disease, where restoring ER-mitochondrial contact rescued locomotive deficits exhibited in the Drosophila.(Basso et al. 2018) In addition to Parkin, the fission protein 1 homologue (Fis1) is also present in the interactomes of PDE2A2 and PDE3A1. Fis1 localises to the OMM where it functions with the ER-localised protein B-cell receptor-associated protein 31 (BAP31) as well as other components of the MAMS, where they are necessary for

the recruitment of procaspase 8. (Wakana et al. 2008) The Fis1-BAP31 interaction and recruitment of procaspase 8 to the MAMs leads to Ca^{2+} release from the ER into the mitochondria, overloading the latter organelle with Ca^{2+}, thus opening mitochondrial permeability transition pore (MPTP) and culminating in apoptosis.(Iwasawa et al. 2011) Indeed, exogenous inducers of apoptosis actually promote Fis1-BAP31 interaction and tethering to the MAMs.(Wang et al. 2011) Fis1 is also implicated in recruiting DRP1 to the mitochondria to induce organelle fission.(Stojanovski et al. 2004) Finally, as aforementioned, PC2 was shown to alter ER-mitochondrial contact and data presented in chapter 7, indicate that PC2 interacts with PDE3A1 and over-expressed PDE2A.(Kuo et al. 2019)

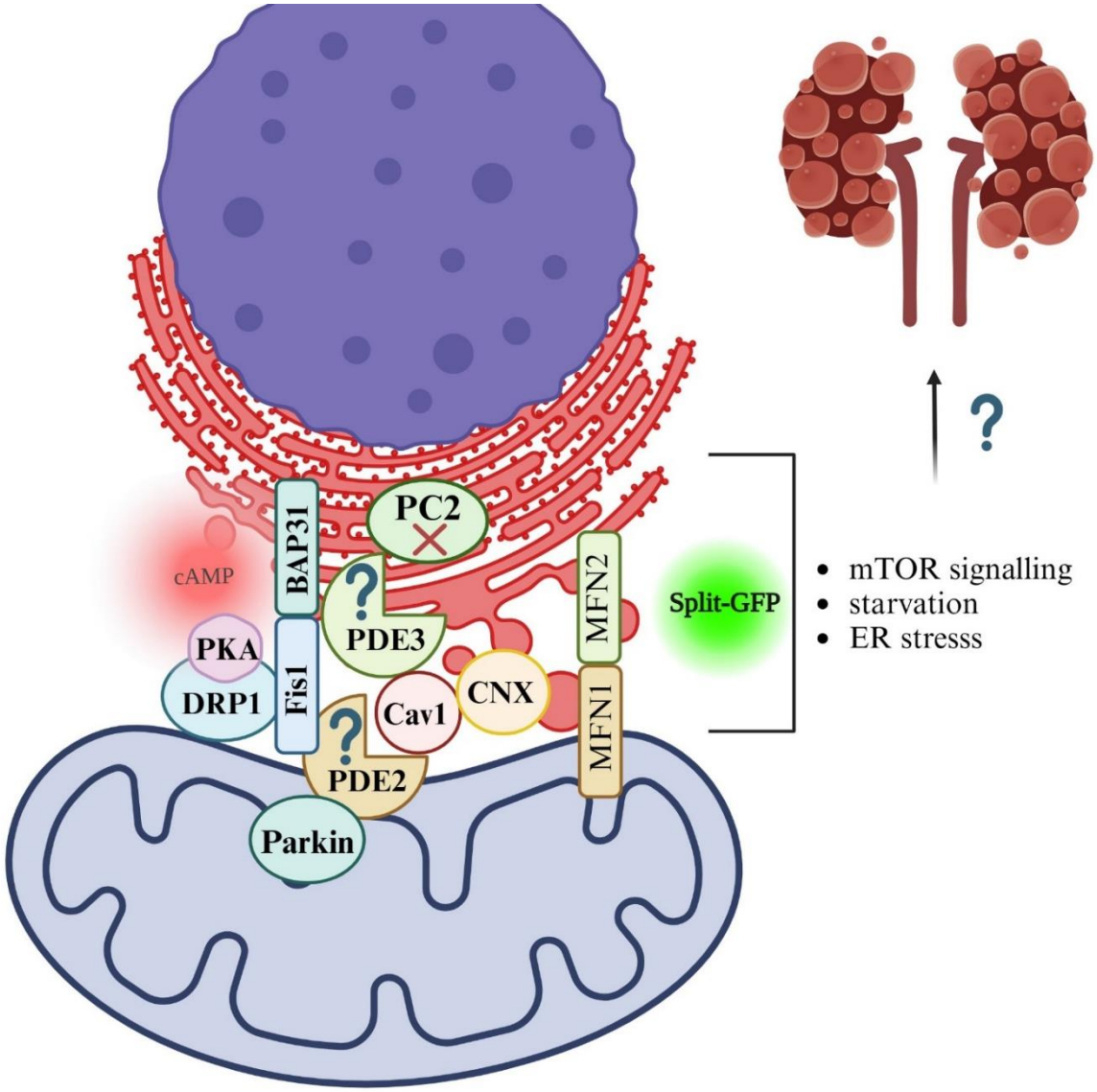

Schematic 13: Model for PDE2A2 at the OMM and PDE3A1 at the ER, interacting with some of the numerous proteins appearing in their proteomes, implicated in ER-mitochondrial contact. PKA phosphorylation of DRP1 at the MAMs suggests cAMP signalling is active in this domain. Pathways that are thought to control organelle contact and potentially interplay with cAMP signalling are listed to the right. This model suggests increased contacts, as seen when PC2 is knocked out, results in cystogenesis.

Given the extensive list of MAM-proteins in the PDE interactomes (**Schematic 13**) and the fact that DRP1 is phosphorylated by PKA to orchestrate organelle crosstalk, the hypothesis that PDEs may function at the MAMs to regulate ER-mitochondrial contact seems plausible. In particular, PDE3A1 may control contact sites through a direct interaction with PC2 at the MAMs. If so, PDE3 inhibition in in vitro cysts could lead to mitigated cystogenesis via altered ER-mitochondrial contact and subsequent shifts in organelle metabolism or signalling.

To evaluate this hypothesis, we had the following objectives:

1. Establish a method to accurately report changes in organelle interactions in IMCD3. For this, we used the Split-GFP construct, targeted to the ER and the OMM, in IMCD3 subjected to several manipulations known to promote organelle interaction, such as ER stress (Tunicamycin), nutrients depletion (starvation), and mTOR inhibition (Rapamycin).
2. Elucidate the effects of PDE inhibition on ER-mitochondrial contacts using split-GFP, as well as other available tools.
3. Measure the effects of PDE inhibition on ER-mitochondrial contacts downstream of treatments known to promote organelle interaction.
4. Discover whether bulk cyclic nucleotide signalling or non-selective PDE inhibition alters ER-mitochondrial contacts.
5. Explore whether there is a correlation between number of ER and mitochondrial contacts and ciliary phenotype of a cell.

The overall aim was to establish whether PDEs function at the MAMs to regulate ER-mitochondrial function. If a cAMP domain, controlled by PDEs, exists at these contact sites, then this finding could have implications for a variety of disease where organelle crosstalk is altered, such as in ADPKD.

Results 1- Confirming PC2/Cav1 interaction

Before assessing PDE involvement in ER-mitochondrial communication, I wanted to test whether PC2 and Cav1 interact, since both PC2 and Cav1 function at ER-mitochondrial contact sites. Another study also demonstrated Cav1 regulates PC2 localisation to the cilium.(Scheidel, Kennedy, and Blacque 2018) In addition, a previous PhD student in the lab, Miguel Lobo, confirmed the interaction of PDE2A isoforms, as well as PDE3A1, with Cav1. Thus, I hypothesized PC2, Cav1, and PDE3A1 might work in concert to regulate organelle dynamics. To test the PC2/Cav1 interaction, HEK293 cells were transfected with mRFP, PC2-

GFP, Cav1-RFP, or co-transfected with Cav1-RFP and PC2-GFP. Pull down was achieved with RFP beads, and an interaction between overexpressed PC2 and overexpressed Cav1 was confirmed (**Figure 39**).

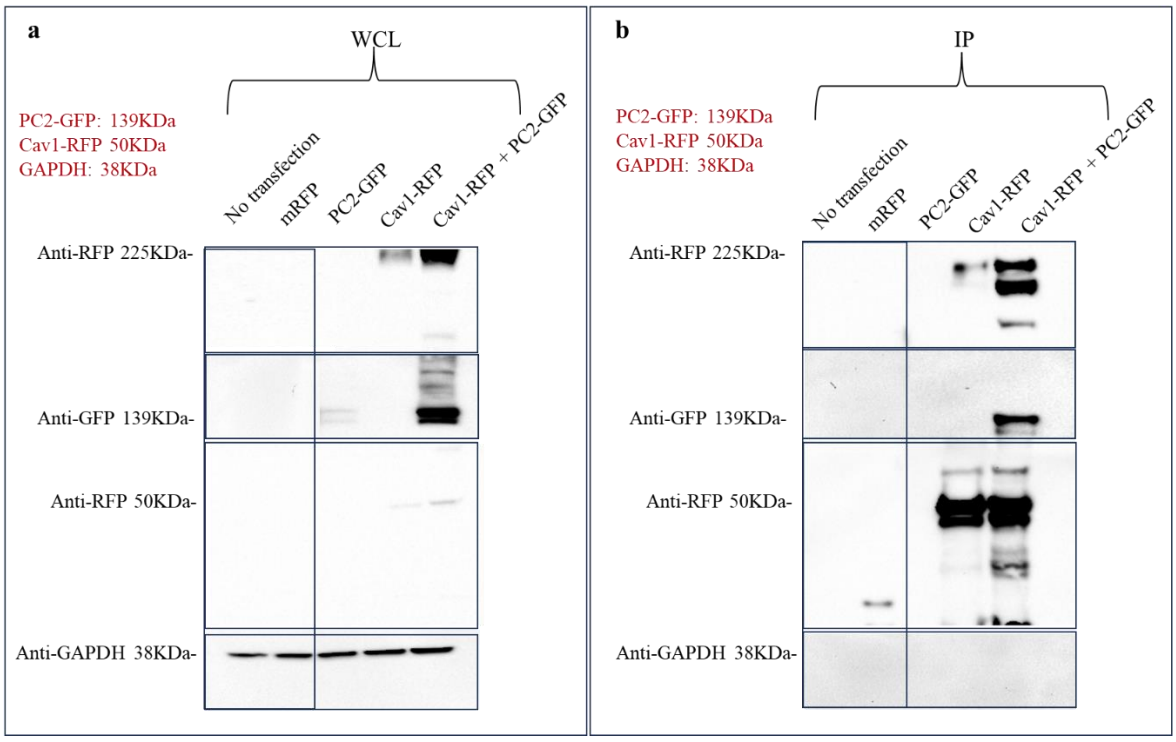

Figure 39: HEK293 transfected with mRFP, PC2-GFP, Cav1-RFP, or co-transfected with Cav1-RFP and PC2-GFP. **a** shows whole cell lysate (WCL) stained for anti-GFP, anti-RFP, or anti-GADPH. **b** shows co-immunoprecipitation (IP) samples, stained for anti-GFP, anti-RFP, or anti-GADPH. Pull down was achieved with RFP. Experiment was only carried out once (n=1), so no statistical analysis was performed.

Results 2-Optimisation of SPLIC$_s$ for measuring ER-mitochondrial contact

To investigate the hypothesis that PDEs regulate ER-mitochondrial contacts, we used the fluorescent tool, split-GFP-based contact site sensor (SPLCS$_s$). The split-GFP is divided so that the first ten β-strands of the GFP β-barrel are targeted to the OMM via fusion to the OMM-resident Tom20 protein (OMM$_{1-10}$) and the 11th β-strand of the GFP is fused to Sac1, an integral membrane protein of the ER.(Cieri et al. 2018) Only when the ER and the mitochondria are at a distance of 10nm or less from each other, the two parts of the GFP reconstitute a complete GFP that is fluorescent (**Figure 40**). Early on, it became apparent that transfection of both components of the split-GFP molecule was not particularly efficient, and

if a difference in fluorescence was observed between conditions, we could not exclude the possibility that this difference in signal was due to genuine changes in ER-mitochondrial contacts, or to a difference in transfection efficiency. In addition, as the two sequences are translated from different plasmids, the OMM_{1-10} component of the split-GFP was found to be transfected to a significantly higher degree than its ER counterpart. Even within the same coverslip, a wide degree of split-GFP fluorescence between individual cells was observed. In an attempt to correct for this variable, coverslips transfected with $SPLIC_s$ were also fixed and stained with anti-GFP antibody (**Figure 40**). As seen in **Figure 40b**, anti-GFP monoclonal antibody recognised the OMM_{1-10} component of split-GFP, though it is unclear whether it also recognised the ER_s component, as some dotted pattern could be seen in cells transfected with ER_s only (**Figure 40c**). The staining of ER_s with anti-GFP could suggest it targets individual proteins on the ER, and though anti-GFP is a monoclonal antibody, there are repetitive sequences shared between OMM_{1-10} and ER_s that could give rise to the same antigen targeted by anti-GFP. However, the dotted pattern is also not dissimilar, though stronger, to that observed in non-transfect IMCD3 stained with the same anti-GFP (**Figure 40e**), possibly suggesting that the red dots observed in ER_s coverslips are background non-specific signal. Yet, cells which express both components of the split-GFP, as evident with GFP fluorescence, show a different anti-GFP pattern to OMM_{1-10} transfection alone. The former staining appears more homogenous, implying that indeed, anti-GFP may be targeting both components of the split-GFP (**Figure 40d**). To confirm whether normalising the signal from the anti-GPF antibody helped improve analysis, we tested split-GFP with known inducers of ER-mitochondrial contacts, such as ER stressor, Tunicamycin, nutrients depletion (Starvation), and mTOR1 inhibitor, Rapamycin (**Figure 40**). Contacts were analysed based on split-GFP fluorescence alone (**Figure 41c**) or split-GFP fluorescence normalised to anti-GFP (**Figure 41b**). Only the split-GFP fluorescence alone reported significant alterations in organelle contact, thus suggesting that normalising to anti-GFP was not a useful approach.

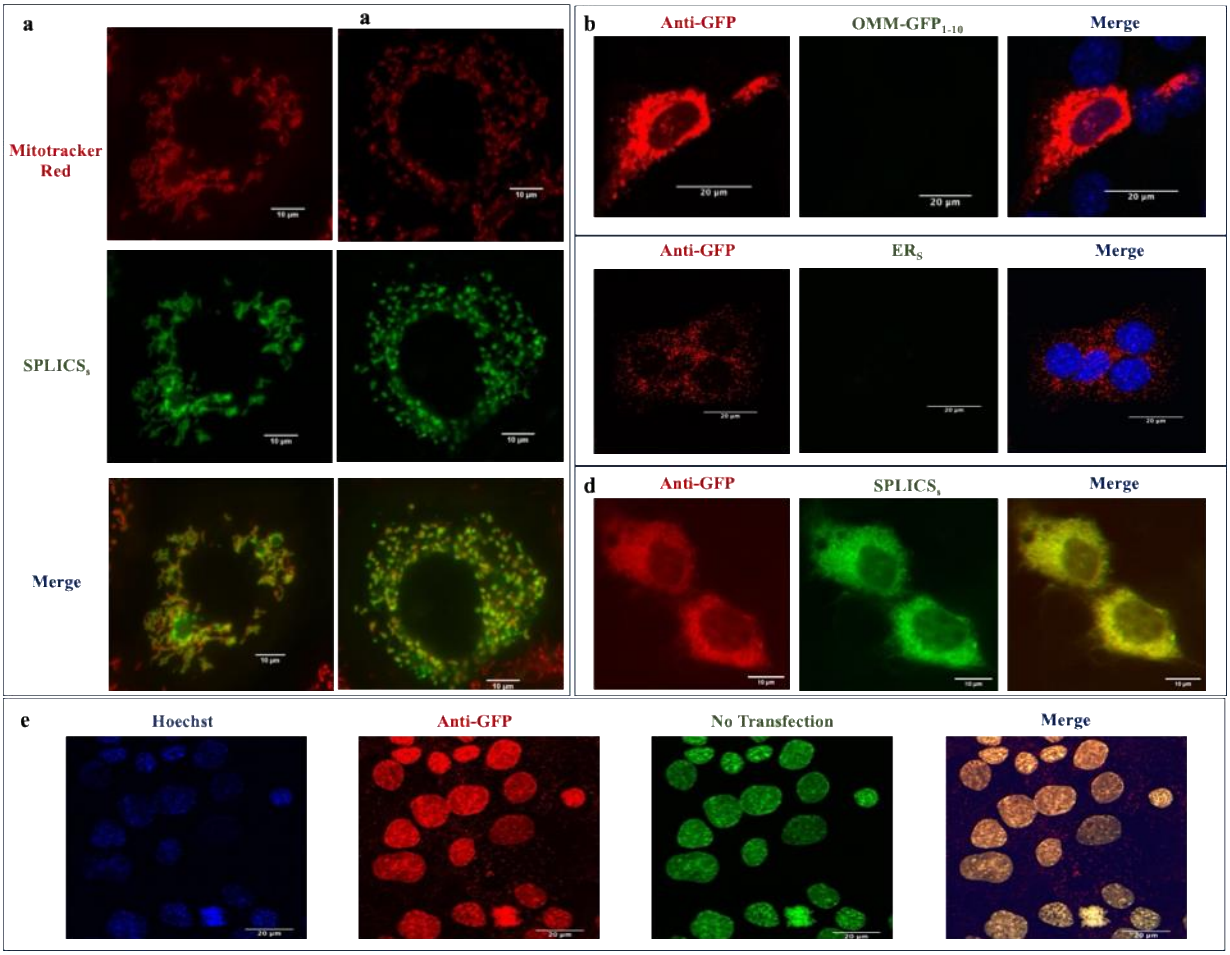

Figure 40: a Example of IMCD3 cells stained for mitotracker red (top), transfected with SPLICs (middle), or overlay of mitochondria and SPLICs (below). **b** IMCD3 transfected with OMM-GFP$_{1-10}$ fixed and stained for anti-GFP. **c** IMCD3 transfected with ER$_S$ fixed and stained for anti-GFP. **d** IMCD3 co-transfected with OMM-GFP$_{1-10}$ and ER$_S$ fixed and stained for anti-GFP. **e** Example of non-transfected IMCD3 stained with anti-GFP and Hoechst.

Results 3-Treatments altering ER-mitochondrial contacts

- After split-GFP was optimised for use in IMCD3, this tool was next used to measure changes in contact sites, in response to various treatments which are known to induce ER-mitochondrial interactions, in order to confirm that our experimental set up functioned properly (**Figure 41**). In particular, we tested the ER-stressor Tunicamycin, which works by inhibiting N-linked glycosylation, a process vital for protein synthesis.(Chen et al. 2023) Previous studies demonstrated increased ER-mitochondrial contacts upon Tunicamycin treatment of Henrietta Lax (HeLa) cells, (Cieri et al. 2018; Bravo-Sagua et al. 2016). Our own experiments, carried out in IMCD3, also found a significant increase in contacts upon Tunicamycin treatment in

the split-GFP fluorescence analysis alone (**Figure 41c**), but saw no marked change with the analysis normalised to anti-GFP staining (**Figure 41b**). In former studies, starvation was shown to increase organelle contact sites in HeLa cells, (Bravo-Sagua et al. 2016; Cieri et al. 2018) but in IMCD3, we found nutrient depletion significantly decreased ER-mitochondrial contact when the analysis was based on GFP fluorescence alone (**Figure 41c**), with no difference reported using the antibody-based correction approach (**Figure 41b**). Finally, treatment with rapamycin, an mTORC1 inhibitor that had been reported to increased ER-mitochondrial interaction in HeLa cells did not show any marked changes in organelle contact in IMCD3, with either analysis approach (**Figure 41b,c**). However, there is a trend, for GFP fluorescence alone, whereby Rapamycin seems to slightly decrease, rather than increase, contacts (**Figure 41c**) .(Bravo-Sagua et al. 2016) Though our findings did not fully recapitulate data obtained in previous published studies, in our hands split-GFP seemed to be able to detect changes in organelle interaction, as we did see an increase in contact upon Tunicamycin treatment, as formerly reported. Additionally, we found $SPLIC_s$ was the best tool for measuring ER-mitochondrial contact, as other approaches were attempted with mixed success, as described below.

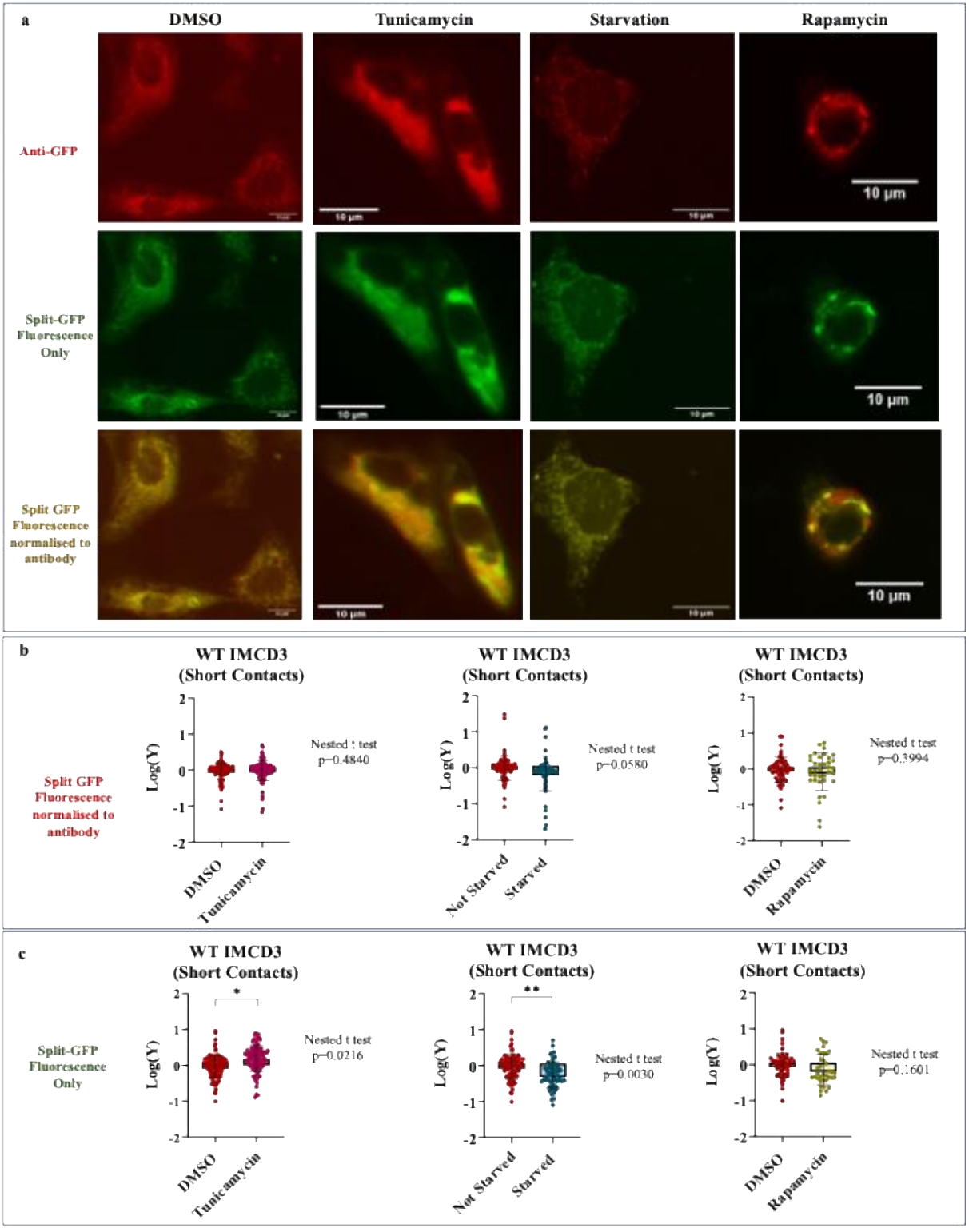

Figure 41: a Example of IMCD3 treated with DMSO, Tunicamycin, Starved, or Rapamycin (left to right) then co-transfected with OMM-GFP$_{1-10}$ and ER$_s$, fixed, and stained for anti-GFP. **b** is quantification of **a**, with SPLIC$_s$ fluorescence normalised to anti-GFP expression (red). **c** is quantification of **a**, with SPLIC$_s$ fluorescence alone. Both for **b** and **c**, data was normalised to DMSO control median, transformed to Log(Y) and analysed using Nested t-test. Bars show Log(Y) mean with SD. Each datapoint represents a single coverslip. N=7 for Tunicamycin, n=6 for starvation, and n=3 for rapamycin experiments, where n represents one round of experimentation from an independent flask passage.

Results 4- FEMP probe reports similar results to $SPLIC_s$

Though results using $SPLIC_s$ in IMCD3 reported mixed conclusions, split-GFP was still the best option tested in our hands, to measure organelle contact. Previously, we attempted to measure contacts using the fluorescence-activating and absorption shifting tag (split-FAST), another split reporter whereby the nFAST and the cFAST domains are targeted to the ER and OMM respectively.(Casas et al. 2023) When HMBR (4-hydroxy-3-methylbenzylidene rhodamine) is administered to cells expressing split-FAST, which are in close proximity, HMBR binds the split-FAST cavity, providing green/yellow fluorescence. Thus fluorescence intensity is an indicator of organelle contact.(Tebo and Gautier 2019) split-FAST is a reversible probe and can detect contacts as they are generated and as they dissolve, which would have made it a preferable tool than split-GFP for our purposes of measuring fluctuations in organelle interaction. However, using this approach we were not able to observe a change in fluorescence upon HMBR administration despite testing a range of HMBR concentrations. Thus, we ruled out this technique after several attempts including in different cell types.

Another tool that was trialled was the FRET-based indicator of ER-mitochondria proximity (FEMP). This technique uses a yellow fluorophore, anchored to the ER and a cyan fluorophore, anchored to the OMM to measure FRET as a readout of organelle distance. When the ER and OMM are in proximity, FRET occurs between the two fluorophores. FRET can also be induced via addition of a rapalog, which creates an artificial link between the two organelles. Induction of artificial links indicates total organelle contacts possible within the cell, and thus one can normalise baseline ratio to this value to compare treatment conditions. **Figure 42a.** shows a schematic of how FEMP works. This tool was promising, as the main issue arising from $SPLIC_s$ was poor transfection efficiency of both components of the split-GFP. It was never certain that ER_s (which had a lower transfection efficiency) was expressed

at comparable levels to $OMM_{1-10,}$ despite our attempt to normalise for transfection efficiency by staining for GFP. In contrast, the two fluorophores, anchored to separate organelles, used in FEMP are expressed from the same mRNA, allowing for equimolar levels of ER and OMM-tagged components.(Naon et al. 2016) IMCD3 cells were thus pretreated with DMSO or one of three PDE inhibitors and either rapamycin or rapalog was added during FRET imaging to achieve maximum organelle contact. **Figure 42b** shows an example ratio trace of an IMCD3 cell pretreated with Bay60, with real-time administration of 1μM rapalog. Based on fluorophore intensities, the FRET response to rapalog was genuine. When we observed successful FEMP imaging, we noted down all experimental conditions (such as sensor intensity), in an effort to reproduce similar results, as previous attempts at FEMP had failed. Unfortunately, out of ten separate days of FEMP experimentation, only a few coverslips, from one day, managed to show any change in FRET upon either rapalog or rapamycin administration (the figure demonstrates one of these responses). Different doses of rapalog/rapamycin were trialled, we extended FEMP experiments up to an hour, thawed fresh IMCD3, tried different drug aliquots and cell types, and transfected with different DNA plasmid concentrations but we were never able to reproduce the results previously observed. It is hypothesized that perhaps the cells already demonstrated maximum organelle contact, so that addition of rapalog would not induce further changes, and therefore there could be no increase with FRET. However, it is unlikely this is the case, as we have shown, using $SPLIC_s$, that in the same cells we see enhanced contacts upon Tunicamycin treatment. Additionally, it would seem physiologically abnormal for IMCD3 to have maximal ER-mitochondrial contact sites at all times, unless they were in stressed conditions. However, as aforementioned we thawed fresh cells and also used freshly prepared media but observed no changes in FEMP signalling. Nevertheless, we quantified the few experiments where FRET did occur. **Figure 42c** shows IMCD3 responses to rapalog, using FEMP, after pre-treatment with PDE inhibitors. A greater response to rapalog suggests fewer initial contacts in the cell. Therefore,

from these results, it appears PDE2 inhibition via Bay60 had no effect on contact numbers, while PDE3 inhibition reduced contacts and PDE4 inhibition increased them.

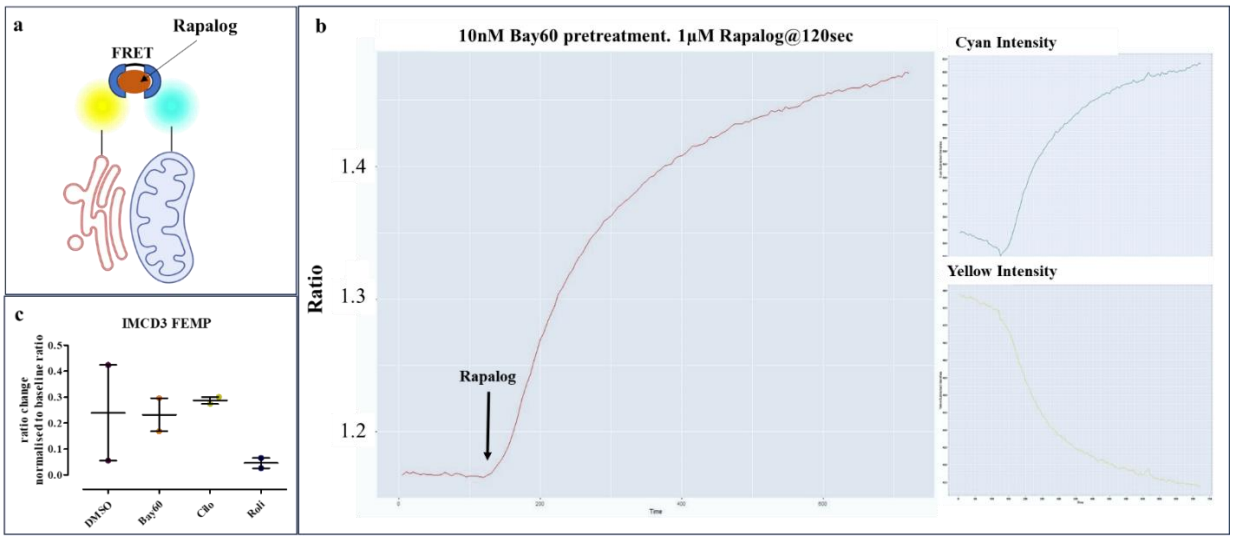

Figure 42: a shows schematic of FRET-based indicator of ER-mitochondria proximity (FEMP) whereby the yellow fluorophore is anchored to the ER and the cyan fluorophore to the OMM. When the ER and OMM are proximate, FRET occurs between the two fluorophores. FRET can also be induced via addition of a rapalog, which creates an artificial link between the two organelles. **b** shows example ratio trace of an IMCD3 cell pretreated with Bay60, with real-time administration of 1µM rapalog. Fluorophore intensities for the trace can be seen to the right. **c** is a quantification of IMCD3 responses to rapalog, using FEMP, after pre-treatment with PDE inhibitors. Each data point is a single cell from independent coverslips. Bars show mean with SD. N=1 so no statistical test was performed.

Results 5- PDEs regulating ER-mitochondrial contact

The fact that PDE3A1 and PDE2A2 (to some degree) interact with PC2, and other proteins which orchestrate ER-mitochondrial contacts, led to the hypothesis that perhaps PDE3 inhibition achieves a reduction in cystogenesis, by altering organelle contacts. Indeed, with a few FEMP experiments, we saw PDE3 inhibition decreased contacts, while PDE4 inhibition increased them. To confirm these observations with more robust data, IMCD3 cells were treated with one of three PDE inhibitors for 24 hours, then transfected with split-GFP, fixed 24 hours after transfection, and stained for anti-GFP. Recombination of the split-GFP is irreversible, so once contacts are achieved, they cannot be undone, hence why cells were treated with inhibitors prior to split-GFP transfection. **Figure 43** shows changes to ER-mitochondrial contact in response to 10nM Bay60 (PDE2 inhibitor), 10µM Cilostamide (PDE3 inhibitor), or 10µM Rolipram (PDE4 inhibitor). Of the inhibitors, only Cilostamide

(PDE3 inhibition) led to marked reduction in organelle contact sites. This decrease was significant when split-GFP fluorescence was normalised to anti-GFP staining (**Figure 43b**) and almost reached statistical significance with the split-GFP fluorescence alone analysis (**Figure 43c**).

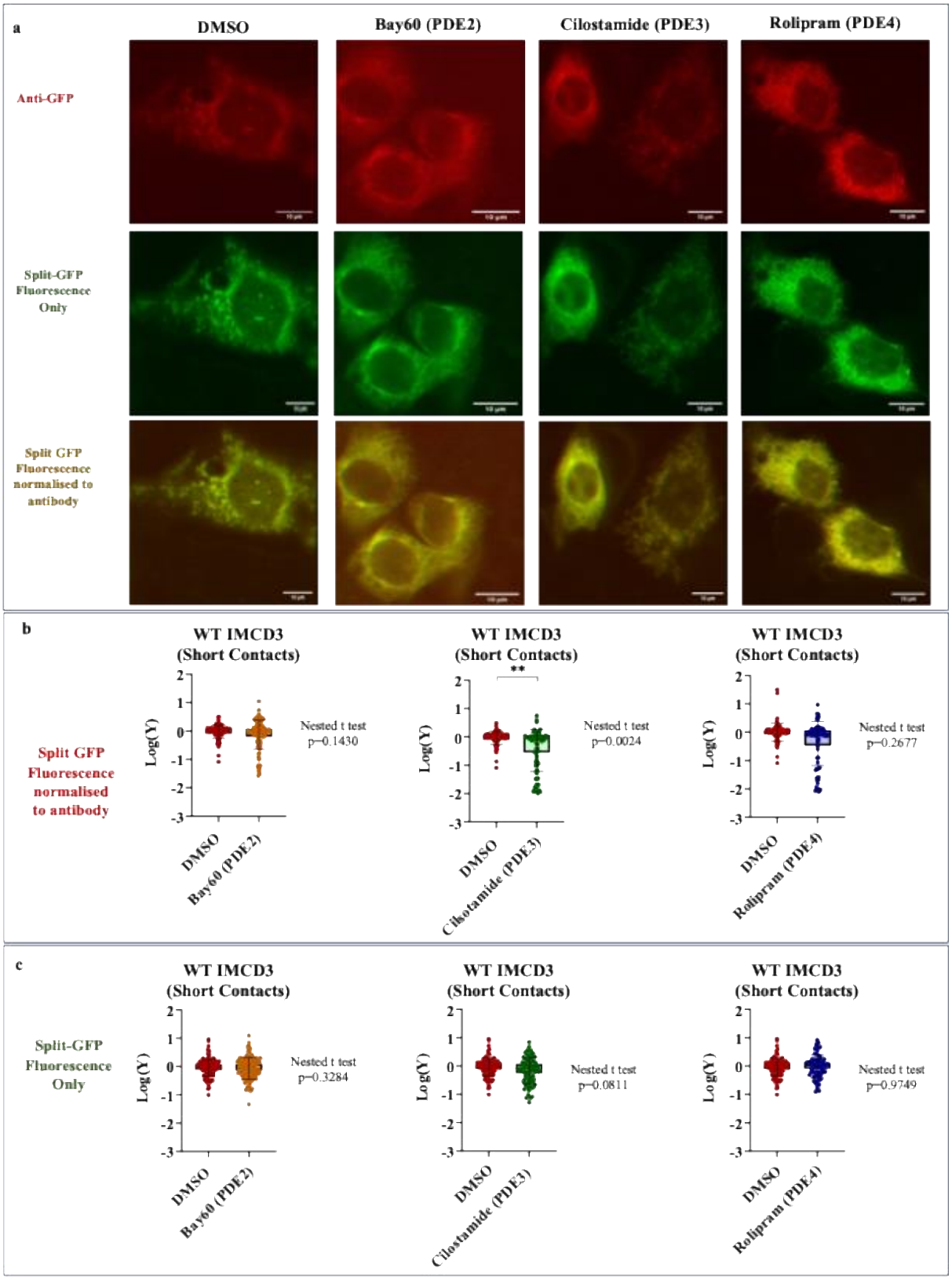

Figure 43: a Example of IMCD3 treated with DMSO, Bay60, Cilostamide, or Rolipram (left to right) then co-transfected with OMM-GFP$_{1-10}$ and ER$_s$, fixed, and stained for anti-GFP. **b** is quantification of **a**, with SPLIC$_s$ fluorescence normalised to anti-GFP expression (red). **c** is quantification of **a**, with SPLIC$_s$ fluorescence alone. Both for **b** and **c**, data was normalised to DMSO control median, transformed to Log(Y) and analysed using Nested t-test. Bars show Log(Y) mean with SD. Each

datapoint represents a single coverslip. N=10, where n represents one round of experimentation from an independent flask passage.

Next, we reasoned that PDEs may function downstream of cellular processes to alter ER-mitochondrial contacts. Any changes in organelle interaction observed upon PDE inhibition in otherwise untreated cells, may be amplified when enzyme inhibition is paired to Tunicamycin treatment, which was previously shown to increase contact sites. **Figure 44** shows the results of experiments whereby IMCD3 were treated with PDE inhibitors followed by Tunicamycin, then transfected with split-GFP and fixed and stained for anti-GFP. Alongside Tunicamycin treatment, all three PDE inhibitors seemed to decrease ER-mitochondrial contacts, with PDE2, PDE3, and PDE4 inhibition showing a significant reduction (**Figure 44c**). However, these results were only observed with the split-GFP alone analysis and were not recapitulated with normalisation to anti-GFP staining (**Figure 44b**).

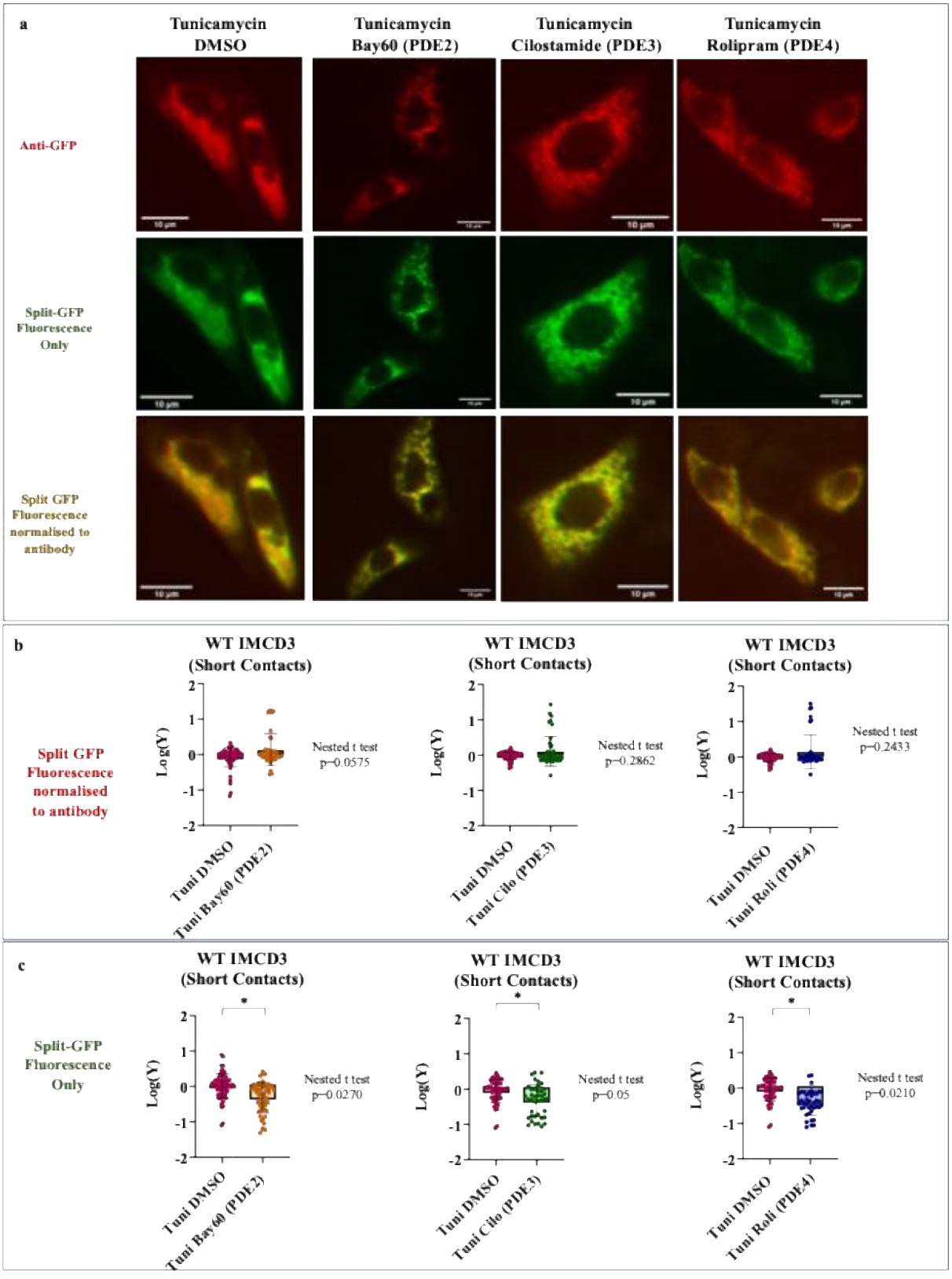

Figure 44: a Example of IMCD3 treated with DMSO and Tunicamycin, Bay60 and Tunicamycin, Cilostamide and Tunicamycin, or Rolipram and Tunicamycin (left to right) then co-transfected with OMM-GFP$_{1-10}$ and ER$_s$, fixed, and stained for anti-GFP. **b** is quantification of **a**, with SPLIC$_s$ fluorescence normalised to anti-GFP expression (red). **c** is quantification of **a**, with SPLIC$_s$ fluorescence alone. Both for **b** and **c**, data was normalised to DMSO control median, transformed to Log(Y) and analysed using Nested t-test. Bars show Log(Y) mean with SD. Each datapoint represents a single coverslip. N=6, where n represents one round of experimentation from an independent flask passage.

Starvation/nutrient-depletion was also shown to impact ER-mitochondrial contact, reducing organelle interaction in IMCD3 (**Figure 41**) but reported to increase contacts in HeLa studies.(Bravo-Sagua et al. 2016; Cieri et al. 2018) Despite this inconsistency, we assessed whether PDEs may function downstream of starvation mechanisms, to alter organelle contacts. Thus, IMCD3 cells were starved and treated with PDE inhibitors, then transfected with split-GFP, fixed, and stained for anti-GFP. Results showed no difference in organelle contacts between any of the PDE inhibitor treatments and the DMSO control, in starved/nutrient-depleted IMCD3 (**Figure 45**). Both methods of analysis led to the same conclusion, suggesting PDEs do not function downstream of starvation mechanisms to alter contact sites.

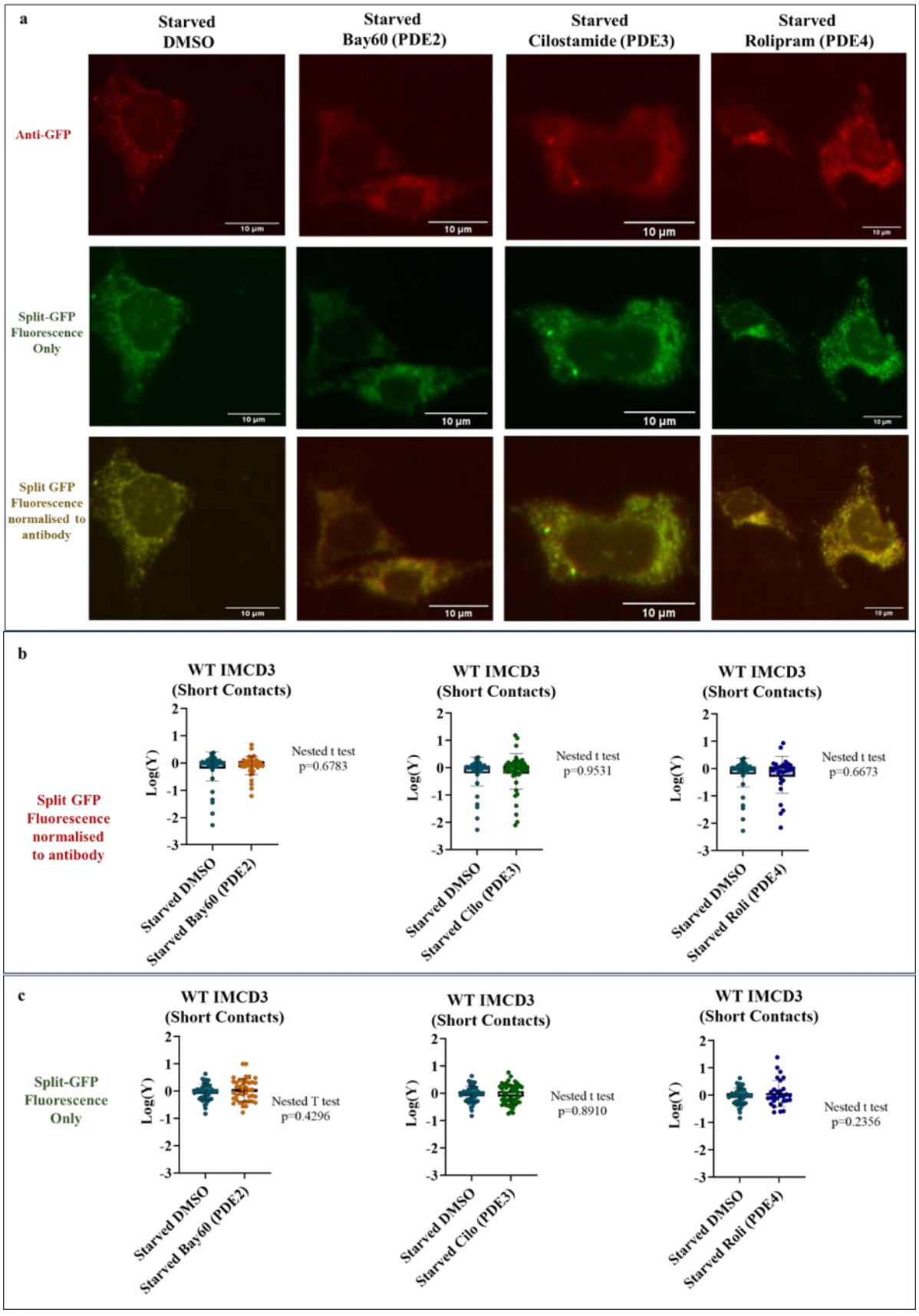

Figure 45: a Example of IMCD3 starved with 0.1% FBS and treated with DMSO, Bay60, Cilostamide, or Rolipram (left to right) then co-transfected with OMM-GFP$_{1-10}$ and ER$_s$, fixed, and stained for anti-GFP. **b** is quantification of **a**, with SPLIC$_s$ fluorescence normalised to anti-GFP expression (red). **c** is quantification of **a**, with SPLIC$_s$ fluorescence alone. Both for **b** and **c**, data was normalised to DMSO control median, transformed to Log(Y) and analysed using Nested t-test. Bars show Log(Y) mean with SD. N=4, where n represents one round of experimentation from an independent flask passage.

Results 6- Cyclic Nucleotides may increase ER-mitochondrial contact

PDEs were shown to alter ER-mitochondrial contact, including when cells were also treated with ER stressor, Tunicamycin. Since PDEs function by hydrolysing cAMP, the next question to answer was whether the cyclic nucleotide itself may influence organelle interaction. For this, IMCD3 cells were treated with increasing doses of FSK, the adenylyl cyclase activator. The cells were then transfected with split-GFP, fixed, and stained for anti-GFP. Analysis with GFP fluorescence alone demonstrated that cAMP does not alter ER-mitochondrial contacts (**Figure 46c**), while the analysis normalised to anti-GFP expression, suggested the second messenger may increase contact sites (**Figure 46b**).

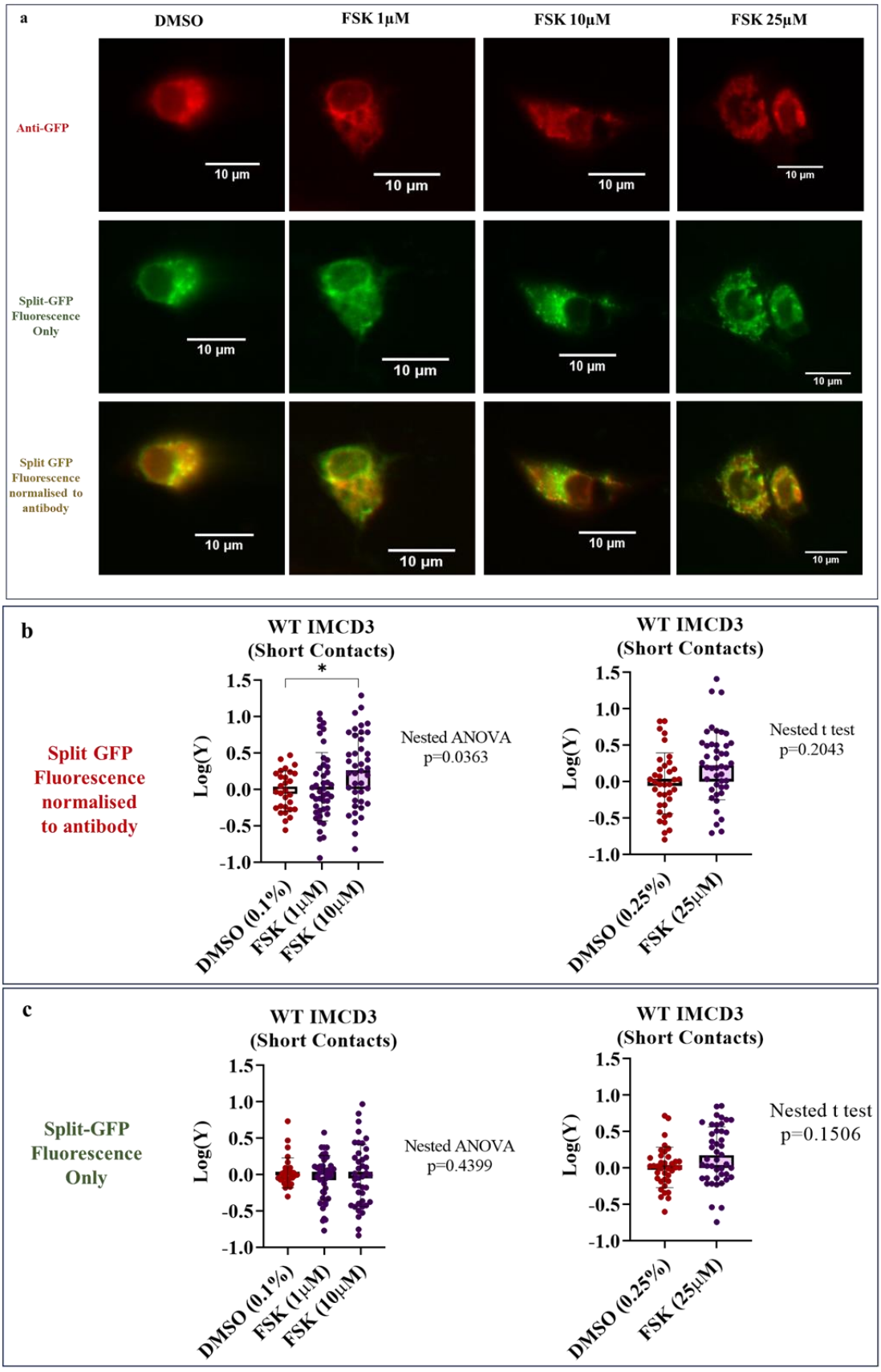

Figure 46: a Example of IMCD3 treated with DMSO (0.1%), 1µM FSK, 10µM FSK, or 25µM FSK (left to right) then co-transfected with OMM-GFP$_{1-10}$ and ER$_s$, fixed, and stained for anti-GFP. **b** is quantification of **a**, with SPLIC$_s$ fluorescence normalised to anti-GFP expression (red). **c** is quantification of **a**, with SPLIC$_s$ fluorescence alone. Both for **b** and **c**, data was normalised to DMSO control median, transformed to Log(Y) and analysed using Nested ANOVA (left) or Nested t-test (Right). Bars show Log(Y) mean with SD. N=4 for 1-10µM FSK and n=3 for 25µM FSK, where n represents one round of experimentation from an independent flask passage.

Since PDE2 and PDE3 not only hydrolyse cAMP but also cGMP, we next sought to determine whether cGMP signalling may alter ER-mitochondria interactions. The same experiment carried out with FSK was reproduced using concentrations of the guanylyl activator (GC) Bay41 instead. **Figure 47c** shows that treatment with Bay41 does not alter ER-mitochondrial contacts, though analysis normalised to anti-GFP suggests a small increase in contacts with augmenting concentrations of activator (**Figure 47b**).

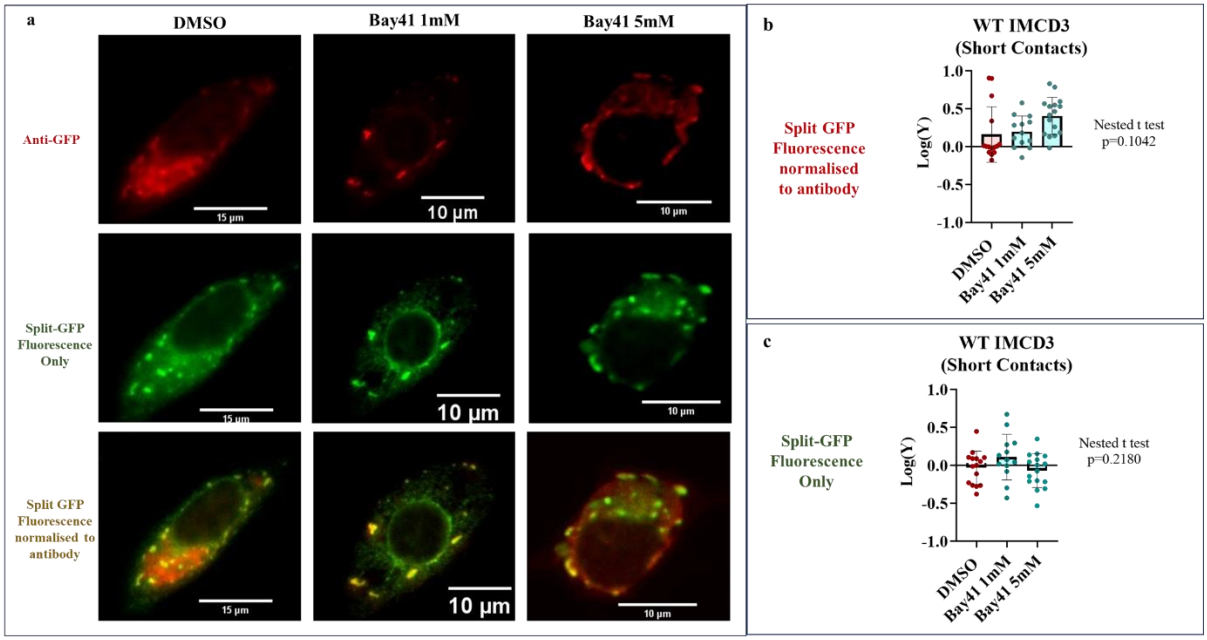

Figure 47: **a** Example of IMCD3 treated with DMSO (0.1%), 1mM Bay41, or 5mM Bay41 (left to right) then co-transfected with OMM-GFP1-10 and ERs, fixed, and stained for anti-GFP. **b** is quantification of a, with SPLICs fluorescence normalised to anti-GFP expression (red). **c** is quantification of a, with SPLICs fluorescence alone. Both for b and c, data was normalised to DMSO control median, transformed to Log(Y) and analysed using Nested ANOVA. Bars show Log(Y) mean with SD. Each datapoint is one coverslip. N=3, where n represents one round of experimentation from an independent flask passage.

While an increase in cAMP signalling propagates cystogenesis, there is evidence to suggest treatment of in vitro cysts with the non-selective PDE inhibitor, IBMX, may help mitigate cystic growth.(Hansen, Kaiser, Leyendecker, Stüven, Krause, Derakhshandeh, Irfan, Sroka, Preval, and Desai 2022) In addition, we have shown that inhibition of individual PDE families reduces ER-mitochondrial contact sites, including during ER stress. Therefore, we

hypothesized that IBMX may be cyst protective due to the PDE inhibitor's effects on ER-mitochondrial interactions. To test this, the split-GFP approach was used in IBMX-treated IMCD3 (**Figure 48**). No effect on ER-mitochondrial contacts was measured on IBMX inhibition, using either analysis approach.

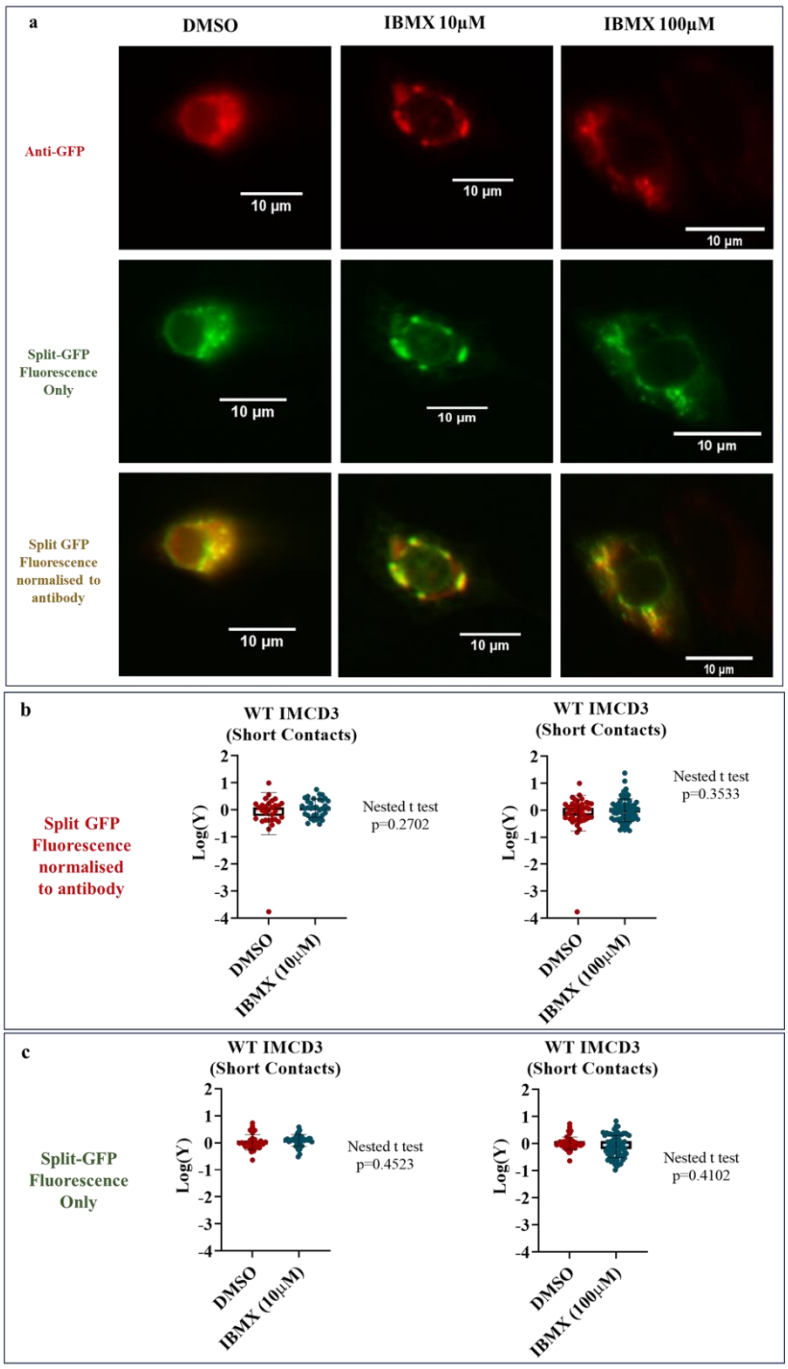

Figure 48: a Example of IMCD3 treated with DMSO, 10µM IBMX, or 100µM IBMX (left to right) then co-transfected with OMM-GFP$_{1-10}$ and ER$_s$, fixed, and stained for anti-GFP. **b** is quantification of **a**, with SPLIC$_s$ fluorescence normalised to anti-GFP expression (red). **c** is quantification of **a**, with SPLIC$_s$ fluorescence alone. Both for **b** and **c**, data was normalised to DMSO control median, transformed to Log(Y) and analysed using Nested t-test. Bars show Log(Y) mean with SD. Each datapoint is one coverslip. N=3 for 10µM IBMX and n=4 for 100µM IBMX, where n represents one round of experimentation from an independent flask passage.

Results 7- Primary Cilium and ER-mitochondrial contact

There is evidence suggesting that ciliary cAMP drives cystogenesis in ADPKD, (Hansen, Kaiser, Leyendecker, Stüven, Krause, Derakhshandeh, Irfan, Sroka, Preval, and Desai 2022) and KO of PC2, in ADPKD, leads to increased ER-mitochondrial contacts.(Kuo et al. 2019) Furthermore, we have shown, using FRET, that PDE hydrolysis of cAMP is dependent on the ciliary phenotype of the cell, with more ER and mitochondrial PDE activity in non-ciliated cells and more PDE hydrolysis of cytosolic cAMP in ciliated IMCD3. In particular, PDE3 and PDE2, but not PDE4 activity, which is ubiquitous, was affected by the ciliary phenotype of a cell. Since the working hypothesis is that PDE2 and PDE3 function at the MAMs, we investigated whether the presence or absence of a cilium may correlate to the distance between the ER and the mitochondria, potentially altering these enzymes' hydrolysing activities of a specific pool of cAMP localising to the MAMs. To test this hypothesis, IMCD3 cells were transfected with $SPLIC_s$, fixed, and stained for ciliary marker Arl13b. SPLICs-positive cells were measured, and ciliary phenotype was assigned based on anti-Arl13b expression (**Figure 49a**). Results showed non-ciliated IMCD3 had markedly more ER-mitochondrial contacts than their ciliated counterparts (**Figure 49b**).

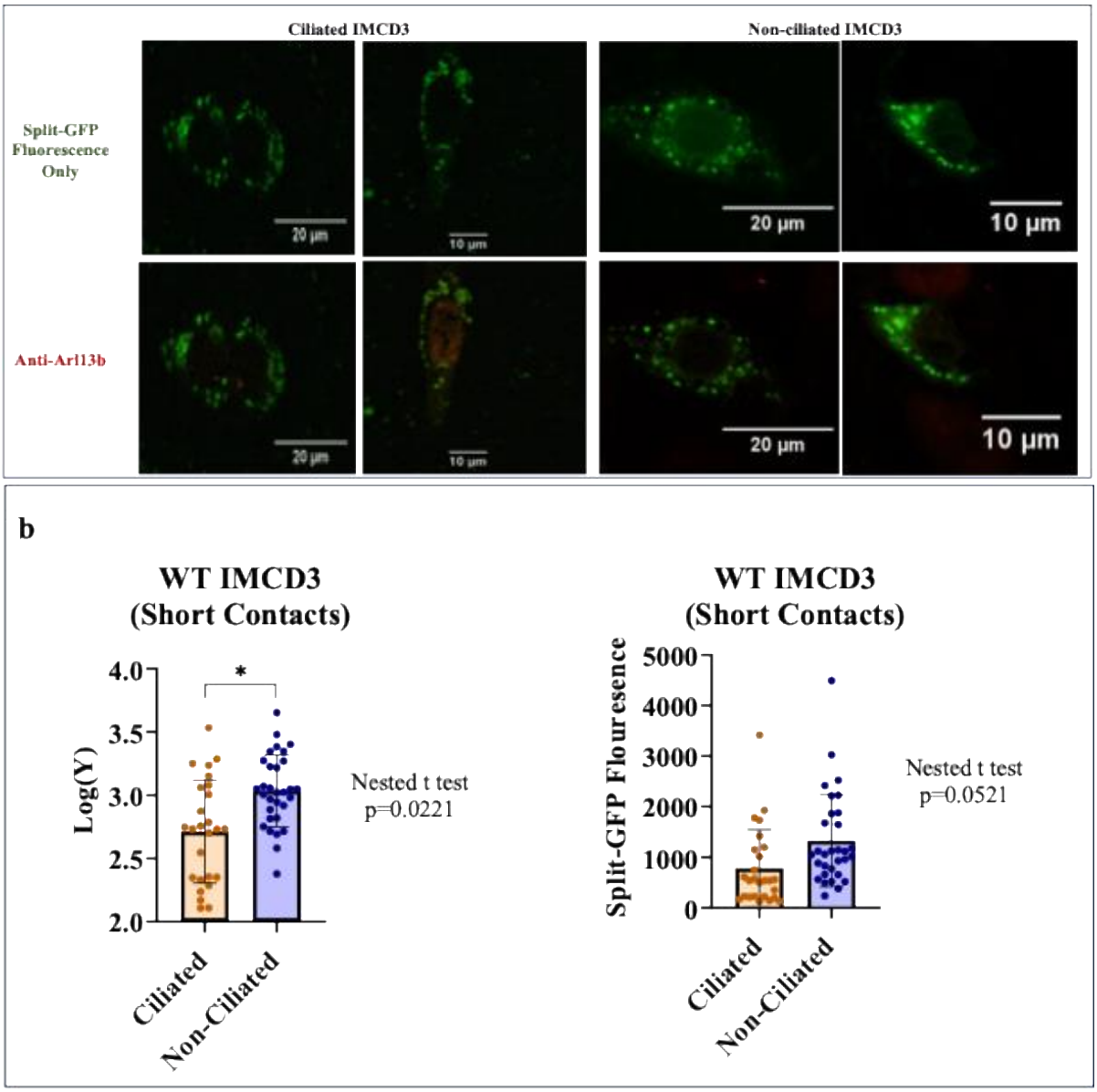

Figure 49: a Example of IMCD3 co-transfected with OMM-GFP$_{1-10}$ and ER$_s$, fixed, and stained for anti-Arl13b. **b** is quantification of **a**, with SPLIC$_s$ fluorescence alone. Data was transformed to Log(Y) and analysed using Nested t-test. To the right is untransformed data. Bars show mean with SD. Each datapoint is one coverslip. N=3, where n represents one round of experimentation from an independent flask passage.

Discussion

PDE3 Inhibition Reduces ER-mitochondrial contacts in IMCD3

ADPKD is a ciliopathy, and thus a disease associated to erratic cAMP and Ca^{2+} signalling in the primary cilium. However, multiple evidence points to renal cystogenesis as a disorder where metabolic function is altered to drive disease progression.(Muto et al. 2022; Menezes

and Germino 2019) Though PC2 has conventionally been thought to localise to the cilium, it can also function at the ER, where it has been shown to regulate organelle contact with the mitochondria (Kuo et al. 2019). Since PDE3A1 and PDE2A2 which localise, among other domains, to the ER and mitochondria respectively, (Shakur et al. 2000; Lobo et al. 2020a) can interact with PC2, as well as other proteins known to function at the MAMs, it was hypothesized that PDE3 may control a pool of cAMP at these organelle contact sites, which in turn regulates cyst formation. To test this hypothesis, we employed split-GFP, that had been previously characterised in HeLa cells (Cieri et al. 2018), to measure ER-mitochondrial contacts in response to PDE inhibitors. PDE3 inhibition decreased ER-mitochondrial contacts, almost significantly, with split-GFP fluorescence alone (**Figure 43**) and also showed a similar trend with FEMP (**Figure 42**). These findings are consistent with our hypothesis that PDE3 inhibition may mitigate cystogenesis by regulating organelle crosstalk.

During ER stress, all PDEs reduce contact sites

In partnership with ER-stress, induced via Tunicamycin, we also observed a significant decrease in contact sites upon inhibition of all three PDE inhibitors (**Figure 44c**). This finding further confirms PDE3 involvement at the MAMs. Additionally, it is not surprising that PDE2 leads to decreased contacts upon ER stress, as this isoform, as aforementioned, is associated with several MAM proteins, especially DRP1 which was shown to function to regulate contacts during organelle stress (Monterisi et al. 2017). Unexpectedly, PDE4 inhibition also decreased contact sites. Of course, in chapter 8, we demonstrated PDE4 can hydrolyse cAMP at both the ER and the OMM, but its activity at these organelles was thought to arise from ubiquitous expression of PDE4 in IMCD3. While PDE3 inhibition leads to decreased cyst growth and contact sites, the fact that PDE2 or PDE4 inhibition achieves the same outcome at the MAMs but aggravates cystogenesis, casts some doubt that downregulation of ER-mitochondrial interactions is cyst-protective. However, Rolipram inhibition of PDE4, using FEMP instead (**Figure 42**), did lead to a comparable increase in contact sites, contrasting the

split-GFP results and aligning with our hypothesis that cystogenesis is aggravated via enhanced ER-mitochondrial contacts.

Unfortunately, there is further discrepancy between previous studies, and our findings. Bravo-Sagua demonstrated that in HeLa cells, PKA phosphorylation of DRP1 enhances contacts, but instead, we have measured a decrease in interactions upon inhibition of each PDE isoform. Since PDEs hydrolyse cAMP, their inhibition leads to increased PKA activity and should thus also increase contact sites. This observation suggests that none of the PDEs regulate phosphorylation of DRP1 to reduce organelle interaction. Alternatively, this is not the only time our findings in IMCD3 did not align with those carried out in HeLa, as nutrient-depletion, which will be discussed later in this section, also gave contradicting results in the two cell types. It is possible that the role of PKA at the MAMs is cell type specific.

Upregulation of bulk cyclic nucleotide signalling did not alter ER-mitochondrial contacts

Since with Tunicamycin we saw a decrease in contact sites upon the inhibition of all three PDEs, we wanted to test whether non-selective PDE inhibition would also decrease contact sites. Additionally, IBMX was shown to have some cyst-protective effect in in vitro assays.(Hansen, Kaiser, Leyendecker, Stüven, Krause, Derakhshandeh, Irfan, Sroka, Preval, and Desai 2022) However, we observed no obvious changes with split-GFP upon IBMX treatment (**Figure 48**). Of note, we did not test IBMX alongside Tunicamycin, so it is possible we would have observed a decrease alongside ER stress. It is also possible promiscuous inhibition of cytosolic PDEs leads to a non-specific surge in cAMP whose downstream functions culminate in a net-zero change in ER-mitochondrial crosstalk. Indeed, when we measured $SPLIC_s$ as a result of AC activation, using FSK, we also did not obtain conclusive results on how cAMP bulk increase affects contact sites (**Figure 46**), despite evidence that PKA does function to alter organelle interaction.(Bravo-Sagua et al. 2019) Again, cytosolic cAMP and localised cAMP nanodomains may work in opposing directions to regulate

organelle interaction. A better experiment to measure cAMP impact on contacts could have been to treat IMCD3 with both FSK and individual PDE inhibitors before measuring contacts with SPLICs. If PDE3 inhibition, with FSK, led to an even more pronounced decrease in split-GFP fluorescence, one could conclude PDE3 works through hydrolysis of cAMP to regulate ER and mitochondria.

PDE2 and PDE3 also hydrolyse cGMP, and in turn are regulated by cGMP. While PDE2 activity is enhanced when cGMP binds its regulatory domain, PDE3 activity is downregulated with cGMP association.(Baillie, Tejeda, and Kelly 2019) This detail formulates the hypothesis that perhaps PDE2A2 at the OMM and PDE3A1 at the ER, orchestrate ER-mitochondrial dynamics in a balanced cycle controlled by cGMP. When PDE3 activity at the ER is inhibited by cGMP, PDE2 hydrolysis at the OMM is stimulated. In the absence of cGMP, PDE3 is the primary hydrolyser of cAMP at the MAMs, while PDE2 is less active. Our results using SPLICs however, did not yield any conclusive analysis for Bay41 treated cells (**Figure 47**). As previously described, a better experiment would have been cGMP stimulation alongside PDE isoform inhibition. To confirm our theory, cGMP with PDE2 inhibition would lead to more pronounced changes in ER-mitochondrial contacts, while cGMP with PDE3 inhibition would abolish significant reductions in organelle interaction. Additionally, simultaneous inhibition of PDE2 and PDE3, not via IBMX, but through Bay60 and Cilostamide, could also have been tested with the possibility of observing a synergistic effect on contact reduction.

Discrepancy in split-GFP reported results may be due to cell type differences

Of importance, SPLICs, and other tools for measuring organelle contact sites are still evolving, so in order to trust our findings upon PDE3 inhibition, we first had to thoroughly test this technique, as it has sparked some controversy on its ability to report on genuine organelle contacts (Giamogante et al. 2020). Early on, we observed great sample variability, even with the same coverslip, so we stained transfected cells with a GFP antibody, in an effort to normalise for transfection efficiency and thus reduce the range of values. According to our

results (**Figure 41b**) we found no significant difference in ER-mitochondrial contacts induced by the different treatment conditions when the $SPLIC_s$ emission intensity was normalised for GFP expression, suggesting our alternative approach may not be as optimal as expected. However, if we look at split-GFP fluorescence alone, it is obvious that $SPLIC_s$ can detect an increase in ER-mitochondrial contacts, as Tunicamycin treatment indeed significantly enhanced organelle interaction (**Figure 41c**). This result is in line with Tunicamycin treatment in HeLa cells (Cieri et al. 2018; Bravo-Sagua et al. 2016) and indicates that the split-GFP fluorescence alone is a more reliable analysis method than normalising to anti-GFP. It is possible, that staining for GFP using an anti-GFP antibody, instead of normalising for transfection efficiency, introduced a further variable which confounded the results. Therefore, conclusions were drawn using the split-GFP fluorescence analysis alone.

We also wanted to validate our results by confirming they mirrored those of previous studies which demonstrate Tunicamycin, nutrient-depletion, and rapamycin increased contact sites. As aforementioned, Tunicamycin increased contact sites in IMCD3, just as they did in HeLa. However, our results disagree with data generated in HeLa cells showing that starvation or nutrient depletion increases contacts. (Cieri et al. 2018; Bravo-Sagua et al. 2019; Bravo-Sagua et al. 2016) It should be noted that what previous studies defined as starvation differed from our approach. In the Bravo-Sagua experiments, glucose starvation was achieved through the use of RPMI medium which contains L-glutamine but was not further supplemented with proteins, lipids, or growth factors normally found in serum. In the same study, amino acid depletion was achieved by using Earle's Balanced Salt Solution (EBSS) medium which contains glucose but no protein. In the Cieri study, Hela cells were treated with Hank's Balanced Salt Solution (HBSS) which contains some glucose but no sodium pyruvate, and which was not supplemented with serum. In contrast, as in our experience IMCD3 cells could not withstand total nutrient depletion, our cells were cultured in DMEM:F12 medium, which comes with low concentrations of glucose and glutamine, and was also supplemented with 0.1% FBS. Though no literature could be found of how incomplete nutrient depletion alters

MAMs compared to total starvation, it is possible that our treatment could not induce the same changes as total starvation, which likely promotes autophagy, but instead worked through an alternative mechanism to decrease organelle contact. Autophagy is the pathway which degrades cell components when nutrients are lacking and is associated with increased ER-mitochondrial contacts. The platform for autophagosome formation is located at the MAMs (Aoyama-Ishiwatari and Hirabayashi 2021), and Miga, a protein required for autophagy, when overexpressed leads to increased organelle contact in drosophila photoreceptor cells.(Xu, Wang, and Tong 2020). Therefore, it seems that Bravo-Sague's methods of starvation reflect upregulation of autophagy and organelle contacts, while our nutrient depletion probably targets a different mechanism.

Of note, none of the PDE inhibitors decreased contacts further, after starvation/nutrient-depletion (**Figure 45**). This finding could have one of two explanations. Either PDEs and cAMP do not work downstream of mechanism induced via nutrient-depletion, whatever they may be, or PDEs function through the same pathway as nutrient-depletion, and their inhibition achieves the same outcomes as upregulation of the pathway. Of course, the first experiment to test these hypotheses would have to identify intracellular processes which may be altered upon our specific nutrient-depleting treatment. One way this could be achieved would be to RNA sequence nutrient-depleted IMCD3.

The final control treatment which was tested, rapamycin, the mTOR inhibitor did not yield any significant difference in ER-mitochondrial contacts, while in HeLa cells this treatment was reported to increase contact sites (**Figure 41**).(Bravo-Sagua et al. 2016) The concentration of rapamycin or incubation period were not stated in the Bravo-Sagua protocol, so it is possible that the observed discrepancy may be due to differences in the protocol used. Our selection of drug dose was based on literature which suggests that lower concentrations of rapamycin target mTORC1 (0.5-100nM) and higher concentrations mTORC2 (0.2-20μM).(Foster and Toschi 2009) We were more interested in mTORC1 due to the greater

evidence for its signalling in ADPKD function. Another possible explanation is that mTORC1 signalling plays different roles in HeLa cells, a human cancer cell line, compared to kidney cells that are derived from mice, IMCD3. For example, though Bravo-Sagua found a decrease in contacts upon Cav1 expression in HeLa, a different study saw enhanced contacts with Cav1 expression in liver cells, so it is possible contact mechanisms are cell type dependent.(Sala-Vila et al. 2016) Due to time restrictions, we could not carry out further experiments, but perhaps should have tested SPLICs with rapamycin and nutrient-depletion treatments in HeLa cells, to confirm whether cell type differences were indeed the reason for opposing findings.

Primary cilium correlate to less ER-mitochondrial contacts in IMCD3

Finally, we also used SPLICs to test whether the presence or absence of a cilium had any correlation to number of ER-mitochondrial contacts, since we had previously shown that ciliary phenotype could alter other intracellular processes, such as PDE hydrolysis of cAMP. Indeed, non-ciliated cells demonstrated more ER-mitochondrial contacts than ciliated cells (**Figure 49**), a novel finding, which had not been previously reported. Published studies have hinted at a possible relationship between contact sites and cilia. In particular, one study carried out in a Parkinson's disease model showed that mitochondrial stress, induced by respiratory complex inhibitors or excessive fission, stimulated ciliogenesis in neuronal cells. DRP1 KD in these cells led to significantly supressed ciliogenesis as well as reduced mitochondrial fragmentation (Bae et al. 2019). Bravo-Sagua demonstrated that DRP1 regulates contact sites, so DRPI might function in an organelle axis which extends to the cilium as well.(Bravo-Sagua et al. 2019) Indeed mitochondria and cilia have already been demonstrated to share common pathways. For example, autophagy, is dependent on ciliary signalling. In fact, the machinery required for ciliogenesis also function in early stages of autophagy, and it is proposed the two processes regulate each other through a feedback loop.(Pampliega et al. 2013; Tang et al. 2013; Cianfanelli and Cecconi 2013) Additionally, in Chapter 6, we observed a decrease in cilia length upon PDE2 inhibition. When we sought to

identify which isoform of PDE2A was responsible for this phenotype, we observed PDE2A2-Dominant Negative (DN)-RFP expression in IMCD significantly decreased both organelle length and percent of ciliated cells (**Figure 24).** PDE2A2 is the isoform which localises to the OMM to regulate mitochondrial morphology and apoptosis.(Monterisi et al. 2017) The possibility of an ER-mitochondria-cilium axis is an exciting one. Though, any experiments trying to prove this phenomenon would struggle to differentiate between correlation and causation. Organelle phenotype and function in relation to one another would be very difficult to untangle, as it is likely orchestrated by a multitude of intertwined and balanced signalling processes.

However, results that non-ciliated cells have more ER-mitochondrial contacts do align with previous FRET data, whereby PDE hydrolysis of cAMP was measured at ER and OMM subdomains, and PDE2 and PDE3 activity at these domains was found to be correlated to a non-ciliary phenotype. Though not significant, PDE2 and PDE3 activities were greater at the ER, and in particular at the OMM, in non-ciliated IMCD3. Ciliated IMCD3 showed no PDE2 or PDE3 activity at the OMM. This suggests that, in non-ciliated cells, where there are more ER-mitochondrial contact sites, PDE2 and PDE3 activity may be upregulated to orchestrate MAM function. Inhibition of PDE3, and to a lesser degree PDE2, decreases the number of contacts. It could be argued that non-ciliated renal cells are not as important as their ciliated counterparts in driving cyst formation. However, what propagates cyst growth is excessive proliferation of dividing cells, which do not have a cilium, as cilia arise from the centrosomes, necessary for cell division.(Ishikawa and Marshall 2011) Therefore, targeting proliferating cells, while not the source of disease, may still prove a beneficial strategy for treating ADPKD (**Schematic 14**).

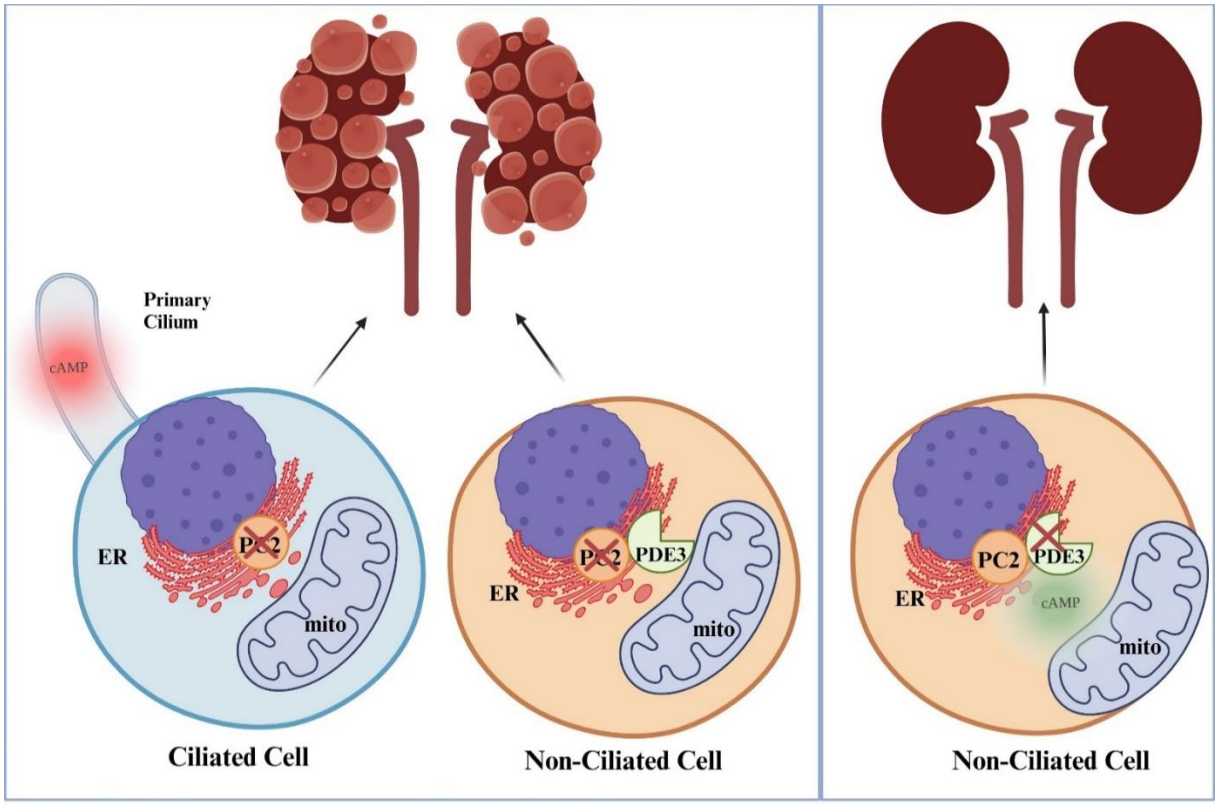

Schematic 14: Working hypothesis based on experimental results. Ciliated cells have fewer ER-mitochondrial contacts, unless PC2 is knocked out, in which case contacts increase and cystogenesis is aggravated. In non-ciliated cells, ER-mitochondrial contacts are also enhanced, particularly with PC2 KO. Non-ciliated cells also have more PDE3 activity at the ER and OMM, which keeps cAMP levels at this nanodomain low. When PDE3 is inhibited in non-ciliated cells, cAMP at the MAMS is increased, and ER-mitochondrial contact is reduced, subsequently mitigating cyst growth.

Conclusion

From these experiments, it is clear the field of inter-organelle crosstalk is still an emerging one, and thus tools to research this topic are still being optimised. Overall, consistent results conclude that PDE3 inhibition is the most robust treatment which decreases ER-mitochondrial contacts, as this was recapitulated with both SPLICs and, to a lesser degree, with FEMP. Relevant to this, PC2 KO, which is known to cause ADPKD, leads to increased organelle interaction.(Kuo et al. 2019) Since we have previously shown that PDE3A1, when overexpressed, can interact with endogenous PC2 and, PDE3 inhibition reduces contact sites, the hypothesis that PDE3A1 may function through an interaction with PC2, to control inter-organelle signalling, subsequently regulating cyst formation, still stands. However, this is not the only hypothesis which may explain reduced in vitro cystogenesis upon PDE3 inhibition,

as other PDEs, such as PDE2 and PDE4, which do not mitigate cystogenesis, have also been implicated in ER-mitochondrial crosstalk during ER stress. In the next chapter we summarise and discuss our findings as a whole, evaluating where PDE3 most likely stands in regulating cystogenesis of ADPKD.

Chapter 10: Discussion

Main Findings Summarised:

1. FRET sensor Arl13B-H187 measured cAMP signalling in the cilium, but no difference between ciliary and cytosolic cAMP was observed. However, ciliated versus non-ciliated cells demonstrated different PDE cAMP-hydrolysing profiles, suggesting the presence or absence of this organelle affects downstream cAMP signalling.
2. PDE4 is the main hydrolyser of cAMP in IMCD3. PDE4 inhibition in in vitro cysts also aggravated cyst formation, supporting evidence that enhanced cAMP signalling drives renal cystogenesis.
3. PDE3 inhibition mitigated cyst formation in FSK-stimulated cystogenesis, despite minimal cAMP hydrolysis by PDE3 observed downstream of AC stimulation. It is hypothesized PDE3 functions in a cAMP nanodomain to regulate cyst growth.
4. PDE3 does not function to alter cilia length, but cAMP does promote organelle elongation, as observed in ADPKD.
5. PDE3 interacts with PC2 at the plasma membrane and the ER, further implicating PDE3 as a potential regulator of cyst growth.
6. PDE3 hydrolyses cAMP at the ER, plasma membrane, and at the OMM of non-ciliated IMCD3, suggesting this enzyme could function at ER-mitochondrial contact sites.
7. PDE3 inhibition consistently decreased ER-mitochondrial contacts in IMCD3, strengthening the hypothesis that PDE3A1 interacts with PC2 to mitigate cyst formation, as PC2 also regulates organelle contact.
8. PDE inhibition reduces contacts during ER stress, highlighting a role for cAMP signalling at the MAMs.
9. Non-ciliated cells have more ER-mitochondrial contacts than their ciliated counterparts, thus the organelle crosstalk axis may also extend to the cilium.

Current treatment for ADPKD is problematic

ADPKD affects 12 million people worldwide.(Igarashi and Somlo 2002) Characterised by the formation of fluid-filled kidney cysts, it is the fourth most common cause of end-stage renal

disease. Yet, there is currently no cure for this ciliopathy. Tolvaptan, a V2R antagonist which blocks GPCR signalling, proved robust in clinical trials, but was also associated with numerous adverse side effects such as polyuria, nocturia, polydipsia, thirst, as well as hepatotoxicity.(Blair 2019) These collateral symptoms beg for the development of a better therapy for ADPKD. Enhanced ciliary cAMP signalling in ADPKD drives cystogenesis, but thanks to the strict compartmentalisation of this second messenger, there is evidence to suggest the same cyclic nucleotide mitigates cyst formation when signalling from a domain in the cell body.(Hansen, Kaiser, Leyendecker, Stüven, Krause, Derakhshandeh, Irfan, Sroka, Preval, and Desai 2022) Thus, identifying these distinguished pools of cyst-protective cAMP could potentially afford ADPKD treatment with subcellular precision. Since cAMP is degraded by PDEs, of which there are numerous unique isoforms, targeting PDEs relevant to cyst protective nanodomains of second messenger could be a selective therapeutic strategy for alleviating renal cystogenesis with minimal side effects. Thus, in this thesis my aim was to identify and characterise cyst-protective nanodomains of cAMP and establish which PDEs regulate these pools of second messenger.

PDE3 inhibition leads to decreased cystogenesis in vitro

In chapter 5, I identified PDE3, when inhibited, mitigates cyst growth in an in vitro assay of renal cystogenesis. Evidence from the literature suggests ciliary cAMP drives cyst formation, but cytosolic cAMP might be cyst protective.(Hansen, Kaiser, Leyendecker, Stüven, Krause, Derakhshandeh, Irfan, Sroka, Preval, and Desai 2022) This indication comes from a study where photo-activatable adenylyl cyclase's (bPACs), targeted to the cilium (cilia-bPAC), when illuminated, lead to in vitro cyst growth. However, when the same construct is instead targeted to the plasma membrane (cyto-bPAC) and stimulated with light, no cyst formation is observed upon increased cytosolic cAMP. The demonstration goes further, as when cilia-bPAC is illuminated in cells treated with Rolipram or IBMX, cystogenesis is aggravated, supporting that enhanced ciliary cAMP is detrimental to renal cells. However, when the same

experiments are carried out in cells expressing cyto-bPAC instead, Rolipram induces cystogenesis, but IBMX does not. This latter result is consistent with our findings that Rolipram, which inhibits PDE4, an enzyme known to hydrolyse cAMP in the cilium(Omar et al. 2019), enhanced ciliary cAMP, and thus aggravated FSK or PGE2-induced cystogenesis in vitro. Further, in the Hansen study, promiscuous PDE inhibition, which includes abolishing cytosolic PDE hydrolysis of cAMP, thus leading to enhanced second messenger signalling in the cytosol, after cyto-bPAC stimulation, does not cause cyst formation. This latter result with IBMX mirrors our finding that PDE3 inhibition, which increased cAMP in non-ciliary locales, mitigated cyst growth in FSK-induced cysts. **Schematic 15** illustrates and compares our outcomes to those of Hansen et al.

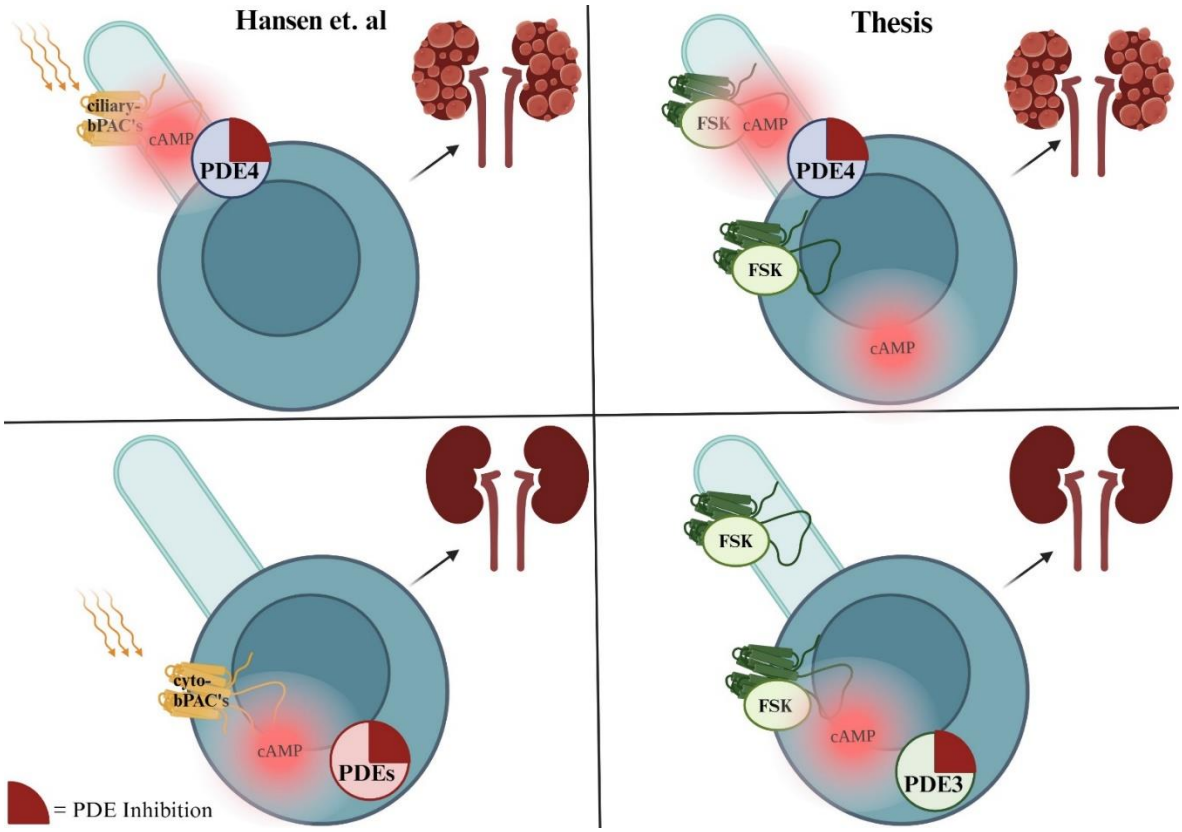

Schematic 15: Comparison of results obtained from the Hansen et. al study (left) and outcomes of this thesis (right). When ciliary-bPAC is illuminated, ciliary cAMP is increased, inducing cystogenesis (top left). If PDEs are inhibited in this model, cystogenesis is further aggravated. If cyto-bPAC is light activated then cytosolic cAMP is enhanced. Paired to cytosolic PDE inhibition, there is no cystogenesis (bottom left). In our in vitro cyst model, cAMP was enhanced using universal AC activator FSK. When PDE4 was inhibited, which can localise to the cilium, cystogenesis was aggravated (top right). In the same assay, when PDE3, instead of PDE4, was inhibited, an increase in cAMP, somewhere in a cytosolic subdomain, mitigated cystogenesis (bottom right).

The discovery that PDE3 inhibition led to a decrease in FSK-induced cystogenesis, was unexpected but exciting. If PDE3 regulates a pool of cAMP which diminishes renal cystogenesis, then PDE3 could be a precise therapeutic target for ADPKD. Yet, in Chapter 5, we did not observe cAMP hydrolysis by PDE3, downstream of FSK stimulation, in cilia or cytosol of ciliated and non-ciliated IMCD3 alike, implying PDE3 should not function in the regulation of renal cystogenesis. To explain these contradictory observations we hypothesized that, rather than through modulation of bulk cytosolic cAMP, PDE3 may regulate a nanodomain of cAMP somewhere in the cell to alter cyst formation.

PDE3's interaction with PC2 gives clues to where PDE3 may function in the cell

Since PDE3 has not been shown to localise to primary cilia, and in Chapter 6 we demonstrated PDE3 inhibition does not mitigate cyst formation by altering cilia length, we needed further clues to identify the nanodomain in which PDE3 functions in the cell. In a proteomics study previously carried out in our lab, PDE3A1 is shown to interact with PC2, which is mutated in 15% of ADPKD cases.(Subramaniam et al. 2023) This interaction was validated, and PDE3A1 was shown to associate with PC2 at the plasma membrane and ER of IMCD3. Therefore, we sought to measure PDE3 hydrolysis of cAMP at these subdomains, and found that PDE3 functions at the ER, the plasma membrane, and OMM of non-ciliated cells at comparable levels. Thus, once again, further evidence was required to decide the direction of our investigations.

Recently, PC2, was demonstrated to regulate ER-mitochondrial contact sites to elicit changes in organelle biogenesis and Ca^{2+} signalling.(Kuo et al. 2019) In addition, many other proteins found in the PDE3A1 interactome, such as Cav1, Calnexin, and Fis1 are also implicated in the regulation of organelle interactions at the MAMs. Thus, we formulated the hypothesis that PDE3 plays a role at ER-mitochondrial contact sites, and that PDE3 inhibition mitigates in vitro cystogenesis by regulating organelle crosstalk.

PDEs, but in particular PDE3, function at ER-mitochondrial contact sites

To test this hypothesis that PDE3 may orchestrate ER contacts with mitochondria, we employed several tools, that measured organelle interactions, with mixed success. Despite some trials, we found PDE3 inhibition decreased ER-mitochondrial contacts consistently, with both $SPLIC_s$ and FEMP. These results upheld our hypothesis that PDE3 may mitigate cystogenesis by governing organelle interaction at the MAMs.

Of note, when we tested PDE inhibition alongside Tunicamycin-induced ER stress, we found a decrease in contact sites upon inhibition of all three PDE isoforms, suggesting increased cAMP, and thus PKA, decreased organelle interaction during ER stress. However, this finding does not align with previous work in cancer cells which demonstrated PKA phosphorylation of DRP1, regulated by Cav1, enhances organelle contacts during ER stress.(Bravo-Sagua et al. 2019) One explanation for these contradictions is that PKA functions differentially in distinct cell types- HeLa versus IMCD3. Indeed, a separate study reported enhanced contacts with Cav1 overexpression in liver cells, contradicting Bravo-Sagua's results whereby Cav1 in HeLa works to prevent such contacts.(Sala-Vila et al. 2016) A different possibility is that cAMP signalling, and its downstream components, have altered functions in disease and homeostasis. For example, it was demonstrated that PDE3 inhibition, in cells isolated from human APDKD tissue, induces cell proliferation, but noticeably decreases proliferation of cells derived from healthy human samples. (Pinto et al. 2016) The same pattern is observed with cAMP, whereby in normal renal tissue, cAMP generally inhibits ERK and subsequent cell proliferation, while we know that in disease, enhanced second messenger signalling leads to the opposite effects.(Hanaoka and Guggino 2000; Yamaguchi et al. 2000b)

A shortfall of our experiments is that contact sites, upon PDE inhibition, were not measured alongside FSK treatment, whereas in in vitro cyst assays, where PDE3 inhibition mitigated cyst formation, cystogenesis was stimulated via AC activation with the diterpene. Therefore, the two experimental conditions are not entirely comparable, and it could be possible that with

original FSK stimulation, PDE3 inhibition would lead to increased contact sites at MAMs. In addition, stimulation of cystogenesis via FSK is not as relevant an ADPKD model as a knock out or mutation in polycystins. Indeed, it was reported that in Pkd2($^{-/WS25}$) mice, PDE3A KO aggravates cystogenesis, not ameliorates it. (Ye et al. 2016) It thus seems possible that PDE3 plays a role in organelle contacts and cyst formation, but the direction of the change in either process cannot be predicted without testing enzyme inhibition in more robust models of ADPKD. A good follow up experiment, if time had allowed, would have been to confirm if PDE3 inhibition in PC2 KO cells reduces contacts even more robustly or whether the change previously observed with Cilostamide treatment is abolished. Both results could suggest PDE3 inhibition works through phosphorylation of PC2 to alter contact sites.

PDE3 may function in a nanodomain with PC2 to regulate ER-mitochondrial contacts and subsequent cyst growth

The hypothesis that PDE3 inhibition works through PC2 to mitigate organelle contacts as well as cystogenesis is even further upheld by the fact that all three PDE isoforms, when inhibited, decreased contacts (measured via $SPLIC_s$) during ER stress. Since PDE2 inhibition did not alter cyst growth and PDE4 inhibition aggravated in vitro cyst formation, if cystogenesis relied on changes in contact sites during ER-stress, then PDE2 and PDE4 inhibition should not have reduced organelle contact. Therefore, the fact that promiscuous inhibition of PDEs is enough to diminish contact sites, but only PDE3 inhibition mitigates cystogenesis, suggests a piece of the puzzle is missing, and that piece may be an interaction between PDE3 and PC2. If there is a pool of cAMP which controls phosphorylation of DRP1 to alter contacts at the MAMs, but PDE3 works on a separate nanodomain of cAMP, also located at these organelles' membranes, but which regulates phosphorylation of PC2 instead, this phenomenon would demonstrate just how precise compartmentalisation of the second messenger truly is.

In contrast, though FEMP had many caveats, the few measurements obtained with this tool did demonstrate PDE2 inhibition did not alter contacts and PDE4 inhibition enhanced them,

aligning perfectly with the idea that increased contact at MAMs correlates to aggravated cystogenesis. It should be noted however, that FEMP experiments were not carried out alongside Tunicamycin treatment and thus may reflect a different signalling mechanism to ER stress at the MAMs. Using SPLICs, with no Tunicamycin treatment, only PDE3 inhibition led to a noticeable decrease in contact sites, with no obvious change in contacts after PDE2 or PDE4 inhibition. This result does hint that the cAMP signalling domain which regulates contacts during ER stress is separate to the second messenger domain which functions at more basal conditions of organelle interaction. The study which demonstrated PC2 KO increases contact sites was also carried out without prior stress induction, thus supporting the idea that PDE3A1 may function to regulate cystogenesis via PC2.

Study limitations

SPLICs, and other tools, have demonstrated that PDE3 inhibition leads to decreased in vitro cystogenesis and reduced ER-mitochondrial contacts. However, with current data, we can only demonstrate decreased organelle interaction correlates to mitigated cystogenesis, but we cannot prove changes in ER-mitochondrial crosstalk are responsible for altered cyst growth when PDE3 is inhibited in vitro. In fact, our findings from Chapter 8 showed significant hydrolysis of cAMP, by PDE3, at AKAP79, which localises at the plasma membrane. Previous studies also report that PDE3A can function alongside CFTR (Ye et al. 2016; Penmatsa et al. 2010). Indeed, PDE3 is linked to Cl^- secretion in shark rectal glands,(De Jonge, Tilly, Hogema, Pfau, Kelley, Kelley, Melita, Morris, Viola, and Forrest Jr 2014) and pig trachea submucosal glands.(Penmatsa et al. 2010) In addition, in principle-collecting duct cells, mpkCCD$_{c14}$, PDE3 inhibition, increases NAPDH oxidase 4 (NOX4), which is believed to contribute to V2R-cAMP-PKA signalling to enhance expression of AQP2.(Feraille et al. 2014) Therefore, while we hypothesize PDE3 functions at the MAMs to regulate cystogenesis, an equally valid alternative is that PDE localises to the plasma membrane where it reduces fluid secretion rather than cellular proliferation to mitigate cyst formation. To rule

out this possibility, we could have assessed whether CFTR and PDE3 interact, looked at phosphorylation of CFTR with/without PDE3 inhibition, or also explored the effect of enzyme inhibition on Cl^- secretion. Unfortunately, time did not allow for these experiments.

In addition to the possibility that PDE3 functions through fluid secretion to alter cyst growth in vitro, there are also study limitations regarding the experiments which have been carried out in this thesis. One of the most prominent pitfalls of this research is that in vitro cystogenesis was achieved through the upregulation of intracellular cAMP via FSK or PGE2, and not through a mutation in one or both Polycystins. AC activation is a promiscuous and indirect method to study renal cystogenesis, as it is known, different pools of cAMP achieve distinct and often disparate functions within the cell. Using FSK to activate ACs would likely target the pool of cAMP responsible for cystogenesis, hence why cyst growth was observed in vitro. However, FSK would also stimulate ACs which are not normally involved in renal cyst formation, and which could alter disease progression or mask physiological truths. PGE2 stimulated cysts are also a misleading model for cyst formation, because while PGE2 has been shown to generate cysts in vitro, it is unlikely PGE2 stimulation is the only mechanism at play in ADPKD. Thus, using PGE2 to induce cystogenesis would give a limited picture of intracellular signalling in the context of ADPKD. Finally, and perhaps more importantly, without studying a model derived from mutations in Polycystins, any results obtained upon PDE inhibition cannot be directly linked to ADPKD, only a broad form of renal cystogenesis. If PDE3 interacts with PC2 and functions through the polycystins to affect cyst growth, it is possible that without the polycystins present or not wholly functioning, manipulation of PDE3 activity could be rendered meaningless in the pursuit of a treatment for ADPKD. It is also possible that in PC1 or PC2 mutated or KO cells, PDE3 inhibition may have the opposite effect on cystogenesis than that observed in FSK or PGE2-dervived cysts. Ultimately, the only way to truly study the effects of PDE3 activity on ADPKD progression would be to implement cell or animal models with mutations in polycystins.

Apart from the lack of an optimal model for the study of ADPKD, some experimental set ups could also have been improved. Measuring ER-mitochondrial contacts proved difficult, as many of the techniques implemented in this pursuit, such as FEMP and splitGFP, were still in the process of optimisation and often led to inconsistent results. However, limited tools aside, the ER-mitochondrial experiments could have been executed so that results were comparable to data obtained through FRET and in vitro cyst assays. As aforementioned, cysts were generated in vitro via FSK or PGE2 treatment. PDE inhibition in the cilia and cytosol of renal cells was measured both with no prior stimulation but also with PGE2 or FSK. Thus, one could conclude that the PDE activity in renal cells, measured via FRET, indicated PDE contribution to cystogenesis in vitro. However, FRET experiments using localised reporters to the ER, OMM, and plasma membrane did not include initial stimulation via FSK or PGE2, and only measured PDE activity at basal levels of cAMP in renal cells. Since cAMP is a versatile second messenger, it is likely that its downstream signalling, including PDE hydrolysing activity, differs in cells with minimal cAMP and in cystic cells which have been stimulated with PGE2 or FSK. Therefore, while I observed PDE3 activity at the ER, OMM, and plasma membrane of renal cells at basal levels of cAMP, I cannot assume that the same PDE3 activity occurs in cystic cells pre-treated with PGE2 or FSK, and cannot make robust conclusions on PDE3's contribution to cAMP hydrolysis in renal cystogenesis at these subcellular domains. Finally, the same caveat occurred when measuring ER-mitochondrial contacts. One argument of this thesis is that PDE3 alters cyst growth by regulation of ER-mitochondrial contact. However, since cysts were generated via FSK or PGE2, cells for ER-mitochondrial experiments should have also been treated with FSK or PGE2 prior to PDE inhibition. As thoroughly mentioned in this thesis and other studies, ER-mitochondrial contacts vary drastically when cells are experiencing different levels of stress or signalling, thus contact sites at basal cAMP may not reflect organelle communication when cAMP is upregulated. Unfortunately, since the ER-mitochondrial contact sites were a new area of research for me, I opted to test one drug treatment at a time to make conclusions simple.

However, this approach only succeeded in rendering the results less relevant to renal cystogenesis.

Overall, this thesis was a learning experience in the development, optimisation, and execution of experimentation and the formulation of hypotheses. In the final section, I will discuss future experiments which could help translate the results obtained so far into a more definitive and translational understanding of PDE3's contribution in ADPKD.

Future Direction

Due to time limitations, our research ended with the hypothesis that PDE3A1 regulates organelle interaction through a direct association with PC2. This crosstalk between the mitochondria and the ER (and possibly the cilium) is believed to regulate cyst growth. However, there were many study limitations which left the link between PDE3, PC2, organelle communication, and regulation of cystogenesis unexplored. Thus, the next step of this research would be to correct for these limitations by measuring PDE inhibition on ER-mitochondrial contact, downstream of PGE2 or FSK stimulation and to also measure PDE activity at localised subcellular domains in the same fashion. This would help clarify whether ER-mitochondrial contacts are relevant to renal cystogenesis, induced via FSK or PGE2, and whether PDEs function at these subdomains during high levels of cAMP signalling, as observed in renal cyst formation.

Since splitGFP and other tools used to measure organelle contacts were inconsistent, it would also be opportune to try other techniques which could solidify PDE3's role in organelle contacts. For example, electron microscopy allows for increased resolution and could be used to faithfully measure the distance between ER and mitochondria in renal cells treated with FSK/PGE2 and PDE inhibitors. Alternatively, physically measuring organelle contacts is not the only approach one could take in this endeavour. It was shown that PC2 KO leads to increased ER and mitochondrial tethering through mitofusin 2. This tethering increases Ca^{2+} transfer from the former to the latter organelle, altering bioenergetics and ultimately

contributing to cystogenesis. It is possible PC2 activity at the ER, independent to the OMM, may be controlling PC2-modulated Ca^{2+} signalling into the mitochondria through Ryanodine or inositol triphosphate (IP3) receptors.(Brill and Ehrlich 2020) Thus, one could explore PDE3's role at the MAMs by measuring whether PDE3 inhibition may also have an effect on Ca^{2+} signalling, particularly from the ER into the mitochondria. Perhaps PDE3 functions through PC2 to alter Ca^{2+} signalling. FRET sensors localising to subcellular domains are available in the lab, which can report real-time changes in intracellular Ca^{2+}. These sets of experiments would implicate PDE3 in the regulation of contact sites and Ca^{2+} exchange. However, to fully connect PDE3 to ADPKD the best approach would be to carry out the experiments comprising this thesis in a cell model with polycystin mutations or KO. IMCD3 with Polycystin 1 only, Polycystin 2 only, or Polycystin 1 and 2 KO, achieved through Crispr/Cas9, were recently obtained in the lab. Comparing PDE3 inhibition in cysts derived from PC KO versus WT IMCD3 could shed light on whether PDE3 contributes to ADPKD disease mechanisms. Measuring PDE3 activity in IMCD3 with PC KO via FRET would indicate whether PDE3 hydrolyses cAMP generated downstream of PC malfunction, like in ADPKD. Testing PDE3 inhibition on ER-mitochondrial contacts of PC KO versus WT IMCD3 would demonstrate whether PDE3 affects these organelle interactions through PC2, or via an independent process.

Finally, provided prior work in PKD cell lines shows a promising role for PDE3 in ADPKD cystogenesis, the next approach would be to test PDE3 inhibition in ADPKD animal models harbouring mutations in polycystins.

Conclusion

ADPKD is a prevalent disease which is characterised by formation of fluid-filled kidney cysts. cAMP signalling in the cilium is thought to drive this ciliopathy, but here we have shown that inhibition of PDE3 increases cAMP in cytosolic organelles and reduces cyst formation in vitro. Thus, PDEs could be a potential therapeutic target for this disease, as they

compartmentalise the cAMP signal at precise nanodomains of second messenger signalling. Disrupting such nanodomains, as a treatment strategy, would likely cause minimal collateral disturbances and thus fewer side effects. We hypothesize that PDE3 functions alongside PC2 to regulate ER-mitochondrial crosstalk, ultimately controlling cyst formation. If cAMP signalling and PDE hydrolysis of second messenger function to orchestrate organelle crosstalk, this finding could have implications not only for ADPKD treatment, but for many diseases where altered organelle crosstalk is emerging as a prevalent contributor of pathogenesis.

Chapter 11: References

Abdul-Majeed, Shakila, Bryan C Moloney, and Surya M Nauli. 2012. 'Mechanisms regulating cilia growth and cilia function in endothelial cells', *Cellular and Molecular Life Sciences*, 69: 165-73.

Agarwal, K. C., and R. E. Parks, Jr. 1983. 'Forskolin: a potential antimetastatic agent', *Int J Cancer*, 32: 801-4.

Agarwal, Shailesh R, Colleen E Clancy, and Robert D Harvey. 2016. 'Mechanisms restricting diffusion of intracellular cAMP', *Scientific reports*, 6: 19577.

Agarwal, Shailesh R, Kathryn Miyashiro, Htun Latt, Rennolds S Ostrom, and Robert D Harvey. 2017. 'Compartmentalized cAMP responses to prostaglandin EP2 receptor activation in human airway smooth muscle cells', *British Journal of Pharmacology*, 174: 2784-96.

Aguiari, G., F. Bizzarri, A. Bonon, A. Mangolini, E. Magri, M. Pedriali, P. Querzoli, S. Somlo, P. C. Harris, L. Catizone, and L. Del Senno. 2012. 'Polycystin-1 regulates amphiregulin expression through CREB and AP1 signalling: implications in ADPKD cell proliferation', *J Mol Med (Berl)*, 90: 1267-82.

Ahmad, F., W. Shen, F. Vandeput, N. Szabo-Fresnais, J. Krall, E. Degerman, F. Goetz, E. Klussmann, M. Movsesian, and V. Manganiello. 2015. 'Regulation of sarcoplasmic reticulum Ca2+ ATPase 2 (SERCA2) activity by phosphodiesterase 3A (PDE3A) in human myocardium: phosphorylation-dependent interaction of PDE3A1 with SERCA2', *J Biol Chem*, 290: 6763-76.

Albert, V., and M. N. Hall. 2015. 'mTOR signaling in cellular and organismal energetics', *Curr Opin Cell Biol*, 33: 55-66.

Annamdevula, Naga S, Rachel Sweat, John R Griswold, Kenny Trinh, Chase Hoffman, Savannah West, Joshua Deal, Andrea L Britain, Kees Jalink, and Thomas C Rich. 2018. 'Spectral imaging of FRET-based sensors reveals sustained cAMP gradients in three spatial dimensions', *Cytometry Part A*, 93: 1029-38.

Anton, Selma E, Charlotte Kayser, Isabella Maiellaro, Katarina Nemec, Jan Möller, Andreas Koschinski, Manuela Zaccolo, Paolo Annibale, Martin Falcke, and Martin J Lohse. 2022. 'Receptor-associated independent cAMP nanodomains mediate spatiotemporal specificity of GPCR signaling', *Cell*, 185: 1130-42. e11.

Aoyama-Ishiwatari, Saeko, and Yusuke Hirabayashi. 2021. 'Endoplasmic reticulum–mitochondria contact sites—emerging intracellular signaling hubs', *Frontiers in Cell and Developmental Biology*, 9: 653828.

Arasaki, Kohei, Hiroaki Shimizu, Hirofumi Mogari, Naoki Nishida, Naohiko Hirota, Akiko Furuno, Yoshihisa Kudo, Misuzu Baba, Norio Baba, and Jinglei Cheng. 2015. 'A role for the ancient SNARE syntaxin 17 in regulating mitochondrial division', *Developmental cell*, 32: 304-17.

Arena, Danielle T, and Aldebaran M Hofer. 2021. 'Cyclic AMP does double duty to support parallel signaling in primary cilium and cytosol', *Cell calcium*, 97: 102436.

Arruda, Ana Paula, Benedicte M Pers, Güneş Parlakgül, Ekin Güney, Karen Inouye, and Gökhan S Hotamisligil. 2014. 'Chronic enrichment of hepatic endoplasmic reticulum–mitochondria contact leads to mitochondrial dysfunction in obesity', *Nature medicine*, 20: 1427-35.

Assenza, M. R., F. Barbagallo, F. Barrios, M. Cornacchione, F. Campolo, E. Vivarelli, D. Gianfrilli, L. Auletta, A. Soricelli, A. M. Isidori, A. Lenzi, M. Pellegrini, and F. Naro. 2018. 'Critical role of phosphodiesterase 2A in mouse congenital heart defects', *Cardiovasc Res*, 114: 830-45.

Bachmann, Verena A, Johanna E Mayrhofer, Ronit Ilouz, Philipp Tschaikner, Philipp Raffeiner, Ruth Röck, Mathieu Courcelles, Federico Apelt, Tsan-Wen Lu, and George S Baillie. 2016. 'Gpr161 anchoring of PKA consolidates GPCR and cAMP signaling', *Proceedings of the National Academy of Sciences*, 113: 7786-91.

Bae, Ji-Eun, Gil Myung Kang, Se Hee Min, Doo Sin Jo, Yong-Keun Jung, Keetae Kim, Min-Seon Kim, and Dong-Hyung Cho. 2019. 'Primary cilia mediate mitochondrial stress responses to promote dopamine neuron survival in a Parkinson's disease model', *Cell Death & Disease*, 10: 952.

Baillie, George S., Gonzalo S. Tejeda, and Michy P. Kelly. 2019. 'Therapeutic targeting of 3′,5′-cyclic nucleotide phosphodiesterases: inhibition and beyond', *Nature Reviews Drug Discovery*, 18: 770-96.

Banales, J. M., T. V. Masyuk, S. A. Gradilone, A. I. Masyuk, J. F. Medina, and N. F. LaRusso. 2009. 'The cAMP effectors Epac and protein kinase a (PKA) are involved in the hepatic cystogenesis of an animal model of autosomal recessive polycystic kidney disease (ARPKD)', *Hepatology*, 49: 160-74.

Bangs, Fiona, and Kathryn V Anderson. 2017. 'Primary cilia and mammalian hedgehog signaling', *Cold Spring Harbor perspectives in biology*, 9: a028175.

Barbeito, Pablo, and Francesc R. Garcia-Gonzalo. 2021. 'HTR6 and SSTR3 targeting to primary cilia', *Biochemical Society Transactions*, 49: 79-91.

Bartok, Adam, David Weaver, Tünde Golenár, Zuzana Nichtova, Máté Katona, Száva Bánsághi, Kamil J. Alzayady, V. Kaye Thomas, Hideaki Ando, Katsuhiko Mikoshiba, Suresh K. Joseph, David I. Yule, György Csordás, and György Hajnóczky. 2019. 'IP3 receptor isoforms differently regulate ER-mitochondrial contacts and local calcium transfer', *Nature Communications*, 10: 3726.

Bassler, J., J. E. Schultz, and A. N. Lupas. 2018. 'Adenylate cyclases: Receivers, transducers, and generators of signals', *Cell Signal*, 46: 135-44.

Basso, V., E. Marchesan, C. Peggion, J. Chakraborty, S. von Stockum, M. Giacomello, D. Ottolini, V. Debattisti, F. Caicci, E. Tasca, V. Pegoraro, C. Angelini, A. Antonini, A. Bertoli, M. Brini, and E. Ziviani. 2018. 'Regulation of ER-mitochondria contacts by Parkin via Mfn2', *Pharmacol Res*, 138: 43-56.

Beavo, J. A., J. G. Hardman, and E. W. Sutherland. 1971. 'Stimulation of adenosine 3',5'-monophosphate hydrolysis by guanosine 3',5'-monophosphate', *J Biol Chem*, 246: 3841-6.

Belibi, Franck A, Gail Reif, Darren P Wallace, Tamio Yamaguchi, Lincoln Olsen, Hong Li, George M Helmkamp Jr, and Jared J Grantham. 2004. 'Cyclic AMP promotes growth and secretion in human polycystic kidney epithelial cells', *Kidney International*, 66: 964-73.

Bender, A. T., and J. A. Beavo. 2006. 'Cyclic nucleotide phosphodiesterases: molecular regulation to clinical use', *Pharmacol Rev*, 58: 488-520.

Bergmann, Carsten. 2015. 'ARPKD and early manifestations of ADPKD: the original polycystic kidney disease and phenocopies', *Pediatric Nephrology*, 30: 15-30.

Bergmann, Carsten, Lisa M. Guay-Woodford, Peter C. Harris, Shigeo Horie, Dorien J. M. Peters, and Vicente E. Torres. 2018. 'Polycystic kidney disease', *Nature Reviews Disease Primers*, 4: 50.

Betz, C., D. Stracka, C. Prescianotto-Baschong, M. Frieden, N. Demaurex, and M. N. Hall. 2013. 'Feature Article: mTOR complex 2-Akt signaling at mitochondria-associated endoplasmic reticulum membranes (MAM) regulates mitochondrial physiology', *Proc Natl Acad Sci U S A*, 110: 12526-34.

Billesbølle, Christian B., Claire A. de March, Wijnand J. C. van der Velden, Ning Ma, Jeevan Tewari, Claudia Llinas del Torrent, Linus Li, Bryan Faust, Nagarajan Vaidehi, Hiroaki Matsunami, and Aashish Manglik. 2023. 'Structural basis of odorant recognition by a human odorant receptor', *Nature*, 615: 742-49.

Blair, H. A. 2019. 'Tolvaptan: A Review in Autosomal Dominant Polycystic Kidney Disease', *Drugs*, 79: 303-13.

Bock, Andreas, Paolo Annibale, Charlotte Konrad, Annette Hannawacker, Selma E Anton, Isabella Maiellaro, Ulrike Zabel, Sivaraj Sivaramakrishnan, Martin Falcke, and Martin J Lohse. 2020. 'Optical mapping of cAMP signaling at the nanometer scale', *Cell*, 182: 1519-30. e17.

Boess, Frank G., Martin Hendrix, Franz-Josef van der Staay, Christina Erb, Rudy Schreiber, Wilma van Staveren, Jan de Vente, Jos Prickaerts, Arjan Blokland, and Gerhard Koenig. 2004. 'Inhibition of phosphodiesterase 2 increases neuronal cGMP, synaptic plasticity and memory performance', *Neuropharmacology*, 47: 1081-92.

Bolger, Graeme, Tamar Michaeli, Tim Martins, Tom St John, Bart Steiner, Linda Rodgers, Michael Riggs, Michael Wigler, and Kenneth Ferguson. 1993. 'A family of human phosphodiesterases homologous to the dunce learning and memory gene product of Drosophila melanogaster are potential targets for antidepressant drugs', *Molecular and Cellular Biology*.

Brand, T. 2005. 'The Popeye domain-containing gene family', *Cell Biochem Biophys*, 43: 95-103.

Bravo, Roberto, Jose Miguel Vicencio, Valentina Parra, Rodrigo Troncoso, Juan Pablo Munoz, Michael Bui, Clara Quiroga, Andrea E Rodriguez, Hugo E Verdejo, and Jorge Ferreira. 2011. 'Increased ER–mitochondrial coupling promotes mitochondrial respiration and bioenergetics during early phases of ER stress', *Journal of cell science*, 124: 2143-52.

Bravo-Sagua, Roberto, Camila López-Crisosto, Valentina Parra, Marcelo Rodriguez-Peña, Beverly A. Rothermel, Andrew F. G. Quest, and Sergio Lavandero. 2016. 'mTORC1 inhibitor rapamycin and ER stressor tunicamycin induce differential patterns of ER-mitochondria coupling', *Scientific reports*, 6: 36394.

Bravo-Sagua, Roberto, Valentina Parra, Camila López-Crisosto, Paula Díaz, AF Quest, and Sergio Lavandero. 2017. 'Calcium transport and signaling in mitochondria', *Compr Physiol*, 7: 623-34.

Bravo-Sagua, Roberto, Valentina Parra, Carolina Ortiz-Sandoval, Mario Navarro-Marquez, Andrea E. Rodríguez, Natalia Diaz-Valdivia, Carlos Sanhueza, Camila Lopez-Crisosto, Nasser Tahbaz, Beverly A. Rothermel, Joseph A. Hill, Mariana Cifuentes, Thomas Simmen, Andrew F. G. Quest, and Sergio Lavandero. 2019. 'Caveolin-1 impairs PKA-DRP1-mediated remodelling of ER–mitochondria communication during the early phase of ER stress', *Cell Death & Differentiation*, 26: 1195-212.

Brill, A. L., and B. E. Ehrlich. 2020. 'Polycystin 2: A calcium channel, channel partner, and regulator of calcium homeostasis in ADPKD', *Cell Signal*, 66: 109490.

Brook-Carter, P. T., B. Peral, C. J. Ward, P. Thompson, J. Hughes, M. M. Maheshwar, M. Nellist, V. Gamble, P. C. Harris, and J. R. Sampson. 1994. 'Deletion of the TSC2 and PKD1 genes associated with severe infantile polycystic kidney disease--a contiguous gene syndrome', *Nat Genet*, 8: 328-32.

Brown, Edward M. 2007. 'Clinical lessons from the calcium-sensing receptor', *Nature Clinical Practice Endocrinology & Metabolism*, 3: 122-33.

Bujakowska, Kinga M, Qin Liu, and Eric A Pierce. 2017. 'Photoreceptor cilia and retinal ciliopathies', *Cold Spring Harbor perspectives in biology*, 9: a028274.

Bukanov, Nikolay O, Laurie A Smith, Katherine W Klinger, Steven R Ledbetter, and Oxana Ibraghimov-Beskrovnaya. 2006. 'Long-lasting arrest of murine polycystic kidney disease with CDK inhibitor roscovitine', *Nature*, 444: 949-52.

Burdyga, Alex, Nicoletta C. Surdo, Stefania Monterisi, Giulietta Di Benedetto, Francesca Grisan, Elisa Penna, Luca Pellegrini, Manuela Zaccolo, Mario Bortolozzi, Pawel Swietach, Tullio Pozzan, and Konstantinos Lefkimmiatis. 2018. 'Phosphatases control PKA-dependent functional microdomains at the outer mitochondrial membrane', *Proceedings of the National Academy of Sciences*, 115: E6497-E506.

Burkhalter, M. D., A. Sridhar, P. Sampaio, R. Jacinto, M. S. Burczyk, C. Donow, M. Angenendt, M. Hempel, P. Walther, P. Pennekamp, H. Omran, S. S. Lopes, S. M. Ware, and M. Philipp. 2019. 'Imbalanced mitochondrial function provokes heterotaxy via aberrant ciliogenesis', *J Clin Invest*, 129: 2841-55.

Buu, Nguyen T, Ru-tai Hui, and Pierre Falardeau. 1993. 'Norepinephrine in neonatal rat ventricular myocytes: association with the cell nucleus and binding to nuclear α1-and β-adrenergic receptors', *Journal of molecular and cellular cardiology*, 25: 1037-46.

Cai, Yiqiang, Georgia Anyatonwu, Dayne Okuhara, Kyu-Beck Lee, Zhiheng Yu, Tamehito Onoe, Chang-Lin Mei, Qi Qian, Lin Geng, and Ralph Wiztgall. 2004. 'Calcium dependence of polycystin-2 channel activity is modulated by phosphorylation at Ser812', *Journal of Biological Chemistry*, 279: 19987-95.

Calvet, J. P. 2015. 'The Role of Calcium and Cyclic AMP in PKD.' in X. Li (ed.), *Polycystic Kidney Disease* (Codon Publications

Copyright: The Author.: Brisbane (AU)).

Cantero Mdel, R., I. F. Velázquez, A. J. Streets, A. C. Ong, and H. F. Cantiello. 2015. 'The cAMP Signaling Pathway and Direct Protein Kinase A Phosphorylation Regulate Polycystin-2 (TRPP2) Channel Function', *J Biol Chem*, 290: 23888-96.

Cárdenas, César, Russell A Miller, Ian Smith, Thi Bui, Jordi Molgó, Marioly Müller, Horia Vais, King-Ho Cheung, Jun Yang, and Ian Parker. 2010. 'Essential regulation of cell bioenergetics by constitutive InsP3 receptor Ca2+ transfer to mitochondria', *Cell*, 142: 270-83.

Casas, Paloma García, Michela Rossini, Linnea Påvénius, Mezida Saeed, Nikita Arnst, Sonia Sonda, Matteo Bruzzone, Valeria Berno, Andrea Raimondi, Maria Livia Sassano, Luana Naia, Patrizia Agostinis, Mattia Sturlese, Barbara A. Niemeyer, Hjalmar Brismar, Maria Ankarcrona, Arnaud Gautier, Paola Pizzo, and Riccardo Filadi. 2023. 'Simultaneous detection of membrane contact dynamics and associated Ca2+ signals by reversible chemogenetic reporters', *bioRxiv*.

Chaudhry, B., and D. J. Henderson. 2019. 'Cilia, mitochondria, and cardiac development', *J Clin Invest*, 129: 2666-68.

Chebib, Fouad T, and Vicente E Torres. 2016. 'Autosomal dominant polycystic kidney disease: core curriculum 2016', *American Journal of Kidney Diseases*, 67: 792-810.

Chen, Xingyi, Chaoran Shi, Meihui He, Siqi Xiong, and Xiaobo Xia. 2023. 'Endoplasmic reticulum stress: molecular mechanism and therapeutic targets', *Signal Transduction and Targeted Therapy*, 8: 352.

Cheng, J., M. A. Thompson, H. J. Walker, C. E. Gray, G. M. Warner, W. Zhou, and J. P. Grande. 2006. 'Lixazinone stimulates mitogenesis of Madin-Darby canine kidney cells', *Exp Biol Med (Maywood)*, 231: 288-95.

Choi, Y. H., A. Suzuki, S. Hajarnis, Z. Ma, H. C. Chapin, M. J. Caplan, M. Pontoglio, S. Somlo, and P. Igarashi. 2011a. 'Polycystin-2 and phosphodiesterase 4C are components of a ciliary A-kinase anchoring protein complex that is disrupted in cystic kidney diseases', *Proc Natl Acad Sci U S A*, 108: 10679-84.

Choi, Yun-Hee, Akira Suzuki, Sachin Hajarnis, Zhendong Ma, Hannah C Chapin, Michael J Caplan, Marco Pontoglio, Stefan Somlo, and Peter Igarashi. 2011b. 'Polycystin-2 and phosphodiesterase 4C are components of a ciliary A-kinase anchoring protein complex that is disrupted in cystic kidney diseases', *Proceedings of the National Academy of Sciences*, 108: 10679-84.

Cianfanelli, Valentina, and Francesco Cecconi. 2013. 'Molecular clearance at the cell's antenna', *Nature*, 502: 180-81.

Cieri, D., M. Vicario, M. Giacomello, F. Vallese, R. Filadi, T. Wagner, T. Pozzan, P. Pizzo, L. Scorrano, M. Brini, and T. Calì. 2018. 'SPLICS: a split green fluorescent protein-based contact site sensor for narrow and wide heterotypic organelle juxtaposition', *Cell Death Differ*, 25: 1131-45.

Cohen, Alex W, Babak Razani, William Schubert, Terence M Williams, Xiao Bo Wang, Puneeth Iyengar, Dawn L Brasaemle, Philipp E Scherer, and Michael P Lisanti. 2004. 'Role of caveolin-1 in the modulation of lipolysis and lipid droplet formation', *Diabetes*, 53: 1261-70.

Colledge, M., and J. D. Scott. 1999. 'AKAPs: from structure to function', *Trends Cell Biol*, 9: 216-21.

Corbin, J. D., and S. L. Keely. 1977. 'Characterization and regulation of heart adenosine 3':5'-monophosphate-dependent protein kinase isozymes', *J Biol Chem*, 252: 910-8.

Cornec-Le Gall, E., R. J. Olson, W. Besse, C. M. Heyer, V. G. Gainullin, J. M. Smith, M. P. Audrézet, K. Hopp, B. Porath, B. Shi, S. Baheti, S. R. Senum, J. Arroyo, C. D. Madsen, C. Férec, D. Joly, F. Jouret, O. Fikri-Benbrahim, C. Charasse, J. M. Coulibaly, A. S. Yu, K. Khalili, Y. Pei, S. Somlo, Y. Le Meur, V. E. Torres, and P. C. Harris. 2018. 'Monoallelic Mutations to DNAJB11 Cause Atypical Autosomal-Dominant Polycystic Kidney Disease', *Am J Hum Genet*, 102: 832-44.

Csordás, G., D. Weaver, and G. Hajnóczky. 2018. 'Endoplasmic Reticulum-Mitochondrial Contactology: Structure and Signaling Functions', *Trends Cell Biol*, 28: 523-40.

De Jonge, Hugo R, Ben C Tilly, Boris M Hogema, Daniel J Pfau, Catherine A Kelley, Megan H Kelley, August M Melita, Montana T Morris, Ryan M Viola, and John N Forrest Jr. 2014. 'cGMP inhibition of type 3 phosphodiesterase is the major mechanism by which C-type natriuretic peptide activates CFTR in the shark rectal gland', *American Journal of Physiology-Cell Physiology*, 306: C343-C53.

De Jonge, Hugo R., Ben C. Tilly, Boris M. Hogema, Daniel J. Pfau, Catherine A. Kelley, Megan H. Kelley, August M. Melita, Montana T. Morris, Ryan M. Viola, and John N. Forrest. 2014. 'cGMP inhibition of type 3 phosphodiesterase is the major mechanism by which C-type natriuretic peptide activates CFTR in the shark rectal gland', *American journal of physiology. Cell physiology*, 306: C343-53.

de Rooij, J., F. J. Zwartkruis, M. H. Verheijen, R. H. Cool, S. M. Nijman, A. Wittinghofer, and J. L. Bos. 1998. 'Epac is a Rap1 guanine-nucleotide-exchange factor directly activated by cyclic AMP', *Nature*, 396: 474-7.

Depry, Charlene, and Jin Zhang. 2011. 'Using FRET-based reporters to visualize subcellular dynamics of protein kinase A activity', *Signal Transduction Protocols*: 285-94.

Dessauer, C. W., V. J. Watts, R. S. Ostrom, M. Conti, S. Dove, and R. Seifert. 2017. 'International Union of Basic and Clinical Pharmacology. CI. Structures and Small Molecule Modulators of Mammalian Adenylyl Cyclases', *Pharmacol Rev*, 69: 93-139.

Di Benedetto, G., A. Zoccarato, V. Lissandron, A. Terrin, X. Li, M. D. Houslay, G. S. Baillie, and M. Zaccolo. 2008. 'Protein kinase A type I and type II define distinct intracellular signaling compartments', *Circ Res*, 103: 836-44.

Diskar, Mandy, Hans-Michael Zenn, Alexandra Kaupisch, Melanie Kaufholz, Stefanie Brockmeyer, Daniel Sohmen, Marco Berrera, Manuela Zaccolo, Michael Boshart, Friedrich W. Herberg, and Anke Prinz. 2010. 'Regulation of cAMP-dependent protein kinases: the human protein kinase X (PrKX) reveals the role of the catalytic subunit alphaH-alphaI loop', *The Journal of Biological Chemistry*, 285: 35910-18.

Doroquez, David B, Cristina Berciu, James R Anderson, Piali Sengupta, and Daniela Nicastro. 2014. 'A high-resolution morphological and ultrastructural map of anterior sensory cilia and glia in Caenorhabditis elegans', *elife*, 3: e01948.

Duldulao, Neil A., Sunjin Lee, and Zhaoxia Sun. 2009. 'Cilia localization is essential for in vivo functions of the Joubert syndrome protein Arl13b/Scorpion', *Development*, 136: 4033 - 42.

Düvel, K., J. L. Yecies, S. Menon, P. Raman, A. I. Lipovsky, A. L. Souza, E. Triantafellow, Q. Ma, R. Gorski, S. Cleaver, M. G. Vander Heiden, J. P. MacKeigan, P. M. Finan, C. B. Clish, L. O. Murphy, and B. D. Manning. 2010. 'Activation of a metabolic gene regulatory network downstream of mTOR complex 1', *Mol Cell*, 39: 171-83.

Elberg, Gerard, Dorit Elberg, Teresa V Lewis, Suresh Guruswamy, Lijuan Chen, Charlotte J Logan, Michael D Chan, and Martin A Turman. 2007. 'EP2 receptor mediates PGE2-induced cystogenesis of human renal epithelial cells', *American Journal of Physiology-Renal Physiology*, 293: F1622-F32.

Erneux, Christophe, Dominique Couchie, Jacques E Dumont, Janina Baraniak, Woljciech J Stec, Emilio Garcia Abbad, Georg PETRIDIS, and Bernd Jastorff. 1981. 'Specificity of cyclic GMP activation of a multi-substrate cyclic nucleotide phosphodiesterase from rat liver', *European Journal of Biochemistry*, 115: 503-10.

Fantus, D., N. M. Rogers, F. Grahammer, T. B. Huber, and A. W. Thomson. 2016. 'Roles of mTOR complexes in the kidney: implications for renal disease and transplantation', *Nat Rev Nephrol*, 12: 587-609.

Feraille, Eric, Eva Dizin, Isabelle Roth, Jean-Paul Derouette, Ildiko Szanto, Pierre-Yves Martin, Sophie de Seigneux, and Udo Hasler. 2014. 'NADPH oxidase 4 deficiency reduces aquaporin-2 mRNA expression in cultured renal collecting duct principal cells via increased PDE3 and PDE4 activity', *PloS one*, 9: e87239.

Fesenko, E. E., S. S. Kolesnikov, and A. L. Lyubarsky. 1985. 'Induction by cyclic GMP of cationic conductance in plasma membrane of retinal rod outer segment', *Nature*, 313: 310-3.

Flowers, E. M., J. Sudderth, L. Zacharias, G. Mernaugh, R. Zent, R. J. DeBerardinis, and T. J. Carroll. 2018. 'Lkb1 deficiency confers glutamine dependency in polycystic kidney disease', *Nat Commun*, 9: 814.

Focșa, I. O., M. Budișteanu, and M. Bălgrădean. 2021. 'Clinical and genetic heterogeneity of primary ciliopathies (Review)', *Int J Mol Med*, 48.

Foster, D. A., and A. Toschi. 2009. 'Targeting mTOR with rapamycin: one dose does not fit all', *Cell Cycle*, 8: 1026-9.

Friedman, Jonathan R, Laura L Lackner, Matthew West, Jared R DiBenedetto, Jodi Nunnari, and Gia K Voeltz. 2011. 'ER tubules mark sites of mitochondrial division', *Science*, 334: 358-62.

Gattone, Vincent H., Tibério M. Siqueira, Charles R. Powell, Chad M. Trambaugh, James E. Lingeman, and Arieh L. Shalhav. 2008. 'Contribution of Renal Innervation to Hypertension in

Rat Autosomal Dominant Polycystic Kidney Disease', *Experimental Biology and Medicine*, 233: 952-57.
Ghesquière, B., B. W. Wong, A. Kuchnio, and P. Carmeliet. 2014. 'Metabolism of stromal and immune cells in health and disease', *Nature*, 511: 167-76.
Giamogante, F., L. Barazzuol, M. Brini, and T. Calì. 2020. 'ER-Mitochondria Contact Sites Reporters: Strengths and Weaknesses of the Available Approaches', *Int J Mol Sci*, 21.
Grantham, Jared J, Vicente E Torres, Arlene B Chapman, Lisa M Guay-Woodford, Kyongtae T Bae, Bernard F King Jr, Louis H Wetzel, Deborah A Baumgarten, Phillip J Kenney, and Peter C Harris. 2006. 'Volume progression in polycystic kidney disease', *New England Journal of Medicine*, 354: 2122-30.
Grantham, JJ, M Ye, VH Gattone, and LP Sullivan. 1995. 'In vitro fluid secretion by epithelium from polycystic kidneys', *The Journal of clinical investigation*, 95: 195-202.
Grieben, Mariana, Ashley C. W. Pike, Chitra A. Shintre, Elisa Venturi, Sam El-Ajouz, Annamaria Tessitore, Leela Shrestha, Shubhashish Mukhopadhyay, Pravin Mahajan, Rod Chalk, Nicola A. Burgess-Brown, Rebecca Sitsapesan, Juha T. Huiskonen, and Elisabeth P. Carpenter. 2017. 'Structure of the polycystic kidney disease TRP channel Polycystin-2 (PC2)', *Nature Structural & Molecular Biology*, 24: 114-22.
Haj Slimane, Z., I. Bedioune, P. Lechêne, A. Varin, F. Lefebvre, P. Mateo, V. Domergue-Dupont, M. Dewenter, W. Richter, M. Conti, A. El-Armouche, J. Zhang, R. Fischmeister, and G. Vandecasteele. 2014. 'Control of cytoplasmic and nuclear protein kinase A by phosphodiesterases and phosphatases in cardiac myocytes', *Cardiovasc Res*, 102: 97-106.
Hajarnis, S., R. Lakhia, M. Yheskel, D. Williams, M. Sorourian, X. Liu, K. Aboudehen, S. Zhang, K. Kersjes, R. Galasso, J. Li, V. Kaimal, S. Lockton, S. Davis, A. Flaten, J. A. Johnson, W. L. Holland, C. M. Kusminski, P. E. Scherer, P. C. Harris, M. Trudel, D. P. Wallace, P. Igarashi, E. C. Lee, J. R. Androsavich, and V. Patel. 2017. 'microRNA-17 family promotes polycystic kidney disease progression through modulation of mitochondrial metabolism', *Nat Commun*, 8: 14395.
Halls, M. L., and D. M. F. Cooper. 2017. 'Adenylyl cyclase signalling complexes - Pharmacological challenges and opportunities', *Pharmacol Ther*, 172: 171-80.
Hambleton, Ryan, Judith Krall, Eliso Tikishvili, Matthew Honeggar, Faiyaz Ahmad, Vincent C Manganiello, and Matthew A Movsesian. 2005. 'Isoforms of cyclic nucleotide phosphodiesterase PDE3 and their contribution to cAMP hydrolytic activity in subcellular fractions of human myocardium', *Journal of Biological Chemistry*, 280: 39168-74.
Han, Seung Jin, Sergio Vaccari, Taku Nedachi, Carsten B Andersen, Kristina S Kovacina, Richard A Roth, and Marco Conti. 2006. 'Protein kinase B/Akt phosphorylation of PDE3A and its role in mammalian oocyte maturation', *The EMBO Journal*, 25: 5716-25.
Hanaoka, K., F. Qian, A. Boletta, A. K. Bhunia, K. Piontek, L. Tsiokas, V. P. Sukhatme, W. B. Guggino, and G. G. Germino. 2000. 'Co-assembly of polycystin-1 and -2 produces unique cation-permeable currents', *Nature*, 408: 990-4.
Hanaoka, Kazushige, and William B Guggino. 2000. 'cAMP regulates cell proliferation and cyst formation in autosomal polycystic kidney disease cells', *Journal of the American Society of Nephrology*, 11: 1179-87.
Hansen, J. N., F. Kaiser, P. Leyendecker, B. Stüven, J. H. Krause, F. Derakhshandeh, J. Irfan, T. J. Sroka, K. M. Preval, P. B. Desai, M. Kraut, H. Theis, A. D. Drews, E. De-Domenico, K. Händler, G. J. Pazour, D. J. P. Henderson, D. U. Mick, and D. Wachten. 2022. 'A cAMP signalosome in primary cilia drives gene expression and kidney cyst formation', *EMBO Rep*, 23: e54315.
Hansen, J. N., S. Rassmann, B. Stüven, N. Jurisch-Yaksi, and D. Wachten. 2021. 'CiliaQ: a simple, open-source software for automated quantification of ciliary morphology and fluorescence in 2D, 3D, and 4D images', *Eur Phys J E Soft Matter*, 44: 18.
Hansen, Jan N, Fabian Kaiser, Philipp Leyendecker, Birthe Stüven, Jens-Henning Krause, Fatemeh Derakhshandeh, Jaazba Irfan, Tommy J Sroka, Kenley M Preval, and Paurav B Desai. 2022. 'A cAMP signalosome in primary cilia drives gene expression and kidney cyst formation', *EMBO reports*, 23: e54315.
Harris, Peter C. 1999. 'Autosomal dominant polycystic kidney disease: clues to pathogenesis', *Human molecular genetics*, 8: 1861-66.

Hashimoto, Y, RK Sharma, and TR Soderling. 1989. 'Regulation of Ca2+/calmodulin-dependent cyclic nucleotide phosphodiesterase by the autophosphorylated form of Ca2+/calmodulin-dependent protein kinase II', *Journal of Biological Chemistry*, 264: 10884-87.

Hatzivassiliou, Georgia, Kyung Song, Ivana Yen, Barbara J Brandhuber, Daniel J Anderson, Ryan Alvarado, Mary JC Ludlam, David Stokoe, Susan L Gloor, and Guy Vigers. 2010. 'RAF inhibitors prime wild-type RAF to activate the MAPK pathway and enhance growth', *Nature*, 464: 431-35.

Hauser, A. S., M. M. Attwood, M. Rask-Andersen, H. B. Schiöth, and D. E. Gloriam. 2017. 'Trends in GPCR drug discovery: new agents, targets and indications', *Nat Rev Drug Discov*, 16: 829-42.

Haycraft, Courtney J, Boglarka Banizs, Yesim Aydin-Son, Qihong Zhang, Edward J Michaud, and Bradley K Yoder. 2005. 'Gli2 and Gli3 localize to cilia and require the intraflagellar transport protein polaris for processing and function', *PLoS genetics*, 1: e53.

Heggö, O. 1966. 'A microdissection study of cystic disease of the kidneys in adults', *The Journal of Pathology and Bacteriology*, 91: 311-15.

Heidorn, Sonja J, Carla Milagre, Steven Whittaker, Arnaud Nourry, Ion Niculescu-Duvas, Nathalie Dhomen, Jahan Hussain, Jorge S Reis-Filho, Caroline J Springer, and Catrin Pritchard. 2010. 'Kinase-dead BRAF and oncogenic RAS cooperate to drive tumor progression through CRAF', *Cell*, 140: 209-21.

Helal, Imed. 2013. 'Autosomal dominant polycystic kidney disease: new insights into treatment', *Saudi Journal of Kidney Diseases and Transplantation*, 24: 230-34.

Henske, E. P., S. Jóźwiak, J. C. Kingswood, J. R. Sampson, and E. A. Thiele. 2016. 'Tuberous sclerosis complex', *Nat Rev Dis Primers*, 2: 16035.

Hepler, J. R., and A. G. Gilman. 1992. 'G proteins', *Trends Biochem Sci*, 17: 383-7.

Hilger, Daniel, Matthieu Masureel, and Brian K. Kobilka. 2018. 'Structure and dynamics of GPCR signaling complexes', *Nature Structural & Molecular Biology*, 25: 4-12.

Ho, Emily K, and Tim Stearns. 2021. 'Hedgehog signaling and the primary cilium: implications for spatial and temporal constraints on signaling', *Development*, 148: dev195552.

Houslay, Miles D, Michael Sullivan, and Graeme B Bolger. 1998. 'The multienzyme PDE4 cyclic adenosine monophosphate–specific phosphodiesterase family: Intracellular targeting, regulation, and selective inhibition by compounds exerting anti-inflammatory and antidepressant actions', *Advances in pharmacology*, 44: 225-342.

Hsieh, A. C., Y. Liu, M. P. Edlind, N. T. Ingolia, M. R. Janes, A. Sher, E. Y. Shi, C. R. Stumpf, C. Christensen, M. J. Bonham, S. Wang, P. Ren, M. Martin, K. Jessen, M. E. Feldman, J. S. Weissman, K. M. Shokat, C. Rommel, and D. Ruggero. 2012. 'The translational landscape of mTOR signalling steers cancer initiation and metastasis', *Nature*, 485: 55-61.

Huangfu, Danwei, Aimin Liu, Andrew S Rakeman, Noel S Murcia, Lee Niswander, and Kathryn V Anderson. 2003. 'Hedgehog signalling in the mouse requires intraflagellar transport proteins', *Nature*, 426: 83-87.

Hunter, Roger W, Carol MacKintosh, and Ingeborg Hers. 2009. 'Protein kinase C-mediated phosphorylation and activation of PDE3A regulate cAMP levels in human platelets', *Journal of Biological Chemistry*, 284: 12339-48.

Igarashi, Peter, and Stefan Somlo. 2002. 'Genetics and pathogenesis of polycystic kidney disease', *Journal of the American Society of Nephrology*, 13: 2384-98.

Irannejad, Roshanak, Jin C. Tomshine, Jon R. Tomshine, Michael Chevalier, Jacob P. Mahoney, Jan Steyaert, Søren G. F. Rasmussen, Roger K. Sunahara, Hana El-Samad, Bo Huang, and Mark von Zastrow. 2013. 'Conformational biosensors reveal GPCR signalling from endosomes', *Nature*, 495: 534-38.

Ishikawa, Hiroaki, and Wallace F. Marshall. 2011. 'Ciliogenesis: building the cell's antenna', *Nature Reviews Molecular Cell Biology*, 12: 222-34.

Ishimoto, Yu, Reiko Inagi, Daisuke Yoshihara, Masanori Kugita, Shizuko Nagao, Akira Shimizu, Norihiko Takeda, Masaki Wake, Kenjiro Honda, Jing Zhou, and Masaomi Nangaku. 2017. 'Mitochondrial Abnormality Facilitates Cyst Formation in Autosomal Dominant Polycystic Kidney Disease', *Molecular and Cellular Biology*, 37: e00337-17.

Iwasawa, Ryota, Anne-Laure Mahul-Mellier, Christoph Datler, Evangelos Pazarentzos, and Stefan Grimm. 2011. 'Fis1 and Bap31 bridge the mitochondria–ER interface to establish a platform for apoptosis induction', *The EMBO Journal*, 30: 556-68-68.

Izreig, S., B. Samborska, R. M. Johnson, A. Sergushichev, E. H. Ma, C. Lussier, E. Loginicheva, A. O. Donayo, M. C. Poffenberger, S. M. Sagan, E. E. Vincent, M. N. Artyomov, T. F. Duchaine, and

R. G. Jones. 2016. 'The miR-17~92 microRNA Cluster Is a Global Regulator of Tumor Metabolism', *Cell Rep*, 16: 1915-28.
Jackson, Edwin K, and Dubey K Raghvendra. 2004. 'The extracellular cyclic AMP-adenosine pathway in renal physiology', *Annu. Rev. Physiol.*, 66: 571-99.
Jackson, Edwin K., and Delbert G. Gillespie. 2013. 'Extracellular 2′,3′-cAMP-adenosine pathway in proximal tubular, thick ascending limb, and collecting duct epithelial cells', *American Journal of Physiology-Renal Physiology*, 304: F49-F55.
Jackson, Edwin K., Zaichuan Mi, Chongxue Zhu, and Raghvendra K. Dubey. 2003. 'Adenosine Biosynthesis in the Collecting Duct', *Journal of Pharmacology and Experimental Therapeutics*, 307: 888-96.
Jacobson, Kenneth A, Ramachandran Balasubramanian, Francesca Deflorian, and Zhan-Guo Gao. 2012. 'G protein-coupled adenosine (P1) and P2Y receptors: ligand design and receptor interactions', *Purinergic signalling*, 8: 419-36.
Jiang, Jason Y, Jeffrey L Falcone, Silvana Curci, and Aldebaran M Hofer. 2019. 'Direct visualization of cAMP signaling in primary cilia reveals up-regulation of ciliary GPCR activity following Hedgehog activation', *Proceedings of the National Academy of Sciences*, 116: 12066-71.
Juhl, A. D., Z. Anvarian, S. Kuhns, J. Berges, J. S. Andersen, D. Wüstner, and L. B. Pedersen. 2023a. 'Transient accumulation and bidirectional movement of KIF13B in primary cilia', *J Cell Sci*, 136.
Juhl, Alice Dupont, Zeinab Anvarian, Stefanie Kuhns, Julia Berges, Jens S Andersen, Daniel Wüstner, and Lotte B Pedersen. 2023b. 'Transient accumulation and bidirectional movement of KIF13B in primary cilia', *Journal of cell science*, 136: jcs259257.
Juilfs, Dawn M., Hans-Jurgen Fulle, Allan Z. Zhao, Miles D. Houslay, David L. Garbers, and Joseph A. Beavo. 1997. 'A Subset of Olfactory Neurons that Selectively Express cGMP-Stimulated Phosphodiesterase (PDE2) and Guanylyl Cyclase-D Define a Unique Olfactory Signal Transduction Pathway', *Proceedings of the National Academy of Sciences of the United States of America*, 94: 3388-95.
Jurevicius, J, and R Fischmeister. 1996. 'cAMP compartmentation is responsible for a local activation of cardiac Ca2+ channels by beta-adrenergic agonists', *Proceedings of the National Academy of Sciences*, 93: 295-99.
Juul, Kristian Vinter, Daniel G. Bichet, Søren Nielsen, and Jens Peter Nørgaard. 2014. 'The physiological and pathophysiological functions of renal and extrarenal vasopressin V2 receptors', *American Journal of Physiology-Renal Physiology*, 306: F931-F40.
Kakade, V. R., S. Tao, M. Rajagopal, X. Zhou, X. Li, A. S. Yu, J. P. Calvet, P. Pandey, and R. Rao. 2016a. 'A cAMP and CREB-mediated feed-forward mechanism regulates GSK3β in polycystic kidney disease', *J Mol Cell Biol*, 8: 464-76.
Kakade, Vijayakumar R., Shixin Tao, Madhumitha Rajagopal, Xia Zhou, Xiaogang Li, Alan S.L. Yu, James P. Calvet, Pankaj Pandey, and Reena Rao. 2016b. 'A cAMP and CREB-mediated feed-forward mechanism regulates GSK3β in polycystic kidney disease', *Journal of Molecular Cell Biology*, 8: 464-76.
Kang, H. M., S. H. Ahn, P. Choi, Y. A. Ko, S. H. Han, F. Chinga, A. S. Park, J. Tao, K. Sharma, J. Pullman, E. P. Bottinger, I. J. Goldberg, and K. Susztak. 2015. 'Defective fatty acid oxidation in renal tubular epithelial cells has a key role in kidney fibrosis development', *Nat Med*, 21: 37-46.
Kathem, S. H., A. M. Mohieldin, and S. M. Nauli. 2014. 'The Roles of Primary cilia in Polycystic Kidney Disease', *AIMS Mol Sci*, 1: 27-46.
Katritch, Vsevolod, Vadim Cherezov, and Raymond C. Stevens. 2013. 'Structure-Function of the G Protein–Coupled Receptor Superfamily', *Annual Review of Pharmacology and Toxicology*, 53: 531-56.
Katsura, TOSHIYA, CORINNE E Gustafson, DENNIS A Ausiello, and DENNIS Brown. 1997. 'Protein kinase A phosphorylation is involved in regulated exocytosis of aquaporin-2 in transfected LLC-PK1 cells', *American Journal of Physiology-Renal Physiology*, 272: F816-F22.
Kiesel, Petra, Gonzalo Alvarez Viar, Nikolai Tsoy, Riccardo Maraspini, Peter Gorilak, Vladimir Varga, Alf Honigmann, and Gaia Pigino. 2020. 'The molecular structure of mammalian primary cilia revealed by cryo-electron tomography', *Nature Structural & Molecular Biology*, 27: 1115-24.
Kim, Choel, Cecilia Y. Cheng, S. Adrian Saldanha, and Susan S. Taylor. 2007. 'PKA-I holoenzyme structure reveals a mechanism for cAMP-dependent activation', *Cell*, 130: 1032-43.

Kim, Joon, Suguna Rani Krishnaswami, and Joseph G Gleeson. 2008. 'CEP290 interacts with the centriolar satellite component PCM-1 and is required for Rab8 localization to the primary cilium', *Human molecular genetics*, 17: 3796-805.
Kishore, Bellamkonda K, Simon C Robson, and Karen M Dwyer. 2018. 'CD39-adenosinergic axis in renal pathophysiology and therapeutics', *Purinergic signalling*, 14: 109-20.
Köchl, Robert, Martina Alken, Claudia Rutz, Gerd Krause, Alexander Oksche, Walter Rosenthal, and Ralf Schülein. 2002. 'The signal peptide of the G protein-coupled human endothelin B receptor is necessary for translocation of the N-terminal tail across the endoplasmic reticulum membrane', *Journal of Biological Chemistry*, 277: 16131-38.
Koptides, Michael, and C Constantinou Deltas. 2000. 'Autosomal dominant polycystic kidney disease: molecular genetics and molecular pathogenesis', *Human genetics*, 107: 115-26.
Kuo, I. Y., A. L. Brill, F. O. Lemos, J. Y. Jiang, J. L. Falcone, E. P. Kimmerling, Y. Cai, K. Dong, D. L. Kaplan, D. P. Wallace, A. M. Hofer, and B. E. Ehrlich. 2019. 'Polycystin 2 regulates mitochondrial Ca(2+) signaling, bioenergetics, and dynamics through mitofusin 2', *Sci Signal*, 12.
Kuo, Ivana Y, Camille Keeler, Rachel Corbin, Andjelka Ćelić, Edward T Petri, Michael E Hodsdon, and Barbara E Ehrlich. 2014. 'The number and location of EF hand motifs dictates the calcium dependence of polycystin-2 function', *The FASEB Journal*, 28: 2332.
Lakhia, Ronak, Matanel Yheskel, Andrea Flaten, Ezekiel B Quittner-Strom, William L Holland, and Vishal Patel. 2018. 'PPARα agonist fenofibrate enhances fatty acid β-oxidation and attenuates polycystic kidney and liver disease in mice', *American Journal of Physiology-Renal Physiology*, 314: F122-F31.
Lee, J. V., A. Carrer, S. Shah, N. W. Snyder, S. Wei, S. Venneti, A. J. Worth, Z. F. Yuan, H. W. Lim, S. Liu, E. Jackson, N. M. Aiello, N. B. Haas, T. R. Rebbeck, A. Judkins, K. J. Won, L. A. Chodosh, B. A. Garcia, B. Z. Stanger, M. D. Feldman, I. A. Blair, and K. E. Wellen. 2014. 'Akt-dependent metabolic reprogramming regulates tumor cell histone acetylation', *Cell Metab*, 20: 306-19.
Leroy, Marie-Josephe, Eva Degerman, Masato Taira, Taku Murata, Lu Hua Wang, Matthew A Movsesian, Elisabetta Meacci, and Vincent C Manganiello. 1996. 'Characterization of two recombinant PDE3 (cGMP-inhibited cyclic nucleotide phosphodiesterase) isoforms, RcGIP1 and HcGIP2, expressed in NIH 3006 murine fibroblasts and Sf9 insect cells', *Biochemistry*, 35: 10194-202.
Leuenroth, Stephanie J, Natasha Bencivenga, Peter Igarashi, Stefan Somlo, and Craig M Crews. 2008. 'Triptolide reduces cystogenesis in a model of ADPKD', *Journal of the American Society of Nephrology*, 19: 1659-62.
Leuenroth, Stephanie J, Dayne Okuhara, Joseph D Shotwell, Glen S Markowitz, Zhiheng Yu, Stefan Somlo, and Craig M Crews. 2007. 'Triptolide is a traditional Chinese medicine-derived inhibitor of polycystic kidney disease', *Proceedings of the National Academy of Sciences*, 104: 4389-94.
Levitzki, A. 1988. 'From epinephrine to cyclic AMP', *Science*, 241: 800-6.
Li, J., F. Qi, H. Su, C. Zhang, Q. Zhang, Y. Chen, P. Chen, L. Su, Y. Chen, Y. Yang, Z. Chen, and S. Zhang. 2022. 'GRP75-faciliated Mitochondria-associated ER Membrane (MAM) Integrity controls Cisplatin-resistance in Ovarian Cancer Patients', *Int J Biol Sci*, 18: 2914-31.
Li, Mingtao, Xiaomin Wang, Mary Kay Meintzer, Tracey Laessig, Morris J Birnbaum, and Kim A Heidenreich. 2000. 'Cyclic AMP promotes neuronal survival by phosphorylation of glycogen synthase kinase 3β', *Molecular and Cellular Biology*.
Li, You, Nikolai T. Klena, George C. Gabriel, Xiaoqin Liu, Andrew J. Kim, Kristi Lemke, Yu Chen, Bishwanath Chatterjee, William Devine, Rama Rao Damerla, Chienfu Chang, Hisato Yagi, Jovenal T. San Agustin, Mohamed Thahir, Shane Anderton, Caroline Lawhead, Anita Vescovi, Herbert Pratt, Judy Morgan, Leslie Haynes, Cynthia L. Smith, Janan T. Eppig, Laura Reinholdt, Richard Francis, Linda Leatherbury, Madhavi K. Ganapathiraju, Kimimasa Tobita, Gregory J. Pazour, and Cecilia W. Lo. 2015. 'Global genetic analysis in mice unveils central role for cilia in congenital heart disease', *Nature*, 521: 520-24.
Lin, C. C., M. Kurashige, Y. Liu, T. Terabayashi, Y. Ishimoto, T. Wang, V. Choudhary, R. Hobbs, L. K. Liu, P. H. Lee, P. Outeda, F. Zhou, N. P. Restifo, T. Watnick, H. Kawano, S. Horie, W. Prinz, H. Xu, L. F. Menezes, and G. G. Germino. 2018. 'A cleavage product of Polycystin-1 is a mitochondrial matrix protein that affects mitochondria morphology and function when heterologously expressed', *Sci Rep*, 8: 2743.

Liu, Xiaowen, Thuy Vien, Jingjing Duan, Shu-Hsien Sheu, Paul G DeCaen, and David E Clapham. 2018. 'Polycystin-2 is an essential ion channel subunit in the primary cilium of the renal collecting duct epithelium', *elife*, 7: e33183.

Liu, Yu, Madhumitha Rajagopal, Kim Lee, Lorenzo Battini, Daniel Flores, G Luca Gusella, Alan C Pao, and Rajeev Rohatgi. 2012. 'Prostaglandin E2 mediates proliferation and chloride secretion in ADPKD cystic renal epithelia', *American Journal of Physiology-Renal Physiology*, 303: F1425-F34.

Liu, Z., Y. Liu, L. Dang, M. Geng, Y. Sun, Y. Lu, Z. Fang, H. Xiong, and Y. Chen. 2021. 'Integrative Cistromic and Transcriptomic Analyses Identify CREB Target Genes in Cystic Renal Epithelial Cells', *J Am Soc Nephrol*, 32: 2529-41.

Lobo, M. J., L. Reverte-Salisa, Y. C. Chao, A. Koschinski, F. Gesellchen, G. Subramaniam, H. Jiang, S. Pace, N. Larcom, E. Paolocci, A. Pfeifer, S. Zanivan, and M. Zaccolo. 2020a. 'Phosphodiesterase 2A2 regulates mitochondria clearance through Parkin-dependent mitophagy', *Commun Biol*, 3: 596.

Lobo, Miguel Goncalo de Oliveira Ferrao. 2018. 'Role of PDE2A in cAMP/PKA Signalling ', The University of Oxford

Lobo, Miguel J., Laia Reverte-Salisa, Ying-Chi Chao, Andreas Koschinski, Frank Gesellchen, Gunasekaran Subramaniam, He Jiang, Samuel Pace, Natasha Larcom, Ester Paolocci, Alexander Pfeifer, Sara Zanivan, and Manuela Zaccolo. 2020b. 'Phosphodiesterase 2A2 regulates mitochondria clearance through Parkin-dependent mitophagy', *Communications Biology*, 3: 596.

Lohse, C., A. Bock, I. Maiellaro, A. Hannawacker, L. R. Schad, M. J. Lohse, and W. R. Bauer. 2017. 'Experimental and mathematical analysis of cAMP nanodomains', *PloS one*, 12: e0174856.

Lohse, Martin J., Andreas Bock, and Manuela Zaccolo. 2024. 'G Protein–Coupled Receptor Signaling: New Insights Define Cellular Nanodomains', *Annual Review of Pharmacology and Toxicology*, 64: 387-415.

Loktev, Alexander V, and Peter K Jackson. 2013. 'Neuropeptide Y family receptors traffic via the Bardet-Biedl syndrome pathway to signal in neuronal primary cilia', *Cell reports*, 5: 1316-29.

Louet, J. F., G. Hayhurst, F. J. Gonzalez, J. Girard, and J. F. Decaux. 2002. 'The coactivator PGC-1 is involved in the regulation of the liver carnitine palmitoyltransferase I gene expression by cAMP in combination with HNF4 alpha and cAMP-response element-binding protein (CREB)', *J Biol Chem*, 277: 37991-8000.

Loukil, A., K. Tormanen, and C. Sütterlin. 2017. 'The daughter centriole controls ciliogenesis by regulating Neurl-4 localization at the centrosome', *J Cell Biol*, 216: 1287-300.

Lovinger, David M., Yolanda Mateo, Kari A. Johnson, Sheila A. Engi, Mario Antonazzo, and Joseph F. Cheer. 2022. 'Local modulation by presynaptic receptors controls neuronal communication and behaviour', *Nature Reviews Neuroscience*, 23: 191-203.

Low, Seng Hui, Shivakumar Vasanth, Claire H Larson, Sambuddho Mukherjee, Nikunj Sharma, Michael T Kinter, Michelle E Kane, Tomoko Obara, and Thomas Weimbs. 2006. 'Polycystin-1, STAT6, and P100 function in a pathway that transduces ciliary mechanosensation and is activated in polycystic kidney disease', *Developmental cell*, 10: 57-69.

Lugnier, C. 2006a. 'Cyclic nucleotide phosphodiesterase (PDE) superfamily: a new target for the development of specific therapeutic agents', *Pharmacol Ther*, 109: 366-98.

Lugnier, Claire. 2006b. 'Cyclic nucleotide phosphodiesterase (PDE) superfamily: A new target for the development of specific therapeutic agents', *Pharmacology & Therapeutics*, 109: 366-98.

Ma, Ming, Xin Tian, Peter Igarashi, Gregory J Pazour, and Stefan Somlo. 2013. 'Loss of cilia suppresses cyst growth in genetic models of autosomal dominant polycystic kidney disease', *Nature genetics*, 45: 1004-12.

Mangoo-Karim, ROBERTO, M Ye, DARREN P Wallace, JARED J Grantham, and LAWRENCE P Sullivan. 1995. 'Anion secretion drives fluid secretion by monolayers of cultured human polycystic cells', *American Journal of Physiology-Renal Physiology*, 269: F381-F88.

Martins, Timothy J, MC Mumby, and JA Beavo. 1982. 'Purification and characterization of a cyclic GMP-stimulated cyclic nucleotide phosphodiesterase from bovine tissues', *Journal of Biological Chemistry*, 257: 1973-79.

Masyuk, Anatoliy I, Sergio A Gradilone, Jesus M Banales, Bing Q Huang, Tatyana V Masyuk, Seung-Ok Lee, Patrick L Splinter, Angela J Stroope, and Nicholas F LaRusso. 2008. 'Cholangiocyte primary cilia are chemosensory organelles that detect biliary nucleotides via P2Y12 purinergic

receptors', *American Journal of Physiology-Gastrointestinal and Liver Physiology*, 295: G725-G34.
Matousovic, K., Y. Tsuboi, H. Walker, J. P. Grande, and T. P. Dousa. 1997a. 'Inhibitors of cyclic nucleotide phosphodiesterase isozymes block renal tubular cell proliferation induced by folic acid', *J Lab Clin Med*, 130: 487-95.
Matousovic, Karel, Yasushi Tsuboi, Henry Walker, Joseph P. Grande, and Thomas P. Dousa. 1997b. 'Inhibitors of cyclic nucleotide phosphodiesterase isozymes block renal tubular cell proliferation induced by folic acid', *Journal of Laboratory and Clinical Medicine*, 130: 487-95.
Meacci, Elisabetta, Masato Taira, Malcolm Moos Jr, Carolyn J Smith, Matthew A Movsesian, Eva Degerman, per Belfrage, and Vincent Manganiello. 1992. 'Molecular cloning and expression of human myocardial cGMP-inhibited cAMP phosphodiesterase', *Proceedings of the National Academy of Sciences*, 89: 3721-25.
Menezes, L. F., and G. G. Germino. 2013. 'Murine Models of Polycystic Kidney Disease', *Drug Discov Today Dis Mech*, 10: e153-e58.
Menezes, L. F., F. Zhou, A. D. Patterson, K. B. Piontek, K. W. Krausz, F. J. Gonzalez, and G. G. Germino. 2012. 'Network analysis of a Pkd1-mouse model of autosomal dominant polycystic kidney disease identifies HNF4α as a disease modifier', *PLoS Genet*, 8: e1003053.
Menezes, Luis Fernando, and Gregory G. Germino. 2019. 'The pathobiology of polycystic kidney disease from a metabolic viewpoint', *Nature Reviews Nephrology*, 15: 735-49.
Mi, Z., Y. Song, J. Wang, Z. Liu, X. Cao, L. Dang, Y. Lu, Y. Sun, H. Xiong, L. Zhang, and Y. Chen. 2022. 'cAMP-Induced Nuclear Condensation of CRTC2 Promotes Transcription Elongation and Cystogenesis in Autosomal Dominant Polycystic Kidney Disease', *Adv Sci (Weinh)*, 9: e2104578.
Miki, Takashi, Masato Taira, Steven Hockman, Fumio Shimada, Jonathan Lieman, Maria Napolitano, David Ward, Masanori Taira, Hideichi Makino, and Vincent C Manganiello. 1996. 'Characterization of the cDNA and gene encoding human PDE3B, the cGIP1 isoform of the human cyclic GMP-inhibited cyclic nucleotide phosphodiesterase family', *Genomics*, 36: 476-85.
Mongillo, M., T. McSorley, S. Evellin, A. Sood, V. Lissandron, A. Terrin, E. Huston, A. Hannawacker, M. J. Lohse, T. Pozzan, M. D. Houslay, and M. Zaccolo. 2004. 'Fluorescence resonance energy transfer-based analysis of cAMP dynamics in live neonatal rat cardiac myocytes reveals distinct functions of compartmentalized phosphodiesterases', *Circ Res*, 95: 67-75.
Mons, N., L. Decorte, R. Jaffard, and D. M. Cooper. 1998. 'Ca2+-sensitive adenylyl cyclases, key integrators of cellular signalling', *Life Sci*, 62: 1647-52.
Monterisi, S., M. J. Lobo, C. Livie, J. C. Castle, M. Weinberger, G. Baillie, N. C. Surdo, N. Musheshe, A. Stangherlin, E. Gottlieb, R. Maizels, M. Bortolozzi, M. Micaroni, and M. Zaccolo. 2017. 'PDE2A2 regulates mitochondria morphology and apoptotic cell death via local modulation of cAMP/PKA signalling', *elife*, 6.
Monterisi, Stefania, Maria Favia, Lorenzo Guerra, Rosa A Cardone, Domenico Marzulli, Stephan J Reshkin, Valeria Casavola, and Manuela Zaccolo. 2012. 'CFTR regulation in human airway epithelial cells requires integrity of the actin cytoskeleton and compartmentalized cAMP and PKA activity', *Journal of cell science*, 125: 1106-17.
Moore, Bryn S, Ann N Stepanchick, Paul H Tewson, Cassandra M Hartle, Jin Zhang, Anne Marie Quinn, Thomas E Hughes, and Tooraj Mirshahi. 2016. 'Cilia have high cAMP levels that are inhibited by Sonic Hedgehog-regulated calcium dynamics', *Proceedings of the National Academy of Sciences*, 113: 13069-74.
Morita, M., S. P. Gravel, V. Chénard, K. Sikström, L. Zheng, T. Alain, V. Gandin, D. Avizonis, M. Arguello, C. Zakaria, S. McLaughlan, Y. Nouet, A. Pause, M. Pollak, E. Gottlieb, O. Larsson, J. St-Pierre, I. Topisirovic, and N. Sonenberg. 2013. 'mTORC1 controls mitochondrial activity and biogenesis through 4E-BP-dependent translational regulation', *Cell Metab*, 18: 698-711.
Movsesian, M., F. Ahmad, and E. Hirsch. 2018. 'Functions of PDE3 Isoforms in Cardiac Muscle', *J Cardiovasc Dev Dis*, 5.
Mukhopadhyay, Saikat, Xiaohui Wen, Navneet Ratti, Alexander Loktev, Linda Rangell, Suzie J Scales, and Peter K Jackson. 2013. 'The ciliary G-protein-coupled receptor Gpr161 negatively regulates the Sonic hedgehog pathway via cAMP signaling', *Cell*, 152: 210-23.
Muto, Yoshiharu, Eryn E. Dixon, Yasuhiro Yoshimura, Haojia Wu, Kohei Omachi, Nicolas Ledru, Parker C. Wilson, Andrew J. King, N. Eric Olson, Marvin G. Gunawan, Jay J. Kuo, Jennifer

H. Cox, Jeffrey H. Miner, Stephen L. Seliger, Owen M. Woodward, Paul A. Welling, Terry J. Watnick, and Benjamin D. Humphreys. 2022. 'Defining cellular complexity in human autosomal dominant polycystic kidney disease by multimodal single cell analysis', *Nature Communications*, 13: 6497.

Nagano, N. 2006. 'Pharmacological and clinical properties of calcimimetics: Calcium receptor activators that afford an innovative approach to controlling hyperparathyroidism', *Pharmacology and Therapeutics*, 109: 339-65.

Nagao, S, K Nishii, D Yoshihara, H Kurahashi, K Nagaoka, T Yamashita, H Takahashi, T Yamaguchi, JP Calvet, and DP Wallace. 2008. 'Calcium channel inhibition accelerates polycystic kidney disease progression in the Cy/+ rat', *Kidney international*, 73: 269-77.

Nagao, S., M. Morita, M. Kugita, D. Yoshihara, T. Yamaguchi, H. Kurahashi, J. P. Calvet, and D. P. Wallace. 2010. 'Polycystic kidney disease in Han:SPRD Cy rats is associated with elevated expression and mislocalization of SamCystin', *Am J Physiol Renal Physiol*, 299: F1078-86.

Nagao, Shizuko, Kazuhiro Nishii, Makoto Katsuyama, Hiroki Kurahashi, Tohru Marunouchi, Hisahide Takahashi, and Darren P Wallace. 2006. 'Increased water intake decreases progression of polycystic kidney disease in the PCK rat', *Journal of the American Society of Nephrology*, 17: 2220-27.

Naon, Deborah, Marta Zaninello, Marta Giacomello, Tatiana Varanita, Francesca Grespi, Sowmya Lakshminaranayan, Annalisa Serafini, Martina Semenzato, Stephanie Herkenne, Maria Isabel Hernández-Alvarez, Antonio Zorzano, Diego De Stefani, Gerald W. Dorn, and Luca Scorrano. 2016. 'Critical reappraisal confirms that Mitofusin 2 is an endoplasmic reticulum–mitochondria tether', *Proceedings of the National Academy of Sciences*, 113: 11249-54.

Nguyen, Anh-Nguyet T, Darren P Wallace, and Gustavo Blanco. 2007. 'Ouabain binds with high affinity to the na, K-ATPase in human polycystic kidney cells and induces extracellular Signal–Regulated kinase activation and cell proliferation', *Journal of the American Society of Nephrology*, 18: 46-57.

Oki, N., S. I. Takahashi, H. Hidaka, and M. Conti. 2000. 'Short term feedback regulation of cAMP in FRTL-5 thyroid cells. Role of PDE4D3 phosphodiesterase activation', *J Biol Chem*, 275: 10831-7.

Omar, F., J. E. Findlay, G. Carfray, R. W. Allcock, Z. Jiang, C. Moore, A. L. Muir, M. Lannoy, B. A. Fertig, D. Mai, J. P. Day, G. Bolger, G. S. Baillie, E. Schwiebert, E. Klussmann, N. J. Pyne, A. C. M. Ong, K. Bowers, J. M. Adam, D. R. Adams, M. D. Houslay, and D. J. P. Henderson. 2019. 'Small-molecule allosteric activators of PDE4 long form cyclic AMP phosphodiesterases', *Proc Natl Acad Sci U S A*, 116: 13320-29.

Ortiz-Sandoval, Carolina G, Sarah C Hughes, Joel B Dacks, and Thomas Simmen. 2014. 'Interaction with the effector dynamin-related protein 1 (Drp1) is an ancient function of Rab32 subfamily proteins', *Cellular logistics*, 4: e986399.

Oyarzún, Carlos, Wallys Garrido, Sebastián Alarcón, Alejandro Yáñez, Luis Sobrevia, Claudia Quezada, and Rody San Martín. 2017. 'Adenosine contribution to normal renal physiology and chronic kidney disease', *Molecular Aspects of Medicine*, 55: 75-89.

Padovano, V., I. Y. Kuo, L. K. Stavola, H. R. Aerni, B. J. Flaherty, H. C. Chapin, M. Ma, S. Somlo, A. Boletta, B. E. Ehrlich, J. Rinehart, and M. J. Caplan. 2017. 'The polycystins are modulated by cellular oxygen-sensing pathways and regulate mitochondrial function', *Mol Biol Cell*, 28: 261-69.

Pal, Kasturi, Sun-hee Hwang, Bandarigoda Somatilaka, Hemant Badgandi, Peter K Jackson, Kathryn DeFea, and Saikat Mukhopadhyay. 2016. 'Smoothened determines β-arrestin–mediated removal of the G protein–coupled receptor Gpr161 from the primary cilium', *Journal of Cell Biology*, 212: 861-75.

Pal, Kuntal, Karsten Melcher, and H. Eric Xu. 2012. 'Structure and mechanism for recognition of peptide hormones by Class B G-protein-coupled receptors', *Acta Pharmacologica Sinica*, 33: 300-11.

Pampliega, Olatz, Idil Orhon, Bindi Patel, Sunandini Sridhar, Antonio Díaz-Carretero, Isabelle Beau, Patrice Codogno, Birgit H. Satir, Peter Satir, and Ana Maria Cuervo. 2013. 'Functional interaction between autophagy and ciliogenesis', *Nature*, 502: 194-200.

Paolocci, E., and M. Zaccolo. 2023. 'Compartmentalised cAMP signalling in the primary cilium', *Front Physiol*, 14: 1187134.

Pei, York. 2001. 'A ‘two-hit’ model of cystogenesis in autosomal dominant polycystic kidney disease?', *Trends in Molecular Medicine*, 7: 151-56.

Pema, M., L. Drusian, M. Chiaravalli, M. Castelli, Q. Yao, S. Ricciardi, S. Somlo, F. Qian, S. Biffo, and A. Boletta. 2016. 'mTORC1-mediated inhibition of polycystin-1 expression drives renal cyst formation in tuberous sclerosis complex', *Nat Commun*, 7: 10786.

Penmatsa, Himabindu, Weiqiang Zhang, Sunitha Yarlagadda, Chunying Li, Veronica G Conoley, Junming Yue, Suleiman W Bahouth, Randal K Buddington, Guangping Zhang, and Deborah J Nelson. 2010. 'Compartmentalized cyclic adenosine 3′, 5′-monophosphate at the plasma membrane clusters PDE3A and cystic fibrosis transmembrane conductance regulator into microdomains', *Molecular biology of the cell*, 21: 1097-110.

Pennanen, Christian, Valentina Parra, Camila Lopez-Crisosto, Pablo E Morales, Andrea Del Campo, Tomás Gutierrez, Pablo Rivera-Mejías, Jovan Kuzmicic, Mario Chiong, and Antonio Zorzano. 2014. 'Mitochondrial fission is required for cardiomyocyte hypertrophy mediated by a Ca2+-calcineurin signaling pathway', *Journal of cell science*, 127: 2659-71.

Peterson, Yuri K., and Louis M. Luttrell. 2017. 'The Diverse Roles of Arrestin Scaffolds in G Protein–Coupled Receptor Signaling', *Pharmacological Reviews*, 69: 256-97.

Pinto, C. S., A. Raman, G. A. Reif, B. S. Magenheimer, C. White, J. P. Calvet, and D. P. Wallace. 2016. 'Phosphodiesterase Isoform Regulation of Cell Proliferation and Fluid Secretion in Autosomal Dominant Polycystic Kidney Disease', *J Am Soc Nephrol*, 27: 1124-34.

Pinto, C. S., G. A. Reif, E. Nivens, C. White, and D. P. Wallace. 2012. 'Calmodulin-sensitive adenylyl cyclases mediate AVP-dependent cAMP production and Cl- secretion by human autosomal dominant polycystic kidney cells', *Am J Physiol Renal Physiol*, 303: F1412-24.

Podrini, C., I. Rowe, R. Pagliarini, A. S. H. Costa, M. Chiaravalli, I. Di Meo, H. Kim, G. Distefano, V. Tiranti, F. Qian, D. di Bernardo, C. Frezza, and A. Boletta. 2018. 'Dissection of metabolic reprogramming in polycystic kidney disease reveals coordinated rewiring of bioenergetic pathways', *Commun Biol*, 1: 194.

Porath, Binu, Vladimir G Gainullin, Emilie Cornec-Le Gall, Elizabeth K Dillinger, Christina M Heyer, Katharina Hopp, Marie E Edwards, Charles D Madsen, Sarah R Mauritz, and Carly J Banks. 2016. 'Mutations in GANAB, encoding the glucosidase IIα subunit, cause autosomal-dominant polycystic kidney and liver disease', *The American Journal of Human Genetics*, 98: 1193-207.

Porpora, Monia, Simona Sauchella, Laura Rinaldi, Rossella Delle Donne, Maria Sepe, Omar Torres-Quesada, Daniela Intartaglia, Corrado Garbi, Luigi Insabato, and Margherita Santoriello. 2018. 'Counterregulation of cAMP-directed kinase activities controls ciliogenesis', *Nature Communications*, 9: 1224.

Pozuelo Rubio, Mercedes, David G Campbell, Nicholas A Morrice, and Carol Mackintosh. 2005. 'Phosphodiesterase 3A binds to 14-3-3 proteins in response to PMA-induced phosphorylation of Ser428', *Biochemical Journal*, 392: 163-72.

Prince, M. R., E. Weiss, and J. D. Blumenfeld. 2023. 'Size Matters: How to Characterize ADPKD Severity by Measuring Total Kidney Volume', *J Clin Med*, 12.

Puri, P., C. M. Schaefer, D. Bushnell, M. E. Taglienti, J. A. Kreidberg, B. K. Yoder, and C. M. Bates. 2018. 'Ectopic Phosphorylated Creb Marks Dedifferentiated Proximal Tubules in Cystic Kidney Disease', *Am J Pathol*, 188: 84-94.

Putnam, W. C., S. M. Swenson, G. A. Reif, D. P. Wallace, G. M. Helmkamp, Jr., and J. J. Grantham. 2007. 'Identification of a forskolin-like molecule in human renal cysts', *J Am Soc Nephrol*, 18: 934-43.

Qian, Feng, Alessandra Boletta, Anil K Bhunia, Hangxue Xu, Lijuan Liu, Ali K Ahrabi, Terry J Watnick, Fang Zhou, and Gregory G Germino. 2002. 'Cleavage of polycystin-1 requires the receptor for egg jelly domain and is disrupted by human autosomal-dominant polycystic kidney disease 1-associated mutations', *Proceedings of the National Academy of Sciences*, 99: 16981-86.

Qian, Feng, F. Joseph Germino, Yiqiang Cai, Xiangbin Zhang, Stefan Somlo, and Gregory G. Germino. 1997. 'PKD1 interacts with PKD2 through a probable coiled-coil domain', *Nature genetics*, 16: 179-83.

Rahn, Tova, Lars Rönnstrand, Marie-Josephe Leroy, Christer Wernstedt, Hans Tornqvist, Vincent C Manganiello, Per Belfrage, and Eva Degerman. 1996. 'Identification of the Site in the cGMP-inhibited Phosphodiesterase Phosphorylated in Adipocytes in Response to Insulin and Isoproterenol (∗)', *Journal of Biological Chemistry*, 271: 11575-80.

Ramalingam, Harini, Sonu Kashyap, Patricia Cobo-Stark, Andrea Flaten, Chun-Mien Chang, Sachin Hajarnis, Kyaw Zaw Hein, Jorgo Lika, Gina M Warner, and Jair M Espindola-Netto. 2021. 'A

methionine-Mettl3-N6-methyladenosine axis promotes polycystic kidney disease', *Cell metabolism*, 33: 1234-47. e7.
Rao, Reena, Satish Patel, ChuanMing Hao, James Woodgett, and Raymond Harris. 2010. 'GSK3β Mediates Renal Response to Vasopressin by Modulating Adenylate Cyclase Activity', *Journal of the American Society of Nephrology*, 21: 428-37.
Raychowdhury, Malay K, Arnolt J Ramos, Peng Zhang, Margaret McLaughin, Xiao-Qing Dai, Xing-Zhen Chen, Nicolás Montalbetti, María del Rocío Cantero, Dennis A Ausiello, and Horacio F Cantiello. 2009. 'Vasopressin receptor-mediated functional signaling pathway in primary cilia of renal epithelial cells', *American Journal of Physiology-Renal Physiology*, 296: F87-F97.
Reeders, Stephen T. 1992. 'Multilocus polycystic disease', *Nature genetics*, 1: 235-37.
Rees, S., W. Kittikulsuth, K. Roos, K. A. Strait, A. Van Hoek, and D. E. Kohan. 2014. 'Adenylyl cyclase 6 deficiency ameliorates polycystic kidney disease', *J Am Soc Nephrol*, 25: 232-7.
Reif, Gail A., Tamio Yamaguchi, Emily Nivens, Hiroyuki Fujiki, Cibele S. Pinto, and Darren P. Wallace. 2011. 'Tolvaptan inhibits ERK-dependent cell proliferation, Cl− secretion, and in vitro cyst growth of human ADPKD cells stimulated by vasopressin', *American Journal of Physiology-Renal Physiology*, 301: F1005-F13.
Reiter, Jeremy F, Oliver E Blacque, and Michel R Leroux. 2012. 'The base of the cilium: roles for transition fibres and the transition zone in ciliary formation, maintenance and compartmentalization', *EMBO reports*, 13: 608-18.
Rezi, Csenge, Alina Frei, Fabiola Campestre, Christina Berggreen, Julie Laplace, Aurelien Sicot, Geyi Li, Søren Johansen, Julie Sørensen, Martin Berchtold, Mohamed Chamlali, Søren Christensen, Karsten Boldt, Zeinab Anvarian, Helen May-Simera, and Lotte Pedersen. 2024. 'Loss of KIF13B causes time-dependent changes in ciliary polycystin-2 levels and extracellular vesicle release', *bioRxiv*.
Riccardi, Daniela, Amy E. Hall, Naibedya Chattopadhyay, Jason Z. Xu, Edward M. Brown, and Steven C. Hebert. 1998. 'Localization of the extracellular Ca2+/polyvalent cation-sensing protein in rat kidney', *American Journal of Physiology-Renal Physiology*, 274: F611-F22.
Rieusset, Jennifer. 2018. 'The role of endoplasmic reticulum-mitochondria contact sites in the control of glucose homeostasis: an update', *Cell Death & Disease*, 9: 388.
Rodbell, M., L. Birnbaumer, S. L. Pohl, and H. M. Krans. 1971. 'The glucagon-sensitive adenyl cyclase system in plasma membranes of rat liver. V. An obligatory role of guanylnucleotides in glucagon action', *J Biol Chem*, 246: 1877-82.
Roos, K. P., K. A. Strait, K. L. Raphael, M. A. Blount, and D. E. Kohan. 2012. 'Collecting duct-specific knockout of adenylyl cyclase type VI causes a urinary concentration defect in mice', *Am J Physiol Renal Physiol*, 302: F78-84.
Ross, E. M., and T. M. Wilkie. 2000. 'GTPase-activating proteins for heterotrimeric G proteins: regulators of G protein signaling (RGS) and RGS-like proteins', *Annu Rev Biochem*, 69: 795-827.
Rowe, I., M. Chiaravalli, V. Mannella, V. Ulisse, G. Quilici, M. Pema, X. W. Song, H. Xu, S. Mari, F. Qian, Y. Pei, G. Musco, and A. Boletta. 2013. 'Defective glucose metabolism in polycystic kidney disease identifies a new therapeutic strategy', *Nat Med*, 19: 488-93.
Rowe, Isaline, Marco Chiaravalli, Valeria Mannella, Valeria Ulisse, Giacomo Quilici, Monika Pema, Xuewen W Song, Hangxue Xu, Silvia Mari, and Feng Qian. 2013. 'Defective glucose metabolism in polycystic kidney disease identifies a new therapeutic strategy', *Nature medicine*, 19: 488-93.
Rushworth, Linda K, Alison D Hindley, Eric O'Neill, and Walter Kolch. 2006. 'Regulation and role of Raf-1/B-Raf heterodimerization', *Molecular and Cellular Biology*.
Sala-Vila, Aleix, Inmaculada Navarro-Lérida, Miguel Sánchez-Alvarez, Marta Bosch, Carlos Calvo, Juan Antonio López, Enrique Calvo, Charles Ferguson, Marta Giacomello, Annalisa Serafini, Luca Scorrano, José Antonio Enriquez, Jesús Balsinde, Robert G. Parton, Jesús Vázquez, Albert Pol, and Miguel A. Del Pozo. 2016. 'Interplay between hepatic mitochondria-associated membranes, lipid metabolism and caveolin-1 in mice', *Scientific reports*, 6: 27351.
Sánchez, I., and B. D. Dynlacht. 2016. 'Cilium assembly and disassembly', *Nat Cell Biol*, 18: 711-7.
Sankaran, Deepa, Neda Bankovic-Calic, Malcolm R Ogborn, Gary Crow, and Harold M Aukema. 2007. 'Selective COX-2 inhibition markedly slows disease progression and attenuates altered prostanoid production in Han: SPRD-cy rats with inherited kidney disease', *American Journal of Physiology-Renal Physiology*, 293: F821-F30.

Scheidel, Noémie, Julie Kennedy, and Oliver E Blacque. 2018. 'Endosome maturation factors Rabenosyn-5/VPS45 and caveolin-1 regulate ciliary membrane and polycystin-2 homeostasis', *The EMBO Journal*, 37: e98248.

Schou, K. B., J. B. Mogensen, A. Aleliunaite, S. Morthorst, I. Veland, S. Christensen, and L. B. Pedersen. 2015. 'Kinesin-3 motor protein KIF13B localizes to centrosomes and primary cilia and regulates ciliary length and signaling', *Cilia*, 4: O3.

Schou, K. B., J. B. Mogensen, S. K. Morthorst, B. S. Nielsen, A. Aleliunaite, A. Serra-Marques, N. Fürstenberg, S. Saunier, A. A. Bizet, I. R. Veland, A. Akhmanova, S. T. Christensen, and L. B. Pedersen. 2017a. 'KIF13B establishes a CAV1-enriched microdomain at the ciliary transition zone to promote Sonic hedgehog signalling', *Nat Commun*, 8: 14177.

Schou, Kenneth B., Johanne B. Mogensen, Stine K. Morthorst, Brian S. Nielsen, Aiste Aleliunaite, Andrea Serra-Marques, Nicoline Fürstenberg, Sophie Saunier, Albane A. Bizet, Iben R. Veland, Anna Akhmanova, Søren T. Christensen, and Lotte B. Pedersen. 2017b. 'KIF13B establishes a CAV1-enriched microdomain at the ciliary transition zone to promote Sonic hedgehog signalling', *Nature Communications*, 8: 14177.

Selbie, L. A., and S. J. Hill. 1998. 'G protein-coupled-receptor cross-talk: the fine-tuning of multiple receptor-signalling pathways', *Trends Pharmacol Sci*, 19: 87-93.

Senatore, Emanuela, Francesco Chiuso, Laura Rinaldi, Daniela Intartaglia, Rossella Delle Donne, Emilia Pedone, Bruno Catalanotti, Luciano Pirone, Bianca Fiorillo, and Federica Moraca. 2021. 'The TBC1D31/praja2 complex controls primary ciliogenesis through PKA-directed OFD1 ubiquitylation', *The EMBO Journal*, 40: e106503.

Shakur, Yasmin, Kazuyo Takeda, Yael Kenan, Zu-Xi Yu, Graham Rena, Daniel Brandt, Miles D Houslay, Eva Degerman, Víctor J. Ferrans, and Vicent C. Manganiello. 2000. 'Membrane Localization of Cyclic Nucleotide Phosphodiesterase 3 (PDE3)', *The Journal of Biological Chemistry*, 275: 38749 - 61.

Shao, Lina, Wassim El-Jouni, Fanwu Kong, Janani Ramesh, Radhe Shantha Kumar, Xiaogang Shen, Jingjing Ren, Shruti Devendra, Arianna Dorschel, and Maoqing Wu. 2020. 'Genetic reduction of cilium length by targeting intraflagellar transport 88 protein impedes kidney and liver cyst formation in mouse models of autosomal polycystic kidney disease', *Kidney International*, 98: 1225-41.

Shen, TIANSHENG, YOSUKE Suzuki, MADELEINE Poyard, NORIHIRO Miyamoto, NICOLE Defer, and JACQUES Hanoune. 1997. 'Expression of adenylyl cyclase mRNAs in the adult, in developing, and in the Brattleboro rat kidney', *American Journal of Physiology-Cell Physiology*, 273: C323-C30.

Shillingford, J. M., N. S. Murcia, C. H. Larson, S. H. Low, R. Hedgepeth, N. Brown, C. A. Flask, A. C. Novick, D. A. Goldfarb, A. Kramer-Zucker, G. Walz, K. B. Piontek, G. G. Germino, and T. Weimbs. 2006. 'The mTOR pathway is regulated by polycystin-1, and its inhibition reverses renal cystogenesis in polycystic kidney disease', *Proc Natl Acad Sci U S A*, 103: 5466-71.

Shillingford, J. M., K. B. Piontek, G. G. Germino, and T. Weimbs. 2010. 'Rapamycin ameliorates PKD resulting from conditional inactivation of Pkd1', *J Am Soc Nephrol*, 21: 489-97.

Shimada, Ichio, Takumi Ueda, Yutaka Kofuku, Matthew T. Eddy, and Kurt Wüthrich. 2019. 'GPCR drug discovery: integrating solution NMR data with crystal and cryo-EM structures', *Nature Reviews Drug Discovery*, 18: 59-82.

Sholokh, A., S. Walter, L. Markó, B. J. McMurray, D. Y. Sunaga-Franze, M. Xu, K. Zühlke, M. Russwurm, T. U. P. Bartolomaeus, R. Langanki, F. Qadri, A. Heuser, A. Patzak, S. K. Forslund, S. Bähring, T. Borodina, P. B. Persson, P. G. Maass, M. Bader, and E. Klussmann. 2023. 'Mutant phosphodiesterase 3A protects the kidney from hypertension-induced damage', *Kidney Int*, 104: 388-93.

Smith, F. Donelson, Jessica L. Esseltine, Patrick J. Nygren, David Veesler, Dominic P. Byrne, Matthias Vonderach, Ilya Strashnov, Claire E. Eyers, Patrick A. Eyers, Lorene K. Langeberg, and John D. Scott. 2017. 'Local protein kinase A action proceeds through intact holoenzymes', *Science*, 356: 1288-93.

Smith, Laurie A, Nikolay O Bukanov, Hervé Husson, Ryan J Russo, Tiffany C Barry, Ava L Taylor, David R Beier, and Oxana Ibraghimov-Beskrovnaya. 2006. 'Development of polycystic kidney disease in juvenile cystic kidney mice: insights into pathogenesis, ciliary abnormalities, and common features with human disease', *Journal of the American Society of Nephrology*, 17: 2821-31.

Sonnenburg, William K, Dalia Seger, Keith S Kwak, Jing Huang, Harry Charbonneau, and Joseph A Beavo. 1995. 'Identification of Inhibitory and Calmodulin-binding Domains of the PDE1A1 and PDE1A2 Calmodulin-stimulated Cyclic Nucleotide Phosphodiesterases (∗)', *Journal of Biological Chemistry*, 270: 30989-1000.

Spirli, Carlo, Valeria Mariotti, Ambra Villani, Luca Fabris, Romina Fiorotto, and Mario Strazzabosco. 2017. 'Adenylyl cyclase 5 links changes in calcium homeostasis to cAMP-dependent cyst growth in polycystic liver disease', *Journal of hepatology*, 66: 571-80.

Sriram, Krishna, and Paul A. Insel. 2018. 'G Protein-Coupled Receptors as Targets for Approved Drugs: How Many Targets and How Many Drugs?', *Molecular Pharmacology*, 93: 251-58.

Stojanovski, D., O. S. Koutsopoulos, K. Okamoto, and M. T. Ryan. 2004. 'Levels of human Fis1 at the mitochondrial outer membrane regulate mitochondrial morphology', *Journal of cell science*, 117: 1201-10.

Stork, P. J., and J. M. Schmitt. 2002. 'Crosstalk between cAMP and MAP kinase signaling in the regulation of cell proliferation', *Trends Cell Biol*, 12: 258-66.

Strait, K. A., P. K. Stricklett, M. Chapman, and D. E. Kohan. 2010. 'Characterization of vasopressin-responsive collecting duct adenylyl cyclases in the mouse', *Am J Physiol Renal Physiol*, 298: F859-67.

Subramaniam, Gunasekaran, Katharina Schleicher, Duangnapa Kovanich, Anna Zerio, Milda Folkmanaite, Ying-Chi Chao, Nicoletta C. Surdo, Andreas Koschinski, Jianshu Hu, Arjen Scholten, Albert J.R. Heck, Maria Ercu, Anastasiia Sholokh, Kyung Chan Park, Enno Klussmann, Viviana Meraviglia, Milena Bellin, Sara Zanivan, Svenja Hester, Shabaz Mohammed, and Manuela Zaccolo. 2023. 'Integrated Proteomics Unveils Nuclear PDE3A2 as a Regulator of Cardiac Myocyte Hypertrophy', *Circulation Research*, 132: 828-48.

Sullivan, Lawrence P, Darren P Wallace, and Jared J Grantham. 1998. 'Epithelial transport in polycystic kidney disease', *Physiological reviews*, 78: 1165-91.

Sun, Fei, Martin J Hug, Neil A Bradbury, and Raymond A Frizzell. 2000. 'Protein kinase A associates with cystic fibrosis transmembrane conductance regulator via an interaction with ezrin', *Journal of Biological Chemistry*, 275: 14360-66.

Sun, Y., Z. Liu, X. Cao, Y. Lu, Z. Mi, C. He, J. Liu, Z. Zheng, M. J. Li, T. Li, D. Xu, M. Wu, Y. Cao, Y. Li, B. Yang, C. Mei, L. Zhang, and Y. Chen. 2019. 'Activation of P-TEFb by cAMP-PKA signaling in autosomal dominant polycystic kidney disease', *Sci Adv*, 5: eaaw3593.

Suofu, Yalikun, Wei Li, Frédéric G Jean-Alphonse, Jiaoying Jia, Nicolas K Khattar, Jiatong Li, Sergei V Baranov, Daniela Leronni, Amanda C Mihalik, and Yanqing He. 2017. 'Dual role of mitochondria in producing melatonin and driving GPCR signaling to block cytochrome c release', *Proceedings of the National Academy of Sciences*, 114: E7997-E8006.

Surdo, Nicoletta C., Marco Berrera, Andreas Koschinski, Marcella Brescia, Matias R. Machado, Carolyn Carr, Peter Wright, Julia Gorelik, Stefano Morotti, Eleonora Grandi, Donald M. Bers, Sergio Pantano, and Manuela Zaccolo. 2017. 'FRET biosensor uncovers cAMP nano-domains at β-adrenergic targets that dictate precise tuning of cardiac contractility', *Nature Communications*, 8: 15031.

Sussman, Caroline R., Xiaofang Wang, Fouad T. Chebib, and Vicente E. Torres. 2020. 'Modulation of polycystic kidney disease by G-protein coupled receptors and cyclic AMP signaling', *Cellular Signalling*, 72: 109649.

Sutendra, Gopinath, Peter Dromparis, Paulette Wright, Sébastien Bonnet, Alois Haromy, Zhengrong Hao, M Sean McMurtry, Marek Michalak, Jean E Vance, and William C Sessa. 2011. 'The role of Nogo and the mitochondria–endoplasmic reticulum unit in pulmonary hypertension', *Science translational medicine*, 3: 88ra55-88ra55.

Taira, M, SC Hockman, JC Calvo, P Belfrage, and VC Manganiello. 1993. 'Molecular cloning of the rat adipocyte hormone-sensitive cyclic GMP-inhibited cyclic nucleotide phosphodiesterase', *Journal of Biological Chemistry*, 268: 18573-79.

Tan, Adrian Y, Tuo Zhang, Alber Michaeel, Jon Blumenfeld, Genyan Liu, Wanying Zhang, Zhengmao Zhang, Yi Zhu, Lior Rennert, and Che Martin. 2018. 'Somatic mutations in renal cyst epithelium in autosomal dominant polycystic kidney disease', *Journal of the American Society of Nephrology*, 29: 2139-56.

Tang, Zaiming, Mary Grace Lin, Timothy Richard Stowe, She Chen, Muyuan Zhu, Tim Stearns, Brunella Franco, and Qing Zhong. 2013. 'Autophagy promotes primary ciliogenesis by removing OFD1 from centriolar satellites', *Nature*, 502: 254-57.

Tao, S., V. R. Kakade, J. R. Woodgett, P. Pandey, E. D. Suderman, M. Rajagopal, and R. Rao. 2015. 'Glycogen synthase kinase-3β promotes cyst expansion in polycystic kidney disease', *Kidney Int*, 87: 1164-75.

Taurin, Sebastien, Nathan Sandbo, Yimin Qin, Darren Browning, and Nickolai O Dulin. 2006. 'Phosphorylation of β-catenin by cyclic AMP-dependent protein kinase', *Journal of Biological Chemistry*, 281: 9971-76.

Taylor, S. S., C. Kim, C. Y. Cheng, S. H. Brown, J. Wu, and N. Kannan. 2008. 'Signaling through cAMP and cAMP-dependent protein kinase: diverse strategies for drug design', *Biochim Biophys Acta*, 1784: 16-26.

Taylor, S. S., E. Radzio-Andzelm, D. R. Knighton, L. F. Ten Eyck, J. M. Sowadski, F. W. Herberg, W. Yonemoto, and J. Zheng. 1993. 'Crystal structures of the catalytic subunit of cAMP-dependent protein kinase reveal general features of the protein kinase family', *Receptor*, 3: 165-72.

Taylor, S. S., P. Zhang, J. M. Steichen, M. M. Keshwani, and A. P. Kornev. 2013. 'PKA: lessons learned after twenty years', *Biochim Biophys Acta*, 1834: 1271-8.

Tebo, Alison G., and Arnaud Gautier. 2019. 'A split fluorescent reporter with rapid and reversible complementation', *Nature Communications*, 10: 2822.

Tewson, Paul H, Scott Martinka, Nathan C Shaner, Thomas E Hughes, and Anne Marie Quinn. 2016. 'New DAG and cAMP sensors optimized for live-cell assays in automated laboratories', *Journal of biomolecular screening*, 21: 298-305.

Tomilin, V. N., and O. Pochynyuk. 2019. 'A peek into Epac physiology in the kidney', *Am J Physiol Renal Physiol*, 317: F1094-f97.

Torres, V, XF Wang, P Harris, and V Gattone. 2003. "Inhibition of renal cystic disease development and progression by a vasopressin (VP) V2 receptor antagonist in the PCK rat." In *Journal of the American Society of Nephrology*, 109A-09A. LIPPINCOTT WILLIAMS & WILKINS 530 WALNUT ST, PHILADELPHIA, PA 19106-3621 USA.

Torres, Vicente E, Arlene B Chapman, Olivier Devuyst, Ron T Gansevoort, Jared J Grantham, Eiji Higashihara, Ronald D Perrone, Holly B Krasa, John Ouyang, and Frank S Czerwiec. 2012. 'Tolvaptan in patients with autosomal dominant polycystic kidney disease', *New England Journal of Medicine*, 367: 2407-18.

Torres, Vicente E, Arlene B Chapman, Olivier Devuyst, Ron T Gansevoort, Ronald D Perrone, Ann Dandurand, John Ouyang, Frank S Czerwiec, Jaime D Blais, and TEMPO 4: 4 Trial Investigators. 2018. 'Multicenter, open-label, extension trial to evaluate the long-term efficacy and safety of early versus delayed treatment with tolvaptan in autosomal dominant polycystic kidney disease: the TEMPO 4: 4 Trial', *Nephrology Dialysis Transplantation*, 33: 477-89.

Torres, Vicente E, Xiaofang Wang, Qi Qian, Stefan Somlo, Peter C Harris, and Vincent H Gattone. 2004. 'Effective treatment of an orthologous model of autosomal dominant polycystic kidney disease', *Nature medicine*, 10: 363-64.

Truong, Melissa E, Sara Bilekova, Semil P Choksi, Wan Li, Lukasz J Bugaj, Ke Xu, and Jeremy F Reiter. 2021. 'Vertebrate cells differentially interpret ciliary and extraciliary cAMP', *Cell*, 184: 2911-26. e18.

Tubbs, E., and J. Rieusset. 2017. 'Metabolic signaling functions of ER-mitochondria contact sites: role in metabolic diseases', *J Mol Endocrinol*, 58: R87-r106.

Tuson, Miquel, Mu He, and Kathryn V Anderson. 2011. 'Protein kinase A acts at the basal body of the primary cilium to prevent Gli2 activation and ventralization of the mouse neural tube', *Development*, 138: 4921-30.

Vandeput, F., N. Szabo-Fresnais, F. Ahmad, C. Kho, A. Lee, J. Krall, A. Dunlop, M. W. Hazel, J. A. Wohlschlegel, R. J. Hajjar, M. D. Houslay, V. C. Manganiello, and M. A. Movsesian. 2013. 'Selective regulation of cyclic nucleotide phosphodiesterase PDE3A isoforms', *Proc Natl Acad Sci U S A*, 110: 19778-83.

Wakana, Y., S. Takai, K. I. Nakajima, K. Tani, A. Yamamoto, P. Watson, D. J. Stephens, H. P. Hauri, and M. Tagaya. 2008. 'Bap31 is an itinerant protein that moves between the peripheral endoplasmic reticulum (ER) and a juxtanuclear compartment related to ER-associated degradation', *Molecular biology of the cell*, 19: 1825-36.

Walker-Gray, Ryan, Florian Stengel, and Matthew G Gold. 2017. 'Mechanisms for restraining cAMP-dependent protein kinase revealed by subunit quantitation and cross-linking approaches', *Proceedings of the National Academy of Sciences*, 114: 10414-19.

Wallace, Darren P. 2011. 'Cyclic AMP-mediated cyst expansion', *Biochimica et Biophysica Acta (BBA) - Molecular Basis of Disease*, 1812: 1291-300.

Walsh, D. A., J. P. Perkins, and E. G. Krebs. 1968. 'An adenosine 3',5'-monophosphate-dependant protein kinase from rabbit skeletal muscle', *J Biol Chem*, 243: 3763-5.
Wang, Bing, Mai Nguyen, Natasha C. Chang, and Gordon C. Shore. 2011. 'Fis1, Bap31 and the kiss of death between mitochondria and endoplasmic reticulum', *The EMBO Journal*, 30: 451-52-52.
Wang, Q., P. Cobo-Stark, V. Patel, S. Somlo, P. L. Han, and P. Igarashi. 2018a. 'Adenylyl cyclase 5 deficiency reduces renal cyclic AMP and cyst growth in an orthologous mouse model of polycystic kidney disease', *Kidney Int*, 93: 403-15.
Wang, Qian, Patricia Cobo-Stark, Vishal Patel, Stefan Somlo, Pyung-Lim Han, and Peter Igarashi. 2018b. 'Adenylyl cyclase 5 deficiency reduces renal cyclic AMP and cyst growth in an orthologous mouse model of polycystic kidney disease', *Kidney International*, 93: 403-15.
Wang, Qingyi, Huiyuan Zhang, Hao Xu, Dongqing Guo, Hui Shi, Yuan Li, Weiwei Zhang, and Yuchun Gu. 2016. '5-HTR3 and 5-HTR4 located on the mitochondrial membrane and functionally regulated mitochondrial functions', *Scientific reports*, 6: 37336.
Wang, X., L. Jiang, K. Thao, C. R. Sussman, T. LaBranche, M. Palmer, P. C. Harris, G. S. McKnight, K. P. Hoeflich, S. Schalm, and V. E. Torres. 2022. 'Protein Kinase A Downregulation Delays the Development and Progression of Polycystic Kidney Disease', *J Am Soc Nephrol*, 33: 1087-104.
Wang, Xiaofang, II Vincent Gattone, Peter C Harris, and Vicente E Torres. 2005. 'Effectiveness of vasopressin V2 receptor antagonists OPC-31260 and OPC-41061 on polycystic kidney disease development in the PCK rat', *Journal of the American Society of Nephrology*, 16: 846-51.
Watnick, Terry J., and Gregory G. Germino. 2013. 'Polycystin-1 and polycystin-2—it's complicated', *Nature Reviews Nephrology*, 9: 249-50.
Weis, W. I., and B. K. Kobilka. 2018a. 'The Molecular Basis of G Protein-Coupled Receptor Activation', *Annu Rev Biochem*, 87: 897-919.
Weis, William I., and Brian K. Kobilka. 2018b. 'The Molecular Basis of G Protein–Coupled Receptor Activation', *Annual Review of Biochemistry*, 87: 897-919.
Weissinger, E. M., G. Eissner, C. Grammer, S. Fackler, B. Haefner, L. S. Yoon, K. S. Lu, A. Bazarov, J. M. Sedivy, H. Mischak, and W. Kolch. 1997. 'Inhibition of the Raf-1 kinase by cyclic AMP agonists causes apoptosis of v-abl-transformed cells', *Mol Cell Biol*, 17: 3229-41.
Wellen, K. E., G. Hatzivassiliou, U. M. Sachdeva, T. V. Bui, J. R. Cross, and C. B. Thompson. 2009. 'ATP-citrate lyase links cellular metabolism to histone acetylation', *Science*, 324: 1076-80.
Wettschureck, Nina, and Stefan Offermanns. 2005. 'Mammalian G Proteins and Their Cell Type Specific Functions', *Physiological Reviews*, 85: 1159-204.
Wheway, Gabrielle, Liliya Nazlamova, and John T Hancock. 2018. 'Signaling through the primary cilium', *Frontiers in Cell and Developmental Biology*, 6: 8.
Wiggins, S. V., C. Steegborn, L. R. Levin, and J. Buck. 2018. 'Pharmacological modulation of the CO(2)/HCO(3)(-)/pH-, calcium-, and ATP-sensing soluble adenylyl cyclase', *Pharmacol Ther*, 190: 173-86.
Wikstrom, Jakob D, Tal Israeli, Etty Bachar-Wikstrom, Avital Swisa, Yafa Ariav, Meytal Waiss, Daniel Kaganovich, Yuval Dor, Erol Cerasi, and Gil Leibowitz. 2013. 'AMPK regulates ER morphology and function in stressed pancreatic β-cells via phosphorylation of DRP1', *Molecular endocrinology*, 27: 1706-23.
Wilson, Emma Louise, and Emmanouil Metzakopian. 2021. 'ER-mitochondria contact sites in neurodegeneration: genetic screening approaches to investigate novel disease mechanisms', *Cell Death & Differentiation*, 28: 1804-21.
Wong, B. W., X. Wang, A. Zecchin, B. Thienpont, I. Cornelissen, J. Kalucka, M. García-Caballero, R. Missiaen, H. Huang, U. Brüning, S. Blacher, S. Vinckier, J. Goveia, M. Knobloch, H. Zhao, C. Dierkes, C. Shi, R. Hägerling, V. Moral-Dardé, S. Wyns, M. Lippens, S. Jessberger, S. M. Fendt, A. Luttun, A. Noel, F. Kiefer, B. Ghesquière, L. Moons, L. Schoonjans, M. Dewerchin, G. Eelen, D. Lambrechts, and P. Carmeliet. 2017. 'The role of fatty acid β-oxidation in lymphangiogenesis', *Nature*, 542: 49-54.
Wong, W., and J. D. Scott. 2004. 'AKAP signalling complexes: focal points in space and time', *Nat Rev Mol Cell Biol*, 5: 959-70.
Wu, Albert Y, Xiao-Bo Tang, Sergio E Martinez, Kaori Ikeda, and Joseph A Beavo. 2004. 'Molecular determinants for cyclic nucleotide binding to the regulatory domains of phosphodiesterase 2A', *Journal of Biological Chemistry*, 279: 37928-38.
Xu, Lingna, Xi Wang, and Chao Tong. 2020. 'Endoplasmic reticulum–mitochondria contact sites and neurodegeneration', *Frontiers in Cell and Developmental Biology*, 8: 428.

Xu, Y., A. J. Streets, A. M. Hounslow, U. Tran, F. Jean-Alphonse, A. J. Needham, J. P. Vilardaga, O. Wessely, M. P. Williamson, and A. C. Ong. 2016. 'The Polycystin-1, Lipoxygenase, and α-Toxin Domain Regulates Polycystin-1 Trafficking', *J Am Soc Nephrol*, 27: 1159-73.

Xu, Z., L. Schaedel, D. Portran, A. Aguilar, J. Gaillard, M. P. Marinkovich, M. Théry, and M. V. Nachury. 2017. 'Microtubules acquire resistance from mechanical breakage through intralumenal acetylation', *Science*, 356: 328-32.

Yamaguchi, T., J. C. Pelling, N. T. Ramaswamy, J. W. Eppler, D. P. Wallace, S. Nagao, L. A. Rome, L. P. Sullivan, and J. J. Grantham. 2000a. 'cAMP stimulates the in vitro proliferation of renal cyst epithelial cells by activating the extracellular signal-regulated kinase pathway', *Kidney Int*, 57: 1460-71.

Yamaguchi, Tamio, Scott J Hempson, Gail A Reif, Anne-Marie Hedge, and Darren P Wallace. 2006. 'Calcium restores a normal proliferation phenotype in human polycystic kidney disease epithelial cells', *Journal of the American Society of Nephrology*, 17: 178-87.

Yamaguchi, Tamio, Clara Lysecki, Ashleigh Reid, Shizuko Nagao, and Harold M Aukema. 2014. 'Renal cyclooxygenase products are higher and lipoxygenase products are lower in early disease in the pcy mouse model of adolescent nephronophthisis', *Lipids*, 49: 39-47.

Yamaguchi, Tamio, Shizuko Nagao, Masao Kasahara, Hisahide Takahashi, and Jared J Grantham. 1997. 'Renal accumulation and excretion of cyclic adenosine monophosphate in a murine model of slowly progressive polycystic kidney disease', *American journal of kidney diseases*, 30: 703-09.

Yamaguchi, Tamio, Jill C Pelling, Nadja T Ramaswamy, Jason W Eppler, Darren P Wallace, Shizuko Nagao, Lorraine A Rome, Lawrence P Sullivan, and Jared J Grantham. 2000b. 'cAMP stimulates the in vitro proliferation of renal cyst epithelial cells by activating the extracellular signal-regulated kinase pathway', *Kidney international*, 57: 1460-71.

Yamaguchi, Tamio, Gail A Reif, James P Calvet, and Darren P Wallace. 2010. 'Sorafenib inhibits cAMP-dependent ERK activation, cell proliferation, and in vitro cyst growth of human ADPKD cyst epithelial cells', *American Journal of Physiology-Renal Physiology*, 299: F944-F51.

Yamaguchi, Tamio, Darren P Wallace, Brenda S Magenheimer, Scott J Hempson, Jared J Grantham, and James P Calvet. 2004. 'Calcium restriction allows cAMP activation of the B-Raf/ERK pathway, switching cells to a cAMP-dependent growth-stimulated phenotype', *Journal of Biological Chemistry*, 279: 40419-30.

Yang, B., N. D. Sonawane, D. Zhao, S. Somlo, and A. S. Verkman. 2008. 'Small-molecule CFTR inhibitors slow cyst growth in polycystic kidney disease', *J Am Soc Nephrol*, 19: 1300-10.

Yang, Dehua, Qingtong Zhou, Viktorija Labroska, Shanshan Qin, Sanaz Darbalaei, Yiran Wu, Elita Yuliantie, Linshan Xie, Houchao Tao, Jianjun Cheng, Qing Liu, Suwen Zhao, Wenqing Shui, Yi Jiang, and Ming-Wei Wang. 2021. 'G protein-coupled receptors: structure- and function-based drug discovery', *Signal Transduction and Targeted Therapy*, 6: 7.

Yao, Gang, Chong Luo, Michael Harvey, Maoqing Wu, Taylor H Schreiber, Yanjun Du, Nuria Basora, Xuefeng Su, Diego Contreras, and Jing Zhou. 2016. 'Disruption of polycystin-L causes hippocampal and thalamocortical hyperexcitability', *Human molecular genetics*, 25: 448-58.

Yasuda, Gen, and William B. Jeffries. 1998. 'Regulation of cAMP production in initial and terminal inner medullary collecting ducts', *Kidney International*, 54: 80-86.

Ye, H., X. Wang, M. M. Constans, C. R. Sussman, F. T. Chebib, M. V. Irazabal, W. F. Young, Jr., P. C. Harris, L. S. Kirschner, and V. E. Torres. 2017. 'The regulatory 1α subunit of protein kinase A modulates renal cystogenesis', *Am J Physiol Renal Physiol*, 313: F677-f86.

Ye, H., X. Wang, C. R. Sussman, K. Hopp, M. V. Irazabal, J. L. Bakeberg, W. B. LaRiviere, V. C. Manganiello, C. V. Vorhees, H. Zhao, P. C. Harris, J. van Deursen, C. J. Ward, and V. E. Torres. 2016. 'Modulation of Polycystic Kidney Disease Severity by Phosphodiesterase 1 and 3 Subfamilies', *J Am Soc Nephrol*, 27: 1312-20.

Zhang, Bo, Uyen Tran, and Oliver Wessely. 2018. 'Polycystin 1 loss of function is directly linked to an imbalance in G-protein signaling in the kidney', *Development*, 145: dev158931.

Zhang, D., Q. Zhao, and B. Wu. 2015. 'Structural studies of G protein-coupled receptors', *Molecules and Cells*, 38: 836-42.

Zhang, J., D. Levy, M. Oydanich, C. A. Bravo, S. Yoon, D. E. Vatner, and S. F. Vatner. 2018. 'A novel adenylyl cyclase type 5 inhibitor that reduces myocardial infarct size even when administered after coronary artery reperfusion', *J Mol Cell Cardiol*, 121: 13-15.

Zimmermann, Karl Wilhelm. 1898. 'Beiträge zur Kenntniss einiger drüsen und epithelien', *Archiv für mikroskopische Anatomie*, 52: 552-706.
Zittema, Debbie, Wendy E. Boertien, André P. van Beek, Robin P.F. Dullaart, Casper F.M. Franssen, Paul E. de Jong, Esther Meijer, and Ron T. Gansevoort. 2012. 'Vasopressin, Copeptin, and Renal Concentrating Capacity in Patients with Autosomal Dominant Polycystic Kidney Disease without Renal Impairment', *Clinical Journal of the American Society of Nephrology*, 7: 906-13.